

**Low oxygen tension modulates the
effects of TNF α and fibronectin
fragments in compressed
chondrocytes**

Reshma Kishan Tilwani

Submitted in partial fulfilment of the requirements of the degree of
Doctor of Philosophy

School of Engineering and Materials Science
Queen Mary University of London
Mile End Road
London, E1 4NS

2016

Statement of Originality

I, Reshma Kishan Tilwani, confirm that the research included within this thesis is my own work or that where it has been carried out in collaboration with, or supported by others, that this is duly acknowledged below and my contribution indicated. Previously published material is also acknowledged below.

I attest that I have exercised reasonable care to ensure that the work is original, and does not to the best of my knowledge break any UK law, infringe any third party's copyright or other Intellectual Property Right, or contain any confidential material.

I accept that the College has the right to use plagiarism detection software to check the electronic version of the thesis.

I confirm that this thesis has not been previously submitted for the award of a degree by this or any other university.

The copyright of this thesis rests with the author and no quotation from it or information derived from it may be published without the prior written consent of the author.

Signature: R. K. Tilwani

Date: 30/09/2016

Acknowledgements

I would firstly like to thank my supervisors Dr Tina Chowdhury, Professor David Lee and especially Professor Dan Bader for their constant support, patience and faith in me throughout the course of my PhD. They have greatly inspired me, helping me to become the researcher that I am today. I couldn't ask for better supervisors.

I would also like to thank Professor Belinda Pinguan-Murphy, from the University of Malaya for partly funding this project, together with other collaborators, including Engineering and Physical Sciences Research Council (EPSRC), the AO foundation and Dr Sandrine Vessillier.

I am also grateful for all my friends from SEMS who have made my journey more enjoyable, including Mr Shaffir Iqbal, Miss Patricia Ceide Martinez, Dr Erica Di Federico, Dr Stephen Thorpe, Dr Estelle Collin, Dr Nick Peake, Dr Eleanor Parker and many more.

Last but not the least; I would like to thank my dearest parents, Mr and Mrs Kishan Tilwani and my loving brother, Mr Lokesh Tilwani for all their patience, love and support through every step of the way. Words cannot express how grateful I am for having such a loving family.

Abstract

Oxygen tension and biomechanical signals are factors that regulate inflammatory mechanisms in chondrocytes. We examined whether low oxygen tension influenced the cells response to TNF α and dynamic compression.

Chondrocyte/agarose constructs were treated with varying concentrations of TNF α (0.1 to 100 ng/ml) and cultured at 5% and 21% oxygen tension for 48 hours. In separate experiments, constructs were subjected to dynamic compression (15%) and treated with TNF α (10 ng/ml) and/or L-NIO (1 mM) at 5% and 21% oxygen tension using an ex-vivo bioreactor for 48 hours. Markers for catabolic activity (NO, PGE₂) and tissue remodelling (GAG, MMPs) were quantified by biochemical assay. ADAMTS-5 and MMP-13 expression were examined by real-time qPCR. 2-way ANOVA and a post hoc Bonferroni-corrected t-test were used to analyse data.

TNF α dose-dependently increased NO, PGE₂ and MMP activity (all $p < 0.001$) and induced MMP-13 ($p < 0.05$) and ADAMTS-5 gene expression ($p < 0.01$) with values greater at 5% oxygen tension than 21%. The induction of catabolic mediators by TNF α was reduced by dynamic compression and/or L-NIO (all $p < 0.001$), with a greater inhibition observed at 5% than 21%. The stimulation of GAG synthesis by dynamic compression was greater at 21% than 5% oxygen tension and this response was reduced with TNF α or reversed with L-NIO.

The present findings revealed that TNF α has dose-dependent catabolic activities and increased production of inflammatory mediators at low oxygen tension. Dynamic compression or the NOS inhibitor downregulated the inflammatory effects induced by TNF α , linking both types of stimuli to reparative activities. Future therapeutics should develop oxygen-sensitive antagonists which are directed to interfering with the TNF α induced pathways.

Table of Contents

Statement of Originality	i
Acknowledgements	ii
Abstract	iii
Chapter 1 – Articular cartilage in health and disease	1
1.1 Characteristics of healthy articular cartilage	2
1.2 Structure and composition of articular cartilage	3
1.2.1 Extracellular matrix components	3
1.2.2 Zonal arrangement of cartilage.....	8
1.3 Oxygen tension in healthy cartilage.....	11
1.3.1 Chondrocyte metabolism under inherent hypoxic conditions	11
1.3.2 Oxygen-dependent signalling pathways.....	12
1.4 Effect of mechanical stimuli on cartilage homeostasis	15
1.4.1 Effect of physiological loading on cartilage homeostasis	16
1.5 Characteristics of diseased articular cartilage	25
1.5.1 Changes at the tissue level	26
1.5.2 Modulation of chondrocyte phenotype during OA.....	27
1.5.3 ECM turnover during OA progression.....	28
1.6 Pro-inflammatory cytokines.....	30
1.6.1 The interleukins	31
1.6.2 TNF α	32
1.6.3 Cytokines activate protein kinase signalling	33
1.6.4 Regulation of MMP gene expression by cytokines	34
1.6.5 Induction of nitric oxide and apoptosis by cytokines	35
1.7 Extracellular matrix fragments.....	40
1.7.1 Effect of FN-fs in cartilage breakdown and osteoarthritis	42
1.7.2 Effect of collagen fragments in the development of osteoarthritis	49

1.8	Effect of mechanical loading on OA progression	52
1.8.1	Effect of biomechanical signals and FN-fs on tissue remodelling and anabolic activities.....	52
1.8.2	Fibronectin fragments signalling	54
1.8.3	Effect of biomechanical signals and Col-fs on tissue remodelling and anabolic activities.....	57
1.9	Nitric oxide and oxygen tension during OA disease progression	60
1.9.1	Nitric oxide in OA.....	60
1.9.2	Effect of oxygen tension and pro-inflammatory cytokines on NO production.....	62
1.9.3	Combined effect of oxygen tension and mechanical loading on NO production.....	63
1.10	Aims and Objectives	65
Chapter 2 – General Methods		66
2.1	Justification of materials used	68
2.1.1	Agarose as a scaffold material.....	68
2.1.2	Oxygen tension	69
2.1.3	Source of chondrocytes	70
2.1.4	Purity of bovine cells	71
2.2	Cell seeded agarose model	72
2.2.1	Preparation of culture media and enzyme solutions.....	72
2.2.2	Isolation of primary chondrocytes from bovine joints.....	73
2.2.3	Preparation of cell seeded agarose constructs.....	75
2.2.4	Digestion of cell seeded agarose constructs	75
2.3	Uninterrupted culture system – Biospherix incubator	76
2.4	Mechanical loading	77
2.4.1	Mechanical loading apparatus	77
2.4.2	System set-up for the application of dynamic loading.....	77
2.5	Biochemical analysis.....	79

2.5.1	DNA quantification.....	79
2.5.2	Quantification of GAG synthesis	80
2.5.3	Quantification of nitric oxide release	81
2.5.4	Quantification of PGE ₂ synthesis	83
2.5.5	Total MMP activity measurement using fluorogenic substrate	86
2.5.5.1	Established assay procedure.....	86
2.5.5.2	MMP Optimization.....	91
2.5.6	TNF α synthesis quantification	102
2.6	Statistics	103
Chapter 3 – Low oxygen tension increases the pro-inflammatory effects induced by TNFα in chondrocytes		104
3.1	Introduction.....	105
3.2	Materials and methods.....	106
3.2.1	Dose response effect of TNF α on the production of catabolic and anabolic mediators in chondrocyte/agarose constructs cultured at 21 and 5% oxygen tension..	106
3.2.2	Temporal effect of exogenous TNF α on cell-free and chondrocyte seeded agarose constructs cultured at 21 and 5% oxygen tension	106
3.3	Results	107
3.3.1	Dose response effect of TNF α on catabolic and anabolic mediators in chondrocyte/agarose constructs cultured at 21 and 5% oxygen tensions.....	107
3.3.1.1	Nitrite release.....	107
3.3.1.2	PGE ₂ release.....	107
3.3.1.3	MMP activity.....	107
3.3.1.4	GAG synthesis.....	108
3.3.1.5	GAG loss.....	108
3.3.1.6	Summary of catabolic and anabolic mediators.....	114
3.3.2	Temporal effect of exogenous TNF α on TNF α release in cell-free and chondrocyte seeded agarose constructs cultured at 21 and 5% oxygen tensions.....	115
3.4	Summary of results	117
3.5	Discussion	118

Chapter 4 – Dynamic compression and oxygen tension modulates the effects of TNFα on protein synthesis in chondrocytes	120
4.1 Introduction.....	121
4.2 Materials and methods.....	122
4.3 Results	123
4.3.1 Effect of dynamic compression on catabolic and anabolic mediators in TNF α stimulated chondrocyte/agarose constructs cultured at 21 and 5% oxygen tension.	123
4.3.1.1 Nitrite release.....	123
4.3.1.2 PGE ₂ release.....	123
4.3.1.3 MMP activity.....	123
4.3.1.4 TNF α synthesis.....	124
4.3.1.5 GAG synthesis.....	124
4.3.1.6 GAG loss.....	124
4.3.1.7 Summary of catabolic and anabolic mediators.....	132
4.4 Summary of results	133
4.5 Discussion	134
Chapter 5 – Optimization of qRT-PCR techniques to examine the combined effects of oxygen tension and TNFα on gene expression in compressed chondrocytes	135
5.1 Introduction.....	136
5.2 Materials and methods.....	137
5.2.1 Effect of dynamic compression on the gene expression of TNF α stimulated chondrocyte/agarose constructs cultured at 21 and 5% oxygen tension..	137
5.2.2 Gene expression levels.....	137
5.2.2.1 RNA isolation.....	137
5.2.2.2 Reverse transcription and cDNA synthesis.....	139
5.2.2.3 Real-time quantitative PCR.....	140
5.3 Statistics	142
5.4 qRT-PCR optimization	143
5.4.1 Introduction.....	143
5.4.2 Primer binding efficiency.....	143

5.5	Results	157
5.6	Discussion	160
Chapter 6 – Extracellular matrix fragments.....		162
6.1	Introduction.....	163
6.2	Materials and methods.....	164
6.2.1	Effect of NT telopeptides on the production of catabolic and anabolic mediators in chondrocyte/agarose constructs cultured at 21, 5 and 2% oxygen tension.....	164
6.2.2	Effect of fibronectin fragments on the production of catabolic and anabolic mediators in chondrocyte/agarose constructs cultured at 21, 5 and 2% oxygen tension.....	166
6.2.3	Effect of dynamic compression on VGVAPG peptide- stimulated chondrocyte/agarose constructs cultured at 21, 5 and 2% oxygen tensions.....	168
6.3	Results	170
6.3.1	Effect of 3 and 50µM NT telopeptides on nitrite release and GAG synthesis in chondrocyte/agarose constructs cultured at 21, 5 and 2% oxygen tension..	170
6.3.2	Dose response effect of lactose on FN-fs-induced NO release and GAG synthesis in chondrocyte/agarose constructs cultured under free-swelling conditions..	173
6.3.3	Optimization of the culture conditions required for lactose to induce anabolic effects in FN-f-treated constructs.....	176
6.3.3.1	Effect of the solubility of lactose in culture media versus DMSO and PBS.....	176
6.3.3.2	Effect of equilibration on the response of FN-fs to lactose in chondrocyte/agarose constructs.....	178
6.3.3.3	Dose response effect of FN-fs with and without lactose in equilibrated chondrocyte/agarose constructs.....	181
6.3.3.4	Dose response effect of FN-fs in chondrocyte/agarose constructs treated with lactose without equilibration.....	185
6.3.3.5	Dose response effect of lactose in FN-f-treated chondrocyte/agarose constructs.....	188
6.3.4	Effect of 21, 5 and 2% oxygen tension on the response of FN-fs to lactose...	190
6.3.5	Effect of dynamic compression on the response of the VGVAPG peptide to lactose at 21 and 5% oxygen tensions..	192
6.4	Discussion	194

6.4.1	Effect of NT telopeptides on the production of catabolic and anabolic mediators in chondrocyte/agarose constructs cultured at 21, 5 and 2% oxygen tension.....	194
6.4.1.1	Model system and species of chondrocytes used.....	194
6.4.1.2	NT telopeptide synthesis.....	195
6.4.1.3	Peptide preparation prior to chondrocyte treatment.....	195
6.4.2	The effect of lactose on FN-fs is oxygen-sensitive and enhanced under hypoxic conditions..	197
6.4.3	The effect of dynamic compression on the response of the VGVAPG peptide to lactose is oxygen-independent..	198
Chapter 7 – General Discussion		199
7.1	Introduction.....	200
7.2	Model System.....	202
7.3	Test Equipment	203
7.4	Biochemical and molecular analysis	204
7.5	Scientific findings	205
7.5.1	The effect of TNF α and the NOS inhibitor, L-NIO on NO production.....	205
7.5.2	The effect of dynamic compression on chondrocytes stimulated with TNF α	209
7.5.3	The effect of oxygen tension in chondrocytes stimulated with TNF α ..	212
7.5.4	The effect of lactose on FN-fs.....	213
7.5.5	The effect of NT telopeptides on chondrocyte metabolism.....	217
7.6	Clinical Implications.....	219
7.7	Future work	220
References		222
Publications and Conference Proceedings		263

List of Figures

Chapter 1

Figure 1.1. Schematic of the synovial joint (a), side view of the femoral condyle (b), and arthroscopic view of a healthy human knee joint (c) (Schulz and Bader, 2007).....	2
Figure 1.2. Illustration of collagen structure from the isolated amino acids to collagen fibrils. The collagen right-handed triple helix is formed from three individual polypeptide chains resulting in a (Gly-X-Y), repeat structure which characterizes all collagen types. The X and Y position is often occupied by proline and hydroxyproline. Each of the three -chains of articular cartilage specific type II collagen fibrils forms an extended lefthanded helix with a pitch of 18 amino acids per turn. The three chains, staggered by one residue relative to each other, are supercoiled around a central axis in a right-handed manner to form the triple helix (Riqozzi et al., 2011).	5
Figure 1.3. The structure of aggrecan	7
Figure 1.4. Zonal arrangement of articular cartilage. Superficial, intermediate and deep zones of articular cartilage demonstrated in Hematoxylin and eosin (H&E) and Safranin O stained full depth sections of the tissue in an adult sheep distal femur (A) and schematic of articular cartilage (B) (An & Martin, 2003, Hardin et al., 2015).	8
Figure 1.5. Organisation of macromolecules within the different zones of articular cartilage. Schematic drawing (a) of articular cartilage demonstrates the zonal arrangement and macromolecular organization by the illustration of PGs (blue) and collagen fibrils (green). Histological staining with Safranin O and fast green (b) of full-depth articular cartilage harvested from bovine medial femoral condyle depicting columnar formation. Subchondral bone is stained green, articular cartilage is red because of its proteoglycan content and calcified cartilage as a mixture of both results in a pink staining (Schulz & Bader, 2007).	9
Figure 1.6. The ECM regions of articular cartilage. Illustration of the various tissue regions within a fragment of articular cartilage (Landínez-Parra et al., 2012).	10
Figure 1.7. Oxygen and glucose gradients in articular cartilage. Schematic of the (A) levels of oxygen and (B) glucose concentration gradient in articular cartilage (Blanco et al., 2010).	12
Figure 1.8. HIF-1 alpha signalling cascades induced by oxygen tension (Based on Henrotin, 2005).	13
Figure 1.9. Change in the T1 relaxation time in the presence of Gd-DTPA (TA[Gd]). Graph reflecting change in the GAG content of the medial femoral condyle of the menisectomized (study) knee, in both the exercise group and the control group (n=30), as a function of self-reported change in physical activity level during the study period. Bars denote the mean T1(Gd) for each of the 3 groups of self-reported change (Roos et al., 2005).....	17

Figure 1.10. Assessment of chondral lesions in ACLT Wister rat models subjected to moderate exercise. Histological grading according to Mankin's score and (B) apoptotic events assessed by immunostaining of activated caspase 3 in the control group (open columns) and exercised rats (grey columns) that had been subjected to ACLT at days 7, 14 and 28, significant beneficial effect of exercise (Galois et al., 2003).....	19
Figure 1.11. Histological lesions in ACLT and exercised rats (A) Histological lesions according to Mankin's score in ACLT rats and those subjected to slight, moderate and intense exercise at days 14 and 28 (Galois et al., 2004).....	20
Figure 1.12. Histological sections of articular cartilage from sham-operated joints, ACLT and exercised rats. (Upper figures) Hematoxylin-Eosin (H&E) staining evaluating cartilage surface integrity and (Bottom figures) toluidine blue (TB) staining revealing proteoglycan content in sham-operated joints (arthrotomy without ACLT), ACLT rats and those subjected to slight (ACLT 15min), moderate (ACLT 30min) and intense (ACLT 60min) exercise (Galois et al., 2004).	20
Figure 1.13. GAG synthesis and [3H]-TdR incorporation were measured in mechanically loaded 3D chondrocyte/agarose constructs. (A) GAG synthesis and (B) [3H] thymidine ([3H]-TdR) incorporation by 3D chondrocyte/agarose constructs subjected to 15% gross strain at frequencies ranging from 0.3 to 3Hz for 48 hours. The values have been normalized to unstrained control levels (100%). Each value represents the mean and SEM of at least 16 replicates from at least two separate experiments. Unpaired Student's t test results indicate differences from control values as follows: *= $p < 0.05$ (Bader and Lee, 1997).	21
Figure 1.14. Structural changes in OA disease progression (Giunta et al., 2015).....	25
Figure 1.15. Hypothetical model that shows the changes of cartilage, subchondral bone, and synovial macrophages during OA development (Siebelt et al., 2014).....	27
Figure 1.16. Schematic representation of key pathological events and some of the potential targets considered for disease modification in osteoarthritis.	29
Figure 1.17. Schematic of signalling pathways induced by pro-inflammatory cytokines.	39
Figure 1.18. Schematic of events involved in early to late stage osteoarthritis..	40
Figure 1.19. Biphasic effects of FN-fs on proteoglycan content (A) and proteoglycan synthesis (B). Cartilage explants were treated with 1, 10 or 100nM 29kDa FN-f continuously with media changes every other day. At intervals, cartilage was subjected to papain digests and measurement of proteoglycan content by DMB assay (left). Similar cultures were subjected to 35S labelling to determine rates of sulphated proteoglycan synthesis (right) (Homandberg et al., 1994, Homandberg et al.,1998).	44
Figure 1.20. Correlation of cartilage proteoglycan content (A) with MMP-3 release (B) and cytokine/ factor release (C) with high FN-f. Cartilage explants were treated with 100nM 29kDa FNof continuously with media changes every other day. In (A), cartilage proteoglycan content was measured in explants; in (B), MMP-3 (stromelysin) was measured by ELISA and in (C), cytokines and growth factors in the media were measured by ELISA (Homandberg et al., 1996, Homandberg et al., 1997).	46

Figure 1.21. Schematic diagram of cartilage destruction by matrix degradation products. Increased proteolytic matrix fragments activate chondrocytes and synovial fibroblasts, leading to the induction of matrix metalloproteinase, nitric oxide and cytokines via cell surface receptors such as integrins that can stimulate catabolic intracellular signals and pathways involving the MAPKs.	48
Figure 1.22. Injection of FN-fs rabbit knee joints causes marked loss of proteoglycan within 2 days. Adolescent rabbits were intra-articular injected with 200µg of a mixture of 29kDa human plasma FN-fs and after 2 days, cartilage recovered and subjected to staining with safranin-O to visualize proteoglycan (Homandberg et al., 2001).....	48
Figure 1.23. Model of interaction of type II collagen N-telo and C-telo regions with ECM and integrins. Bacteria collagenase cleaves type II collagen while leaving the N-telo and C-telo crosslinked regions intact. Such digest mixtures have been shown to upregulate MMPs. The N-telopeptide has been shown to bind annexin V but interaction with integrins might also occur for both types of peptides, as discussed (Henroitin, 2009).	50
Figure 1.24. Dynamic compression (15%. 1 Hz) inhibits NH ₂ -FN-f induced NO release (A) and restores cell proliferation (B) and proteoglycan synthesis (C) in chondrocyte/agarose constructs (48 hrs) (Raveenthiran and Chowdhury, 2009).	52
Figure 1.25. Effect of FN-f or IL-1β and dynamic compression on NO release (A) and GAG synthesis (B) in chondrocyte/agarose constructs cultured at 5 and 21% oxygen tension for 48hr. Constructs were cultured under uninterrupted experimental conditions with 0 or 1µM FN-f or 10ng/ml IL-1β and/or 1mM L-NIO. Error bars represent the mean and SEM of 8 to 12 replicates from three separate experiments, where (*) indicates comparisons between unstrained and strained values. In unstrained constructs, (+++) indicates comparisons between FN-f and FN-f + L-NIO; (ψ or ψψψ) indicates comparisons between untreated and IL-1β; (δδδ) indicates comparisons between IL-1β and IL-1β + L-NIO. (Raveenthiran and Chowdhury, 2009).	53
Figure 1.26. Effect of 0.1M α lactose (SGAL), 100µg/ml GRGDSP (α ₅ β ₁), 100µg/ml GRADSP (control), 1µg/ml anti-TLR4 in chondrocyte monolayer culture treated with 1µM of the 29kDa NH ₂ -heparin-binding FN-fs for 48 hours. The effects on NO production were then observed. (*) P < 0.05 indicates significant comparisons between constructs treated with fragment alone and those treated with fragment and inhibitor as shown [n=4, data obtained previously from the host lab in collaboration with Drs Parker and Peake (unpublished)].....	55
Figure 1.27. Effect of 0.1M α lactose in chondrocyte monolayer culture and 3D chondrocyte/agarose culture treated with 1µM of the 29kDa NH ₂ -heparin-binding FN-fs for 48 hours. The effects on NO production were then observed. (***) P < 0.001 indicate significant comparisons between constructs treated with fragment and those treated with fragment and inhibitor as shown [n=4, ata obtained previously from the host lab in collaboration with Drs Parker and Peake (unpublished)].....	56
Figure 1.28. Bioreactor vessel components (Chowdhury et al., 2010).	57

Figure 1.29. Continuous compression applied for longer periods resulted in a greater magnitude of stimulation of fibronectin (A) and MMP-3 (B) expression even in the presence of telopeptides or FN-fs (Chowdhury et al., 2010).	58
Figure 1.30. Effect of NT and CT telopeptides and dynamic compression (15%, 1 Hz) on NO release (A) and sGAG content (B). Unstrained and strained constructs were cultured with 50 μ M NT or CT peptide and/or 1mM 1400 W for 48 hours (n=8). SN and SC peptides (50 μ M) were used as negative controls. NH ₂ -FN-f (1 μ M) was used as a positive control. (*) indicates significant comparisons in unstrained constructs for no treatment vs fragment; (ψ) indicates significant comparisons in unstrained constructs for fragment vs fragment + 1400 W; + P < 0.05, ++ P < 0.01, +++ P < 0.001 indicates significant comparisons between treatment conditions as shown (n=6, Chowdhury et al., 2010).	59

Chapter 2

Figure 2.1. Flow chart illustrating the <i>ex-vivo</i> methods and protein analysis employed in the present study.....	67
Figure 2.2. Isolation of full depth articular cartilage from bovine metacarpalphalangeal joint.	74
Figure 2.3. The Biospherix incubator.	76
Figure 2.4. The <i>ex vivo</i> 3D/bioreactor system. Bose bioreactor cell straining apparatus (A) integrated with the Biospherix (B). Inset in (A) shows custom designed compressive mounting plate with loading pins positioned above a 24-well culture plate.	78
Figure 2.5. DNA standard curve obtained from fluorometer at an emission and excitation wavelength of 355nm and 460nm, respectively, which was then used to determine the concentration of DNA in each chondrocyte/agarose construct (Error bars represent SD of 3 replicates).....	79
Figure 2.6. Standard curve for chondroitin 4-sulphate complexed with DMB and measured at an absorbance of 595nm (Error bars represent SD of 2 replicates).	81
Figure 2.7. Nitrite standard curve (Error bars represent SD of 2 replicates).	82
Figure 2.8. PGE ₂ standard curve ranging from 39 to 1250pg/ml.	85
Figure 2.9. Fluorescence changes in MMP-1 activity to show kinetic performance during incubation with time (sec). Note the initial rate of hydrolysis before the reaction reached plateau. The change of fluorescence with time should be calculated from the linear part of the reaction (green square).	86
Figure 2.10. Kinetic profile obtained from performing the established fluorogenic substrate peptide assay on culture supernatants obtained from treating chondrocyte/agarose constructs with 0 or 10ng/ml of TNF α for 48 hours. RFU = Relative fluorescence unit.....	88
Figure 2.11. Flow chart illustrating the trial and error steps taken in optimizing the MMP fluorogenic substrate assay, starting from the established assay..	90
Figure 2.12. Kinetic profile obtained from performing the established fluorogenic substrate peptide assay on culture supernatants obtained from chondrocyte/agarose constructs	

cultured with 0 or 10ng/ml of TNF α for 48 hours in the presence and absence of ZnCl $_2$. RFU = Relative fluorescence unit.....	91
Figure 2.13. Kinetic profile obtained from employing black, flat-bottomed, uncoated 96-well plates to perform the fluorogenic substrate peptide assay on culture supernatants obtained from chondrocyte/agarose constructs cultured with 0 or 10ng/ml of TNF α for 48 hours, in the presence of ZnCl $_2$. RFU = Relative fluorescence unit.	92
Figure 2.14. Black, flat-bottomed, 96-well plates were employed to perform the fluorogenic substrate assay on culture supernatants obtained from culturing chondrocyte/agarose constructs for 48 hours with 0 or 10ng/ml of TNF α . The gain at which the fluorometer was set was increased from 10%, at increments of 10, up to 60% gain and the effects were observed on the kinetic profiles. RFU = Relative fluorescence unit.	98
Figure 2.15. Black, flat-bottomed, 96-well plates were employed to perform the fluorogenic substrate assay on culture supernatants obtained from culturing chondrocyte/agarose constructs for 48 hours with 0 or 10ng/ml of TNF α . The cycle number was set to 200 cycles and the effects were observed on the kinetic profiles. RFU = Relative fluorescence unit.....	99
Figure 2.16. Kinetic profile obtained from carrying out the fluorogenic substrate assay on culture supernatants obtained from culturing chondrocyte/agarose constructs for 48 hours with TNF α , using excitation/emission filters with values 355nm/440nm. RFU = Relative fluorescence unit. (***) = p<0.001.	101
Figure 2.17. Kinetic profile obtained from carrying out the fluorogenic substrate assay on culture supernatants obtained from culturing chondrocyte/agarose constructs for 48 hours with TNF α , using excitation/emission filters with values 355nm/440nm. RFU = Relative fluorescence unit.	101
Figure 2.18. TNF α standard curve ranging from 0 to 6000pg/ml (n=2)..	102

Chapter 3

Figure 3.1. Effect of 21 and 5% oxygen tension on nitrite release in chondrocytes treated with varying concentrations of TNF α . Chondrocyte/agarose constructs were cultured for 48 hours with varying concentrations of TNF α (0.1 to 100 ng/ml) and/or L-NIO (1 mM) and the effects of 21% (A) and 5% (B) oxygen tension were examined on nitrite release. Error bars represent the mean and SEM values for 6-18 replicates from four separate experiments. (+++) indicates significant comparisons between untreated and cytokine treated constructs cultured at 21% and 5% oxygen tension; (***) indicates significant comparisons between TNF α and TNF α + L-NIO.	109
Figure 3.2. Effect of 21 and 5% oxygen tension on PGE $_2$ release in chondrocytes treated with varying concentrations of TNF α . Chondrocyte/agarose constructs were cultured for 48 hours with varying concentrations of TNF α (0.1 to 100 ng/ml) and/or L-NIO (1 mM) and the effects of 21% (A) and 5% (B) oxygen tension were examined on PGE $_2$ release. Error bars represent the mean and SEM values for 6-18 replicates from four separate experiments. (+++) indicates significant comparisons between untreated and cytokine treated constructs	

cultured at 21% and 5% oxygen tension; (***) indicates significant comparisons between TNF α and TNF α + L-NIO.	110
Figure 3.3. Effect of 21 and 5% oxygen tension on MMP activity in chondrocytes treated with varying concentrations of TNF α . Chondrocyte/agarose constructs were cultured for 48 hours with varying concentrations of TNF α (0.1 to 100 ng/ml) and/or L-NIO (1 mM) and the effects of 21% (A) and 5% (B) oxygen tension were examined on MMP activity. Error bars represent the mean and SEM values for 6-18 replicates from four separate experiments. (+++) indicates significant comparisons between untreated and cytokine treated constructs cultured at 21% and 5% oxygen tension; (* or **) indicates significant comparisons between TNF α and TNF α + L-NIO.	111
Figure 3.4. Dose-dependent effects of TNF α on matrix synthesis at 21 and 5% oxygen tension. Chondrocyte/agarose constructs were cultured with varying concentrations of TNF α (0.1 to 100 ng/ml) and/or L-NIO (1 mM) for 48 hours and the effects of 21% (A) and 5% (B) oxygen tension were examined on GAG synthesis. Error bars represent the mean and SEM values for 6-18 replicates from four separate experiments. (+ or +++) indicates significant comparisons between untreated and cytokine treated constructs cultured at both oxygen tensions; (***) indicates significant comparisons between TNF α and TNF α + L-NIO at both oxygen tensions.	112
Figure 3.5. Dose-dependent effects of TNF α on matrix degradation at 21 and 5% oxygen tension. Chondrocyte/agarose constructs were cultured with varying concentrations of TNF α (0.1 to 100 ng/ml) and/or L-NIO (1 mM) for 48 hours and the effects of 21% (A) and 5% (B) oxygen tension were examined on GAG loss. Error bars represent the mean and SEM values for 6-18 replicates from four separate experiments. (+++) indicates significant comparisons between untreated and cytokine treated constructs cultured at both oxygen tensions; (***) indicates significant comparisons between TNF α and TNF α + L-NIO at both oxygen tensions.	113
Figure 3.6. Temporal effect of exogenous TNF α . Cell-free and chondrocyte seeded agarose constructs were treated with 10ng/ml of TNF α for 48 hours at 21% (A, B) and 5% (C) oxygen tension and the temporal effect of the cytokine was examined on TNF α release in the culture supernatant. Error bars represent the mean and SEM values for 4-11 replicates from three separate experiments. (*) p<0.05 indicates significant comparison between cytokine treated constructs cultured at 0 hours and those cultured for 48 hours at 5% oxygen tension.	116

Chapter 4

Figure 4.1. Effect of dynamic compression (15%, 1Hz) on nitrite release in chondrocyte/agarose constructs treated with TNF α (0 or 10ng/ml) and/or L-NIO (1mM) at 21% (A) and 5% (B) oxygen tension for 48 hours. Error bars represent the mean and SEM values for 8-12 replicates from four separate experiments. (** or ***) indicates significant

comparisons between the different treatment conditions. All other comparisons were not significant (not indicated). 1

Figure 4.2. Effect of dynamic compression (15%, 1Hz) on PGE₂ release in chondrocyte/agarose constructs treated with TNF α (0 or 10ng/ml) and/or L-NIO (1mM) at 21% (A) and 5% (B) oxygen tension for 48 hours. Error bars represent the mean and SEM values for 8-12 replicates from four separate experiments. (***) indicates significant comparisons between the different treatment conditions. All other comparisons were not significant (not indicated). 1

Figure 4.3. Effect of dynamic compression (15%, 1Hz) on MMP activity in chondrocyte/agarose constructs treated with TNF α (0 or 10ng/ml) and/or L-NIO (1mM) at 21% (A) and 5% (B) oxygen tension for 48 hours. Error bars represent the mean and SEM values for 8-12 replicates from four separate experiments. (***) indicates significant comparisons between the different treatment conditions. All other comparisons were not significant (not indicated). 1

Figure 4.4. Effect of dynamic compression (15%, 1Hz) on TNF α release in chondrocyte/agarose constructs treated with TNF α (0 or 10ng/ml) and/or L-NIO (1mM) at 21% (A) and 5% (B) oxygen tension for 48 hours. Error bars represent the mean and SEM values for 6-8 replicates from two separate experiments. (*or ***) indicates significant comparisons between the different treatment conditions. All other comparisons were not significant (not indicated). 1

Figure 4.5. Effect of dynamic compression (15%, 1Hz) on GAG synthesis in chondrocyte/agarose constructs treated with TNF α (0 or 10ng/ml) and/or L-NIO (1mM) at 21% (A) and 5% (B) oxygen tension for 48 hours. Error bars represent the mean and SEM values for 8 replicates from two separate experiments. (***) indicates significant comparisons between the different treatment conditions. All other comparisons were not significant (not indicated). 1

Figure 4.6. Effect of dynamic compression (15%, 1Hz) on GAG loss in chondrocyte/agarose constructs treated with TNF α (0 or 10ng/ml) and/or L-NIO (1mM) at 21% (A) and 5% (B) oxygen tension for 48 hours. Error bars represent the mean and SEM values for 8 replicates from two separate experiments. (***) indicates significant comparisons between the different treatment conditions. All other comparisons were not significant (not indicated). 1

Chapter 5

Figure 5.1. Standard curve obtained from 1:5 serial dilution of cDNA sample using 18S primers at a concentration of 500nM..... 144

Figure 5.2. Standard curve obtained from 1:5 serial dilution of cDNA sample using ADAMTS-5 primers at a concentration of 500nM..... 145

Figure 5.3. Standard curve obtained from 1:5 serial dilution of cDNA sample using MMP-13 primers at a concentration of 500nM..... 145

Figure 5.4. Amplification curves obtained on carrying out qRT-PCR on nuclease-free PCR-grade water and cDNA samples, using 18S, MMP-13 and ADAMTS-5 primers in a three-step thermal cycling programme, according to the standard conditions stated in section 5.2.2.3.	146
Figure 5.5. Amplification curves obtained on employing a new batch of plate sealer for qRT-PCR on nuclease-free PCR-grade water and cDNA samples, using 18S, MMP-13 and ADAMTS-5 primers in a three-step thermal cycling programme, according to the standard conditions stated in section 5.2.2.3.	147
Figure 5.6. Amplification curves obtained on employing KAPA master mix for qRT-PCR on nuclease-free PCR-grade water and cDNA samples, using MMP-13 primer pairs in a three-step thermal cycling programme.	149
Figure 5.7. Amplification plots obtained on performing qRT-PCR on nuclease-free PCR-grade water (NTC) and cDNA samples in duplicates, using MMP-13 primer pairs in a three-step thermal cycling programme with and without MgCl ₂	150
Figure 5.8. Amplification plots obtained on performing qRT-PCR on nuclease-free PCR-grade water (NTC) and cDNA samples in duplicates, using ADAMTS-5 primer pairs in a three-step thermal cycling programme with and without MgCl ₂	152
Figure 5.9. Amplification plots obtained on performing qRT-PCR on nuclease-free PCR-grade water (NTC) and cDNA samples, using ADAMTS-5 primer pairs in a two-step thermal cycling programme without MgCl ₂	154
Figure 5.10. Amplification plots obtained on performing qRT-PCR on nuclease-free PCR-grade water (NTC) and cDNA samples, using MMP-13 primer pairs in a two-step thermal cycling programme without MgCl ₂	155
Figure 5.11. Amplification plots obtained on carrying out qRT-PCR on nuclease-free PCR-grade water (NTC) and cDNA samples, using 18S primer pairs in a two-step thermal cycling programme without MgCl ₂	156
Figure 5.12. The effects of TNF α and dynamic compression on ADAMTS-5 gene expression at 21 and 5% oxygen. Data obtained from the two experiments carried out have been divided into experiment 1 (A, B) and experiment 2 (C, D) in order to determine the presence of significant differences between the two sets of experiments. Chondrocyte/agarose constructs were subjected to dynamic compression (15%, 1 Hz) in the presence or absence of TNF α (0 or 10 ng/ml) and/or L-NIO (1 mM) at 21 and 5% oxygen tension for 6 hours. Error bars represent the mean and SEM values for 3 replicates from a single experiment.	158
Figure 5.13. The effects of TNF α and dynamic compression on MMP-13 gene expression at 21 and 5% oxygen. Data obtained from the two experiments carried out have been divided into experiment 1 (A, B) and experiment 2 (C, D) in order to determine the presence of significant differences between the two sets of experiments. Chondrocyte/agarose constructs were subjected to dynamic compression (15%, 1 Hz) in the presence or absence of TNF α (0 or 10 ng/ml) and/or L-NIO (1 mM) at 21 and 5% oxygen tension for 6 hours. Error bars represent the mean and SEM values for 3 replicates from a single experiment.	159

Chapter 6

- Figure 6.1.** Flow chart illustrating *ex-vivo* methods and protein analysis for the investigation of the effects of N-telopeptides on chondrocyte metabolism. 165
- Figure 6.2.** Flow chart illustrating *ex-vivo* methods and protein analysis for the investigation of the effects of FN-fs on chondrocyte metabolism. 167
- Figure 6.3.** Flow chart illustrating the steps taken for the optimization of the culture conditions and concentrations required for lactose to inhibit FN-fs induced catabolic activities.....168
- Figure 6.4.** Effect of 21, 5 and 2% oxygen tension on (A) nitrite release and (B) GAG synthesis in chondrocytes treated with 3 μ M of NT telopeptides and/or L-NIO (1mM), and/or NS-398 (100mM) for 48 hours. 10ng/ml of TNF α in the presence and absence of both inhibitors represented a positive control. Error bars represent the mean and SEM values for 4 replicates from one experiment. (***) indicates significant comparisons between treatment conditions at 21%, 5% and 2% oxygen tension..... 1
- Figure 6.5.** Effect of 21, 5 and 2% oxygen tension on (A) nitrite release and (B) GAG synthesis in chondrocytes treated with 50 μ M of NT telopeptides and/or L-NIO (1mM) for 48 hours. 10ng/ml of TNF α in the presence and absence of both inhibitors represented a positive control. Error bars represent the mean and SEM values for 4 replicates from one experiments. (***) indicates significant comparisons between treatment conditions at 21%, 5% and 2% oxygen tension..... 172
- Figure 6.6.** Effect of varying concentrations of lactose on (A) nitrite release and (B) GAG synthesis in chondrocytes treated with 1 μ M FN-f. Chondrocyte/agarose constructs were cultured for 48 hours with varying concentrations of lactose (0.1 to 100 mM) and/or FN-fs (1 μ M) and the effects were examined on (A) nitrite release and (B) GAG synthesis. TNF α was used as a positive control. Error bars represent the mean and SEM values for 4 replicates from one experiment. (***) p<0.001 indicate significant comparisons between treatment conditions..... 174
- Figure 6.7.** Effect of lactose prepared in culture media on (A) nitrite release and (B) GAG synthesis in chondrocytes treated with 1 μ M FN-f. Chondrocyte/agarose constructs were cultured for 48 hours with 100mM lactose and/or 1 μ M of FN-fs and the effects were examined on (A) nitrite release and (B) GAG synthesis. Error bars represent the mean and SEM values for 4 replicates from one experiment. (*) p<0.05 and (***) p<0.001, indicate significant comparisons between treatment conditions... .. 177
- Figure 6.8.** Effect of 0 or 72 hours of equilibration on (A) nitrite release and (B) GAG synthesis in chondrocytes treated with FN-f and lactose. Chondrocyte/agarose constructs were subjected to either 0 or 72 hours equilibration followed by 48 hours of culture with 1 μ M FN-fs in the presence or absence of 100mM lactose. The effects were then examined on (A) nitrite release and (B) GAG synthesis. Error bars represent the mean and SEM values for 4

- replicates from one experiment. (*) $p < 0.05$, (**) $p < 0.01$ and (***) $p < 0.001$, indicate significant comparisons between treatment conditions..... 180
- Figure 6.9.** Dose response effect of FN-fs (0.25 to 2 μ M) on equilibrated chondrocyte/agarose constructs. Chondrocyte/agarose constructs were subjected to 72 hours equilibration followed by 48 hours of culture with 0.25, 0.5, 1 and 2 μ M FN-fs. The effects were then examined on (A) nitrite release and (B) GAG synthesis. Error bars represent the mean and SEM values for 4 replicates from one experiment. (*) $p < 0.05$ and (***) $p < 0.001$, indicate significant comparisons between treatment conditions..... 182
- Figure 6.10.** Dose response effect of FN-fs (0.01 to 1 μ M) on equilibrated chondrocyte/agarose constructs. Chondrocyte/agarose constructs were subjected to 72 hours equilibration followed by 48 hours of culture with 0.25, 0.5, 1 and 2 μ M FN-fs. The effects were then examined on (A) nitrite release and (B) GAG synthesis. Error bars represent the mean and SEM values for 4 replicates from one experiment. (*) $p < 0.05$ and (***) $p < 0.001$, indicate significant comparisons between treatment conditions.....183
- Figure 6.11.** Dose response effect of FN-fs in equilibrated chondrocytes treated with lactose. Chondrocyte/agarose constructs were subjected to 72 hours of equilibration, followed by 48 hours of culture with varying concentrations of FN-fs (0.01 to 1 μ M) and/or 100mM of lactose and the effects were examined on (A) nitrite release and (B) GAG synthesis. Error bars represent the mean and SEM values for 4 replicates from one experiment. (*) $p < 0.05$ and (***) $p < 0.001$, indicate significant comparisons between treatment conditions..... 184
- Figure 6.12.** Dose response effect of FN-fs in chondrocytes treated with lactose without equilibration. Chondrocyte/agarose constructs were subjected to 0 hours of equilibration, followed by 48 hours of culture with varying concentrations of FN-fs (0.01 to 1 μ M) and/or 100mM of lactose and the effects were examined on (A) nitrite release and (B) GAG synthesis. Error bars represent the mean and SEM values for 4 replicates from one experiment. (*) $p < 0.05$, (**) $p < 0.01$ and (***) $p < 0.001$, indicate significant comparisons between treatment conditions.. 186
- Figure 6.13.** Effect of varying concentrations of lactose on (A) nitrite release and (B) GAG synthesis in chondrocytes treated with 0.01 μ M FN-f. Chondrocyte/agarose constructs were subjected to 0 hours of equilibration, followed by 48 hours of culture with varying concentrations of lactose (1 to 100 mM) and/or FN-fs (1 μ M) and the effects were examined on (A) nitrite release and (B) GAG synthesis. Error bars represent the mean and SEM values for 4 replicates from one experiment. (***) $p < 0.001$, indicate significant comparisons between treatment conditions.. 189
- Figure 6.14.** Effect of hypoxia on the response of FN-fs to lactose. Chondrocyte/agarose constructs were cultured for 48 hours with 0.01 μ M of FN-fs in the presence or absence of 100mM lactose at 21, 5 and 2% oxygen tensions and the effects were examined on (A) nitrite release and (B) GAG synthesis. Error bars represent the mean and SEM values for 4

replicates from one experiment. (*) p<0.05, (**) p<0.01 and (***) p<0.001, indicate significant comparisons between treatment conditions..... 1

Figure 6.15. Effect of the VGVAPG peptide and lactose on chondrocyte/agarose constructs subjected to dynamic loading at 21 and 5% oxygen tensions. Dynamically loaded chondrocyte/agarose constructs were treated with 10µg/ml of the VGVAPG peptide in the presence and absence of 100mM lactose for 48 hours at 21 and 5% oxygen tensions and the effects were examined on (A) nitrite release and (B) GAG synthesis. Error bars represent the mean and SEM values for 4 replicates from one experiment. (*) p<0.05, (**) p<0.01 and (***) p<0.001, indicate significant comparisons between treatment conditions.. 1

Chapter 7

Figure 7.1. Flow chart illustrating the test protocols employed to achieve the aims and objectives of the present study (UT denotes untreated constructs).. 201

Figure 7.2. Flow chart illustrating the signalling cascades triggered on stimulating chondrocyte/agarose constructs with TNFα.. 209

Figure 7.3. Flow chart illustrating the activation of calcium ions upon stimulating chondrocyte/agarose constructs with dynamic compression..... 210

Figure 7.4. Flow chart illustrating the positive feedback loop of catabolic events induced by FN-fs and MMPs. SF = synovial fluid and AC = articular cartilage..... 215

List of Tables

Chapter 1

Table 1.1. Effect of various oxygen tensions on ECM synthesis in chondrocytes.	14
Table 1.2. Clinical studies showing the effects of exercise regimens on cartilage health.	16
Table 1.3. The effects of physiological joint loading on collagen and proteoglycan content in animal studies.	18
Table 1.4. The effects of physiological loading on cartilage metabolism in vitro.	22
Table 1.5. The effects of TNF α and/or IL-1 β on the production of catabolic mediators in chondrocytes.	37
Table 1.6. Effect of different sized FN-fs on cartilage degeneration.	45

Chapter 2

Table 2.1. Reagent concentration in the preparation of culture media for chondrocyte culture.	73
Table 2.2. Composition of reagents supplied used for PGE ₂ quantification.	84
Table 2.3. Reagents required for the preparation of 10X substrate assay buffer.	87
Table 2.4. Reagents required for the preparation of 1x substrate assay buffer.	88
Table 2.5. Plate reader settings for fluorogenic MMP substrate assay.	89
Table 2.6. Parameters altered throughout the optimization process of the fluorogenic peptide substrate assay.	93
Table 2.7. Components of substrate assay buffer A and B.	100

Chapter 3

Table 3.1. Statistical level of differences between cultures at 21% and 5% oxygen tensions, stimulated with different concentrations of TNF α with respect to five catabolic and anabolic mediators in the unstrained condition.	114
---	-----

Chapter 4

Table 4.1. The effects of oxygen tension and dynamic compression on catabolic/remodelling activities in chondrocyte/agarose constructs treated with TNF α	131
Table 4.2. Statistical level of differences between cultures at 21% and 5% oxygen tensions stimulated with 10ng/ml of TNF α , with respect to six catabolic and anabolic mediators in both strained and unstrained conditions.	132

Chapter 5

Table 5.1. Ct values of NTC and cDNA samples, from carrying out qRT-PCR using MMP-13 primer pairs in a three-step thermal cycling programme, with and without MgCl₂..... 151

Table 5.2. Ct values of NTC and cDNA samples, from carrying out qRT-PCR using ADAMTS-5 primer pairs in a three-step thermal cycling programme, with and without MgCl₂.
..... 153

Chapter 1 – Articular cartilage in health and disease

1.1 Characteristics of healthy articular cartilage

Articular cartilage is a complex connective tissue that covers the ends of bones in the synovial joint (Fig. 1.1). Its main functions are to distribute loads minimising the peak stresses in the subchondral bone and to provide a load-bearing surface, with minimal friction and wear (Mirzayan, 2006). The tissue is neither vascularised nor innervated and coupled with a relatively low cell density, exhibits limited repair capacity (Heywood et al 2004). Under healthy conditions, cartilage appears to be a relatively thin white tissue turning slightly yellow with age. The typical location and appearance of native articular cartilage within a synovial joint is illustrated in figure 1.1.

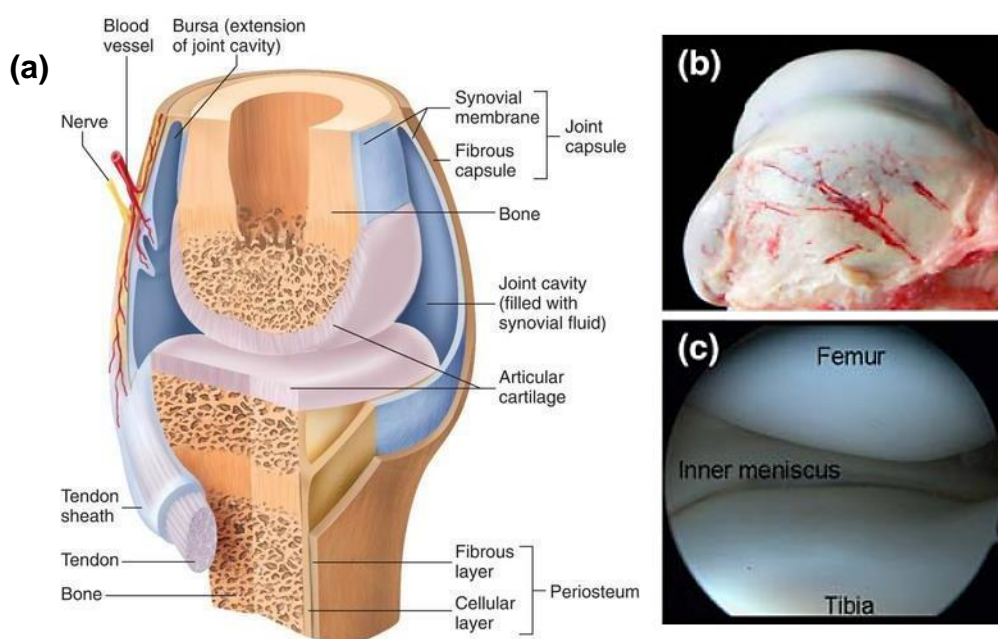


Figure 1.1. Schematic of the synovial joint (a), side view of the femoral condyle (b), and arthroscopic view of a healthy human knee joint (c) (Schulz and Bader, 2007).

1.2 Structure and composition of articular cartilage

Articular cartilage is composed of an extracellular matrix (ECM) which is synthesized and maintained by chondrocytes, which form 1-10% of the total tissue volume (Mirzayan, 2006, Kim et al. 2008; Mow et al. 1999, Muir et al., 1995). The ECM is primarily composed of water (60-80%), type II collagen (10-20%), proteoglycans (4-7%), and glycoproteins (<5%) which are relatively small in size (Anderson 1962, Knudson and Knudson 2001). The composition of the ECM and their interactions give the tissue its load-bearing capacity and, with the bathing synovial fluid, its lubrication and low frictional properties (Mov, Ratcliffe, Poole, 1992).

Chondrocytes exist in a unique physiological and mechanical environment in the ECM and exhibit different sizes, shapes, and possibly metabolic activity in the various zones of cartilage. Each chondrocyte is surrounded by its ECM, has few cell-to-cell contacts, and relies on diffusion from the synovial space for its nutritional supply (Williams, 2007). The interactions between chondrocytes and the ECM regulate important biological processes such as cell attachment, growth and differentiation, hence maintaining cartilage homeostasis (Loeser, 2000).

1.2.1 Extracellular matrix components

Water is most concentrated near the articular surface (80%) and decreases in an approximately linear manner with increasing depth to a concentration of approximately 65% in the deep zone (Lipshitz et al., 1980; Maroudas, 1979). This fluid contains many free mobile cations e.g., Na⁺, K⁺, and Ca²⁺, that greatly influence the mechanical and physiochemical behaviour of cartilage (Gu et al., 1998; Lai et al., 1991; Linn & Sokoloff, 1965; Maroudas 1979). The fluid component of articular cartilage is also essential in maintaining the health of this avascular tissue because it permits gas, nutrient, and waste product movement back and forth between chondrocytes and the surrounding nutrient-rich synovial fluid (Linn & Sokoloff, 1965; Maroudas, 1979).

A small percentage of the water in cartilage resides intracellularly and approximately 30% is strongly associated with the collagen fibrils (Maroudas et al., 1991). The interaction between collagen, proteoglycans and water, via the Donnan osmotic pressure, is considered important in regulating the structural organization of the ECM and its swelling properties. Most of the water thus occupies the interfibrillar space of the ECM and is free to move when a load or pressure gradient or other electrochemical motive forces are applied to the tissue. Indeed, when exposed to large compressive forces, approximately 70% of the water may be

displaced from the loaded region. This interstitial fluid movement is important in controlling the mechanical behaviour and joint lubrication (Gu et al., 1998; Maroudas 1979).

Collagen consists of approximately 1000 amino acids, with a glycine at every third location of an alpha chain. Each collagen molecule is coiled into a left-handed helix, and three alpha helices coil around each other into a right-handed helix called the tropocollagen molecule (Fig. 1.2; Eyre, 1980). Collagen contains significant amounts of both hydroxyproline, which stabilizes the triple helix, and hydroxylysine, which allows collagen to bind covalently to carbohydrates (Eyre, 1980). The types of collagen found in articular cartilage can be divided into fibril-forming and non-fibril-forming. Whereas types II and XI form fibrils, types VI, IX and X collagen do not, although each are found to contribute to the ECM structure. The type of collagens in normal and degenerative articular cartilage has been extensively studied. Of the 23 different types of collagen identified to date, articular cartilage contains at least five types: I, II, VI, IX and XI. Types II, IX and XI are cartilage-specific, cross linked fashion that forms the cartilage extracellular framework. Type II collagen provides the basic architecture and Type XI copolymerise with Type II collagen in the matrix. Type VI collagen is found in normal articular cartilage. In osteoarthritis, Type VI collagen is increased in the pericellular region in the middle and deep zones of articular cartilage, but is reduced in the superficial layer relative to normal cartilage. Type IX collagen (1% of total collagen in cartilage) is covalently linked to the surface of Type II collagen fibrils. Collagen Type X is restricted to the underlying calcified zone of articular cartilage (An & Martin, 2003). Type II collagen fibrils contribute to the stiffness and strength of cartilage. Its fibril thickness and diameter is affected by the other collagen types, particularly collagen type IX which varies through the depth of cartilage. Type II collagen is the most abundant types of collagen in hyaline cartilage, accounting for 90-95% of the collagen in the matrix. It is associated with type XI collagen to form a mesh. Type VI collagen is a microfibrillar collagen that forms elastic fibres and is preferentially located in the pericellular region of chondrocytes. Type IX collagen is classified as fibril-associated collagen fibrils with interrupted triple helices, and may function to act as a bridge between collagen fibrils and aggrecan. Type X collagen is classified as a network forming collagen and, although its function is not entirely clear; it is found mineralized in the calcified zone of cartilage. The collagen fibrils are stabilized by cartilage oligomeric matrix protein, a 100,000-kDa protein that is present in cartilage and tendons, with multiple binding sites (An & Martin, 2003).

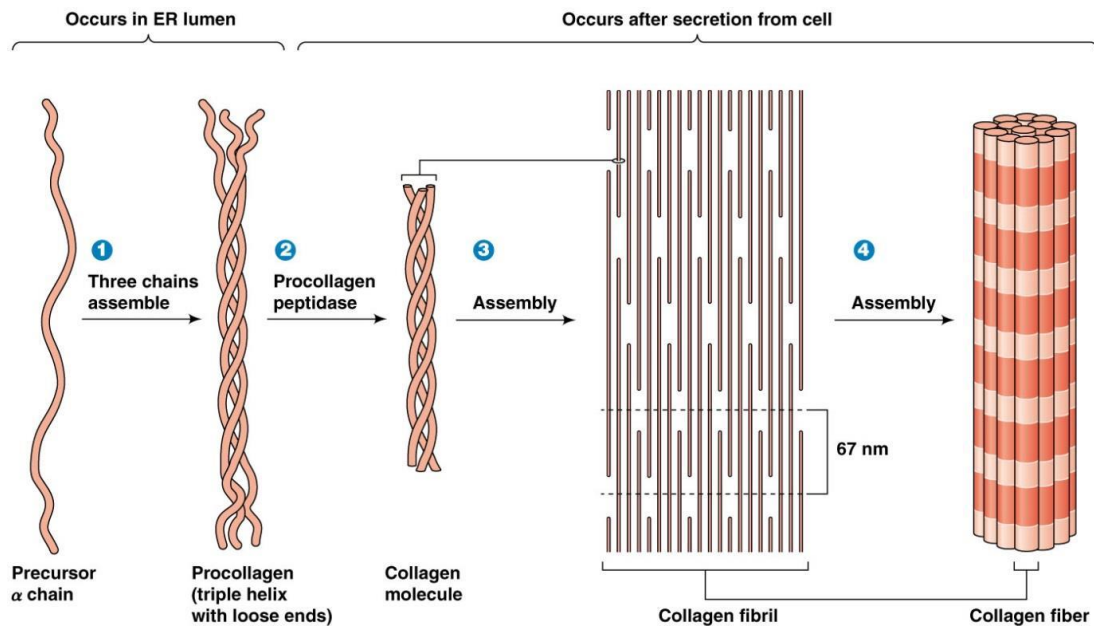


Figure 1.2. Illustration of collagen structure from the isolated amino acids to collagen fibrils. The collagen right-handed triple helix is formed from three individual polypeptide chains resulting in a (Gly-X-Y), repeat structure which characterizes all collagen types. The X and Y position is often occupied by proline and hydroxyproline. Each of the three α -chains of articular cartilage specific type II collagen fibrils forms an extended left-handed helix with a pitch of 18 amino acids per turn. The three chains, staggered by one residue relative to each other, are supercoiled around a central axis in a right-handed manner to form the triple helix (Rigozzi et al., 2011).

Proteoglycans are large ECM molecules composed of a protein core covalently bound to glycosaminoglycan (GAG) chains, the latter of which are long chains of non-branching polysaccharides, consisting of repeating disaccharide units. There is usually a sulphated group, namely SO_4^{2-} , per disaccharide. Less often, there are non-sulphated or disulphated disaccharides. This high occurrence of sulphated disaccharide and the presence of carboxyl (CO_2H^-) ionic groups give an overall negative charge to the GAG, which is crucial in controlling the hydration of cartilage and ultimately the mechanical properties of the tissue (An & Martins, 2003). The two main types of GAG in articular cartilage are keratan sulphate and chondroitin sulphate (Fig. 1.3; Ng et al., 2003). Both sulphated GAGs contain variations within their own groups, such as differences in disaccharide units, sulphation, and amino acid epimerization (Schulz & Bader, 2007). The biosynthesis and control of both GAGs are not well understood. It has been shown that the amount of keratan sulphate in cartilage increases with age. The ratio of the two GAGs also varies with the depth of cartilage. Other GAGs present in the cartilage include dermatan sulphate, which is chondroitin sulphate with epimerized amino acids, and heparin sulphate (Woessner & Howell, 1993).

Proteoglycans are hydrophilic in nature producing the water affinity of articular cartilage (Mirzayan, 2006). The charge-carrying capacity of proteoglycans combined with the interstitial water phase including small cations provides an ideal environment for interactions. Two major classes of proteoglycans reside in articular cartilage: large aggregating

proteoglycan monomers or aggrecans, and small proteoglycans, including decorin, biglycan, and fibromodulin (Schulz & Bader, 2007). The tissue may also contain other small proteoglycans that have not yet been identified. Proteoglycans are key molecules in the mechanical behaviour of articular cartilage. They also play a role in cell behaviour and mediate cell interactions. Proteoglycan aggregates form as a result of the noncovalent interactions between hyaluronan and other small non-collagenous proteins (NCPs). The formation of these aggregates provides, in part, the spatial relationship between the constituents reflected in its mechanical properties (An & Martin 2003).

The noncollagenous proteins and glycoproteins are poorly studied with occasional monosaccharide and oligosaccharides attached. They are found within the ECM and are likely to be involved in maintaining structure. These include anchoring CII, a chondrocyte surface protein; cartilage oligomeric protein (COMP), an acidic protein found within the territorial matrix; and fibronectin and tenascin (Williams, 2007).

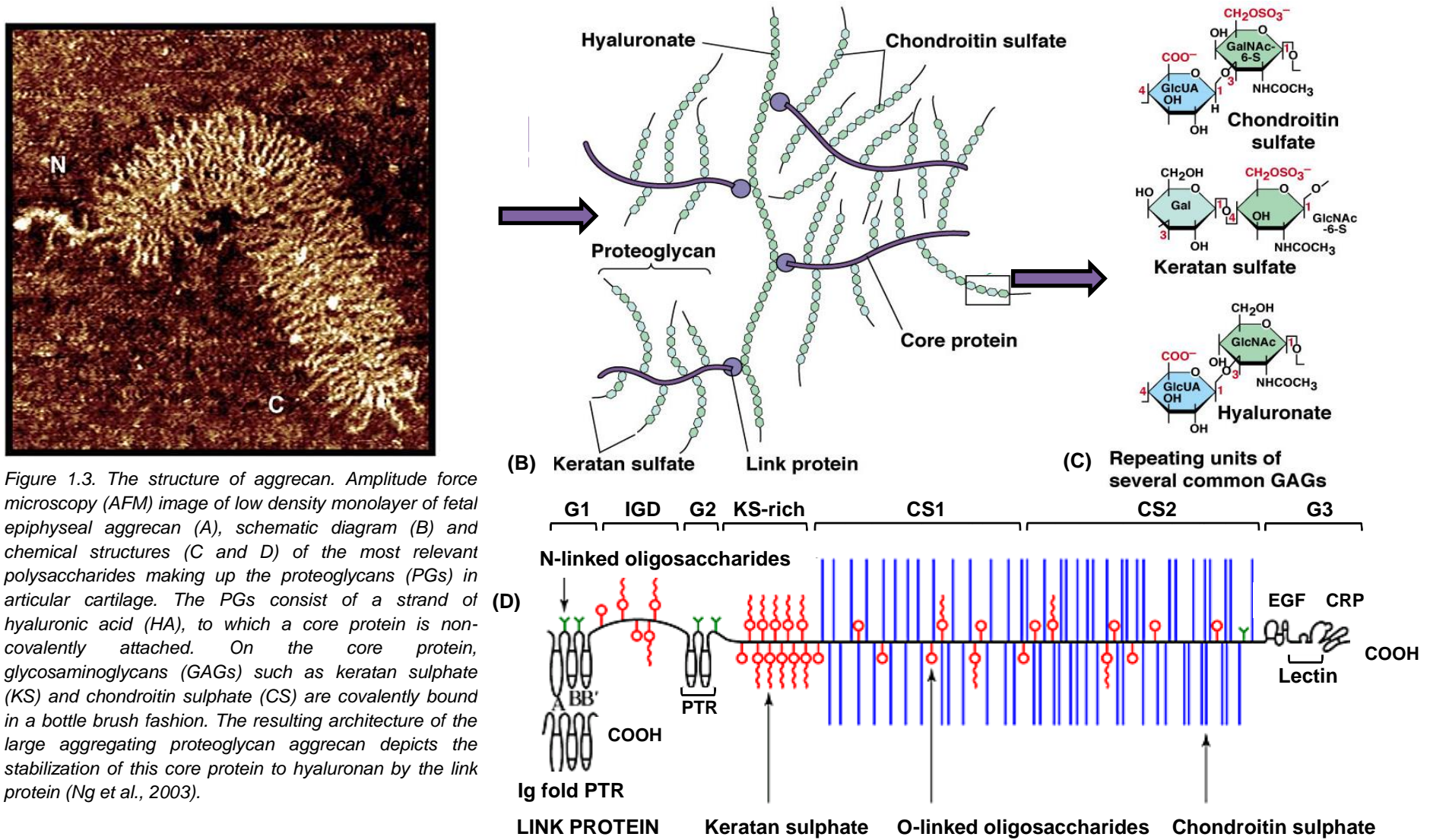


Figure 1.3. The structure of aggrecan. Amplitude force microscopy (AFM) image of low density monolayer of fetal epiphyseal aggrecan (A), schematic diagram (B) and chemical structures (C and D) of the most relevant polysaccharides making up the proteoglycans (PGs) in articular cartilage. The PGs consist of a strand of hyaluronic acid (HA), to which a core protein is non-covalently attached. On the core protein, glycosaminoglycans (GAGs) such as keratan sulphate (KS) and chondroitin sulphate (CS) are covalently bound in a bottle brush fashion. The resulting architecture of the large aggregating proteoglycan aggrecan depicts the stabilization of this core protein to hyaluronan by the link protein (Ng et al., 2003).

1.2.2 Zonal arrangement of cartilage

The structure and composition of articular cartilage at the microscopic level varies significantly with depth and can be separated into four poorly defined zones; superficial, transitional, deep zones and a zone of calcified cartilage (Fig. 1.4, An & Martin, 2003, Hardin et al., 2015).

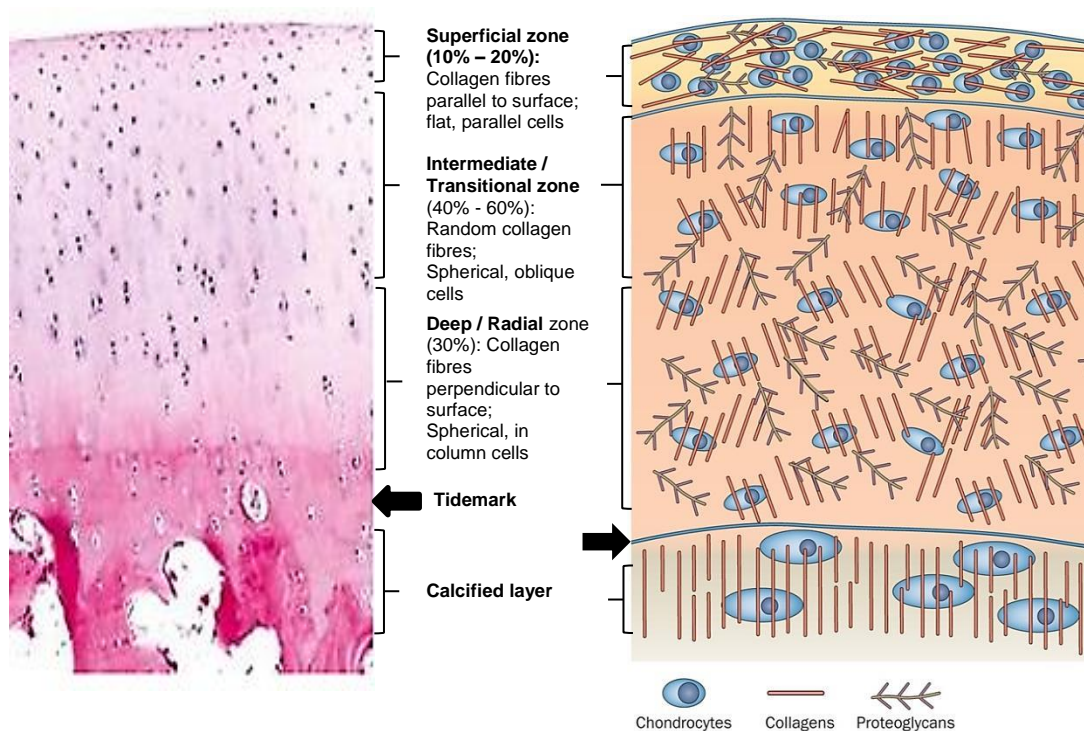


Figure 1.4. Zonal arrangement of articular cartilage. Superficial, intermediate and deep zones of articular cartilage demonstrated in Hematoxylin and eosin (H&E) and Safranin O stained full depth sections of the tissue in an adult sheep distal femur (A) and schematic of articular cartilage (B) (An & Martin, 2003, Hardin et al., 2015).

The **superficial zone** consists of two layers. The outermost layer is composed of fine fibrils with little polysaccharide and no cells that cover the joint surface and is often referred to as the lamina splendens, which can be shed from the articular surface in some regions (Clarke, 1971). The superficial zone lies directly below this and consists of tightly packed collagen fibres orientated parallel to the articular surface, in which flattened disc-shaped cells exist with low proteoglycan (PG) content. This zone is in close proximity to the synovial fluid and its integrity is essential for the fortification and maintenance of the underlying layers. It contributes greatly to the mechanical response of cartilage in resisting the compressive, tensile and shear forces generated during joint articulation (Buckwalter et al., 1987). Indeed, damage to this superficial zone is one of the first detectable structural changes in the experimentally induced degeneration of articular cartilage, leading to a reduction in its mechanical behaviour and a potential release of molecules that stimulate an inflammatory and/or immune response (An & Martin, 2003).

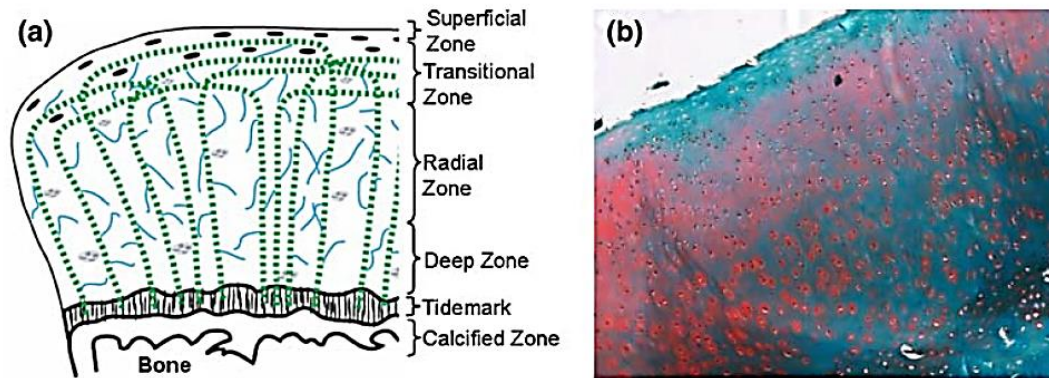


Figure 1.5. Organisation of macromolecules within the different zones of articular cartilage. Schematic drawing (a) of articular cartilage demonstrates the zonal arrangement and macromolecular organization by the illustration of PGs (blue) and collagen fibrils (green). Histological staining with Safranin O and fast green (b) of full-depth articular cartilage harvested from bovine medial femoral condyle depicting columnar formation. Subchondral bone is stained green, articular cartilage is red because of its proteoglycan content and calcified cartilage as a mixture of both results in a pink staining (Schulz & Bader, 2007).

The **transitional zone** is thicker than the superficial zone, and demonstrates a difference in cellularity and organization. The cells in the transitional zone are spheroidal in shape and synthesize a matrix that has larger-diameter collagen fibrils, a higher proportion of proteoglycan and lower concentrations of water and collagen than the matrix of the superficial zone. The chondrocytes in the **middle (radial)** zone are spheroidal in shape, and tend to align themselves in columns perpendicular to the joint surface. The largest diameter collagen fibrils are found in this radial zone associated with the highest concentration of proteoglycans, and the lowest concentration of water. The collagen fibres are aligned perpendicular to the articular surface in this zone. The **deepest calcified zone** forms a mechanical transition between the relatively deformable cartilage above and the hard bone below. A so-called "**tidemark**" delineates the extent of mineralization, yet collagen fibres continue across this line. The calcified cartilage layer makes up the final zone that separates the middle zone from the underlying subchondral bone (An & Martin, 2003).

The extracellular matrix is compartmentalised into three separate domains, known as the **pericellular**, the **territorial** and the **interterritorial matrices** (Fig. 1.6, Landínez-Parra et al., 2012). The **pericellular matrix** surrounds the chondrocytes and is thus in close proximity to the cell membrane. It contains mainly proteoglycans, type VI collagen as well as glycoproteins and other noncollagenous proteins. The **territorial matrix** abuts the pericellular matrix and contains primarily collagen, forming a basket-like meshwork around the cell. It is thicker than the pericellular matrix and possibly functions to protect the cells during loading. The largest of the three matrix compartments is the **interterritorial matrix**, which also contains the largest collagen fibrils. It is the orientation of these collagen fibres that accounts for the differences seen in the four distinct cartilage zones typically parallel in the superficial zone and perpendicular in the deep zone. Accordingly, the interterritorial

matrix is predominantly responsible for the mechanical properties of the tissue (Mirzayan, 2006).

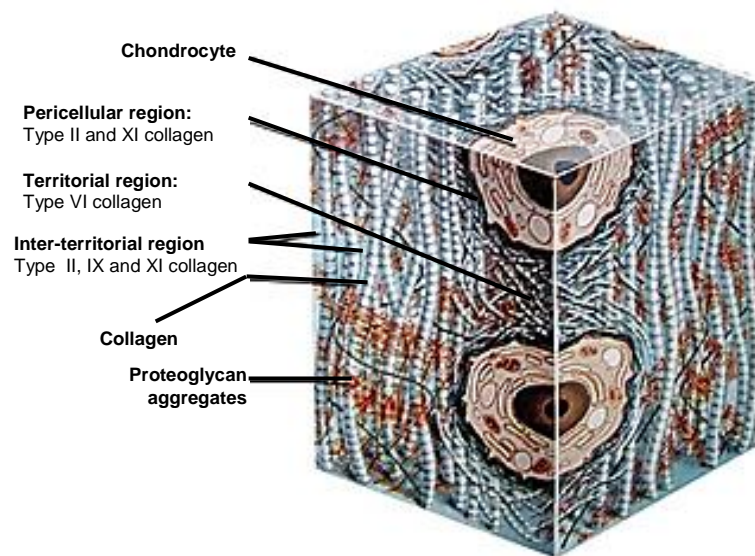


Figure 1.6. The ECM regions of articular cartilage. Illustration of the various tissue regions within a fragment of articular cartilage (Landínez-Parra et al., 2012).

1.3 Oxygen tension in healthy cartilage

The oxygen tension in cartilage ranges from approximately 8% in the superficial zones to as low as 1% in the deep zone with nutrients supplied from the synovial space via diffusion predominantly through the articular surface (Falchuk, Goetzl, Kulka, 1970, Brighton & Heppenstall, 1971, Fig 1.7). At these low oxygen tensions, chondrocytes are well adapted in maintaining their phenotype, promoting ECM production and in the regulation of cartilage homeostasis (Heywood, Bader & Lee, 2006, Falchuk, Goetzl, Kulka, 1970; Nevo, Beit-Or, Eilam, 1988). Oxygen tension is therefore an essential criterion when developing models for tissue engineering cartilage *in vitro*. Furthermore, the presence of reactive oxygen species (ROS) are highly involved in the regulation of cartilage homeostasis and have been previously found to promote tissue degeneration. ROS exists as molecules, ions or radicals which are involved in cell signalling and cell physiology. On exceeding the antioxidant capacity of chondrocytes, ROS will induce an 'oxidative stress' which promotes alterations in cartilage structure and function such as ECM degradation and possibly cell death (Henrotin et al., 2005).

1.3.1 Chondrocyte metabolism under inherent hypoxic conditions

At >1% oxygen tension, chondrocytes generate adenosine triphosphate (ATP) via glycolytic pathways (Lee & Urban, 1997). However, RNA synthesis is limited at oxygen tensions <1% resulting in the reduction of glucose intake and lactate production (Grimshaw & Mason, 2000). It has been well documented that the density of mitochondria found in the superficial regions of articular cartilage is greater when compared to the deep regions of the tissue (Stockwell, 1991). Hence, at higher oxygen levels, chondrocytes have the ability to undergo aerobic metabolism, in order to sustain the production of energy (Lane, Brighton, Menkowitz, 1977). In addition, oxygen consumption is known to be inhibited when chondrocytes are supplied with high concentrations of glucose. This effect, known as the "Crabtree effect", explains the fact that chondrocytes function under hypoxic conditions. Furthermore, previous studies demonstrated that although the oxygen consumption by chondrocytes is lower when compared to other cell types, potassium cyanide can reduce the oxygen consumption in chondrocytes only by 80-90%, suggesting that some percentage of oxygen is still being consumed by non-mitochondrial oxidases (Otte, 1991).

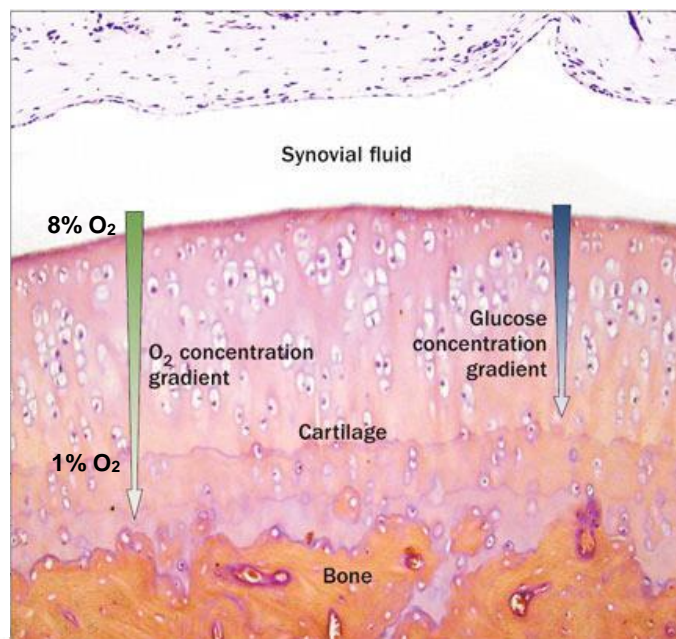


Figure 1.7. Oxygen and glucose gradients in articular cartilage. Schematic of the (A) levels of oxygen and (B) glucose concentration gradient in articular cartilage (Blanco et al., 2010).

1.3.2 Oxygen-dependent signalling pathways

It is well established that the molecule, hypoxia-inducible factor-1 α (HIF-1 α), is expressed by a wide range of mammalian cell types including murine epiphyseal chondrocytes, bovine and human articular chondrocytes (Pfander et al., 2003, Cramer et al., 2004, Pufe et al., 2004, Coimbra et al., 2004). It might be proposed that chondrocytes use the same oxygen-dependent signalling pathways as other cell types. At 21% oxygen tension, HIF-1 α undergoes hydroxylation in response to an oxygen-triggered mechanism. The process is catalysed with the help of the enzyme, prolyl hydroxylase (PHD), in conjunction with Fe²⁺ and vitamin C, which allows it to bind to the von von Hippel-Lindau tumor suppressor protein (pVHL), resulting in the enzymatic degradation of the HIF-1 α (Safran & Kaelin, 2003). In contrast, HIF-1 α does not undergo degradation via hydroxylation at 5% oxygen tension. Instead, the molecule forms a heterodimer, HIF-1 β , which is highly expressed by the translocation of HIF-1 α into the nucleus of the cell. Following this, the heterodimer then binds to the HIF-1 binding sites in hypoxia response elements (HRE) of the DNA and consequently activates hypoxia-inducible genes (Schmid, Zhou, Brune, 2004). Previous studies have demonstrated these oxygen-dependent signalling pathways (Henrotin et al., 2005), as indicated in the schematic in Fig.1.8 via the activation of HIF-1 α in other cell types although many of these pathways have not been identified in chondrocytes. Indeed, at 5% oxygen tension epiphyseal chondrocytes showed an upregulation in ECM synthesis via HIF-1 α (Lin et al., 2004, Cramer et al., 2004). Furthermore, HIF-1 α has been demonstrated to

regulate ATP levels via glycolysis, making it an essential factor in oxygen-sensitive mechanisms in chondrocytes (Pfander et al., 2003).

It has been well documented in tissue engineering studies that low oxygen tension promotes the expression of chondrogenic phenotype and the synthesis of cartilage-specific ECM components. For example, the expression of type II collagen was greater than that of type I collagen in bovine chondrocytes cultured at 5% oxygen tension compared to those cultured at 21% O₂ (Kurz et al., 2004, Domm et al., 2002). Hypoxia has also demonstrated an increase in GAG and type II collagen synthesis in various culture systems in a series of studies as detailed in table 1.1.

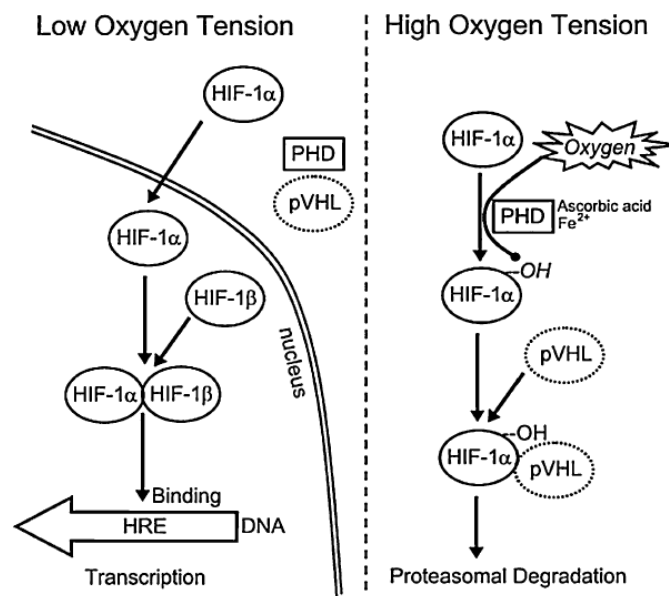


Figure 1.8. HIF-1 alpha signalling cascades induced by oxygen tension (Based on Henrotin, 2005).

Table 1.1: Effect of various oxygen tensions on ECM synthesis in chondrocytes.

Species	Model system	Oxygen tension	Major effect	References
Bovine	Chondrocyte pellet or microcarrier culture Microcarrier medium change: Perfusion/stepwise (stirrer speed: 50-80 rpm)	4, 10.5 and 21%	At each O ₂ tension / bioreactor culture: Consumption, proliferation rate & lactate release on glucose consumption (+/-) (↑) GAG production and chondrocyte – lacunae structures	Malda et al., 2004a
Human	Chondrocyte pellet culture	5 and 19%	5% O ₂ (Phase I): (↑) GAG, collagen type II, HIF-1α. (↓) MMP-1, -13 mRNA and protein 19% O ₂ (Phase II): (↓) GAG production, collagen type II (↑) MMPs, (↑) type II collagen fragments and disorientation of collagen fibrils. 5% O ₂ (Phase II): Additional (↑) GAG, collagen type II, (↓) MMP-13 mRNA and protein.	Strobel et al., 2010
Bovine	Chondrocyte/polyurethane constructs, dynamic compression and surface motion	5 and 21%	5% / 21% O ₂ : (↑) GAG, type II collagen/aggrecan mRNA (↓) type I collagen mRNA and protein Mechanical loading (ML): (↑) collagen type II gene expression No effect on aggrecan mRNA level ML + 5% O ₂ : Stable phenotype (↓) collagen type I mRNA	Wernike et al., 2008
Bovine	Chondrocyte/polylactic acid constructs	5 and 20%	At both O ₂ tensions: Cell proliferation, collagen content (+/-). 5% / 21% O ₂ : GAG synthesis rate and GAG content	Saini & Wick, 2004
Human	Nasal septum chondrocyte, pellet culture/bioreactor	1, 5.25, 21%	1% & 5% Vs 21% O ₂ : (↑) GAG and type II collagen content 1% Vs 5% O ₂ : (↑) type IX collagen 21% Vs 5% & 1% O ₂ : (↓) GAG, DNA, type II and IX collagen content, (↑) type I collagen	Malda et al., 2004b

1.4 Effect of mechanical stimuli on cartilage homeostasis

Mechanical loading is known to maintain the functional integrity of articular cartilage, as well as regulating joint tissue homeostasis. There has been limited progress in the development of long-term, safe and effective therapies for OA disease progression. This is due, in part, to the wide range of experimental models which have been used to elucidate the signalling pathways induced by mechanical stimuli and pro-inflammatory cytokines. Additionally, there is insufficient knowledge on cartilage mechanopathophysiology, such as the manner in which mechanical stimuli influences chondrocyte function and matrix synthesis. As a result, it is difficult to detect key chondroprotective pathways for the design of new and effective treatments for OA.

All tissues of the joint are known to be influenced by mechanical loading via a range of mechanical and chemical factors such as joint injury, joint misalignment / instability, obesity, genetics, age and impaired muscle function. Also, the nature of mechanical stimuli applied to the joint, including its duration and magnitude, affects cartilage matrix turnover. For example, the duration and magnitude of mechanical stimuli influences matrix turnover. Collectively, studies have shown that the application of moderate mechanical stimuli on various experimental models maintained the functional integrity of articular cartilage in addition to low matrix turnover. In contrast, non-physiological mechanical stimuli have resulted in cartilage degradation and an onset in inflammatory signalling cascades. Thus, the identification of the signalling pathways responsible for the mediation of mechanical loading is essential in designing novel biophysical therapies which incorporate both anti-inflammatory agents and defined exercise for OA treatment (Bader, Salter, Chowdhury, 2011).

It is well known that moderate or physiological mechanical loading maintains joint homeostasis and the functional integrity of articular cartilage with a low turnover of matrix constituents. Accumulative evidence also suggests that the duration, nature and magnitude of mechanical loading also influences the turnover of matrix constituents. As a result, a range of approaches have been developed to study the effects of mechanical loading on cartilage signal transduction pathways (or cartilage homeostasis) and OA disease progression. However, each approach is associated with a range of limitations which makes it problematic to determine the exact physiological relevance of the experimental findings. This section will examine the protective role of physiological loading in *in vitro* and animal studies as well as describe the intracellular mechanisms which mediate the effects of mechanical stimuli. Additionally, the possible use of controlled exercise therapy will be discussed in combination with agents for the development of integrated biophysical therapies for OA.

1.4.1 Effect of physiological loading on cartilage homeostasis

Clinical trials

Mechanical stimuli applied at moderate levels are known to maintain cartilage integrity via low matrix turnover (Table 1.2). Individuals that are involved in controlled exercise and activities are less likely to develop OA, as dynamic compression is applied to the joints within a physiological range (Jordan et al., 2003, Fransen, McConnell, Bell, 2002). Indeed, an increase in cartilage thickness, GAG content levels, and joint mobility together with decreased joint pain has been reported in OA patients undergoing strengthening exercises and aerobic activities (Roddy, Zhang, Doherty, 2005, Jansen et al., 2011, Jansen et al., 2010, Manninen et al., 2001).

Table 1.2: Clinical studies showing the effects of exercise regimens on cartilage health.

Subjects	Intervention / loading regime	Major effect	References
45 subjects who underwent partial medial meniscus resection 3–5 years previously	Supervised exercise 3 times weekly for 4 months	(↑) GAG content (↓) pain and joint symptoms	Roos and Dahlberg, 2005
35 subjects without knee OA	Aerobic walking and quadriceps strengthening exercise for 18 months	Normal distribution of proteoglycans, (↓) pain and disability from knee OA	Roddy et al., 2005
11 randomised control trials	Exercise	(↓) pain and disability	Van Baar et al., 1999
805 subjects	Cumulative physical exercise for low (<6862) or high (>8654) hour	(↓) risk in knee OA	Manninen et al., 2001
1279 subjects (+/-) OA, middle aged/elderly, BMI Below/above median	Recreational walking or jogging at low and high levels of activity	High BMI, overweight, middle aged, and elderly persons: no (↑) in risk of OA	Felson et al., 2007

In a seminal MRI-based study involving patients, who had undergone a partial resection of the meniscus, and were subsequently subjected to moderate exercise 3 times per week for 4 months, results indicated an improvement in GAG content as reflected in the values of dGEMRIC (delayed gadolinium enhanced magnetic resonance imaging of cartilage) at baseline and follow-up, with results represented as a change in the T1 relaxation time in the presence of Gd-DTPA (T1[Gd]). Additionally, there was an increase in activity levels in the exercise group compared to that of the control group as indicated in Fig.1.9, suggesting a strong correlation between self-reported change in physical activity level and change in T1(Gd) as expressed by dGEMRIC. Furthermore, such exercises provided protection for cartilage against subsequent degeneration (Roos & Dahlberg, 2005). However, this protective mechanism induced by subjecting patients to therapeutic exercises depends on

individual factors such as the patient's body mass index, age, smoking and previous joint injury (Felson et al., 2007, Perrot et al., 2009). In clinical trials, it has been shown that intense physical activities can be performed by both OA patients and healthy individuals, provided these activities do not result in pain or injury to the joint (Vignon et al., 2006). Recreational exercise was shown to be beneficiary to some patients in terms of improved joint activity and decreased pain. However, a protective mechanism was not induced by recreational exercise nor was the probability of OA occurring increased in healthy middle-aged or elderly subjects (Felson et al., 2007, Messier, 2010, van Baar et al., 1999, Ettinger et al., 1997, Creaby et al., 2010). Nevertheless, the ideal exercise modality including the dosage of agents and duration for integrated biophysical therapy has not been clearly determined due to variable therapeutic loading regimes and diagnostic techniques incorporated into clinical trials.

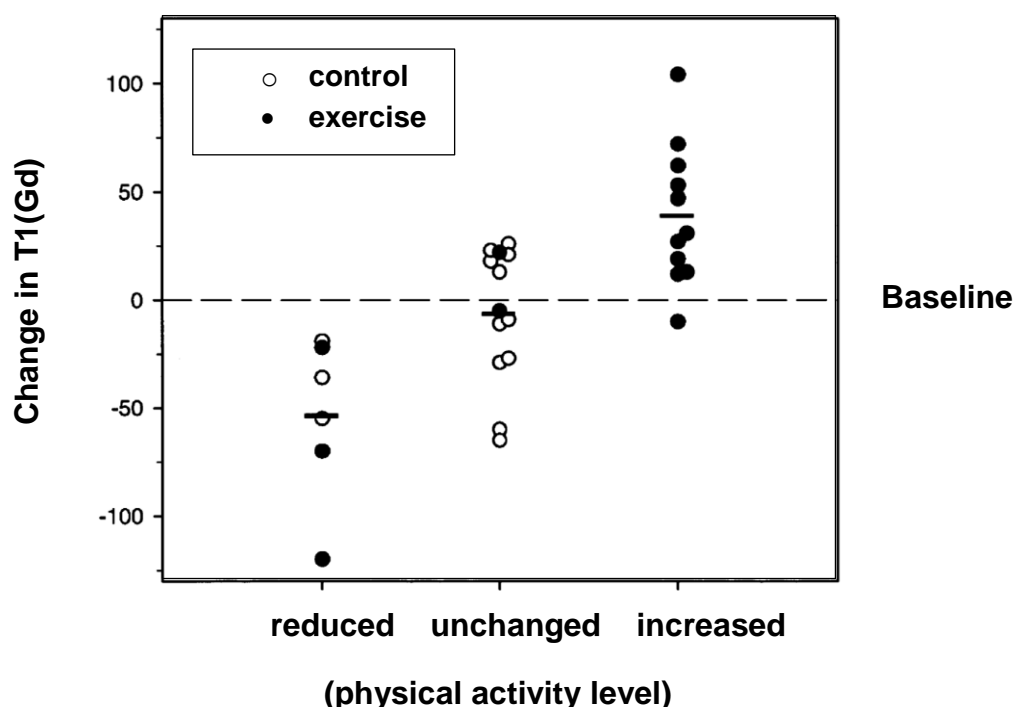


Figure 1.9. Change in the T1 relaxation time in the presence of Gd-DTPA (TA[Gd]). Graph reflecting change in the GAG content of the medial femoral condyle of the menisectomized (study) knee, in both the exercise group and the control group ($n=30$), as a function of self-reported change in physical activity level during the study period. Bars denote the mean T1(Gd) for each of the 3 groups of self-reported change (Roos et al., 2005).

It must be noted that consecutive studies which examined the effect of moderate exercise on cartilage properties demonstrated conflicting results (Roos and Dahlberg, 2005, Fransen et al., 2002). Indeed, recreational exercise reduced pain and joint disability in certain subjects (Table 2). However, in middle-aged and elderly individuals without OA, therapeutic exercise did not increase nor protect against the risk of the incidence of OA (Felson et al., 2007, Messier, 2010, Van Baar et al., 1999, Ettinger et al., 1997, Creaby et al., 2010). Clearly, comparing findings between clinical studies remains a delinquent due to the varying

diagnostic standards and loading regimens incorporated in these studies. Nonetheless, knowledge on the risks and benefits associated with physical activities will provide essential information which will have significant impact in clinical practice.

In vivo studies

The application of mechanical loading within the physiological range has generally been shown to be beneficial in animal models as evident in Table 3. For instance, an increase in GAG content was observed in canine models which were subjected to moderate exercise, especially in younger animals (Buckwalter, 1995, Kiviranta et al., 1988). Similarly, enhanced cartilage thickness and proteoglycan content were demonstrated in hamster models which underwent daily exercise for 6 to 12km/day (Otterness, 1998).

Table 1.3: The effects of physiological joint loading on collagen and proteoglycan content in animal studies.

Beagle dog model	Running exercise: 4 km/day, uphill, 15 weeks	(↑) proteoglycan content and cartilage thickness	Helminen et al., 2000
Hamster model	Running exercise: 6 to 12 km/day	(↑) proteoglycan content	Otterness et al., 1998
Foal model	Conditioning exercise: Increased workload by 30%	(↓) cartilage degeneration index	Van Weeren et al., 2008
Rabbit model	Increased loading following 8 weeks of splinting	(↑) maturation of tissue and increased collagen content	Saamanen et al., 1987
Rabbit model	Running exercise: varied age, 15 months exercise	Improved collagen organisation in young and reversed OA in older animals	Julkunen et al., 2010
OA rat model	Running exercise: 15 km over 28 days	(↓) apoptosis and chondral erosions	Galois et al., 2003

One seminal study involving an OA Wister rat model subjected the animals to moderate exercise at a constant speed of 300mm/s for 30mins over a 28 day period post ACLT. Apoptotic events in the cartilage were assessed by immunostaining of activated caspase 3, whereas the severity of chondral lesions graded using Mankin's scoring (Galois et al., 2003). Mankin's grading score represents a well-established strategy for determining the severity of cartilage damage in humans, by assessing the depth and size of cartilage lesions in the joint. In effect, Mankin's score was directly proportional to the loss of cartilage observed during assessment of the progression of the disease (Rutgers et al., 2010).

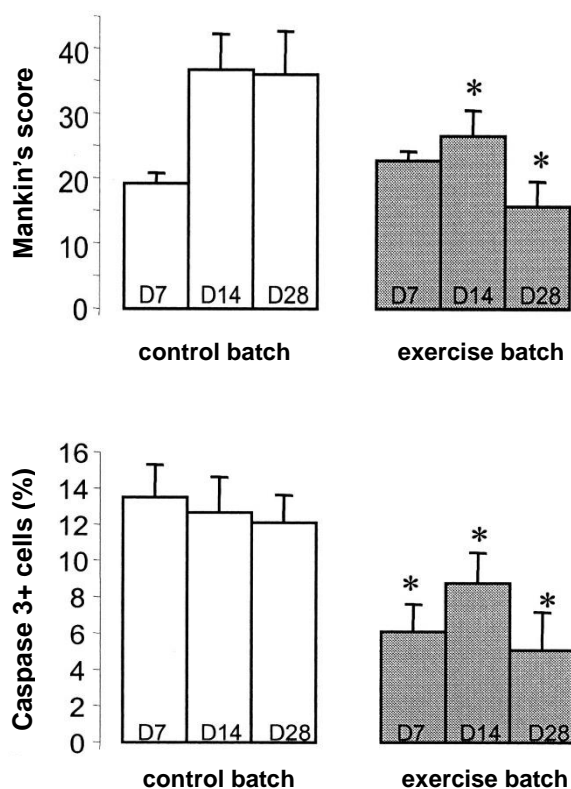


Figure 1.10. Assessment of chondral lesions in ACLT Wister rat models subjected to moderate exercise. Histological grading according to Mankin's score and (B) apoptotic events assessed by immunostaining of activated caspase 3 in the control group (open columns) and exercised rats (grey columns) that had been subjected to ACLT at days 7, 14 and 28, significant beneficial effect of exercise (Galois et al., 2003).

Results indicate a significant decrease in both parameters for the experimental group at days 14 and 28, as indicated in figure 1.10. The authors extended their study (Galois et al., 2004) to include a range of exercise levels as shown in figure 1.11. At day 14, slight and moderate exercises demonstrated a significant decrease in histological lesions when compared to the control ACLT and intense exercise groups. In slight and moderate exercise groups, lesions were further reduced at day 28. Proteoglycan depletion and clefts were mostly pronounced in ACLT rats and intense exercise groups followed by those subjected to slight and moderate exercises respectively (Fig. 1.12, Galois et al., 2004).

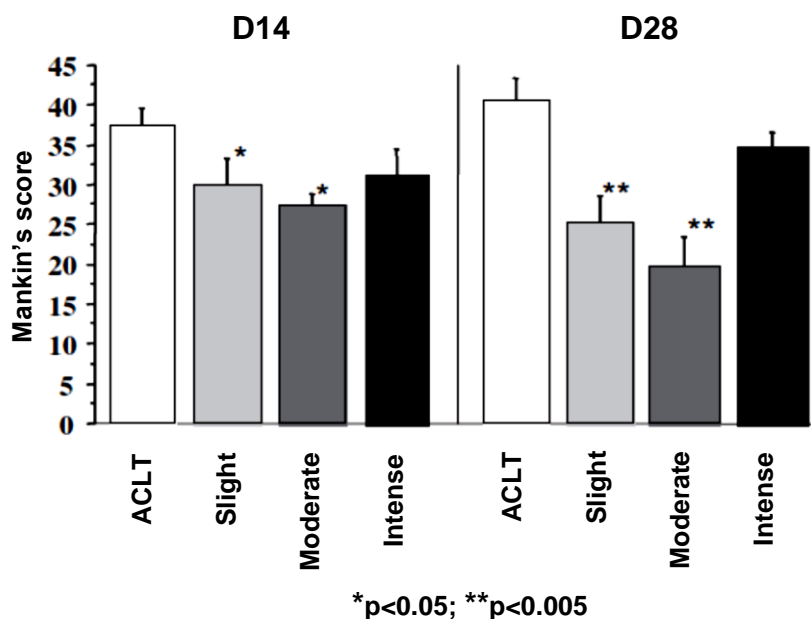


Figure 1.11. Histological lesions in ACLT and exercised rats (A) Histological lesions according to Mankin's score in ACLT rats and those subjected to slight, moderate and intense exercise at days 14 and 28 (Galois et al., 2004).

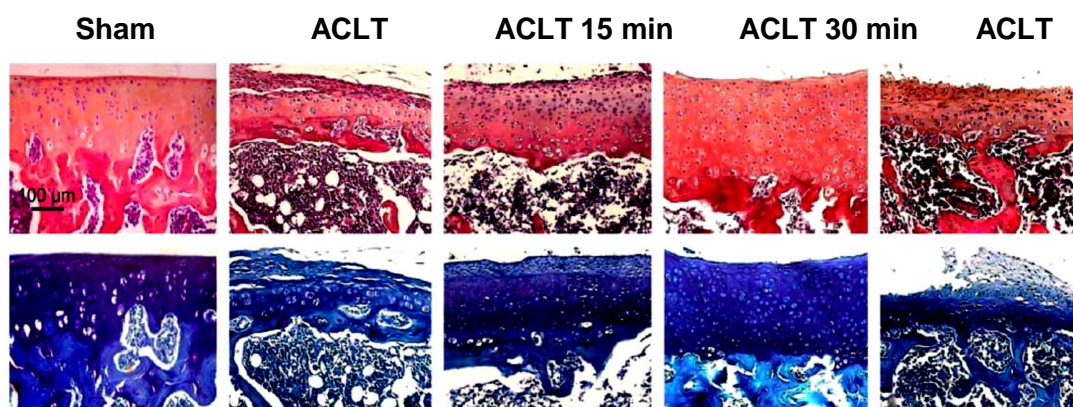


Figure 1.12. Histological sections of articular cartilage from sham-operated joints, ACLT and exercised rats. (Upper figures) Hematoxylin-Eosin (H&E) staining evaluating cartilage surface integrity and (Bottom figures) toluidine blue (TB) staining revealing proteoglycan content in sham-operated joints (arthrotomy without ACLT), ACLT rats and those subjected to slight (ACLT 15min), moderate (ACLT 30min) and intense (ACLT 60min) exercise (Galois et al., 2004).

In other studies, early joint loading strengthened the collagen network, increased the resistance of cartilage against OA and enhanced the maturation of ECM proteins in hamsters (Helminen et al., 2000, Julkunen et al., 2010, Saamanen et al., 1987, Van Weeren et al., 2008). Collectively, these animal studies suggest that the employment of physiological loading regimes improve the load-bearing capacity of articular cartilage, justifying the fact that regular exercise over a lifetime will decrease the risk of incidence of OA during later stages (Galois et al., 2003, Buckwalter, 1995, Kiviranta et al., 1988, Helminen et al., 2000, Julkunen et al., 2010, Saamanen et al., 1987, van Weeren et al., 2008).

In vitro studies

The influence of physiological mechanical loading on *in vitro* studies has long been recognised to enhance anabolic signalling pathways and protective properties (Table 4). Indeed, the application of physiological mechanical stimuli such as hydrostatic pressure, stretching, dynamic compression and fluid-induced shear stress at low frequencies ranging from 0.01 to 1 Hz on monolayer, 3D biomaterial or explant cultures generally exhibited anabolic activities, such as increase in chondrocyte proliferation levels, elevated PG synthesis and enhanced gene expression levels of aggrecan, fibronectin and collagen type II (Guilak et al., 1994, Sah et al., 1989, Kim, Grodzinsky, Plaas, 1996, Bader, Salter, Chowdhury, 2011). As an example, chondrocyte / agarose constructs subjected to 15% compressive strain in either a static or dynamic manner showed that proteoglycan synthesis depended on the rate of frequency incorporated, with maximum proteoglycan synthesis achieved at 1Hz, unlike cell proliferation, quantified by thymidine incorporation, which was upregulated for each of the dynamic frequencies ranging from 0.3 to 3.0Hz (Figure 1.13; Lee and Bader, 1997).

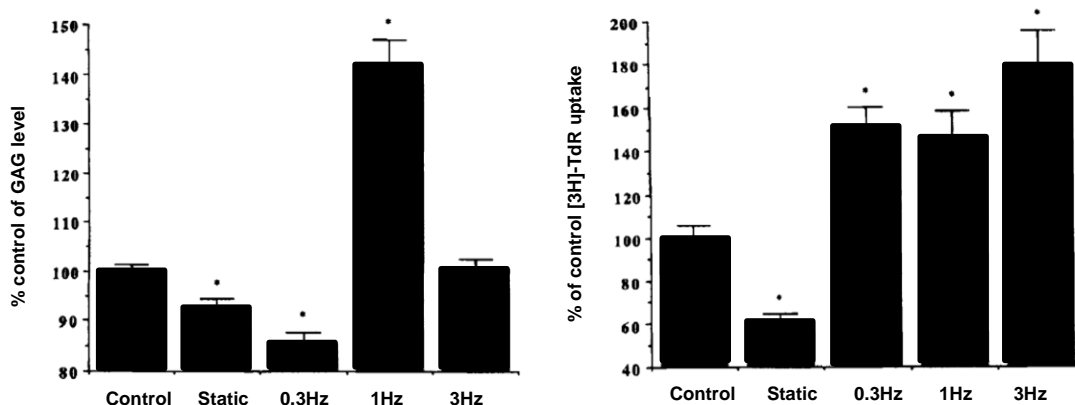


Figure 1.13 GAG synthesis and [3H]-TdR incorporation were measured in mechanically loaded 3D chondrocyte/agarose constructs. (A) GAG synthesis and (B) [3H] thymidine ([3H]-TdR) incorporation by 3D chondrocyte/agarose constructs subjected to 15% gross strain at frequencies ranging from 0.3 to 3Hz for 48 hours. The values have been normalized to unstrained control levels (100%). Each value represents the mean and SEM of at least 16 replicates from at least two separate experiments. Unpaired Student's *t* test results indicate differences from control values as follows: *= $p < 0.05$ (Bader and Lee, 1997).

However, direct comparison of findings from *in vitro* models, such as explant and 3D biomaterial cultures, has proven difficult due to the limitations of these model systems. For example, the use of explant models makes it problematic to exclude the alterations induced by biochemical and mechanical factors which, in turn, influence the intracellular signalling pathways and chondrocyte metabolism. Also, 3D chondrocyte / agarose constructs do not exactly mimic the *in vivo* physiological mechanical loading environment of cartilage (Bader, Salter, Chowdhury, 2011). Furthermore, the incorporation of various loading modalities,

different culture periods and the time points at which mechanical stimuli is applied to the culture system makes it inevitably difficult to compare between *in vitro* studies (Sauerland, Raiss, Steinmeyer, 2003, Chowdhury et al., 2003, Ackermann and Steinmeyer, 2005, Steinmeyer et al., 1997). Therefore, evidence justifying the importance of determining the optimum mechanical loading properties for the induction of anabolic signalling cascades is yet to be achieved.

Table 1.4. The effects of physiological loading on cartilage metabolism *in vitro*.

Species	Model system	Loading regime	Major effect	References
Human	Monolayer	Hydrostatic pressure: 1,5 and 10MPa at 1 Hz for durations of 4hr per day for 4 days	(↑) aggrecan and type II collagen gene expression	Ikenoue et al., 2003
Human	Monolayer	Cyclic pressure-induced strain: 0.3Hz, 6 hours	(↑) aggrecan gene expression	Millward-Sadler et al., 2000
Bovine	Monolayer	Hydrostatic pressure: 10MPa, 1Hz, 4 days	(↑) proteoglycan mRNA and type II collagen mRNA syntheses	Smith et al., 2000
Bovine	Explants	Cyclic compression: 1MPa, 0.5 Hz, 3 days	(↑) proteoglycan synthesis	Steinmeyer et al., 1999
Bovine	Explants	Dynamic compression: 1MPa, repeated 2 and 4 sec, 1.5 hr Dynamic compression: 2% strain, 0.1Hz for 2 days with IGF-I treatment Dynamic compression: 1-5% strain, 1Hz for 8hr	(↑) proteoglycan synthesis and [³ H] proline incorporation	Parkkinen et al., 1992, Bonassar et al., 2001, Sah et al., 1989
Bovine	Agarose	Dynamic compression: 3% strain at 0.01 to 1Hz, 43 days	(↑) proteoglycan and collagen synthesis	Buschmann et al., 1995
Bovine	Agarose	Dynamic compression: 10% strain at 1Hz, 3 x 1hr on, 1hr off, 5 days/week for 21 days	(↑) equilibrium aggregate modulus, sGAG and collagen synthesis	Mauck et al., 2000
Bovine	Agarose	Dynamic compression: 15% strain, 0.3, 1 and 3Hz, 48 hour	(↑) cell proliferation and proteoglycan synthesis, (↓) nitrite release	Lee and Bader, 1997; Lee et al., 1998
Bovine	Agarose: bi-layered structure of 3% (wt/vol; bottom) and 2% (wt/vol, top).	Dynamic compression: 10% strain at 1Hz for 3hr/day, 5 days/week for 4 weeks	Day 28: (↑) GAG and type II collagen in both 2% (wt/vol) and 3% (wt/vol) layers. 2% Vs 3% (wt/vol): (↑) GAG and type II collagen in 3% (wt/vol) layer compared to 2% (wt/vol).	Ng et al., 2006
Mouse	Agarose: 2% w/v type VII constructs	Sinusoidal compression: 10% strain, 1Hz for 1hr on, 1hr off, 3 times/day for 7 to 28 days at intervals of 7 days.	(↑) type II collagen mRNA expression levels at days 14, 21 and 28 with maximum increase at day 7.	Chokalingam et al., 2009
Bovine	Agarose: 2% w/v constructs	Sinusoidal shear strain: 0.5% strain	(↑) GAG concentration after 28 days	Miyata et al., 2008

		superimposed on 20% static compression between 0.01 and 0.5Hz		
Canine	Agarose: 2% w/v type VII constructs	Sliding contact loading at 5% and 1Hz, superimposed on: *10% unconfined compressive strain or *10% tare strain for 3hr/day, 5 days/week	No significant changes in GAG and collagen content between all the control groups	Bian et al., 2010
Bovine	Self-assembling peptide agarose hydrogels	Sinusoidal unconfined compression: 2.5% strain superimposed on 5% static strain offset strain at 1Hz; 30min to 1 hour cycles of compression followed by FS for 0.5, 1, 3, 5 or 7hr for 22 days.	Day 5 – 14: (↓) [³ H] proline incorporation in strained samples compared to FS samples Day 10 – 11: (↑) GAG content in strained samples compared to FS samples Day 16: Further (↑) GAG content in strained samples compared to FS samples	Kisiday et al., 2004
Bovine	PGA	Hydrostatic pressure: 3.5MPa, 5s on, 15s off for 20min every 4hr	(↑) proteoglycan concentration No significant increase in type II collagen	Carver et al., 1999
Bovine	Non-woven PGA scaffolds	Static compression: 10, 30 and 50% strain for 24hr Dynamic compression: saw-tooth waveform, 5 and 50% strain superimposed to 10% , 0.001 or 0.1Hz for 24hr	static compression at 10 and 30% strain: no effect on GAG synthesis static compression at 50% strain: (↓) GAG synthesis dynamic compression at both 0.001Hz and 0.1Hz: (↑) GAG synthesis	Davisson et al., 2002
Human	PEGT/PBT scaffolds	Sinusoidal compression: 5% strain, 0.1Hz superimposed on 5% strain offset, 6 cycles of 2hr loading for 3 – 17 days	(↑) GAG content after 17 days (↓) type I collagen mRNA levels after 17 days (↑) type II collagen mRNA expression in 17 days	Demartean et al., 2003
Bovine	PEG hydrogels	Sinusoidal unconfined compression: 5 – 20% strain, 0.3Hz: *25,920 cycles/day loading for 1 week (IL) or *6,480 cycles /day (1hr on, 1hr off, CL).	IL loading: (↑) AGC and type II collagen expression levels after 1 week. (↓) type II collagen expression during 1 week FS, post IL loading CL loading: (↑) AGC expression levels after 1 week.	Nicodemus and Bryant, 2010

			No changes in type II collagen expression.	
Bovine	PEG, PEG-Fibrinogen (PF) and PGE-Albumin (PA) functionalized scaffolds	Dynamic compression: 15% strain, 1 Hz for 24hr or 28 days	(↑) GAG production and type II collagen in all three scaffold types in the following order: PA > PEG > PF	Appelman et al., 2011
Rabbit	Gelatin/chitosan scaffolds	Cyclic compression: 40% strain at 0.1Hz for: *6hr/day for 3 weeks (long term compression) or *3 or 9hr (short term compression).	3hr short term compression: (↑) GAG mRNA expression levels, type I and II collagen. 9hr short term compression: (↓) Type II collagen mRNA expression levels.	Wang et al., 2009
Porcine	Hydroxyapatite scaffolds	Dynamic compression: 10 and 20% strain, 1Hz, 3000 cycles/day loading with 30 min of rest, 6hr/day for 14 days	No significant changes in GAG/DNA ratio and collagen/DNA ratio between strained samples and controls.	Hoeng et al., 2011
Bovine	Porous calcium phosphate (CPP) constructs	Shear strain: 2, 6 and 12% strain superimposed on 5% unconfined static compression at 1Hz, 400 or 2000 cycles in 48hr. Static compression at 5% strain offset = control	(↑) proteoglycans and collagen in shear strained samples compared to controls.	Waldman et al., 2003a
Bovine	Porous calcium phosphate (CPP) constructs	*2% sinusoidal shear strain or *5% sinusoidal compression of: 1Hz, 400 cycles/day for 4 weeks of either:	(↑) proteoglycan and collagen content in the following order: Shear > compression > static culture	Waldman et al., 2003b
Bovine	Porous calcium phosphate constructs	Cyclic compressive loading: 9.81mN for 15, 30 and 60min for a period of 1, 8 and 15 days at 1Hz	Day 1: (↑) proteoglycan and collagen content Day 15: (↓) proteoglycan content	Waldman et al., 2004
Bovine	Porous PU scaffolds	Shear strain: 5 – 15% strain superimposed on 5% static compressive strain at 1Hz	Day 21: (↑) GAG content Day 35: (↑) GAG and type II collagen	Salzmann et al., 2009

Taken together, the *in vitro* studies demonstrate conclusively that the application of loading in 2D and 3D models is beneficial in the enhancement of anabolic signalling cascades and biosynthesis of anabolic proteins.

1.5 Characteristics of diseased articular cartilage

Osteoarthritis (OA) is a progressive, degenerative joint disease characterized by deteriorating cartilage. The disease is associated with ageing or individuals who are sedentary and/or obese. In the UK, OA affects 15% of the population and costs the NHS £30 billion each year (Oxford Economics, 2008). OA prevalence increases with age, from minimal values for individuals aged between 25 and 34 years to 20-40% occurrence in those aged above 70 years (Guccione, 1997, Felson et al., 1987, Hernborg and Nilsson, 1973, Lawrence et al., 1966, Bergstrom et al., 1986). The disease is more prevalent in males up to the ages of 45 years, although the reverse is evident after this age due to the inhibitory effect of estrogen on MMP synthesis in males (Claassen et al., 2010). OA can be successfully managed by joint replacement in the elderly population, although this treatment will inevitably result in limited functionality and overall physical activity.

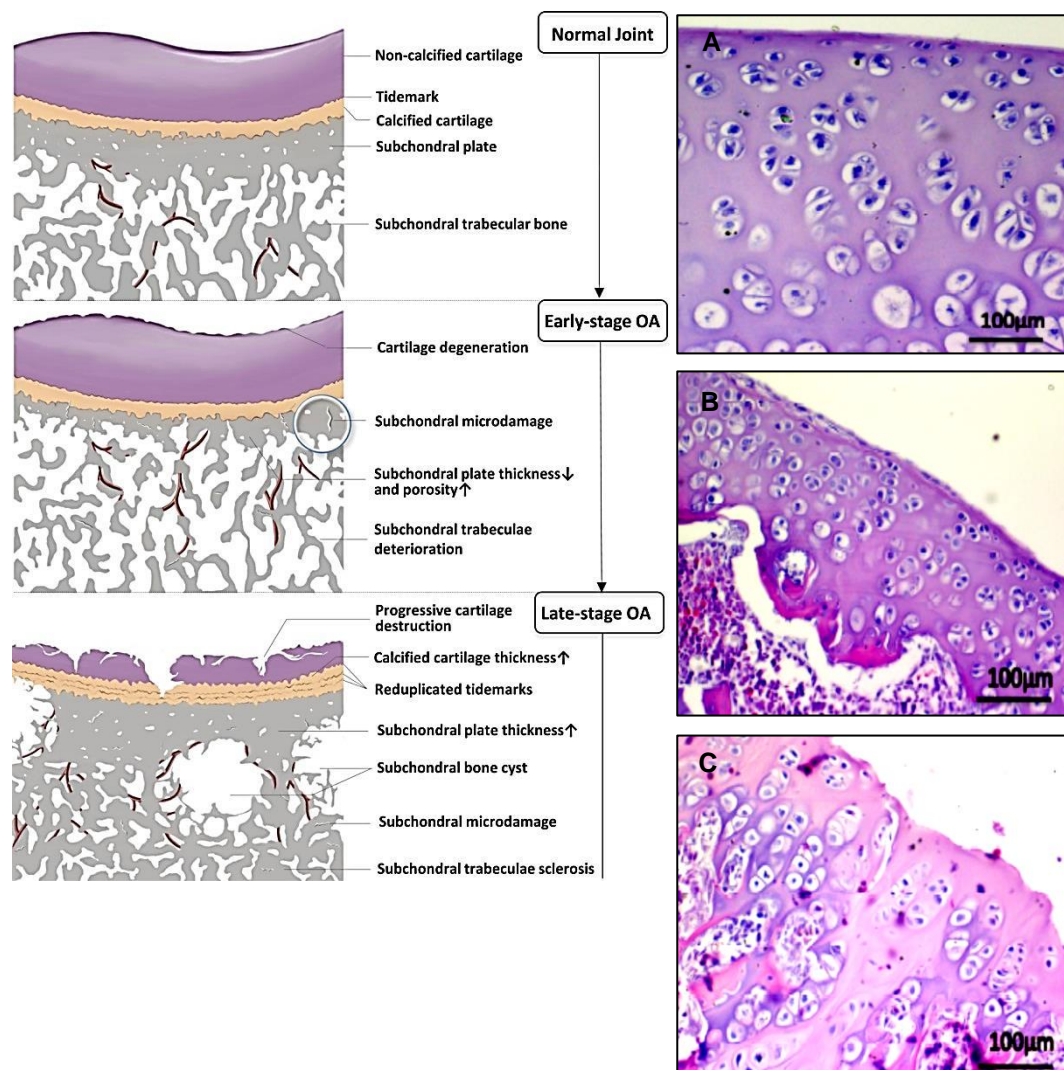


Figure 1.14. Structural changes in OA disease progression (Giunta et al., 2015).

1.5.1 Changes at the tissue level

OA is a multifactorial disease, associated with obesity, age, previous joint injury, misalignment, muscle weakness and genetic predisposition (Denisov et al., 2010; Roos & Dahlberg, 2005; Troyer, 1982). The disease is characterised by progressive loss of the load bearing surfaces and the formation of new osteoarticular tissue at the edges of the joint and pain (Moskowitz, 1992; Goldring, 2000a; Aigner and Stove, 2003; Goldring and Goldring, 2007). The formation of fibrillations at the superficial layer is the initial hallmark of cartilage damage which extends to the middle and deep zones of the tissue. An increase in proliferation of chondrocytes is observed adjacent to areas undergoing fibrillation, resulting in the formation of cell clusters in the diseased tissue (Mankin and Lippiello, 1971). This effect may be due to greater accessibility to proliferative factors present in the synovial fluid resulting from the loss of integrity of the collagen network (Lee et al., 1993). Proteoglycans have also been shown to swell, due to an increase in the water content of cartilage, leading to reduced stiffness and enhanced permeability of the tissue. Indeed, as the disease progresses there is an overall reduction in both cell number and extracellular matrix content (Hulth et al., 1972). Towards the final stages of OA, full thickness loss of cartilage is observed (Fig. 1.14), especially in the focal load bearing regions. Such changes can be radiologically detected in individuals, as the joint space narrows, particularly in those aged 65 years with an increase in prevalence of up to 80% in individuals aged over 75 years (Arden and Nevitt, 2006). Ongoing alterations in the subchondral bone during the progression of the disease include the formation of edema and osteosclerosis (Aigner et al., 1995; Day et al., 2004). Furthermore, cysts are formed in the synovial fluid from debris generated during the breakdown of cartilage and the underlying bone which result in the onset of an inflammatory response of the synovium (Goldenberger et al., 1982; Martel-Pelletier et al., 1999). Cells may sense alterations in charge density, stiffness and osmolarity due to ECM damage and, as a result, release mediators which enhance matrix synthesis, induce cell proliferation and degradation in an attempt to contribute to tissue repair (Dingle et al., 1979).

It is well recognised that the precise cause of OA is complex in nature and involves multiple mechanical, biological and biochemical factors (Byers et al., 1977). An increase in thickness of the subchondral bone and a lack of tissue lubrication were first thought to be the principal causes of OA. Such features led to enhanced breakdown of the articular surface on the application of high mechanical loads and friction at the joint surface (Simon et al., 1972; Walker et al., 1969). Other studies showed reduced or no expression of lubricin correlated with OA pathology, highlighting the significance of protecting the articulating surfaces against repetitive and high intensity mechanical loading (Young et al., 2006; Rhee et al., 2005; Teeple et al., 2008). In addition, alterations in fibrillogenesis and degeneration of the collagen network leads to OA disease progression (Pelletier et al., 1983; Maroudas, 1976).

However, recent studies have started to reveal the molecular processes which may be responsible for structural and biochemical modifications during OA. Indeed, degradative enzymes and pro-inflammatory cytokines induce an imbalance in cartilage homeostasis, resulting in a continuous degeneration of ECM molecules. Consequently, a loss in mechanical properties of cartilage, such as stiffness is observed during the application of physiological loading regimes. Although the signalling cascades during the early stages of OA have not been revealed, identification of these processes may lead to the design of novel diagnostic tools and pharmacological therapies that intervene at an early stage of the disease, before the initiation of an imbalance of cartilage homeostasis.

1.5.2 Modulation of chondrocyte phenotype during OA

In an attempt to evoke self-repair mechanisms OA chondrocytes increase production of collagen (type II, VI, IX and XI) and aggrecan (Lorenz et al., 2005). However, such unregulated activities of chondrocytes result in the formation of fibrillations and the disorganisation of the ECM (Pritzker et al., 2006). In certain situations, this may lead to an induction of type X collagen, collagenase activity and alkaline phosphatase, similar to cells present in the hypertrophic region of the growth plate (Von der et al., 1992). Type X collagen and MMP-13 are direct transcriptional targets of HIF-2 α , which appears in OA cartilage or activated by pro-inflammatory stimuli or even in the presence of high oxygen tension (Yang et al., 2010; Saito et al., 2010). However, hypertrophic markers are not considered as reliable markers for the detection of cartilage degeneration (Brew et al., 2010).

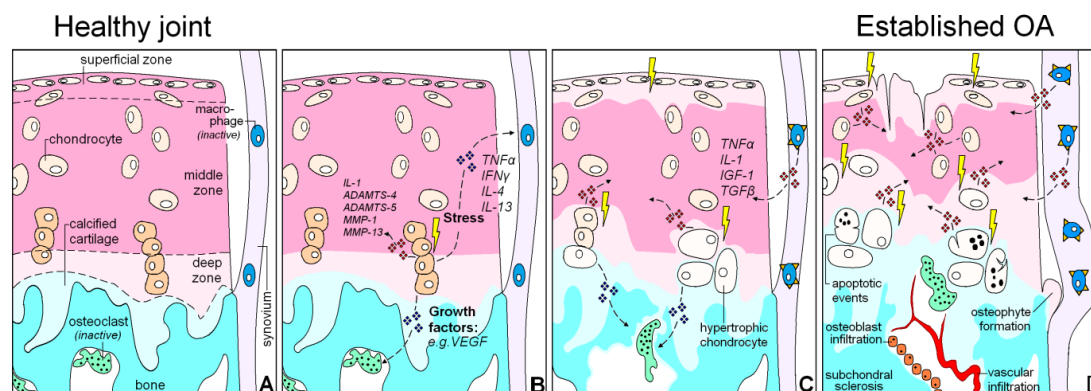


Figure 1.15. Hypothetical model that shows the changes of cartilage, subchondral bone, and synovial macrophages during OA development (Siebelt et al., 2014).

The expression of SOX-9, a molecule responsible for the expression of aggrecan and type II collagen, is rapidly lost in chondrocytes when cultured in monolayer. This may be a modulation on the phenotype of chondrocytes due to a change in extracellular environment, evident in monolayer or the presence of growth factors, rather than a phase in differentiation. However transducing OA chondrocytes with SOX-9 induces the recommencement of ECM production (Tew et al., 2005). Nevertheless, even *in vivo* chondrocytes with restored

phenotypic expressions are unable to sustain the growth and remodelling of cartilage which already experienced an interrupted autocrine signalling cascade (Dell'Accio et al., 2011; De Bari et al., 2004). Collectively, these findings suggest that mechanical signals, matrix degrading enzymes and pro-inflammatory cytokines have a substantial impact on the modulation of chondrocyte phenotype which, in turn, induces an imbalance in cartilage homeostasis.

1.5.3 ECM turnover during OA progression

During cartilage homeostasis, MMPs and ADAMTSs (a disintegrin and metalloproteinase with thrombospondin motif) play an essential role in maintaining the balance between the synthesis and breakdown of extracellular matrix components in an attempt at chondrocytes to induce self-repair. During OA progression, there is an observed upregulation in aggrecan and type II collagen. However, there is an overall breakdown of matrix proteins in response to enhanced MMP activity (Lorenzo et al., 2004; Hermansson et al., 2004). Additionally, the increased expression of COL2A1 during the late stages of the disease may prove to be ineffective due to the inability of the impaired cartilage to reproduce the same collagen organisation achieved during initial cartilage development.

Multiple studies have demonstrated increased levels of MMPs in the OA joint. Indeed, an upregulation of collagenases including MMP-1, 8 and 13 mRNAs was found in the superficial layer of human OA cartilage. Similarly, gelatinases including MMP-2 and 9 were upregulated in the same zone of the tissue. In the middle and deep zones of human OA cartilage, enhanced MMP-3 (stromelysin) expression was observed (Tetlow et al., 2001; Freemont et al., 1997). Furthermore, increased levels of MMP-3 were demonstrated in OA synovial fluid (Lohmander et al., 1993). NITIGE³⁷³ and VDIPEN³⁴¹ aggrecan fragments derived from ADAMTS and MMPs, respectively, were present in OA cartilage (Lark et al., 1997). While both groups of proteases play an essential role in cleaving aggrecan during the early stage of the disease process, previous studies in cartilage explants demonstrated a further increase in MMP activity during late stage OA when compared to ADAMTS activity (Little et al., 2002). Additionally, synovial fluid obtained from OA joints demonstrated enhanced levels of aggrecan fragments during the initial stages of OA, hence suggesting the involvement of aggrecanase activity (Sandy et al., 1991).

Initially, ADAMTS-5 was established as the only key aggrecanase in both OA and inflammatory models (Glasson et al., 2005; Stanton et al., 2005). Indeed, the presence of ADAMTS-5 was revealed using immunohistochemistry in canine cartilage following anterior cruciate ligament (ACL) transection. Similarly, ADAMTS-5 was found in cartilage from the femoral head of OA patients when compared to healthy controls (Roach et al., 2005; Boileau et al., 2007). However, it was shown that knocking down ADAMTS-4 and 5 by RNA

interference technology reversed cartilage breakdown implicating the involvement of aggrecanases in OA (Song et al., 2007).

However, the nature of catabolic signalling cascades during the early stages of the disease process are complex and the subject of much research. For example, the absence of syndecan-4 in transgenic mice demonstrated protection from proteoglycan loss, due to decreased ADAMTS-5 activity. As syndecan-4 is known to be associated with the phenotype of hypertrophic chondrocytes, changes in the cell phenotype may result in an accumulation of aggrecanases, consequently leading to early proteoglycan loss (Echtermeyer et al., 2009; Bertrand et al., 2010). Nevertheless, the primary catabolic mediators that lead to cartilage breakdown during OA pathogenesis are pro-inflammatory cytokines, especially tumour necrosis factor alpha (TNF α) and interleukin-1 β (IL-1 β), which are well known to modulate chondrocyte phenotype and activate catabolic signalling cascades, as indicated in the schematic in figure 1.16 (Fernandes et al., 2002, Fraser et al., 2003, Goldring and Berenbaum, 2004, Kobayashi et al., 2005).

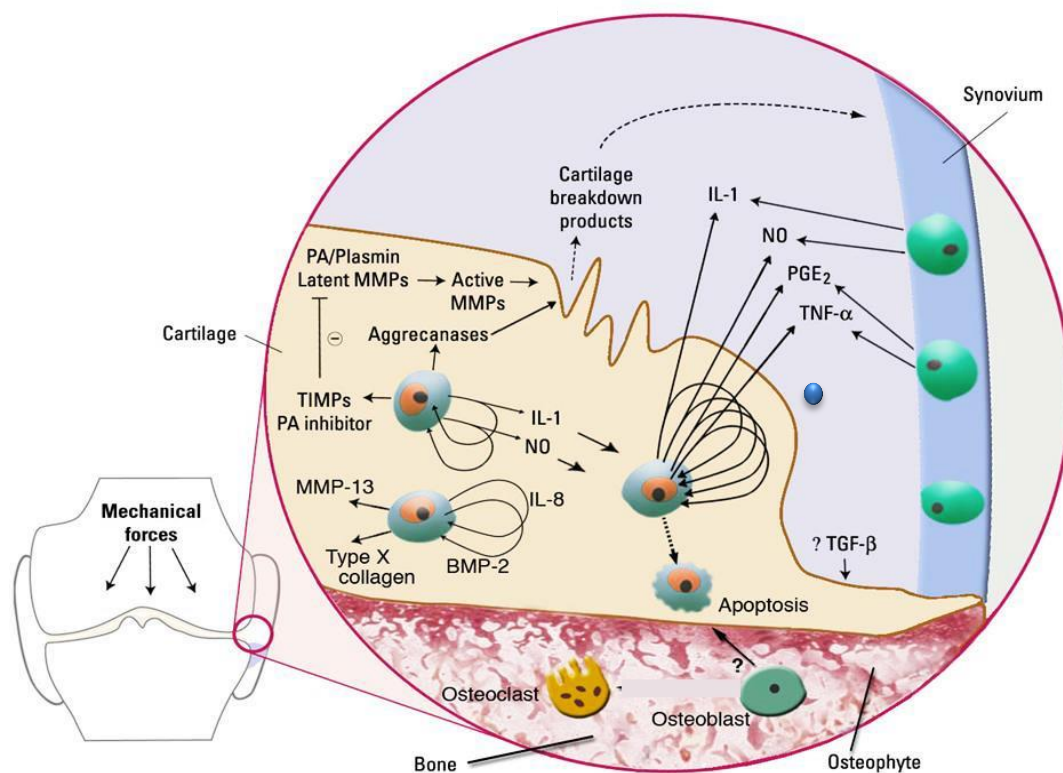


Figure 1.16. Schematic representation of key pathological events and some of the potential targets considered for disease modification in osteoarthritis.

1.6 Pro-inflammatory cytokines

Although OA has been regarded as a non-inflammatory disease due to the absence of infiltration of active leukocytes into the joint at the early stages of the disease, there is compelling evidence that cartilage degradation during OA is a result of an upregulation in inflammation induced by chondrocytes (Goldring, 2000b, Pelletier et al., 2001b, Attur et al., 2002). A large number of clinical and animal studies have demonstrated increased levels of pro-inflammatory cytokines and enhanced local inflammation in OA joints, respectively (Westacott and Sharif, 1996, Fernandes et al., 2002, Goldring, 2000a, Rai et al., 2008). The expression and production of matrix degrading proteases have been shown to be induced by elevated levels of pro-inflammatory cytokines in chondrocyte *in vitro* studies, demonstrating the fundamental role of these cytokines (Shlopov et al., 2000, Fernandes et al., 2002). Indeed, synovial fluid from dogs subjected to anterior cruciate ligament transection (ACLT) demonstrated increased levels of TNF α and IL-6, both of which are essential cytokines in OA disease progression (Venn et al., 1993). Similarly, mongrel dogs which underwent cranial cruciate ligament transection showed elevated levels of MMP-3, TNF α and its receptors (Kammermann et al., 1996).

Previous studies have demonstrated that during OA disease progression, elevated levels of cytokines were initially detected in the synovial membrane, followed by the diffusion of these cytokines through the synovial fluid into articular cartilage (Sakkas et al., 1998, Martel-Pelletier et al., 1999). These cytokines and their receptors including IL-1, TNF α , IL-6, IL-1 receptor type I and IL-1 β converting enzyme were also observed to be expressed by chondrocytes (Moos et al., 1999, Guerne et al., 1990). Additionally, chondrocytes stimulated by diffused cytokines were shown to upregulate MMP expression, prostaglandin E₂ (PGE₂) and nitric oxide (NO) release (Hedborn and Hauselmann, 2002). It is well known that NO and PGE₂ have the ability to influence chondrocyte homeostasis. The combination of these catabolic mediators together with the suppression of ECM synthesis with increased levels of cytokines, while promoting cartilage degradation, suggests that OA progression is regulated by pro-inflammatory cytokines, even though the disease is primarily believed to be initiated by biomechanical factors (Pelletier et al., 2001, Attur et al., 2002).

IL-1 β , TNF α , IL-6 and IL-17 are the most relevant cytokines in OA pathogenesis. Increased sensitivity of chondrocytes to IL-1 β and TNF α may be due to the elevated density of IL-1 β receptors (IL-1Rs) (Martel-Pelletier et al., 1999) and TNF α receptors (TNF-R1 or TNF-R55) on these cells during the disease progression (Martel-Pelletier et al., 1999). These findings consequently formed the incentive for the incorporation of inhibitors of IL-1 β and TNF α as potential therapeutics for OA (Pelletier et al., 1993, Van den Berg, 1999), especially since similar inhibitors were employed for the successful treatment of rheumatoid arthritis (Weinblatt et al., 2003, Fleischmann et al., 2003), a condition characterised by the elevation

of both IL-1 β and TNF α . For example, Martel-Pelletier incorporated the use of IL-1R antagonist (IL-1Ra) for the suppression of MMP expression induced by exogenous IL-1 in chondrocytes, which resulted in a marginal reduction of endogenous IL-1Ra in OA chondrocytes (Martel-Pelletier et al., 1999).

1.6.1 The interleukins

In OA joints the presence of both pro-inflammatory cytokines (IL-1, IL-11 and IL-17) and regulatory cytokines (IL-6 and IL-8) have been detected, with IL-1, IL-6 and IL-17 being the most essential interleukins in OA pathogenesis (Lotz, 2001, Martel-Pelletier et al., 1999).

IL-1 was initially identified only in OA synovium (Towle et al., 1997, Martel-Pelletier et al., 1999). However, over the years, its importance was further validated through studies demonstrating elevated levels of IL-1 α and IL-1 β in synovial fluid from OA patients (Westacott and Sharif, 1996). Both cytokines have also been identified at the articular surface of OA cartilage from immunohistochemical studies, with increased levels of IL-1 β particularly identified in the ECM surrounding OA chondrocytes found in the superficial layer. Additionally, maximum levels of IL-1 were found in OA cartilage explants at early stages of the disease (Pelletier and Martel-Pelletier, 1989). Similarly, significant levels of IL-1 β have been observed in the superficial layer of OA cartilage specimens subjected to immunostaining, unlike age-matched non-arthritic full thickness cartilage specimens which exhibited no traces of IL-1 β (Tetlow et al., 2001).

IL-1 is synthesized as a 31kDa inactive precursor, which is proteolytically converted into its 17kDa bioactive form by the IL-1 β -converting enzyme (ICE/caspase-1, Martel-Pelletier, et al., 1999). In healthy synovial fluid, Westacott and Sharif found only minimum levels of IL-1, especially in its active form (Westacott and Sharif, 1996). In contrast, increased levels of IL-1 were found in the synovial fluid of OA patients. Interestingly, no presence of the cytokine was detected in OA plasma from patients of the same study, suggesting that IL-1 only acts locally; thereby changing cartilage metabolism in OA affected joints (Holt et al., 1992). In a separate study, the inhibition of type II collagen synthesis was observed in chondrocyte monolayer cultures treated with IL-1 (Chandrasekhar et al., 1990). It has been well established that low concentrations of IL-1 also induce the expression of ADAMTS and MMPs (Tetlow et al., 2001). Indeed, proteoglycan levels were shown to decrease following treatment of cartilage explants with IL-1 (Saklatvala, 1987). Additionally, genes associated with the modulation of OA chondrocyte phenotype, such as COL2A1 have also been shown to be suppressed by IL-1 β (Goldring and Goldring, 2004).

1.6.2 TNF α

Several studies have implicated TNF α in OA pathogenesis and progression (Fernandes et al., 2002). TNF α is synthesized as a membrane bound precursor which is then proteolytically cleaved into its bioactive form by the TNF α converting enzyme (TACE), shown to be highly expressed in OA cartilage, together with TNF α p55 receptors (Gearing et al., 1994, Attur et al. 2002, Martel-Pelletier et al., 1999). *In vitro*, however, the effects of TNF α on chondrocytes are amplified at concentrations produced by OA synovium. This was demonstrated by an increase in the level of TNF receptors observed on normal chondrocytes stimulated with either OA synovial fluid or culture supernatant from OA synoviocytes (Webb et al., 1997, Westacott et al., 2000). Such findings resulted in the suggestion of development of therapeutic strategies targeting the suppression of TNF α from binding to its receptors or the inhibition of TNF α activation by TACE for the treatment of OA. The activation of p55 receptors by TNF α was shown to increase synthesis of NO, PGE₂, MMPs and cytokines such as IL-6, IL-8 that degrade collagen type II, IX and XI and inhibit matrix synthesis in a concentration-dependent manner (Lefebvre et al., 1990, Reginato et al., 1993, Campbell et al., 1990, LeGrand et al., 2001, Alaaeddine et al., 1999, Gearing et al., 1994, Attur et al. 2002, Martel-Pelletier et al., 1999). Collectively, these studies demonstrate the importance of TNF α in cartilage degradation, a feature which is inevitable in OA disease progression (Malemud, 1999, Petterson et al., 2002, Islam et al., 2002, Greenwel et al., 2000).

On binding of the bioactive form of TNF α to TNFR1, the structure of the receptor is altered such that the death domain (DD) is activated. This then enables the adaptor protein (TNF receptor type 1 – associated death domain; TRADD) to bind to the DD, subsequently activating a series of phosphorylation events, which are mediated by mitogen-activated protein kinases (MAPK) subtypes such as c-Jun-N-terminal (JNK) and p38 MAPK (Garrington and Johnson, 1999). Initially, MAPK kinase kinases (MAPKKK) is activated and undergoes phosphorylation, after which it activates MAPKK and then MAPK. Translocation of MAPKK and MAPK into the nucleus then occurs, where they regulate the phosphorylation of transcription factors such as activating protein-1 (AP-1), involved in the activation of MMP-13 (Lim and Kim, 2011). Studies have demonstrated that IL-1 β is also involved in the phosphorylation of AP-1 through p38 MAPK and JNK activation, leading to the trans-activation of MMP promoters (Iwamoto et al., 1990, Ahmed et al., 2003, Tower et al., 2003, Muddasani et al., 2007, Im et al., 2007, Sampieri et al., 2008, Lim and Kim, 2011).

Another transcription factor which is known to be activated by TNF α as well as IL-1 β is nuclear factor kappa B (NF- κ B, Yasuda, 2011). Upon activation of this pathway, the inactive NF- κ B dimers which were previously bound to I κ B molecules in the cytoplasm then become free to translocate into the nucleus of the cell, following phosphorylation and degradation of the I κ B molecules by I κ B kinases (IKK, Oeckinghaus and Ghosh, 2009, Niederberger and

Geisslinger, 2008). Consequently, the transcription of an array of target genes is activated by the translocated NF- κ B molecules, inhibiting the anabolic activities of chondrocytes and inducing the production of several matrix degrading enzymes (Ge et al., 2011, Liu-Bryan and Terkeltaub, 2010). As a result, the overall degradation of articular cartilage occurs. Additionally, NF- κ B molecules have been shown to upregulate the expression of other cytokines including IL-1 β , TNF α , IL-6 and IL-8 (Saklatvala et al., 1993, Saklatvala, 2007), consequently leading to the formation of a positive feedback loop which results in the sustained activation of NF- κ B (Kapoor et al., 2011). Several *in vitro* studies have demonstrated that TNF α -induced inflammatory effects which are mediated by MAPK and NF- κ B molecules have been shown to increase proteoglycan depletion, the expression of catabolic mediators including MMPs, NO, iNOS, COX-2 and PGE₂ and apoptosis in human, rabbit, canine or bovine chondrocytes cultured in monolayer, explant or 3D alginate models (Sondergaard et al., 2010, Carames et al., 2008, Zwerina et al., 2006, Ulivi et al., 2008; Marcu et al., 2010, Little et al., 1999, Sabatini et al., 2000, Gilbert et al., 2002, Goodstone and Hardingham, 2002, Kuroki et al., 2005, Sabatini et al., 2001, Schuerwegh et al., 2003, Kobayashi et al., 2005, Lefebvre et al., 1990, Reginato et al., 1993, Campbell et al., 1990). Furthermore, sustained activation of NF- κ B molecules from the positive feedback loop results in the induction of other regulatory transcription factors such as HIF-2 α , which leads to the production of MMP-13 and ADAMTS-5, as mentioned earlier under section 1.5.2. These *in vitro* studies demonstrating the pathophysiological effects of TNF α in cartilage correlate with previous animal studies which showed that selective inhibition of iNOS, reduced the symptoms of inflammation and biomechanical abnormalities in osteoarthritic joints (Pelletier et al., 1999, Pelletier et al., 1996). The importance of TNF α -induced catabolic effects is also evident in clinical studies, which demonstrated enhanced TNF α levels in OA joints and synovial fluids obtained following anterior cruciate ligament rupture (Cameron et al., 1994, Irie et al., 2003).

1.6.3 Cytokines activate protein kinase signalling

Advances in our understanding of the signal transduction pathways associated with cytokines has created a platform upon which these signalling cascades can be identified as novel potential targets for the development of OA therapies. Indeed, the response of chondrocytes to pro-inflammatory cytokines is regulated by signal transduction pathways. For example, an upregulation in iNOS and MMP expression together with an augmented increase in cytokine production was observed in chondrocytes stimulated with IL-1 and TNF α (Malemud, Islam and Haqqi, 2003, Ridley et al., 1997). Human chondrocyte monolayer cultures stimulated with IL-1 and TNF α demonstrated the activation of mitogen-activated protein kinases (MAPKs) and their subtypes: p38 kinases and c-Jun N-terminal kinase (JNK)-1 and JNK-2 time dependently. Additionally, extracellular signal regulated kinase (ERK) was shown to be activated by TNF α (Geng, Valbrecht and Lotz, 1996). In an

extended study, MAPKs and their subtypes: JNK, p38 kinases, including ERK were activated dose and time-dependently on treating rabbit articular chondrocytes with IL-1. However, JNK was observed to be favourably stimulated upon treatment with TNF α (Scherle et al., 1997). As such, it is worth examining the extent to which MAPKs are activated in response IL-1 and TNF α and whether it is a result of variations in the species of chondrocytes incorporated and/or the level of protein kinase activation.

Although several studies have proven that protein kinases can be activated by pro-inflammatory cytokines, it has also been well documented that cytokines and other catabolic mediators can be regulated by upstream protein kinases. For instance, MAPKs have been shown to regulate MMPs, prostaglandin synthase and IL-6 selectively, along with IL-1 activity (Ridley et al., 1997). Another study revealed that IL-1 and TNF α were regulated by p38 kinase and JNK, which in turn upregulated the expression of MMP-1, -3 and -13 (Liacini et al., 2002, Ahmed et al., 2003). Additionally, NO release in OA chondrocytes was found to be regulated by various protein kinases, including MAPK-activated protein kinase (MAPKAPK), which may also be accountable for iNOS expression (Martel-Pelletier et al., 1999).

1.6.4 Regulation of MMP gene expression by cytokines

TNF α and IL-1 β are essential regulators of MMP expression and enzyme protein synthesis, which are involved in the disruption of cartilage and synovium homeostasis during OA disease progression (Shlopov et al., 1997, Malemud et al., 2003, He et al., 2002). Recent studies demonstrated the induction of ECM degradation by IL-1 β and TNF α in OA cartilage explants. However it was also observed that these two cytokines were not always co-expressed (Barakat et al., 2002). IL-1 β and TNF α were also implicated in the upregulation of MMP expression. However ADAMTS-4 was specifically stimulated by IL-1 in bovine chondrocytes, including articular and nasal cartilage explants (Martel-Pelletier et al., 1999, Pratta et al., 2003). The MMPs which are crucial in OA pathogenesis include: MMP-1, -3, -8, -9 and -13 along with aggrecanases which belong to the ADAMTS family. Some of the ECM components of cartilage capable of being degraded by MMPs include collagen, link protein, proteoglycans and fibronectin which are all vital in cartilage function. Aggrecan and versican have also been shown to be substrates of cytokine-induced MMP-3, -8, -13 and aggrecanases (Malemud, 1999, Malemud et al., 2003).

Although there is substantial interest in determining how and which cytokines modulate MMP expression, the mechanisms by which activated MMPs are suppressed by tissue inhibitor of metalloproteinases (TIMPs) and other MMP inhibitors is also of great importance. TIMPs are regulators of activated MMPs (Smith, 1999). Four types of TIMPs primarily exist in human tissues, namely: TIMP-1, TIMP-2, TIMP-3 and TIMP-4, with TIMP-4 being the

most relevant in OA joints. In OA cartilage, Huang et al demonstrated elevated levels of TIMP-4 when compared to healthy cartilage, suggesting that the regulation of MMP activity is mostly mediated by TIMP-4 in OA joints (Bigg et al., 1997, Huang et al., 2002). As such, studies suggesting OA disease process to be a result of an MMP/TIMP imbalance (Martel-Pelletier et al., 1994) need to be re-examined.

1.6.5 Induction of nitric oxide and apoptosis by cytokines

Nitric oxide is one of the major catabolic mediators of OA. Clinical studies have demonstrated increased levels of NO, reactive oxygen species (ROS) and nitrates released by OA cartilage into the synovial fluid and serum of OA patients (Karan et al., 2003), due to an upregulation of inducible nitric oxide synthase (iNOS; Martel-Pelletier and Pelletier, 2010). Elevated levels of the catabolic mediator are also present in OA synovium, capable of activating cartilage MMPs (Murrell et al., 1995, Grabowski et al., 1997). Another essential catabolic mediator of OA is cyclooxygenase-2 (COX-2), which has been shown to be highly expressed together with its product PGE₂ (Murakami et al., 2000, Vane and Botting, 1998a). In human OA cartilage explants, increased levels of PGE₂ were shown to be in correlation with enhanced expression of COX-2 (Amin et al., 1997). Consequently, increased chondrocyte apoptosis was observed, leading to enhanced cartilage damage (Notoya et al., 2000, Pelletier et al., 2001a, Goldring and Berenbaum, 2004). These studies suggest that concentrations of PGE₂ similar to those secreted during inflammation increase chondrocyte apoptosis and cartilage degradation (Amin et al., 1997, Attur et al., 2008). In contrast, low concentrations of PGE₂ have been shown to induce anabolic events (DiBattista et al., 1996) and inhibit of MMP-1 and -13 mediated activities in certain studies (Tchetina et al., 2007).

Cytokines are well known to regulate NO production. An upregulation of iNOS was recently demonstrated in lipopolysaccharide (LPS), TNF α and IL-1 β treated chondrocytes, which led to enhance NO production and apoptosis (Maier et al., 1994, Blanco et al., 1995). Similarly, TNF α has been observed to increase NO levels as well as superoxide production in both OA synoviocytes and chondrocytes (Ahmadzadeh et al., 1990, Maier et al., 1994). Additionally, in human OA chondrocytes, elevated levels of NO release were induced by IL-1 β and IL-17 (Singh et al., 2002). An upregulation in the expression of iNOS was observed in OA cartilage when compared to RA or healthy cartilage (Melchiorri et al., 1998; Amin et al., 1995), resulting in post-translational modifications of the type II collagen network (Hughes et al., 2010). Apoptosis has proven to be the primary cause for the limited self-repair capabilities of OA cartilage (Malemud et al., 2003). Apoptosis induced by NO release has been associated with PGE₂ production via the expression of COX-2 (Notoya et al., 2000). Nevertheless, NO-induced apoptosis by sodium nitroprusside has been shown to be inhibited by TNF α -stimulated COX-2 expression (Relic et al., 2002).

Collectively, these studies suggest that the inhibition of pro-inflammatory cytokine-induced catabolic mediators such as MMPs, NO and PGE₂ is of utmost importance in OA treatment. It has been well documented through numerous *in vitro* and animal studies that the inhibition of IL-1 by the human recombinant IL-1 receptor antagonist (IL-1Ra) – anakinra, results in positive effects on the structural integrity of cartilage. Indeed, in canine OA models, intra-articular injection of anakinra resulted in the downregulation of collagenase activity and a reduction in the development of both cartilage lesions and osteophytes, when compared to placebo treated models (Caron et al., 1996). However, the use of the IL-1Ra in multi-centre trials for the treatment of OA did not have any substantial effect on the turnover of cartilage ECM and knee pain (Chevalier et al., 2009), unlike its use in RA patients, which noticeably reduced cartilage erosion and joint pain (Jiang et al., 2000). Furthermore, knock down of IL-1, iNOS, IL-1 converting enzyme or stromelysin-1 in surgically induced OA mice models resulted in the rapid generation of cartilage lesions, suggesting that the presence of low concentrations of IL-1 is essential for the maintenance of normal ECM turnover (Clements et al., 2003). Indeed, a decrease in NO release and a regulation in PGE₂ levels were observed together with an increase in IL-1Ra synthesis in IL-1 stimulated human articular chondrocytes when treated with the nonsteroidal anti-inflammatory drugs (NSAIDs): aspirin and aceclofenac (Maneiro et al., 2001). Similarly, in human OA cartilage explants, an increase in the synthesis of IL-1Ra was observed on incorporating the iNOS inhibitor, 1400W (Vuolteenaho et al., 2003).

Table 1.5: The effects of TNF α and/or IL-1 β on the production of catabolic mediators in chondrocytes.

Species	Model system	Treatment	Cytokines	Upstream activators		Mediators			Cell response	Reference
				MAPK	NF- κ B	NO	PGE ₂	MMPs		
Canine	Surgically induced OA (transection of cranial cruciate ligament)	-	(\uparrow) TNF α					(\uparrow) MMP-3		Kammermann et al., 1996
Bovine	3D co-culturing of human RA synovial fibroblasts with bovine cartilage explants embedded in agarose	TNF α (10ng/ml) and/or IL-1 β (5ng/ml). 14 days	(\uparrow) IL-6 (\uparrow) IL-8					(\uparrow) MMP-1, 3	(\downarrow) ECM content	Pretzel et al., 2008
Murine	LPS treated mice Adjuvant-induced arthritic (AIA)-induced male Lewis rats	-	(\uparrow) TNF α (\uparrow) IL-6	(\uparrow) p38-MAPK					(\uparrow)GAG loss (\downarrow) Bone mineral density (\downarrow) bone content	Badger et al., 2000
Human	Umbilical vein endothelial cells (HUVEC)	TNF α (50ng/ml), 15-30 min		(\uparrow) ERK, p38 MAPK, JNK						Zhou et al., 2007
Murine	Prechondrocyte or mature chondrocyte, monolayer culture	TNF α (30ng/ml), 72hr		(\uparrow) ERK/MAPK	(\uparrow) NF- κ B				(\downarrow) types I and II collagen (\downarrow) link protein	Seguin & Bernier, 2003
Human	Fibrosarcoma cells or wild-type mouse embryonic fibroblasts (MEFs) monolayer culture	TNF α (20ng/ml), 30min			(\uparrow) NF- κ B				(\downarrow) cell viability	Varfolomeev et al., 2008
Human	OA synovial fibroblasts	TNF α (5ng/ml), 48hr			(\uparrow) NF- κ B		(\uparrow) COX-2 (\uparrow) PGE ₂			Alaaeddine et al., 1999
Human	Chondrocyte/alginate beads	TNF α or IL-1 β (10ng/ml), 72hr			(\uparrow) NF- κ B		(\uparrow) COX-2	(\uparrow) MMP-9	(\downarrow) type II collagen (\downarrow) integrin 1 β receptor expression	Mehdi et al., 2007
Porcine	Chondrocyte monolayer	TNF α (100pg/ml) and/or IL-1 β				(\uparrow) NO (\uparrow) iNOS TNF α > IL-			(\downarrow) aggrecan synthesis (\uparrow) HA	Goodstone and Hardingham,

		(5000pg/ml) for 72hr.				1 β			(\uparrow) HA synthase-2 TNF α = IL-1 β	2002
Bovine	Chondrocyte monolayer	IL-1 α at 0.1, 1, 10 and 100ng/ml and, TNF α (100ng/ml) for 48hr.				(\uparrow) NO production			(\downarrow) cell viability and (\downarrow) proliferation at 100ng/ml (\uparrow) apoptosis	Schuerwegh et al., 2003
Canine	Chondrocyte monolayer and alginate beads	IL-1 β (100ng/ml) and / or TNF α (50ng/ml), 6 to 72hr	(\uparrow) IL-1 β (\uparrow) IL-6, 8 (\uparrow) GM- CSF (\uparrow)TNF α			(\uparrow) iNOS (\uparrow) NO	(\uparrow) COX-2 (\uparrow) PGE ₂	(\uparrow) MMP-3, 13 (\uparrow)	(\downarrow) collagen type II (\downarrow) aggrecan	Rai et al., 2008
Human	OA menisci explants	IL-1 β and/ or TNF α				(\uparrow) NOS-2 expression, (\uparrow) NO release further with either cytokine	(\uparrow) COX-2 expression (\uparrow) PGE ₂ production further with either cytokine			LeGrand et al., 2001
Human	Chondrocyte monolayer OA chondrocytes	TNF α (200U/ml) and/ or IL- 1 α (100U/ml)	(\uparrow) IL-6 (\uparrow) IL-8			(\uparrow) NO		(\uparrow) MMP-1 (\uparrow) MMP-3	No change in chitonase-like protein	Dozin et al., 2002
Human	Chondrocyte monolayer	TNF α (10ng/ml) and / or IL- 1 β (5ng/ml) for 24hr					(\uparrow) PGE ₂ production		(\uparrow) apoptosis, (\uparrow) DNA fragmentation, (\uparrow) condensed nuclei	Caramé's et al., 2008
Human	Chondrocyte monolayer	TNF α (10 ⁻⁸ M)					(\uparrow) PGE ₂ production		Cartilage resorption	Bunning & Russell, 1989
Bovine	Explants	TNF α (50– 100 ng/ml) for 24hr						(\uparrow) pro- and active MMP-2, 9 synthesis	(\uparrow) proteoglycan release, cell death	Gilbert et al, 2003

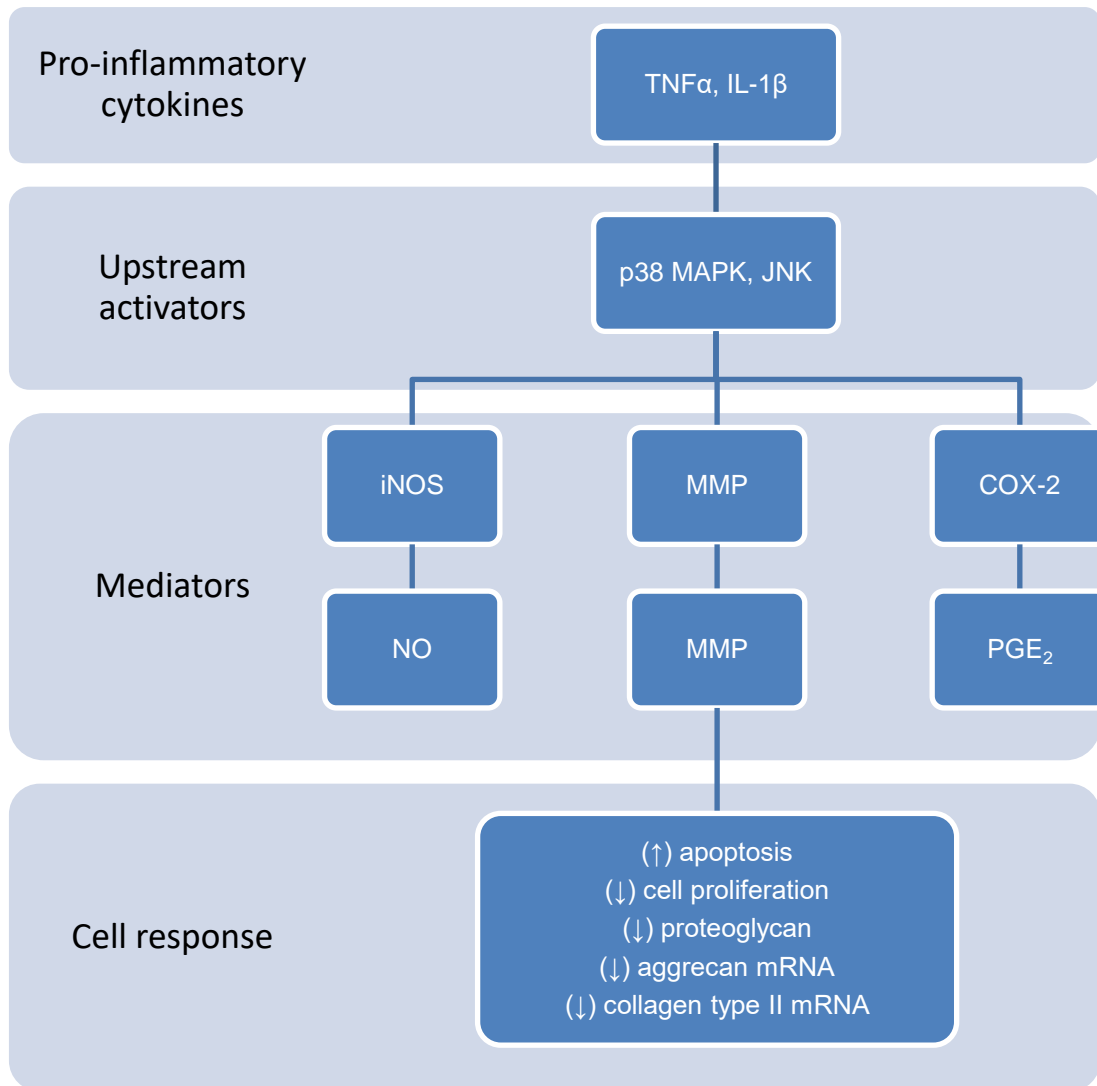


Figure 1.17. Schematic of signalling pathways induced by pro-inflammatory cytokines.

1.7 Extracellular matrix fragments

During OA disease progression, the presence of enhanced levels of fibronectin (FN) in both cartilage tissue and synovial fluid may be a result of increased synthesis and retention of FN in the ECM (Clemmensen and Andersen, 1982, Miller et al., 1984; Brown and Jones, 1992; Wurster and Lust, 1984; Wurster et al., 1986; Wurster and Lust, 1985; Wurster et al., 1986). These elevated levels of FN in the ECM are eventually reduced due to metabolic burden on chondrocytes, leading to the production of fibronectin fragments (FN-fs). FN-fs are also capable of being produced by MMPs present in the synovial fluid during moderate cartilage degradation, leading to the break down of FN into fragments, which result in the generation of FN-f concentrations similar to those found in OA synovial fluid (Homandberg et al., 1998). These FN-fs then penetrate the tissue and bind to the pericellular matrix (Xie and Homandberg, 1993, Homandberg et al., 1992), inducing a series of catabolic activities. These FN-f-induced catabolic activities are mediated by matrix proteases, including MMP-1, -3 and -13 as well as pro-inflammatory cytokines such as IL-1 and TNF α , consequently leading to cartilage breakdown and progression of tissue lesions (Mehraban et al., 1998), hence forming a positive feedback loop of tissue degradation. These studies suggest that FN-fs are involved upstream of the OA disease process, compared to pro-inflammatory cytokines and other catabolic mediators which act downstream of the disease process. As such, this 'stand alone' chapter elucidates the effects of extracellular matrix fragments, with particular reference to FN-fs and collagen fragments (Col-fs), in chondrocyte metabolic activities for the identification of key targets for OA therapy. Figure 1.18 is a schematic illustrating the role of matrix fragments in the early and late stages of OA.

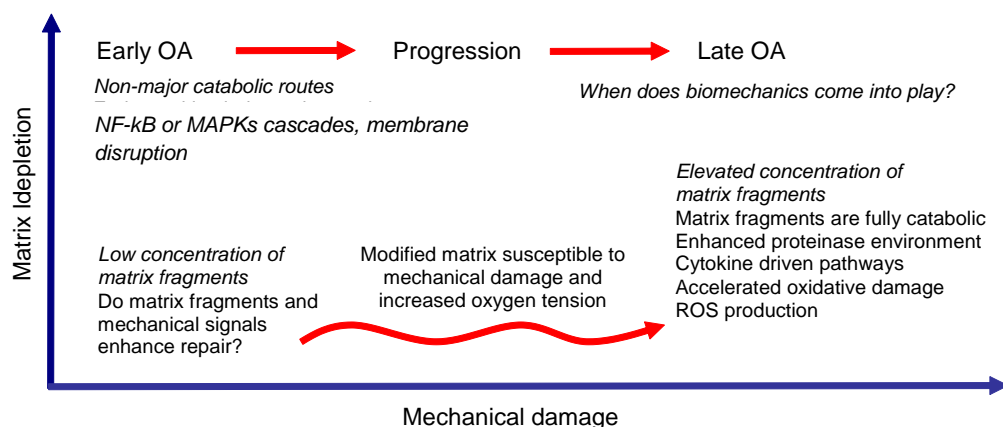


Fig. 1.18. Schematic of events involved in early to late stage osteoarthritis.

Chondrocytes present in the damaged extracellular matrix will either amplify the catabolic processes and contribute to changes in tissue remodelling or enhance anabolic pathways which initiate reparative signals. The catabolic/anabolic effects in damaged cartilage are dependent on the concentration of matrix fragments and phase of the OA disease process.

Indeed, low concentrations of matrix fragments induce anabolic activities, in contrast to high concentrations which enhance catabolic processes. FN-fs are well recognised as key mediators which derive catabolic processes in cartilage. In clinical studies, FN-fs were found in both rheumatoid and osteoarthritic cartilage tissues and injection of FN-fs into rabbit knee joints exert catabolic effects mediated by matrix MMPs and cytokines such as IL-1. For example, Griffiths et al., (1989) detected the presence of FN-fs ranging between 24kDa to 200kDa in RA and OA synovial fluids. Matrix fragments serve as sensors during cell metabolism and play an essential role in initiating pathways either for facilitating degeneration or enhancing reparative signals. The latter might be either a product of a secondary effect of cartilage degeneration or related to the manner of fragment signalling.

Although different types of FN-fs are involved during cartilage degeneration, the amino terminal 29kDa FN-f, was found to be the most potent in contributing to matrix degeneration in human cartilage (Homandberg et al., 1998). Other fragment systems are additionally involved in the regulation of cartilage homeostasis, including Col-fs derived from type II collagen and hyaluronan fragments (HA-fs). These fragment systems demonstrate catabolic activities, but have less potent effects compared to FN-fs, and may indeed act similarly in the manner in which the pathways are regulated. However, very little is known about the way in which these fragment systems induce signalling cascades in normal and diseased cartilage. Furthermore, the question on whether these systems significantly overlap with the pathways induced by FN-fs are unreported.

1.7.1 Effect of FN-fs in cartilage breakdown and osteoarthritis

The levels of FN were reported to increase in animal models which represent OA and human cartilage explants (Miller et al., 1984; Brown and Jones, 1992; Wurster and Lust, 1984; Wurster et al., 1986; Wurster and Lust, 1985; Wurster et al., 1986). This increase may be due to both elevated synthesis and retention of FN in the ECM, in an attempt to induce self-repair. Nevertheless, these elevated levels of FN eventually decrease due to metabolic burden on the chondrocytes. It has also been well documented that the levels of FN are enhanced significantly in synovial fluid from 171µg/ml to 568 and 721µg/ml during OA and RA, respectively (Scott et al., 1981, Carnemolla et al., 1984).

An increase in the level of FN mostly results in the enhancement of FN-fs in both cartilage tissue and synovial fluid during disease progression. Elevated levels of FN-fs have also been observed in both RA and OA synovial fluid (Clemmensen and Andersen, 1982). The FN-fs detected in OA synovial fluid had a total mass ranging between 30kDa and 200kDa (Xie et al., 1992). In human OA cartilage, the 29kDa amino-terminal FN-fs (NH₂-FN-fs) were largely detected in tissue extracts with specific antibodies (Homandberg et al., 1998, Zack et al., 2006). Other studies have confirmed the presence of FN-fs ranging between 24kDa and 200kDa, which represent most of the entire portion of FN in the cartilage tissue. Such levels of FN-fs have been found in cartilage damaged by trauma, OA, RA and also in infected synovial fluid (Griffiths et al., 1989).

FN-fs found in synovial fluid could arise from synovium, cartilage or plasma FN. The presence of alternatively spliced FN isoforms, which are tissue specific, has also been reported. However, synovial fluid contains more than one form. The levels of FN isoforms synthesized in synovial fluid and cartilage tissue vary considerably from those formed in other tissues. In cartilage tissue, enhanced levels of an ED-b[+] form and cartilage specific isoforms, [V+C]- are detected, which lack considerable segments found in isoforms of other tissues (Wurster et al., 1997). These findings were similar to observations made in canine OA models, in which levels of ED-b[+] elevated throughout the ECM of the cartilage (Zhang et al., 1995). In addition, an escalation of the same isoform was detected at the RNA in human OA cartilage (Rencic et al., 1995). In contrast, the types of FN isoforms found in human OA synovial fluid include synovial fluid isoform and ED-a[+] isoform, (Hino et al., 1995) with the latter being present only at basal levels (Rencic et al., 1995). Accordingly, FN-fs found in synovial fluid may theoretically be derived from cartilage, synovial fluid as well as plasma FN. Despite the presence of several types of FN isoforms in synovial fluid, the origin of the fragments cannot be distinguished from one another as these isoforms have a conserve sequence in the amino terminus. This was confirmed by testing the activities of FN-fs derived from bovine cartilage, plasma and synovial fluid and revealing that all the FN-

fs were equally active during chondrolysis. It can therefore be established that the activity of FN-fs are independent of FN isoform or tissue origin.

The 140kDa FN-f consists of an RGD sequence which varies from those existing in other isoforms, due to the presence of its alternately spliced regions. However, the 140kDa FN-f is assumed to be as dynamic as its counterpart from synovial fluid or cartilage tissue (Homandberg et al., 1998). In addition to this, it was demonstrated that FN-fs were produced via moderate cartilage degradation to levels found in OA synovial fluids (Homandberg et al., 1998). Elevated levels of FN-fs increase MMP-1, 3 and 13 levels leading to collagen and fibronectin degradation and activation of catabolic activities. However, the pathways will change during the OA disease process.

FN-fs from different species/models mediate catabolic effects (Table 1.6). The activities of the fragments are independent of the type of proteinase used to generate the FN-fs. This is due to the fact that similar domains are obtained irrespective of the specific bonds cleaved. For example, FN-f mixtures generated by thrombin and cathepsin D are as active as those obtained from human plasma via MMP-3. FN-fs obtained from bovine cartilage, plasma or synovial fluid are equally active. FN-fs derived from OA synovial fluids have proven to be damaging, since the cartilage damaging capabilities of the resultant synovial fluid mediate catabolic effects (Homandberg et al., 1998). Indeed, in OA animal models MMP-3 levels were enhanced in synovial fluids resulting in cartilage breakdown and progression of tissue lesions (Mehraban et al., 1998). Synovial MMPs may therefore breakdown FN into fragments which penetrate the tissue and bind to the pericellular matrix leading to cartilage degradation (Xie and Homandberg, 1993, Homandberg et al., 1992). Several studies performed by Homandberg et al. demonstrated that to cartilage degradation increased MMPs, a brief decrease proteoglycan synthesis by up to 50% (Xie et al., 1993, Xie et al., 1994) and an elevation in the rates at which proteoglycan content was lost from cartilage explants (Homandberg and Hui., 1994, Homandberg and Wen, 1998, Homandberg et al., 1992). Similar observations were found in other cartilage explant studies in which FN-fs induced explants released more than 50% of the entire proteoglycan content into serum within few days. The concentrations of FN-fs incorporated were similar to those detected in OA synovial fluid (Xie and Homandberg, 1993, Xie et al., 1993). It has been recently established that since the native precursor of FN-f is inactive, FN-fs are generated via proteolysis of FN. Also, it has been proven that FN-fs do not function as proteinases, as they require metabolic energy, protein synthesis as well as mRNA for their catabolic activities to proceed (Homandberg et al., 1992). Evidence of attempted repair by FN-fs in cartilage explants have been identified by studies in which the rates of proteoglycan synthesis increased up to 140% of the control values on the removal of FN-fs from the culture media. Despite this, proteoglycan content did not return to their normal values. FN-fs may attempt to repair. However, success was not achieved under such circumstances (Homandberg and Hui, 1994, Homandberg and Wen, 1998).

In order to study the dose response effects of FN-fs on cartilage metabolism, two types of protocols were initially used by Homandberg et al: the incorporation of (i) serum-free media and (ii) serum supplemented media. The first was used in order to determine the rates constants of proteoglycan and their release into media (Homandberg et al., 1992; Xie and Homandberg, 1993, Xie et al., 1994), providing information on the kinetics of matrix degradation. Such measurements were possible due to the greater proteolytic response created by serum-free cultures. In contrast, the later protocol was incorporated in order to carry out longer term cultures, so that information on steady state metabolism will be provided, demonstrating the activity of FN-fs in more physiologic conditions. This was achieved by the significantly reduced rate of proteoglycan depletion provided by the serum supplemented media, which also allowed cartilage to express anabolic responses to degeneration. With these conditions, it was observed that at the lowest concentrations of 1nM 29kDa FN-fs, there was an immediate elevation in the rate of proteoglycan synthesis together with a rise in the proteoglycan content as shown in Fig. 1.19A. On increasing the FN-fs concentration by a factor of 10, a decrease in the proteoglycan content was detected, but with a delay. Between 10 to 100nM of FN-fs concentrations, proteoglycan synthesis decreased, followed by a gradual restoration of its rate of synthesis, leading to significantly high levels of proteoglycan (Fig. 1.19B; Homandberg and Hui, 1994, Homandberg and Wen, 1998).

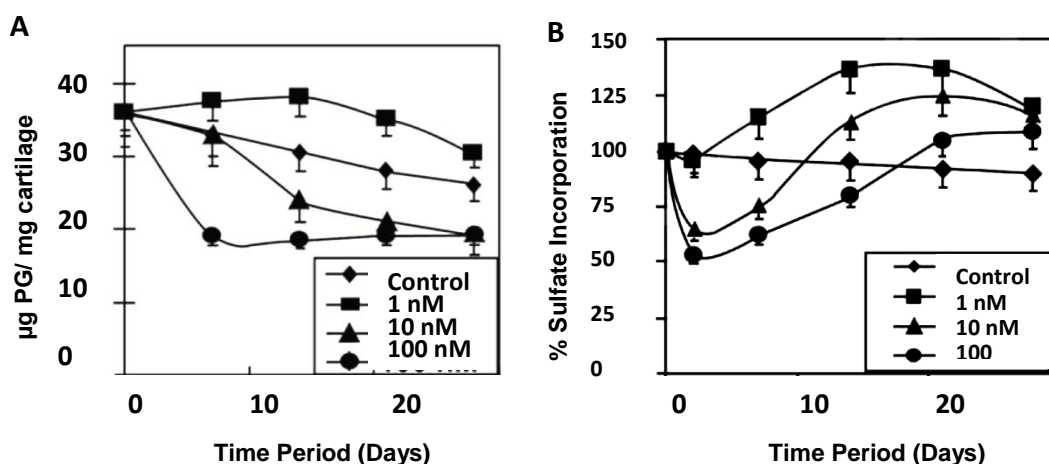


Figure 1.19. Biphasic effects of FN-fs on proteoglycan content (A) and proteoglycan synthesis (B). Cartilage explants were treated with 1, 10 or 100nM 29kDa FN-f continuously with media changes every other day. At intervals, cartilage was subjected to papain digests and measurement of proteoglycan content by DMB assay (left). Similar cultures were subjected to ^{35}S labelling to determine rates of sulphated proteoglycan synthesis (right) (Homandberg et al., 1994, Homandberg et al., 1998).

Table 1.6: Effect of different sized FN-fs on cartilage degeneration.

Species / model system	Fragment type	Major effects	Reference
Bovine, explants and monolayer	29kDa FN-f (100 nM)	(↑) iNOS expression, NO, MMP-1, 13 production. Proteoglycan depletion.	Pichika and Homandberg, 2004
Bovine, explants and monolayer	29 and 140kDa FN-f	(↑) IGF BP-2, 3, 5 in monolayer. Release of IGFBP-2 and IGF-1 in explants	Purple et al., 2002
Human OA and RA, explants	40kDa COOH-FN-f	(↑)NO production via CD44 (↑) MMP-1, 2, 9, 13	Yasuda et al., 2003
Rabbit, explants and monolayer	FN-f containing alternately spliced domain	(↑)Proteoglycan release from explant culture; (↑) IL-1 α and IL-1 β prior to (↑) MMP-1 gene expression	Saito et al., 1999
Bovine, explants	50kDa gelatin-binding FN-f, COOH-FN-fs	(↑) type II collagen cleavage by collagenase; (↑) production of proMMP-3,13 and proteoglycan depletion	Yasuda and Poole, 2002
Porcine, explant and monolayer	45kDa COOH or gelatin binding FN-f	(↑) MMP-3 and 13, aggrecanase activity	Stanton et al., 2002
Human, monolayer	29, 50 or 70kDa FN-f	Upregulation of TLR-1, 2 and 5.	Su et al., 2005
Bovine, alginate beads	29kDa FN-f or IL-1 α	Dose- and time-dependent inhibition of proteoglycan synthesis and (↑)CD44 expression	Chow et al., 1995
Human, monolayer	120kDa FN-f	Elevation of MMP-13 and p38 MAPK	Forsyth et al., 2002
Human and bovine, explants; <i>In vivo</i> OA rabbit model	29kDa FN-f	(↑)cytokines, MMPs and (↓) proteoglycan content; Enhanced cleavage of aggrecanase epitope	Homandberg et al., 1997, Kang et al., 1999
Human, explants, FN-fs derived from cartilage and synovial fluids	29kDa FN-f (0.1-1 μ M)	(↑) MMP-3, IGF-1, IL-1 β , IL-1 α , IL-6, IGF-I, TGF- β , TNF- α . 50% reduction in proteoglycan content	Homandberg et al., 1996, Homandberg et al., 1997, Homandberg et al., 1998
Human, monolayer	110kDa FN-f	(↑) IL-6, IL-8, and chemokines via NF- κ B	Pulai et al., 2005
Rheumatoid synovial cells, monolayer	COOH-terminal Heparin-binding FN-fs	(↑) MMP-3, 13	Yasuda et al., 2003
Rabbit, monolayer	110kDa FN-f	(↑) MMP-3	Arner and Tortorella., 1995
Fibrocartilaginous cells, monolayer	120kDa FN-f	(↑)MMP-1, 3	Hu et al., 2000
Human, monolayer	29kDa FN-f	(↑) NO, IL-1 via FAK and p38 MAPK	Gemba et al., 2002
Bovine, agarose	29 and 40kDa FN-f	(↑)NO, iNOS, COX-2, PGE ₂ , MMP-3, 13 and IL-1	Raveenthiran and Chowdhury, 2009

High concentrations of FN-fs ranging between 0.1 and 1 μ M had substantial effects at day 7 culture (Fig. 1.20A & 1.20B), which included enhanced levels of IL-1 β , IL-1 α , IL-6, MMP-3, TNF α , IGF-I and TGF β as shown in (Fig. 1.20C; Homandberg et al., 1996, Homandberg et al., 1997).

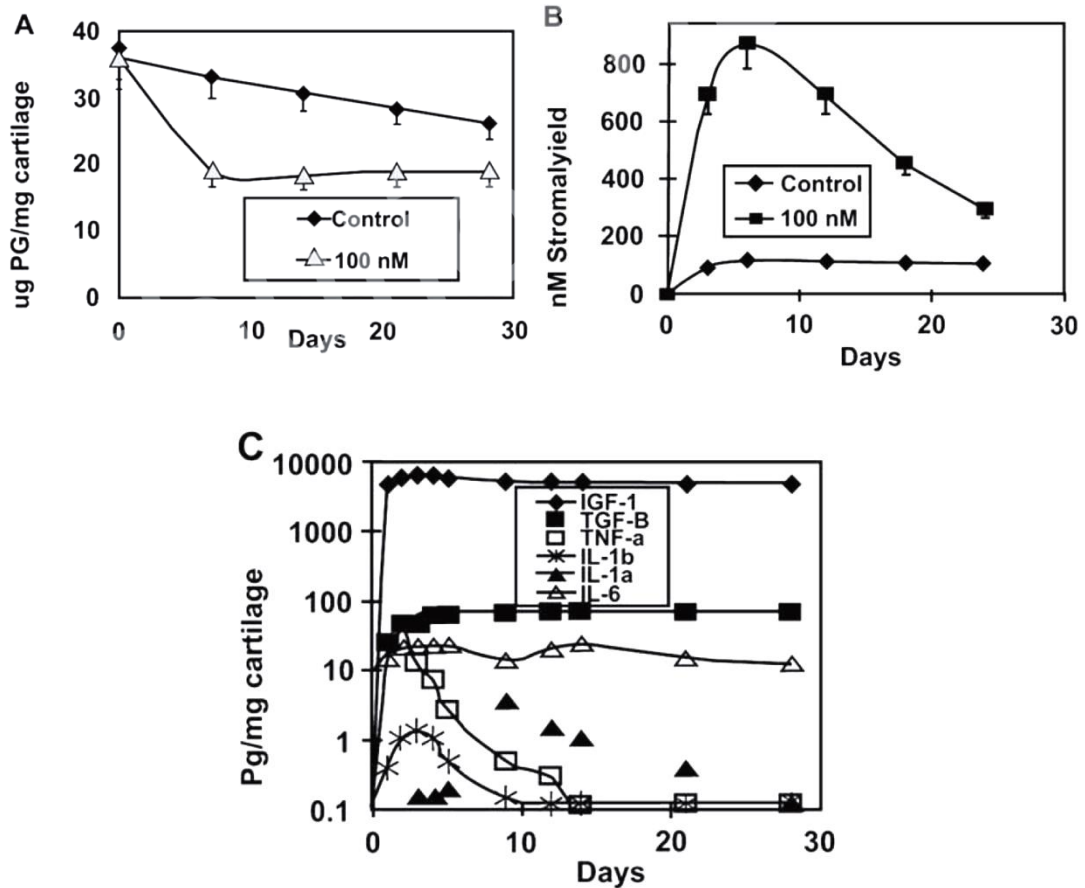


Figure 1.20. Correlation of cartilage proteoglycan content (A) with MMP-3 release (B) and cytokine/factor release (C) with high FN-f. Cartilage explants were treated with 100nM 29kDa FN-f continuously with media changes every other day. In (A), cartilage proteoglycan content was measured in explants; in (B), MMP-3 (stromelysin) was measured by ELISA and in (C), cytokines and growth factors in the media were measured by ELISA (Homandberg et al., 1996, Homandberg et al., 1997).

From the above findings it can be derived that at low concentrations of FN-fs, anabolic repair processes are activated, whereas catabolic insults result from elevated levels of FN-fs. However, as catabolic processes diminish, anabolism predominates once again, leading to enhanced levels of proteoglycan content and increased rates of proteoglycan synthesis.

It is well known that there is an upregulation of proteinases during cartilage breakdown. Examples of the types of proteinases detected during cartilage degradation include: MMP-1, -2, -3 -9 and -13. Emphasis is directed mainly towards MMP-3 since it contributes significantly to the degradation process (Bewsey et al., 1996). This was confirmed by studies in which FN-f treated bovine cartilage explants showed a decrease in the rate of cartilage damage when supplemented with MMP-3 specific antibodies (Xie et al., 1994). An

upregulation in MMP-3 was observed in human cartilage explants on culturing them in DMEM supplemented with 10% serum for 2 days with 100nM 29kDa, when compared to untreated controls. This difference was identified in Paraffin embedded sections stained with anti-MMP-3 and HRP-secondary antibody (Homandberg et al., 2007). Since MMP-3 can degenerate FN macromolecules into small FN-fs (Homandberg et al., 1998), it subsequently results in an upregulation of FN-fs during OA which, in turn will substantially elevate levels of MMP-3 expression in a positive feed-back loop. Furthermore, it has also been shown that FN-fs increase levels of MMP-13, which are enhanced in parallel with MMP-3 when tested with bovine cartilage explants (Forsyth et al., 2002). Also, the aggrecanase epitope cleavage can be enhanced by FN-fs (Homandberg et al., 1997, Kang et al., 1999).

High concentrations of FN-fs result in an upregulation of several types of cytokines, including TNF α , IL-1 (Saito et al., 1999), IL-1 α , IL-1 β , IL-6 and IL-8 in human cartilage as previously mentioned above (Pulai et al., 2005). These observations were confirmed with neutralising antibodies which blocked cytokine production in response to FN-f (Homandberg et al., 1996, Homandberg et al., 1997). Additionally, FN-fs exhibit elevated cytokine pathways not only in chondrocytes, but also in several other cell types (Kamiya et al., 2004). Indeed, interleukin receptor antagonist protein (IRAP) was shown to inhibit catabolic activities in IL-1 β treated chondrocytes. However, the effect of IRAP on blockade of cytokine release varied significantly and was dependent on the type of model system, potency of IRAP and species. For each of these studies, the capability of IRAP to block exogenous IL-1 was considered as the control. However the unsuitability of such a control may be due to the increased struggle in blocking IL-1, especially when it is upregulated and highly concentrated around the cell compared to exogenous IL-1 which becomes diluted upon addition (Homandberg, 2007). Furthermore, the use of IRAP does not confirm complete depletion of MMPs since TNF α is also elevated by FN-fs (Homandberg et al., 1997).

Recent studies with bovine cartilage explants proved that the upregulation of MMPs was driven initially by MAP kinases and NF κ B cascades (Fig. 1.21; Ding et al., 2009), followed by cytokines in the later stages, after 48 hours of culture (Ding et al., 2006). Such observations were consistent with studies in which MAP kinases, PKC and PYK2 inhibitors resulted in a decrease in MMP content within the first 24 hours of culture, during which substantial levels of TNF α and IL-1 were not identified. FN-f induced MMPs were not completely blocked during the first 24 hours of culture using IRAP. However, IRAP proved to be significantly more effective at 48 hours and beyond. Also, it can be suggested that changes detected in the MMP levels during long term explant cultures, were mainly due to the effects of cytokines after 24 hours, due to the more physiological conditions provided for them to be activated (Homandberg, 2007). The pathways involve upstream activation of NF κ B and p38 in fragment treated chondrocytes (Homandberg et al., 2006).

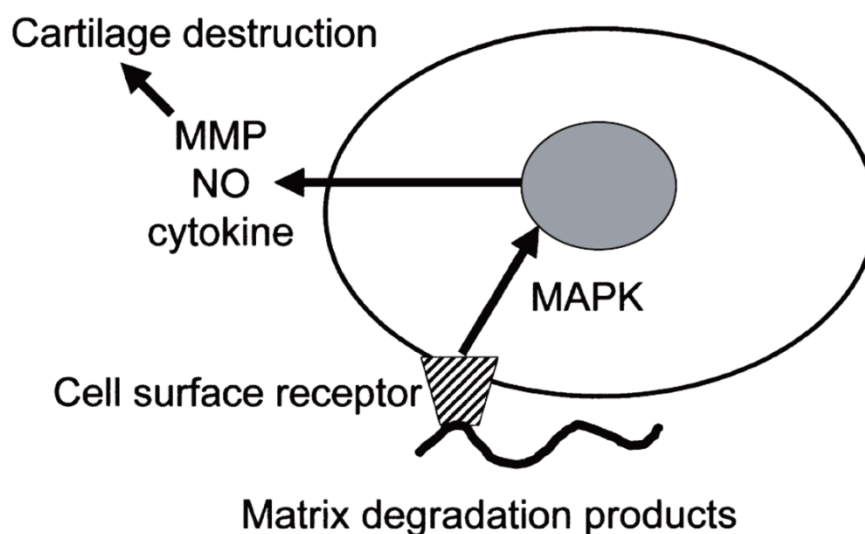


Figure 1.21. Schematic diagram of cartilage destruction by matrix degradation products. Increased proteolytic matrix fragments activate chondrocytes and synovial fibroblasts, leading to the induction of matrix metalloproteinase, nitric oxide and cytokines via cell surface receptors such as integrins that can stimulate catabolic intracellular signals and pathways involving the MAPKs.

Chondrolytic properties of FN-fs were demonstrated by Homandberg et al., (1993) by injecting FN-fs into rabbit knee joints and detecting a loss of up to 50% of the total proteoglycan in articular cartilage. Recent studies show that such loss of proteoglycan was experienced within 2 days of injection of the fragments into the joints. During this period of time proteoglycan synthesis is temporarily suppressed, MMP-3 content was plateaued and the NITEGE (Asn-Ile-Thre-Glu-Gly-Glu) epitope of aggrecan was exposed (Homandberg et al., 2001). Despite this, a slow increase in the synthesis of proteoglycan to supernormal levels was observed, demonstrating anabolic responses, which lead to proteoglycan restoration as shown in figure 1.22. Proteoglycan restoration however was dependent on the age of the knee joint into which FN-fs were injected. Studies by Williams et al., (1996) demonstrated that in adolescent rabbits, Proteoglycan was restored only within 2 weeks of injecting FN-fs into rabbit knee joints. Unlike this, the restoration of proteoglycan in skeletally mature rabbits required months (Williams et al., 2003).

Safranin-O

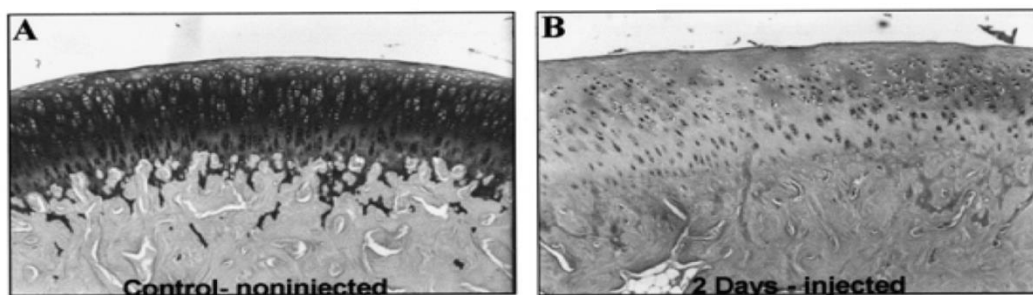


Figure 1.22. Injection of FN-fs rabbit knee joints causes marked loss of proteoglycan within 2 days. Adolescent rabbits were intra-articular injected with 200 μ g of a mixture of 29kDa human plasma FN-fs and after 2 days, cartilage recovered and subjected to staining with safranin-O to visualize proteoglycan (Homandberg et al., 2001).

FN-f damaged cartilage tissue can be repaired via the reduction of catabolic pathways or the compensation for catabolic stress. Such repair can be achieved by the use of agents which may have anti-catabolic or anabolic approaches of action, capable of shifting or compensating for catabolic pathways that are still in operation even after the removal of FN-fs. With the use of FN-f cartilage damage model, which represents a suitable OA model, such observations were justified. The model provided means of testing agents which might potentially block FN-fs damage or promote cartilage repair. It proved to be suitable due to its lack in capability of naturally restoring proteoglycan on the removal of FN-fs (Homandberg and Hui, 1994). Examples of agents which were proven to be partially or completely effective in the reduction of cartilage damage and restoration of proteoglycan in pre-damaged cartilage include: synthetic peptide analogues of the cell binding sequence located in FN (Homandberg and Hui, 1994), IGF-1, the growth factor including N-acetylcysteine and other anti-oxidants (Homandberg et al., 1996a, Homandberg et al., 1997). Also, OP-1 (osteogenic protein-1), another growth factor (Koepp et al., 1999, Im et al., 2003), was proven to block the upregulation of MMP-13, induced by FN-fs and enhance cartilage repair in other studies. In addition to this, high molecular weight HA was found to block FN-f induced damage and promote repair (Kang et al., 1999, Homandberg et al., 1997).

1.7.2 Effect of collagen fragments in the development of osteoarthritis

Type II Collagen, which is the main type of collagen present in articular cartilage increases in the late stages of OA, which may lead to enhanced levels of collagen fragments (Col-fs) being generated (Lorenzo et al., 2004). Also, it has been well documented that while there is an increase in collagen synthesis in cartilage lesions, the content level decreases (Squires et al., 2003). However, the relationship between the increase in collagen synthesis and Col-f production is still unknown. In human OA cartilage, up to 40mg of Col-fs per gm are released from damaged cartilage, which suggests that up to 20% of the total collagen in cartilage tissue undergoes degradation (Billinghurst et al., 1987). Also, the presence of Col-fs of up to 6µg/ml was demonstrated in synovial fluid of rabbits treated surgically to induce OA (Felice et al., 1999).

Despite the fact that several types of Col-fs arise from type II collagen during cartilage degradation, the most significant types detected are the amino (N) and carboxyl (C)-telopeptides. Figure 1.23 depicts a model representing the interactions of integrins and ECM with type II collagen N-telo and C-telo regions. These telopeptides are released upon attack of MMP-3 on the crosslinking segments of type II collagen. C-telopeptides were proved to be linked with the occurrence and progression of radiographic OA in the hip and knee (Reijman et al., 2004). Urine from OA patients were shown to have increased levels of C-telopeptides

(Jung et al., 2004) which directly correlates to elevated cartilage turnover (Christgau et al., 2004). Also C-telopeptides were enhanced after cartilage injury (Lohmander et al., 2003) and were found in vast amounts in the synovial fluid of rabbit models which represent OA (Lindhorst et al., 2005). N-telopeptides have been used as markers for cancer (Reijman et al., 2004). It is highly likely that other types of collagen are capable of contributing to the release of Col-fs. However, majority of the contribution is expected from type II collagen, which implies that N and C-telopeptides are immensely involved in cartilage degradation.

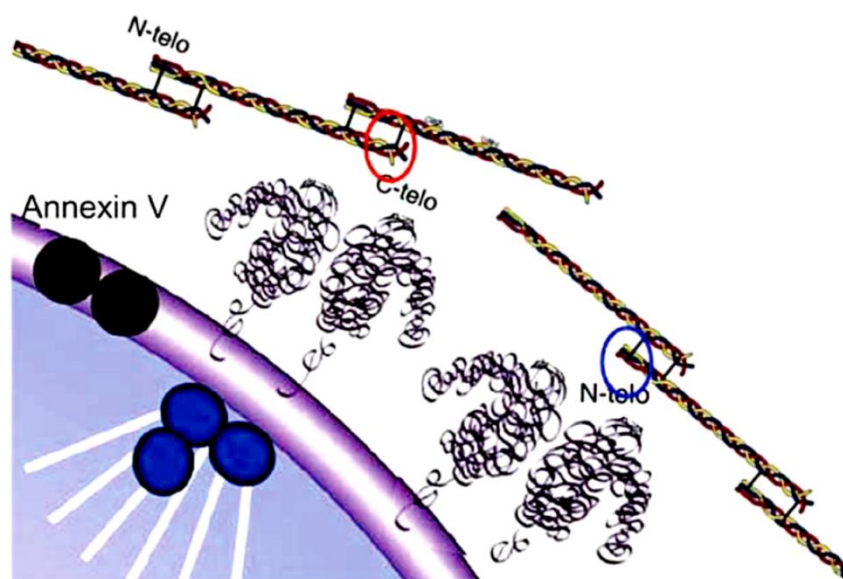


Figure 1.23. Model of interaction of type II collagen N-telo and C-telo regions with ECM and integrins. Bacteria collagenase cleaves type II collagen while leaving the N-telo and C-telo crosslinked regions intact. Such digest mixtures have been shown to upregulate MMPs (Jennings et al., 2001). The N-telopeptide has been shown to bind annexin V but interaction with integrins might also occur for both types of peptides, as discussed (Lucic et al., 2003).

Col-fs demonstrate highly potent catabolic activities during cartilage breakdown and progression of tissue lesions. Various types of collagen peptides have a wide range of inflammatory or tissue damaging effects on various types of other cells. For example, CNBr peptides of type II collagen stimulate the production of collagenase by synovial cells (Golds and Poole, 1984), regulate the production of MMP-8 via gelatinase (Rice and Banda, 1995), alter types II and IX collagen turnover in bovine cartilage explants (Yasuda et al., 1999) or induce IL-1 α and IL-1 β from human monocytes (Goto et al., 1988). Also, the C-terminal fragment of type XVIII collagen is responsible for the induction of clusters and disorientates actin stress fibres via c-src activation (Wickstrom et al., 2002). Such response is achieved by the interaction of the C-terminal fragment with $\alpha_5\beta_1$, the FN receptor. Accordingly, it can be suggested that Col-fs, as with FN-fs are capable of enhancing catabolic effects in various tissue types. In early studies of the effects of Col-fs on articular cartilage, a decrease in the level of proteoglycan and an upregulation of MMP-1, -3 and -13 were demonstrated upon the action of bacterial collagenase digests on cartilage explants. The fragments obtained

from such digests were <10kDa in size and enriched with N and C telopeptides (Jennings et al., 2001). Subsequently, studies were carried out on synthetic N and C telopeptides which were shown to bind with a nonintegrin receptor, annexin V (Guo, Ding and Homandberg, 2009, Lucic et al., 2003). These synthetic telopeptides as with collagen fragments also demonstrated an upregulation in MMP-2, -3, -9 and -13 message levels (Fichter et al., 2006). Peptides of type II collagen have also shown to induce cleavage of aggrecan and type II collagen in cartilage (Yasuda et al., 2006).

In comparison to FN-fs, synthetic N and C telopeptides and collagenase generated type II Col-fs were shown to be less potent, at concentrations of 10-100µg/ml. These Col-fs also demonstrated a slightly lower potential in decreasing proteoglycan levels in cartilage explants compared to that of FN-fs (Guo, Ding and Homandberg, 2009). Accordingly, Col-fs may overlap with pathways induced by FN-fs and may share mechanistic features. This creates the potential for the existence of a single global mechanism describing the two fragment systems, which might be used for therapeutic interventions during disease progression.

1.8 Effect of mechanical loading on OA progression

1.8.1 Effect of biomechanical signals and FN-fs on tissue remodelling and anabolic activities

Early studies by Steinmeyer et al. (1997) demonstrated increased levels of FN in bovine cartilage explants on the application of intermittent cyclic loading. Similar observations were demonstrated in canine cartilage explants subjected to cyclic loading (Farquhar et al., 1996). Biomechanical signals are well known to influence cartilage homeostasis and tissue remodelling via the enhancement of synthetic activities, which overlap with inflammatory pathways (Guilak et al., 2004, Loeser, 2006, Bader et al., 2011). The mediators responsible for initiation of the early stages of matrix damage are quite complex and hence involve both biological and mechanical factors. Enhancement of synthetic signals via mechanical loading was demonstrated in chondrocyte/agarose constructs treated with NH₂-hep I and COOH-hep II FN-fs (Fig. 1.24).

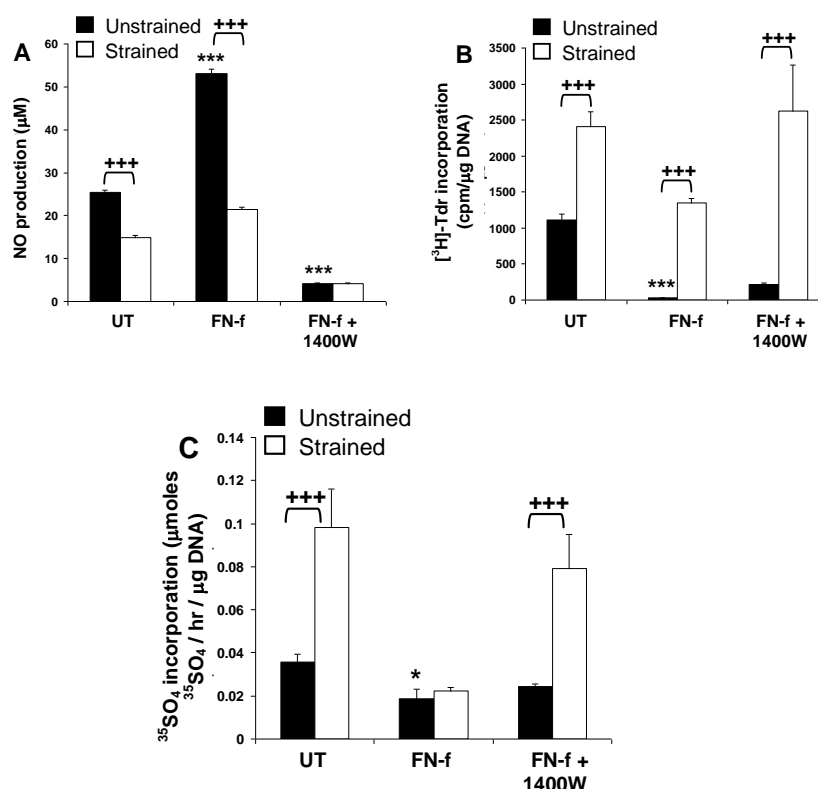


Figure 1.24. Dynamic compression (15%, 1 Hz) inhibits NH₂-FN-f induced NO release (A) and restores cell proliferation (B) and proteoglycan synthesis (C) in chondrocyte/agarose constructs (48 hrs) (Raveenthiran and Chowdhury, 2009).

This study by Chowdhury demonstrated that compressive loading blocks FN-f induced NO production and restores matrix synthesis in chondrocyte/agarose constructs. This represents

the first study to show that mechanical signals inhibit catabolic activities induced by FN-fs (Fig. 1.24; Raveenthiran and Chowdhury, 2009). Another study also demonstrated similar observations in chondrocyte/agarose models induced with the 29kDa NH₂-terminal FN-fs (Fig. 1.25; Parker et al., 2013).

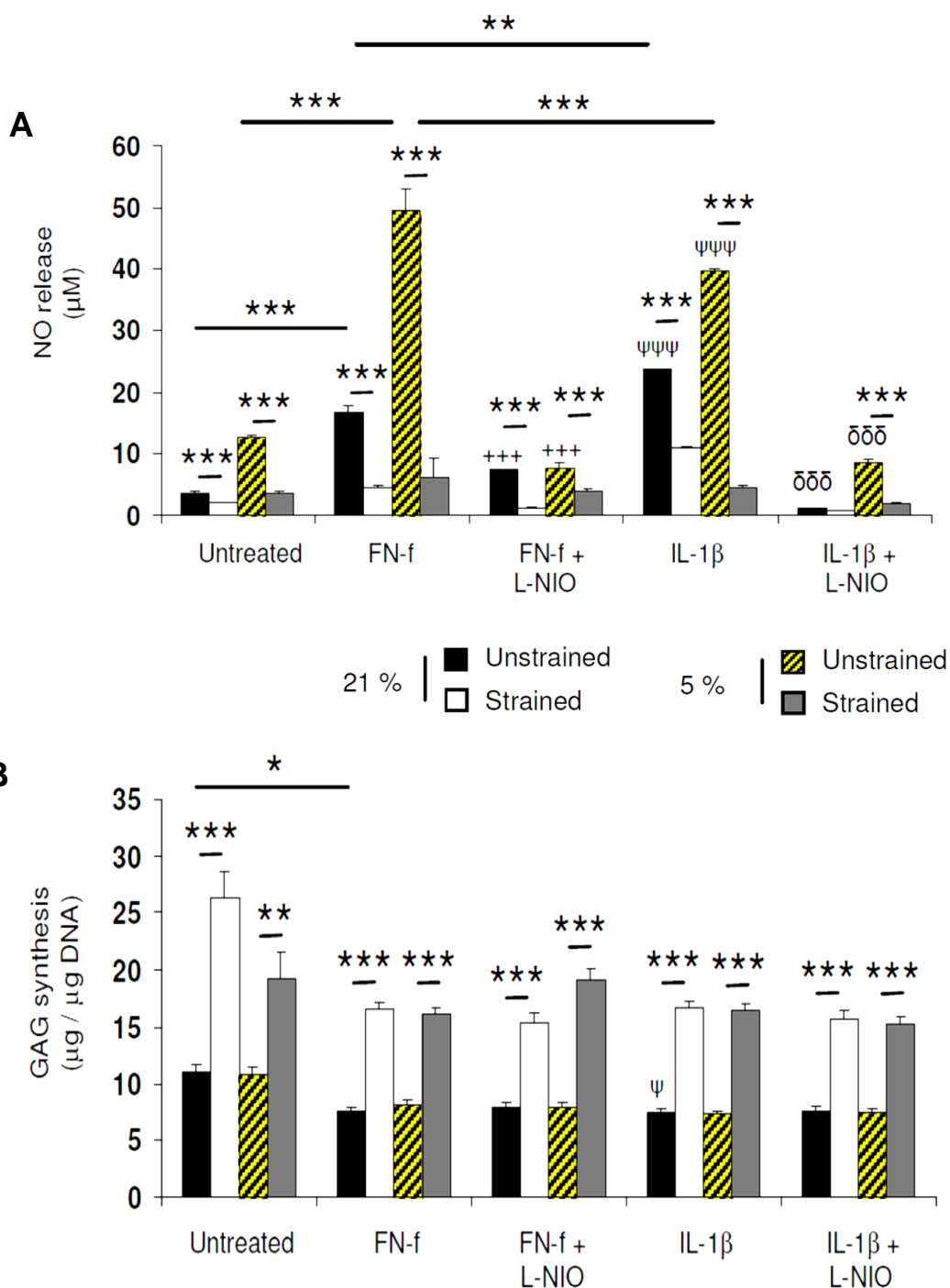


Figure 1.25. Effect of FN-f or IL-1 β and dynamic compression on NO release (A) and GAG synthesis (B) in chondrocyte/agarose constructs cultured at 5 and 21% oxygen tension for 48hr. Constructs were cultured under uninterrupted experimental conditions with 0 or 1 μM FN-f or 10ng/ml IL-1 β and/or 1mM L-NIO. Error bars represent the mean and SEM of 8 to 12 replicates from three separate experiments, where (*) indicates comparisons between unstrained and strained values. In unstrained constructs, (+++) indicates comparisons between FN-f and FN-f + L-NIO; (ψ or $\psi\psi\psi$) indicates comparisons between untreated and IL-1 β ; ($\delta\delta\delta$) indicates comparisons between IL-1 β and IL-1 β + L-NIO. (Raveenthiran and Chowdhury, 2009).

Recent data demonstrates that compressive loading inhibits NO production, MMPs and cytokine production induced by collagen telopeptides or NH₂-FN-fs and increased anabolic activities (fibronectin, collagen, sGAG) in chondrocyte/agarose constructs (Chowdhury et al., 2010). The enhanced matrix synthesis by mechanical signals might therefore constitute an initial repair response. In healthy tissue, a small proportion of matrix proteins will undergo normal matrix turnover and be released due to proteolytic digestion by MMPs. However, mechanical signals may indirectly contribute to a pool of matrix proteins, which later give rise to catabolic activities involving overproduction of both MMPs and released matrix fragments. Consequently, matrix fragment signalling in conjunction with mechanical signals may add to a vicious cycle for accelerated MMP production and be a predisposing factor for OA (Chowdhury et al., 2010, Raveenthiran and Chowdhury, 2009).

The response of chondrocytes to mechanical signals has been proven to be dependent on the type of loading regime, its duration and whether loading was applied during early or late stage of the disease process. For instance, mechanical signals which exceed a certain level increase expression of catabolic and anabolic activities in chondrocytes. Mechanical signals that mimic injury and overloading will accelerate mild damage with an early rebuilding phase by increasing MMPs and metabolic activity. It is conceivable that the remodelling phase may occur indirectly through the effect of altered patterns of mechanical loading and increased production of growth factors (TGF β 1, IGF-1, bFGF) and cytokines (IL-4) (Bader et al., 2011, Guilak et al., 2004, Loeser, 2006). There is now strong evidence which implicates the $\alpha_5\beta_1$ integrin as a receptor for both mechanical loading and matrix fragments implicating overlapping pathways for these signals (Millward-Sadler and Salter, 2004, Homandberg et al., 2002) Integrin-mediated mechanotransduction will contribute to chondroprotective events resulting in an attempt by cells to stimulate anabolic processes locally and assist in tissue remodelling. However, conditions such as obesity or trauma, that represents excessive or injurious loading will increase catabolic activities and accelerate matrix damage possibly via abnormal integrin signals (Fitzgerald et al., 2004, Kurz et al., 2004, De Croos et al., 2006). Furthermore, oxygen tension will influence matrix turnover which, in turn, affects the ability of the tissue to respond to normal mechanical signals (James et al., 1990, Stevens et. al., 1991). It is not known whether oxygen tensions which exist in a diseased state (>7%) will aggravate mechanical and matrix fragment induced signals.

1.8.2 Fibronectin fragments signalling

Although the biochemical effects of FN-fs have been previously examined, the signalling cascades through which these catabolic effects occur have yet to be confirmed. There is strong evidence which implicates the $\alpha_5\beta_1$ integrin as a receptor for both biomechanical signals and matrix fragments suggesting potential overlapping pathways for these signals. Also, TLR4 has been reported to bind to matrix fragments, including HA and heparin

sulphate, suggesting that it may be a possible receptor for FN-fs. Additionally, it has been suggested that CD44 may bind to fibronectin. Based on these studies, preliminary tests were carried out in the host laboratory in collaboration with Drs Eleanor Parker and Nicholas Peake (unpublished), to examine the effects of blocking $\alpha_5\beta_1$, TLR4 and CD44 receptors on NO production in FN-f-treated bovine chondrocyte monolayer culture (Figure 1.26).

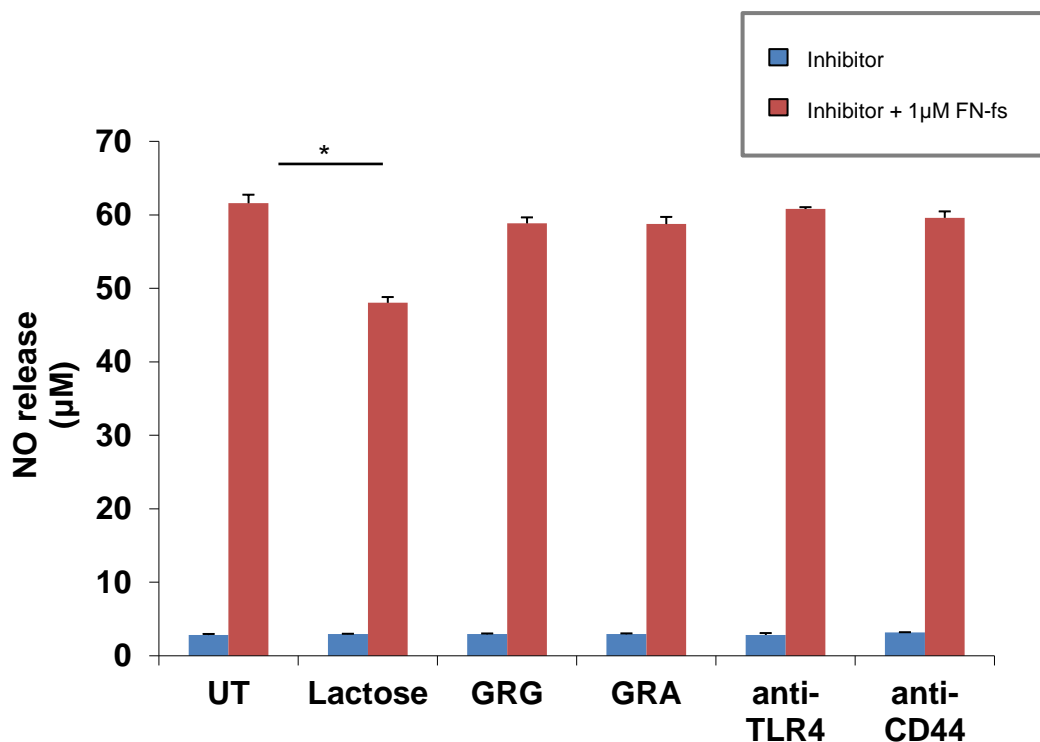


Figure 1.26. Effect of 0.1M α lactose (SGAL), 100µg/ml GRGDSP ($\alpha_5\beta_1$), 100µg/ml GRADSP (control), 1µg/ml anti-TLR4 in chondrocyte monolayer culture treated with 1µM of the 29kDa NH_2 -heparin-binding FN-fs for 48 hours. The effects on NO production were then observed. (*) $P < 0.05$ indicates significant comparisons between constructs treated with fragment and those treated with fragment and inhibitor as shown [$n=4$, data obtained previously from the host lab in collaboration with Drs Parker and Peake (unpublished)].

Significant reductions in NO production were not observed on blocking any of the aforementioned receptors in chondrocytes cultured in monolayer cultures for 48 hours (figure 1.26). Excluding samples treated with lactose, the maximum reduction in NO production achieved was approximately 14%, with the use of anti-TLR4, compared to the other inhibitors. Recent studies have identified the presence of a sequence of consensus pattern, XGXXPG in several matrix proteins, including elastin and collagen, where the VGVAPG motif is repeated particularly in elastin. A spliced variant of lysosomal β -galactosidase called the elastin binding protein (EBP), and also known as SGAL, is a primary receptor of elastin peptides as well as the XGXXPG ligand. Additionally, it has been shown that lactose acts as an inhibitor of XGXXPG, binding to SGAL/EBP. As such, it can be suggested that FN-f signalling occurs through EBP via the binding of EBP to the XGXXPG consensus pattern, which might be present in fibronectin and its fragments. In

order to prove the presence of the *XGXXPG* consensus pattern in 29kDa NH₂-heparin-binding FN-fs, α lactose monohydrate was used to inhibit FN-f-induced NO production in the model described in figure 1.26. The results revealed that lactose was the most successful at inhibiting FN-fs-induced NO production in chondrocytes compared to the other inhibitors employed. Subsequently, a preliminary study was carried out in the host laboratory in collaboration with Drs Eleanor Parker and Nicholas Peake (unpublished), to compare the effects of lactose on FN-f-treated chondrocytes in 3D agarose constructs, to those cultured in monolayer, as shown in figure 1.27.

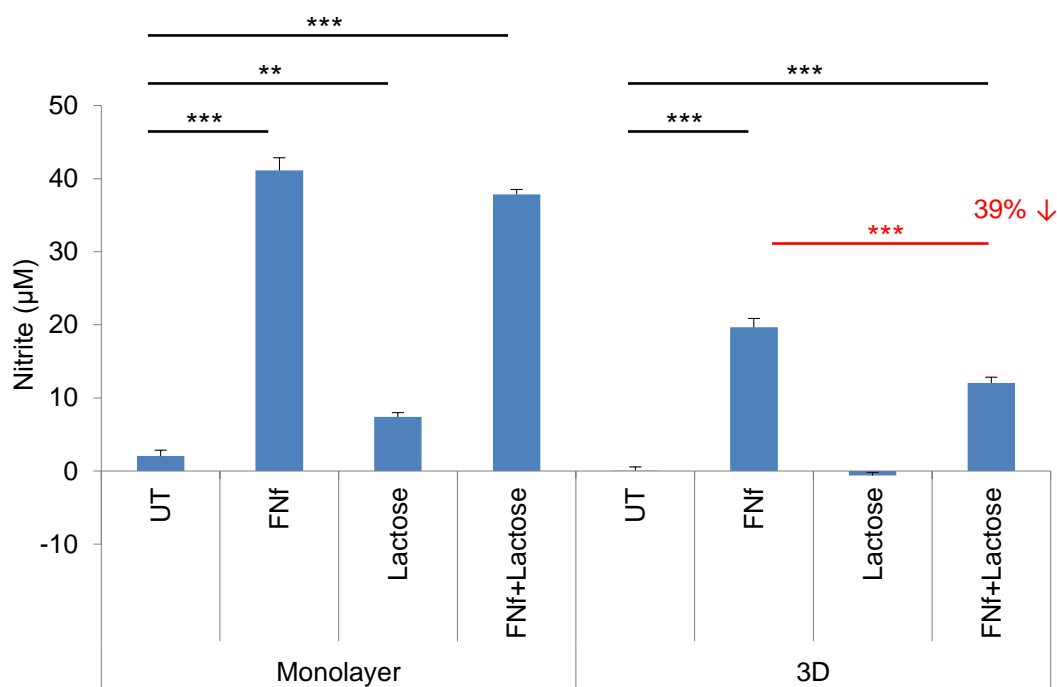


Figure 1.27. Effect of 0.1M α lactose in chondrocyte monolayer culture and 3D chondrocyte/agarose culture treated with 1 μ M of the 29kDa NH₂-heparin-binding FN-fs for 48 hours. The effects on NO production were then observed. (***) $P < 0.001$ indicate significant comparisons between constructs treated with fragment and those treated with fragment and inhibitor as shown [$n=4$, data obtained previously from the host lab in collaboration with Drs Parker and Peake (unpublished)].

From this, it was observed that lactose had a greater inhibitory effect on FN-f-induced NO production in chondrocytes cultured in 3D agarose constructs, when compared to those cultured in monolayer. Based on these results, the aims and objectives of the thesis were defined, as shown in section 1.10.

1.8.3 Effect of biomechanical signals and Col-fs on tissue remodelling and anabolic activities

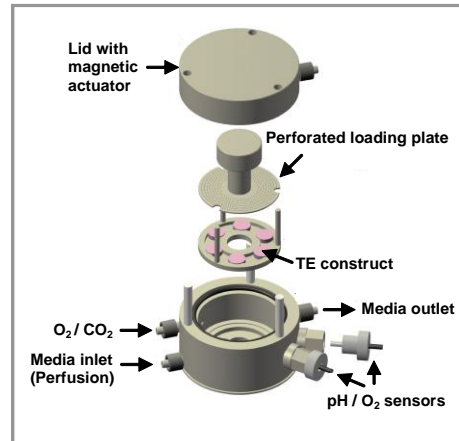


Figure 1.28. Bioreactor vessel components (Chowdhury et al., 2010).

Mechanical loading will influence the pathways induced by Col-fs. This was demonstrated with porcine chondrocytes seeded in agarose gel and subjected to intermittent or continuous loading regimes, with N-terminal (NT) telopeptides, C-terminal (CT) telopeptides and NH₂-FN-fs (Chowdhury et al., 2010). The bioreactor device is shown in figure 1.28. Matrix fragments increased levels of MMP-3, MMP-13, cytokines and NO release. However, MMP upregulation was time-dependant and influenced by the concentration and type of matrix fragment. Catabolic activities were reversed with mechanical loading with or without the iNOS inhibitor leading to restoration of GAG content (Fig 1.29). Thus, physiological mechanical loading may contribute to early anabolic signals and compete with catabolic processes induced by ECM fragments. The incorporation of pharmacology and mechanical loading to downregulate inflammatory responses form an essential tool to further study the interactions of cells signalling and biomechanics in OA.

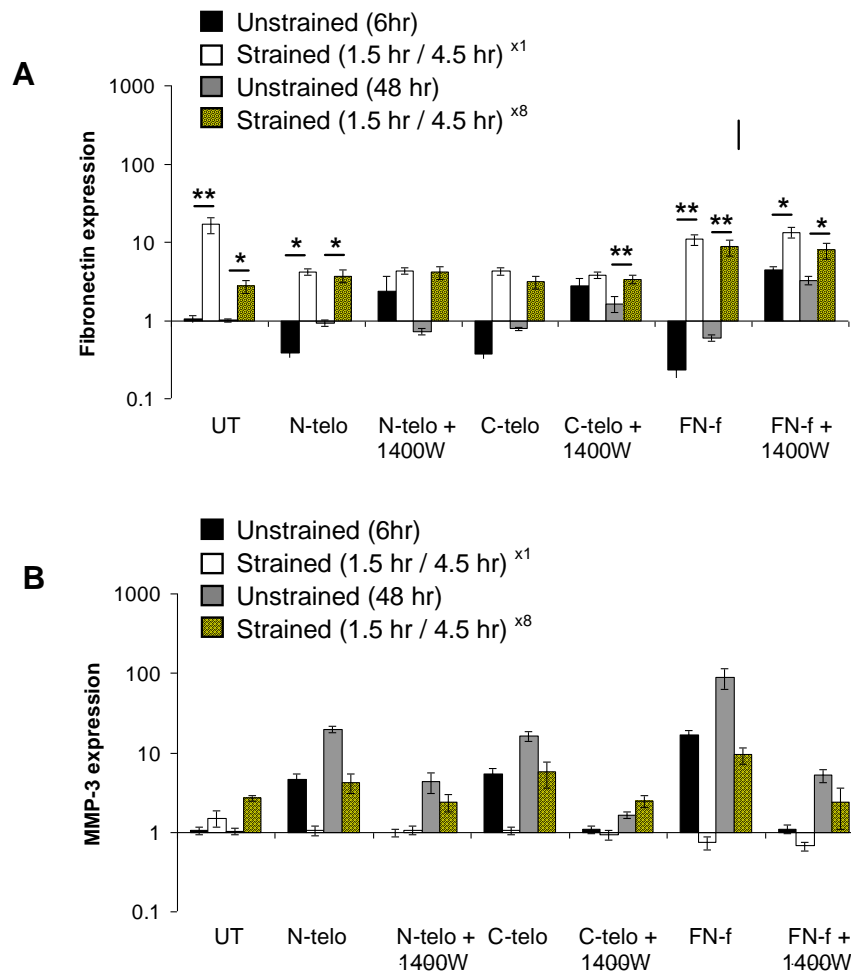


Figure 1.29. Continuous compression applied for longer periods resulted in a greater magnitude of stimulation of fibronectin (A) and MMP-3 (B) expression even in the presence of telopeptides or FN-fs (Chowdhury et al., 2010).

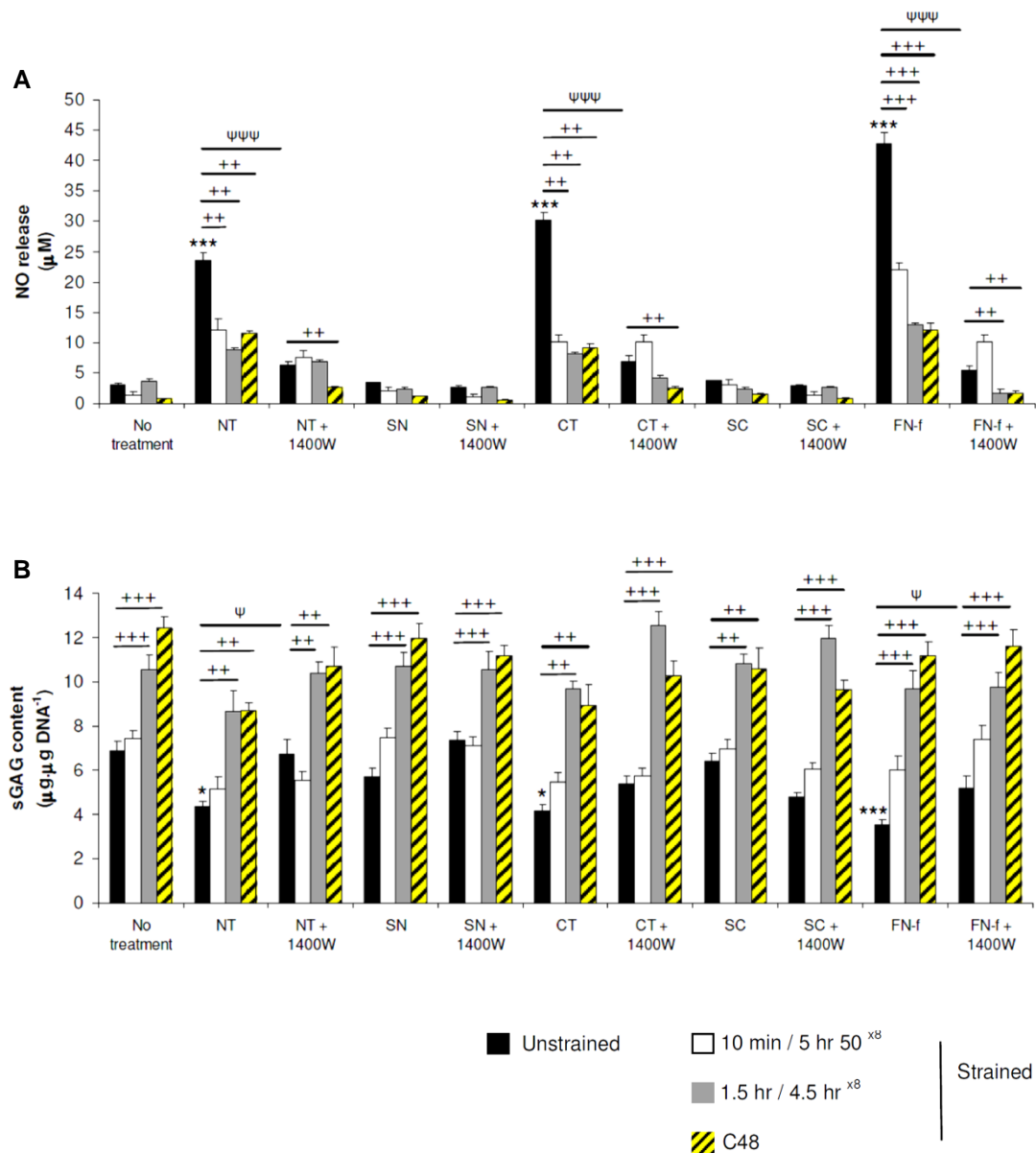


Figure 1.30. Effect of NT and CT telopeptides and dynamic compression (15%, 1 Hz) on NO release (A) and sGAG content (B). Unstrained and strained constructs were cultured with 50 μM NT or CT peptide and/or 1mM 1400 W for 48 hours ($n=8$). SN and SC peptides (50 μM) were used as negative controls. $\text{NH}_2\text{-FN-f}$ (1 μM) was used as a positive control. (*) indicates significant comparisons in unstrained constructs for no treatment vs fragment; (ψ) indicates significant comparisons in unstrained constructs for fragment vs fragment + 1400 W; + $P < 0.05$, ++ $P < 0.01$, +++ $P < 0.001$ indicates significant comparisons between treatment conditions as shown ($n=6$, Chowdhury et al., 2010).

1.9 Nitric oxide and oxygen tension during OA disease progression

The increased levels of NO and PGE₂ which are induced by elevated levels of both pro-inflammatory cytokines and mechanical stress during OA, can be significantly influenced by oxygen tension. A complex reaction exists between NO and PGE₂ which can also be altered by oxygen tension, suggesting that low oxygen tension in articular cartilage may have a tremendous impact on the inflammatory response of cartilage to OA compared to ambient conditions. Although inhibitors of NO have been considerably incorporated in various experimental models in the treatment of OA, they have not been used in a clinical setting. As such, elucidating the mechanisms by which oxygen tension can influence the stimulation of inflammatory mediators in response to pro-inflammatory cytokines and mechanical stress may contribute to the development of dual inhibitors of inflammatory mechanisms in the therapeutic intervention of OA.

Increased production of inflammatory mediators via the enhanced presence of pro-inflammatory cytokines and mechanical stress decreases the oxygen supply in cartilage during OA disease process. The decrease in oxygen tension during progression of the disease can be a result of a reduction in the density of capillaries and the deep localisation of capillaries within the synovial capsule (Stevens et al., 1991). As a result, it can be suggested that OA cartilage is more hypoxic compared to healthy articular cartilage (James et al., 1990).

1.9.1 Nitric oxide in OA

During OA, elevated levels of the catabolic mediator, NO are observed (Amin et al., 1997; Farrell et al., 1992; Sakurai et al., 1995). The gas is capable of readily interacting with superoxide anions (O₂⁻) to form peroxynitrites, which nitrate specific proteins. Nitrotyrosine antibodies can be used for the detection of these nitrated proteins, especially in OA cartilage as demonstrated by the presence of increased nitrated collagen peptides in OA tissue. Additionally, peroxynitrites have been detected in OA chondrocytes (Deberg et al., 2005).

OA has also been associated with a decrease in the protein expression of superoxide dismutase (SOD) as demonstrated in clinical studies and animal models of OA (Regan et al., 2005). An increase in pro-inflammatory cytokines and mechanical stress has been correlated with elevated levels of NO in OA disease process (Guilak et al., 2004). Although the signalling cascades by which NO induces cartilage degeneration is unclear, it has been well established that an increase in NO levels lead to alterations in chondrocyte metabolisms such as the stimulation of MMPs, regulation of cytokine expression and the inhibition of both

cell proliferation and matrix protein synthesis, including proteoglycan and collagen synthesis, which consequently lead to chondrocyte apoptosis (Lotz et al., 1999; Pelletier et al., 1999; Studer et al., 2000). During the conversion of L-arginine to citrulline, NO is produced with the help of oxygen which acts as an electron acceptor. The terminal guanidino nitrogen is catalytically eliminated during this process by the enzyme, NOS (Kwon et al., 1990). It must be noted that the NOS isoform primarily responsible for the production of NO in articular cartilage is iNOS (Sakurai et al., 1995). NO has also been shown to induce the development of reactive oxygen species (ROS) and changes in the redox signalling cascades which play essential roles in OA pathogenesis (Henroitin et al., 2003). The enzyme cytochrome oxidase which exists on mitochondrion membrane is known to catalyse the transfer of electrons to oxygen as part of the electron transport chain for the subsequent production of adenosine triphosphate (ATP). NO can hinder cytochrome oxidase resulting in a decrease in the electron transport chain, consequently leading to the development of superoxide anions and alterations in the redox state of cells. These superoxide anions then readily interact with NO, resulting in the formation of the potentially more toxic peroxynitrite (ONOO⁻), via the combination of the unpaired electrons on each of the two molecules. 3-nitrotyrosine is formed from peroxynitrite, which is now believed to be responsible for most of the catabolic activities of NO. Nevertheless, peroxynitrite can be detoxified depending on its microenvironment. Superoxide anions can be converted into hydrogen peroxides (H₂O₂) via the antioxidant, superoxide dismutase (SOD). Cell proliferation, apoptosis, gene transcription as well as necrosis can be induced by hydrogen peroxide, depending on its concentration. Hydrogen peroxide can be converted into oxygen and water via catalase, thereby reducing oxidative stress (Fermor et al., 2007).

SOD plays an essential role in maintaining a balance in the cellular concentrations of NO and O₂⁻. Extracellular SOD (EC-SOD) primarily resides in the ECM of the tissue due to the presence of its positively charged heparin-binding site (Fattman et al., 2003) which binds to the negatively charged proteoglycans and collagen in the ECM of the tissue (Petersen et al., 2004). During OA disease progression, decreased levels of EC-SOD are found in articular cartilage, resulting in an imbalance between the cellular concentrations of NO, O₂⁻ and SOD, demonstrating its importance in the maintenance of tissue homeostasis (Regan et al., 2005). Furthermore, S-nitrosothiols which are essential regulators of enzyme and cell function can be produced upon interaction of NO with reactive cysteine thiol (Hess et al., 2005).

An increase in pro-inflammatory cytokines or mechanical stress is known to also enhance levels of the catabolic mediator, PGE₂. PGE₂ has been shown to be suppressed by NO in certain cell types, with elevated levels of PGE₂ observed on suppressing NO production in articular cartilage in response to pro-inflammatory cytokines or mechanical stress (Amin et al., 1997, Cernanec et al., 2002). The underlying mechanisms responsible for the interaction between NO and PGE₂ is unclear. However, it has been suggested that NO-induced PGE₂

inhibition may be due to nitration of tyrosine residue (*Tyr*³⁸⁵), leading to downregulation in COX-2 activity which consequently results in a decrease in PGE₂ levels.

1.9.2 Effect of oxygen tension and pro-inflammatory cytokines on NO production

As previously described, an increase in the levels of pro-inflammatory cytokines including TNF α and IL-1 is associated with OA disease progression, which consequently leads to an elevation in NO production (Stadler et al., 1991, Sakurai et al., 1995). TNF α antagonists as well as IL-1Ra have been shown to exhibit beneficial effects in both OA and RA animal models, including clinical RA studies (Evans et al., 1998). Additionally, infliximab, the anti-TNF α antibody has demonstrated effective therapeutic properties in blood monocytes-lymphocytes from RA patients, such that decrease in TNF effects with infliximab correlated with a downregulation in the expression of iNOS (Perkins et al., 1998).

Hypoxia/reoxygenation events as well as low oxygen tensions have shown to have significant influences on NO production in response to pro-inflammatory cytokines. For instance, porcine cartilage explants treated with 10ng/ml of either IL-1 α or TNF α for 72 hours at 1% oxygen tension led to a decrease in NO production compared to those cultured at 20% oxygen tension (Cernanec et al., 2002). In contrast, bovine chondrocyte monolayer cultures subjected to concentrations of IL-1 β ranging from 0.2 to 1nM for a period of 48hr resulted in a decrease in NO production at 20% oxygen tension compared to either 1% or 5% oxygen tension (Mathy-Hartert et al., 2005). Alterations in the findings of these studies may be due to factors such as the model system incorporated as well as culture conditions.

An increase in NO production was observed in IL-1 α or TNF α treated porcine cartilage explants on reoxygenating them from 1% to 20% oxygen tension compared to those which remained at 20% oxygen tension (Cernanec et al., 2002). Similarly, reoxygenation of murine macrophages treated with interferon γ from 1% oxygen tension resulted in an increase in NO production compared to those which remained at 20% oxygen tension. Additionally, replenishment of the cytokine in cultures maintained consistently under ambient conditions led a much smaller increase in NO production when compared to those reoxygenated following hypoxic treatment. These findings suggest that this increase in NO production may be due to the upregulation of iNOS which is then protein translated upon reoxygenation (Melillo et al., 1996).

Although the signalling cascades via which low oxygen tension influences NO production is still unclear, a constant attempt is being made to explore these mechanisms. For instance, an upregulation in p42/p44 MAPK expression was observed in human articular chondrocytes

subjected to 5% oxygen tension, when compared to those cultured at 21% oxygen tension (Dudhia et al., 2000). These findings suggest that varied oxygen tensions may influence the extent to which these upstream kinases are activated.

Since oxygen tension influences NO production in response to pro-inflammatory cytokines and mechanical stress, it can be suggested that oxygen tension also influences PGE₂ production, in addition to NO. For instance, an increase in the levels of PGE₂ was observed on inhibiting IL-1 α -induced NO levels using the iNOS inhibitor, 1400W at 1% oxygen tension. These findings suggest that the suppressive effects of NO on PGE₂ are only manifested at severely low oxygen tensions (Cernanec et al., 2002). Similarly, on replenishing TNF α after 72 hours of incubation, an increase in PGE₂ production was observed at 20% oxygen tension. However, the same effects were not demonstrated in IL-1 α -treated cartilage explants cultured under the same conditions, implying that IL-1 α and TNF α may influence the interaction of catabolic mediators in different manners.

In addition to the catabolic effects NO has on cartilage, the gas is also capable of having protective effects *in vitro* (Evans et al., 1996). The degree to which NO can induce degenerative changes depends on the ratio of NO to oxygen, which determines the quantity of NO derivatives produced, including peroxynitrite and nitrosothiols. This is because, NO and peroxynitrites have different effects on the biological responses of chondrocytes. For instance, NO alone is incapable of inducing cell apoptosis, unless it is in combination with ROS (Mathy-Hartert et al., 2003, Del Carlo and Loeser, 2002). Similarly, elevated levels of NO production are observed on transducing lapine chondrocytes with iNOS (Studer et al., 1999). Additionally, there are variations in the activation of NF- κ B in response to NO and peroxynitrite produced in chondrocytes treated with pro-inflammatory cytokines (Clancy et al., 2004). Collectively, these studies suggest that the effect of NO on chondrocytes is dependent on the balance between NO, O₂⁻ and SOD, which in turn is influenced by oxygen tension.

1.9.3 Combined effect of oxygen tension and mechanical loading on NO production

Joint instability, sedentary life style as well as pain are all factors of abnormal joint loading, which can result in changes in the metabolic activities of chondrocytes, leading to cartilage degeneration, an inevitable feature in both OA and RA disease process (Minor, 1999). Abnormal joint loading is capable of further altering the joint physiology during progression of the disease which can become more distinctive upon weakening of the supporting muscles.

NO release can be stimulated by both physiological and non-physiological loading. However, the level of NO production is influenced by the magnitude of stress applied to articular cartilage (Agarwal et al., 2004). Intermittent loading and shear stress induce the production of NO (Lee et al., 1998, Lane Smith et al., 2000).

Mechanically stimulated NO production can be influenced by oxygen tension. For instance, an increase in the levels of NO were observed on culturing cartilage explants at 5% oxygen tension when compared to either 1% or 20% oxygen tension. However, the application of mechanical compression to these explants did not induce any further changes in NO production. On the other hand, cartilage explants subjected to mechanical compression at 1% oxygen tension led to a decrease in NO production when compared to 20% oxygen tension. Interestingly, 5% oxygen tension did not have any significant effects on NO production when subjected to the same conditions but at 20% oxygen tension (Fermor et al., 2005, Hashimoto et al., 2006). From these studies it can be suggested that NO production is suppressed by very low oxygen tensions, such as 1% oxygen tension.

Cyclic loading of the joint is known to alter the oxygen tension of articular cartilage. While oxygen can readily diffuse into articular cartilage, larger molecules find it more difficult to diffuse into the tissue. However, this process can be facilitated by the application of cyclic loading to the joint which in turn will influence the supply of nutrients and hence the metabolic activity and oxygen consumption of cartilage (Piscoya et al., 2005). However, it is worth noting that static compression can inhibit the diffusion of solutes through the tissue (Quinn et al., 2001).

Mechanically induced PGE₂ levels have been shown to be influenced by both oxygen tension and NO (Fermor et al., 2005). Although the studies mentioned above observed the effects of hypoxia on pro-inflammatory cytokines and mechanical loading separately, the combined effect of pro-inflammatory cytokines and mechanical signals at low oxygen tension has never been examined. The elucidation of mechanisms by which oxygen tension can influence the stimulation of inflammatory mediators in response to both pro-inflammatory cytokines and mechanical stress is essential in the development of dual inhibitors of inflammatory mechanisms in the therapeutic intervention of OA. As such, the present study examined the effect of oxygen tension and TNF α on catabolic and anabolic activities in chondrocyte/agarose constructs subjected to dynamic compression.

1.10 Aims and Objectives

Aim

The overall aim of this project was to examine the effects of oxygen tension on a well-established chondrocyte seeded model exposed to a combination of biomechanical and biochemical stimuli, the latter of which were specifically related to pro-inflammatory cytokines and matrix fragments. This multidisciplinary approach will have implications in the management of progressive osteoarthritis.

Objectives

- Examine the optimum culture period of TNF α , considering its short half-life and mode of action.
- Determine the dose-response effects of TNF α and the combined effects of dynamic compression and TNF α , on markers of catabolic activities and tissue remodelling, in chondrocyte/agarose constructs co-stimulated with the NOS inhibitor, under normoxic and hypoxic culture conditions, using an ex-vivo bioreactor.
- Determine the effects of dynamic compression on the gene expression of degradative enzymes in chondrocyte/agarose constructs treated with TNF α in the presence and absence of L-NIO under normoxic and hypoxic conditions.
- Optimize the culture conditions required to determine the dose-dependent effects of lactose on the production of nitrite and GAG synthesis in chondrocyte/agarose constructs treated with the 29kDa NH₂-heparin-binding FN-f under normoxic culture conditions.
- Examine the effects of varying oxygen tensions on the production of nitrite and GAG synthesis in chondrocyte/agarose constructs co-stimulated with FN-fs and lactose.
- Examine the combined effects of dynamic compression and varying oxygen tensions on the production of nitrite and GAG synthesis in chondrocyte/agarose constructs co-stimulated with lactose and VGVAPG peptides.
- Investigate the effects of commercially available amino terminal telopeptides on the anabolic and catabolic activities of chondrocyte/agarose constructs under both normoxic and hypoxic culture conditions, in the presence and absence of NOS and COX inhibitors.

Chapter 2 – General Methods

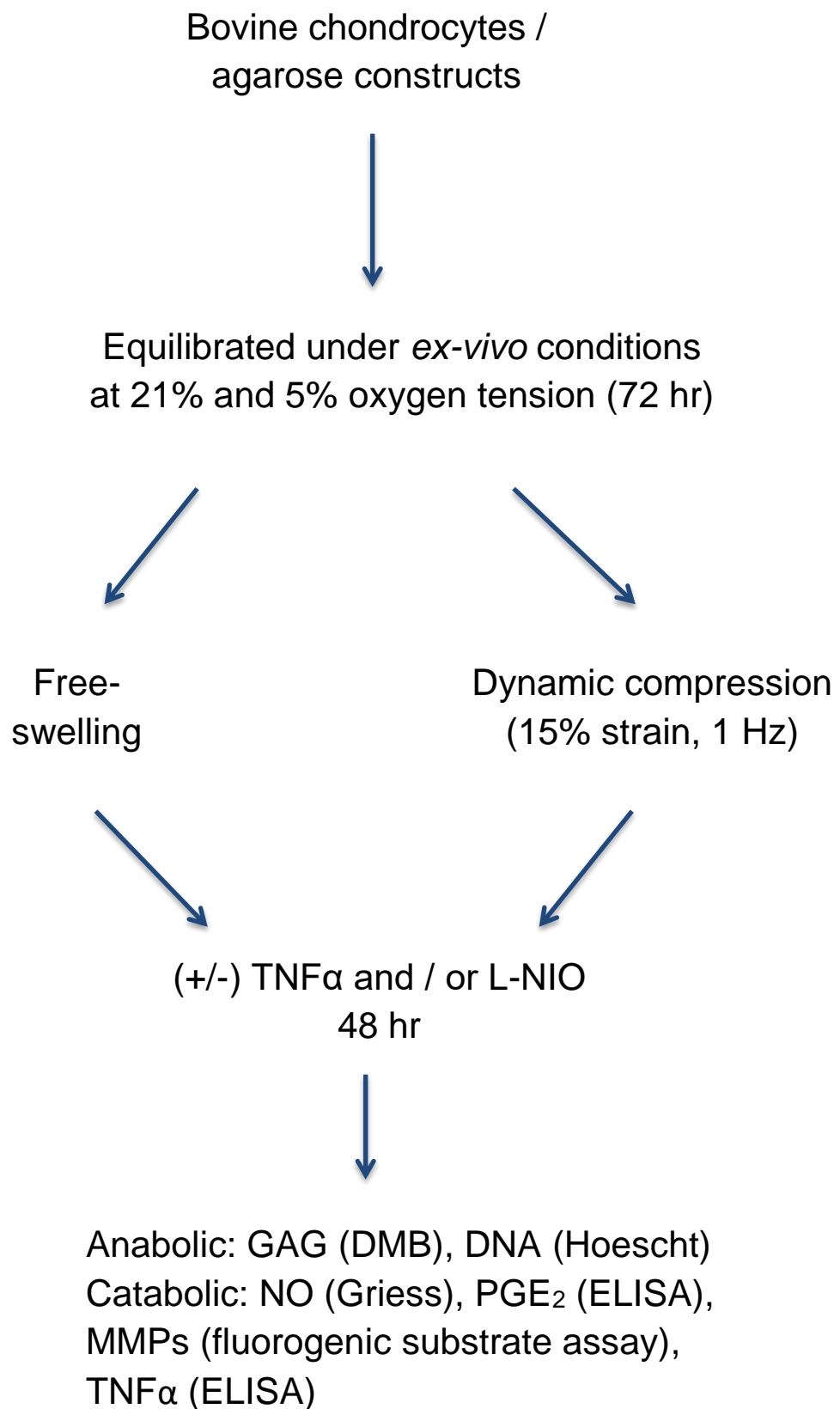


Figure 2.1. Flow chart illustrating the *ex-vivo* methods and protein analysis employed in the present study.

2.1 Justification of materials used

This chapter describes the 3D cell seeded agarose model employed throughout the experimental work, including the protocols and the cell straining apparatus adopted, as well as justifications for the materials and methods used. In the case of individual studies, the specific protocols incorporated are reported in the methods section of the appropriate chapters.

2.1.1 Agarose as a scaffold material

Over the past few years, there has been a significant change in the way cartilage mechanotransduction has been investigated, starting from the use of cartilage explants to the employment of 3D hydrogel constructs to study the effects of various loading modalities and inflammatory mediators on matrix synthesis in chondrocytes (Buschmann et al., 1995, Lee and Bader, 1997). More recently, attention has been focused on the intracellular signalling pathways which induce alterations in matrix synthesis on the application of external loads and inflammatory mediators in chondrocytes. In both approaches cartilage explants, although physiologically relevant, have inevitably resulted in complexity of data in relating input to output parameters (Aydelotte and Kuettner, 1988, Chang and Poole, 1996, Chowdhury et al., 2008). Accordingly, hydrogels provide an alternative and simpler solution to interpret the data. Indeed they have been widely used as scaffolds in tissue engineering due to their multiple sources and inherent properties, including their ability to withstand forces when subjected to mechanical testing, the ease with which they can be conformed into various shapes and sizes, their viscoelastic behaviour as well as their biocompatibility. Although many hydrogels have been used for culturing chondrocytes in a 3D environment, as demonstrated in table 1.4, the naturally occurring polymer, agarose, has been most extensively used for a number of reasons:

- The 3D homogenous model has been shown to maintain chondrocyte viability and phenotype for up to 70 days in culture (Lee and Bader, 1995; Buschmann et al., 1992, Aydelotte et al., 1988). This was confirmed by the ability of the seeded chondrocytes to retain their rounded morphology in agarose and induce the production of aggrecan and type II collagen.
- Agarose is capable of delivering mechanical stability by withstanding the application of compressive strains within physiological levels, which is transduced to the embedded chondrocytes, while maintaining reproducibility (Freeman et al., 1994, Knight et al., 1998, Chowdhury et al., 2001, Chowdhury et al., 2003, Akanji et al.,

2008, Chowdhury et al., 2008 Knight et al., 2006, Pingguan-Murphy et al., 2006, Lee and Bader, 1997, Chowdhury et al., 2008).

- Agarose allows sufficient diffusion of nutrients and disposal of waste products in a bioreactor system (Heywood 2004, 2006). In addition, its pore size allows the effective diffusion of pro-inflammatory cytokines, such as IL-1 β and TNF α , which enables it to be used to examine the combined effects of inflammatory agents and mechanical loading, on chondrocyte metabolism under both normoxic and hypoxic conditions (Aydelotte et al., 1992).
- Agarose has the potential to be degraded by agarase, thereby enabling space for extracellular matrix production over time.
- Agarose is amenable for analysis of cell proliferation and synthesis of both anabolic and catabolic markers, using standard biochemical assays.

The major limitation of the model is that it differs from the complex constituents and architecture of the cartilage ECM. Indeed the associated chondrocytes do not bind to agarose as in native ECM within the pericellular region. This will clearly influence the manner in which the mechanical signals will be transduced to the surface of chondrocytes.

Notwithstanding this limitation, it was decided that chondrocytes seeded in 3D agarose constructs would represent the most appropriate model system to address the aims and objectives of the present study.

2.1.2 Oxygen tension

The consideration of the oxygen tension represents an essential criterion when developing models for tissue engineering cartilage *in vitro*. Throughout this thesis, chondrocyte/agarose constructs cultured at 21% oxygen tension represented the standard culture conditions, which have been used by the vast majority of previous researchers. Indeed it is equivalent to the oxygen concentration in the atmosphere. Given the study aims, this normoxic condition was compared to those cultured at 5% oxygen tension, in order to examine the effects of hypoxia on chondrocyte metabolism, since healthy articular cartilage is well known to exist under low oxygen tensions *in vivo*. 5% oxygen tension was selected, since it lies within the range of oxygen tension present in healthy cartilage *in vivo*, which varies from approximately 8% in the superficial zone to as low as 1% in the deep zone (Falchuk, Goetzl, Kulka, 1970, Brighton & Heppenstall, 1971). At these low oxygen tensions, chondrocytes are well adapted in maintaining their phenotype, promoting ECM production and in the regulation of cartilage homeostasis (Heywood, Bader & Lee, 2006, Falchuk, Goetzl, Kulka, 1970; Nevo, Beit-Or,

Eilam, 1988). Given the availability of the equipment in the host laboratory, in particular the oxygen controlled incubators, only one hypoxic condition was examined for the majority of the experimental work.

2.1.3 Source of chondrocytes

It is accepted that human chondrocytes would provide the ideal source for clinical relevance. However, these cells are not readily available and when sourced from different individuals, often from joint surgery, they are highly variable in nature and highly dependent on the integrity of the cartilage from which they are extracted.

Accordingly, chondrocytes from bovine articular cartilage were used in this study as the tissue is readily available, relatively cheap and their use in agarose gel has been well characterised (Lee and Bader, 1995; Buschmann et al., 1992). Freshly slaughtered cattle aged <18 months (Dawn Cardington, Bedfordshire, UK) were selected for the isolation of full depth slices of articular cartilage, since the extracted chondrocytes are less prone to exhibiting pro-inflammatory symptoms associated with aged and/or injured chondrocytes, which would inevitably interfere with the signalling pathways induced by the exogenous factors to which the cells would be subjected.

Bovine chondrocytes were preferred over chondrocytes isolated from other animal species, since it has been well documented that bovine and human chondrocytes share similar features, such as identical phenotypes, as well as biochemical and biomechanical properties. For this reason, together with the fact that a significant cell population is obtained per joint, when compared to other species such as porcine cartilage, chondrocytes were isolated from bovine metacarpalphalangeal joints.

Additionally, the use of primary chondrocytes has proved ideal in cartilage mechanobiology studies incorporating 3D cell seeded scaffolds, since they are capable of synthesizing the required amount of pericellular matrix to facilitate mechanotransduction pathways, while preventing over-protective mechanisms to be developed. This is achieved by culturing them for a period of approximately 72 hours (Buschmann et al., 1992).

Furthermore, the source of human chondrocytes yields cells which are highly variable in terms of integrity of the cartilage from which they are derived (Chung and Burdick, 2007).

2.1.4 Purity of bovine cells

Although articular cartilage is known to be an anisotropic tissue, divided into four poorly defined zones, the cells isolated from full depth slices of bovine articular cartilage were not subjected to phenotyping in this study. This is because heterogeneous mixtures of cells from immature animals are typically incorporated into scaffolds which have been shown to yield chondrocytes that synthesize abundant levels of cartilaginous matrix, rich in type II collagen and aggrecan. Although this confirms the maintenance of chondrocyte phenotype, it is worth noting that the resulting 3D construct lacks zonal organisation (Chung and Burdick, 2007). Additionally, these cells have been previously characterized in 3D agarose constructs, as detailed in section 2.1.1 (Buschmann et al., 1992, Lee and Bader, 1995).

2.2 Cell seeded agarose model

The cell seeded agarose model involved seeding chondrocytes in agarose gel to form cylindrical shaped constructs. Chondrocytes from bovine articular cartilage were used in this study as the tissue is readily available and since the use of these cells in agarose gel has been well characterised (Lee and Bader, 1995; Buschmann et al., 1992). Hydrogels have been widely used as scaffolds in tissue engineering due to their multiple sources and inherent properties including their ability to withstand forces when subjected to mechanical testing, the ease with which they can be conformed into various shapes and sizes, their viscoelastic behaviour as well as their biocompatibility. In particular, the naturally occurring polymer, agarose, has been extensively employed in the tissue engineering of cartilage, as this 3D homogenous model has been shown to maintain chondrocyte viability and phenotype for up to 70 days in culture (Lee and Bader, 1995; Buschmann et al., 1992, Aydelotte et al., 1988). This was demonstrated by the ability of the seeded chondrocytes to retain their rounded morphology in agarose and induce the production of aggrecan and type II collagen. Additionally, chondrocyte-agarose models allow the effects of inflammatory agents on chondrocyte metabolism to be investigated (Aydelotte et al., 1992). Furthermore, agarose is capable of withstanding the application of compressive strains within physiological levels, which is transduced to the embedded chondrocytes, while maintaining reproducibility (Freeman et al., 1994, Knight et al., 1998, Chowdhury et al., 2001, Chowdhury et al., 2003, Akanji et al., 2008, Chowdhury et al., 2008).

2.2.1 Preparation of culture media and enzyme solutions

Culture media

The culture medium used throughout the experimental work was prepared using the reagents listed in Table 2.1. Initially, 4-(2-hydroxyethyl)-1-piperazineethanesulfonic acid (HEPES) buffer, L-glutamine, penicillin, streptomycin and L-ascorbic acid were added to 124ml of Foetal Calf Serum (FCS). The resultant FCS solution was filtered using a 0.22 μ m pore cellulose acetate filter, in order to ensure sterility, into 500ml of Dulbecco's Modified Eagle's Medium (DMEM, all from Sigma-Aldrich Ltd, Gillingham, Dorset, UK). The prepared culture media (DMEM + 20% FCS) with a pH of 7.4, was then aliquoted into 150ml sterile universal plastic containers (Sterilin, Caerphilly, UK) and stored at -20°C.

Table 2.1: Reagent concentration in the preparation of culture media for chondrocyte culture.

Reagent	Stock Concentration	Final Concentration	Quantity
DMEM	N/A	N/A	500ml
HEPES	1M	20mM	10ml
L-glutamine	200mM	2 μ M	5ml
Penicillin	5mg/ml	5 μ g/ml	5ml
Streptomycin	5mg/ml	5 μ g/ml	5ml
L-ascorbic acid	N/A	0.85 μ M	0.075g
FCS	N/A	20%(w/v)	124ml

Pronase and collagenase solutions

For the isolation of primary chondrocytes from bovine articular cartilage, the enzymes, pronase and collagenase were used. Pronase solution was prepared by adding 1g (per vial) of pronase powder (Sigma-Aldrich Ltd, Gillingham, Dorset, UK) with an activity of 5.9units/mg to 175ml of DMEM + 20% FCS. The resulting solution, with a final activity of 33.71units/ml, was then filtered using a 0.22 μ m pore cellulose acetate filter in order to ensure sterility and stored at -20°C in 10ml aliquots.

Collagenase solution was prepared by adding 1 vial of collagenase powder (1g, type XI clostridium histolyticum, Sigma-Aldrich Ltd, Gillingham, Dorset, UK) to the required volume of culture media, to obtain a solution with a final activity of 100units/ml. It is worth noting that the volume of DMEM + 20% FCS required for the preparation of this solution was calculated based on the specific activity of the batch of collagenase powder employed. Following this, the resultant solution was filtered using a 0.2 μ m pore filter and divided into 30ml aliquots, which were then stored at -20°C.

2.2.2 Isolation of primary chondrocytes from bovine joints

The present study incorporated the use of bovine chondrocytes which was obtained from tissue acquired from the local abattoir (Humphreys and Sons, Essex) with authorization of the relevant meat inspectors. The metacarpalphalangeal joints of freshly slaughtered cattle aged 18-24 months were initially washed thoroughly in hot water to eliminate any attached debris. The joints were then partially immersed in a disinfectant, Virkon for 5 min, followed by 70% Industrial methylated spirits (IMS) for an additional 15mins. In a sterilized dissecting tray, each joint was then transferred into a class II cabinet in order to isolate slices of articular cartilage under sterile conditions.

Using a no.20 scalpel blade, a longitudinal cut was made along the length of the joint, followed by a perpendicular cut across the short pastern. The hide on each side was then peeled back, exposing the joint capsule. Using 70% IMS, the joint surface was then cleaned while ensuring that any hair from the surface was removed. An insertion was then made into the joint capsule by following the groove round under it, while cutting back the surrounding ligaments and tendons such that the joint was dislocated, exposing the condyle surface. This was achieved using a no.11 scalpel blade. Once the joint was opened, full depth slices of articular cartilage were then carved from the proximal load bearing regions of the metacarpal surface using a no.10 scalpel blade (Fig. 2.2). The slices of cartilage were then incubated in a Ø50mm petri dish containing DMEM + 20% FCS at 37°C in 5% CO₂ and 21% O₂ for 24 hours. This was followed by finely dicing the cartilage tissue using a scissor motion, in order to enhance digestion and incubating them on rollers for 1h at 37°C in 10ml of pronase solution. The pronase solution was then removed and the tissue was then incubated for a further 16 hours at 37°C in 30ml of collagenase solution. Following enzymatic digestion, the cell supernatant containing released chondrocytes was passed through a 70µm pore cell sieve and centrifuged at 733xg (2000 rpm) for 5 min using a mid bench centrifuge (ALC International Multispeed Model PK131R). The supernatant was removed and resulting cell pellet was then washed twice and re-suspended in 20ml of DMEM + 20% FCS. Chondrocyte viability and yield were then assessed after which the cells were resuspended at a concentration of 8 x 10⁶ cells/ml.

A minimum of three joints were isolated per experiment, conditional to the number of cells required.



Figure 2.2. Isolation of full depth articular cartilage from bovine metacarpalphalangeal joint.

To assess the cell yield and viability in the cell suspension obtained from isolation; 20µl of the cell suspension was mixed with an equal volume of 0.4% trypan blue and added to the 0.1mm deep chamber of the haemocytometer. This mixture was then examined under the microscope at a magnification of x10, ensuring that the phenomenon of Newton's rings was observed. Non-viable cells were identified by their blue-stained cytoplasm, whereas viable

cells with an intact membrane exhibited clear cytoplasms. Typically, 95-100% cell viability was obtained from each cell suspension following isolation.

2.2.3 Preparation of cell seeded agarose constructs

Following the trypan blue dye exclusion assay, cells were re-suspended in medium at a concentration of 8×10^6 cells/ml for the preparation of 3D chondrocyte / agarose constructs. A suspension of agarose type VII in Earle's Balanced Salt Solutions (EBSS, Sigma Chemical Co., Poole, UK) was prepared at a concentration of 6% (w/v) and autoclaved at 121°C for 45 min, after which it was transferred to a 60°C oven for 1 hour and then allowed to cool on rollers at 37°C. Once the molten agarose was cooled, an equal volume of cell suspension was carefully added to it to yield a final cell concentration of 4×10^6 cells/ml in 3% (w/v) agarose. The chondrocyte/agarose suspension was mixed on rollers to achieve a uniform cell density and then transferred into a sterile stainless steel mould, containing holes of 5mm in diameter and 5mm in height. The agarose was allowed to gel at 4°C for 10 min to yield cylindrical constructs of the mould dimensions, which were then removed and transferred into a 24-well tissue culture plate. All constructs were equilibrated in 1 ml of DMEM + 20% FCS at 37°C in 5% CO₂ for 72 hours, after which they were subjected to various test/ex-vivo conditions as described subsequently.

2.2.4 Digestion of cell seeded agarose constructs

At the end of the application of various test conditions, constructs and their corresponding media were removed and stored at -20°C prior to biochemical analysis and at -80°C prior to qRT-PCR analysis. Digest buffer was prepared by first supplementing 480ml of phosphate buffer saline (PBS, Sigma-Aldrich Ltd, Gillingham, Dorset) solution with 5mM of ethylenediaminetetra-acetic acid (EDTA) and 5mM of L-cysteine hydrochloride monohydrate, followed by adjusting its pH to 6.0. Each construct was then incubated in 1ml of digest buffer at 70°C, after which they were allowed to cool at 37°C for 30mins. Constructs were then digested overnight at 37°C with 10 unit/ml agarase followed by 1 hour at 60°C with 2.8 unit/ml papain (All from Sigma-Aldrich Ltd, Gillingham, Dorset, UK), as previously described (Lee and Bader, 1997, Lee and Knight, 2004).

2.3 Uninterrupted culture system – Biospherix incubator

The effect of 5% and 21% oxygen tension were examined in constructs cultured under free-swelling conditions in a glove-box style workspace integrated within a closed incubator (Fig. 2.3; Biospherix Ltd, Lacona, NY, USA) to ensure that the experimental conditions during set-up were uninterrupted, as previously described (Heywood et al., 2006).



Figure 2.3. The Biospherix incubator

2.4 Mechanical loading

2.4.1 Mechanical loading apparatus

A novel *ex-vivo* bioreactor (Bose ElectroForce, Gillingham, UK) was incorporated for the application of intermittent uni-axial compressive strain to 3D chondrocyte/agarose constructs cultured at 5% and 21% oxygen tensions. The cell-straining apparatus (Fig. 2.4A) comprised of a controlled loading system which was placed in the Biospherix incubator (Fig. 2.4B) to maintain a sterile tissue culture environment. Application of dynamic compression was achieved through an electromagnetically controlled vertical actuator which was connected to a load cell capable of withstanding a maximum of 225N (BOSE ElectroForce System Group, Minnesota, USA). The vertical movement of the actuator was assessed by a Linear Variable Differential Transformer (LVDT DG 2.5 Guided, SolartronMetrology, RS Components Ltd, Corby, UK), which was linked via a central rod to a custom designed mounting plate located within a Perspex chamber. With the help of a locking screw the relative movement of the central rod to the Perspex chamber was controlled. The mounting plate consisted of a matrix of 24 holes which were equally disturbed across its five segments. These segments were held together in place by locating rods and clamping nuts. Each of the 24 holes accommodated an equal number of 316L stainless steel loading pins (\varnothing 4mm \times height 31mm, 2g mass) connected to circular platen heads (\varnothing 11mm). The innermost holes restrained the vertical motion of 12 stainless steel pins, while the outer ones allowed free movement of the other 12 identical loading pins. Prior to set-up of the cell-straining apparatus, the Perspex chamber, mounting plate and loading pins were all sterilized and placed in a class II cabinet flow hood to maintain sterile conditions (Lee and Bader, 1997).

2.4.2 System set-up for the application of dynamic loading

Constructs were transferred into individual wells of a 24-well culture plate (Costar, High Wycombe, UK) and loaded onto the mounting plate in the Perspex chamber such that each pin was located directly above each centrally located construct in the 24-well plate. The 12 innermost pins were then released, ensuring that each pin was in contact with the surface of a cylindrical construct. This was followed by clamping the pins to keep them in place. Once the mounting plate and constructs were aligned, 1ml of DMEM + 20% FCS was supplemented to each construct by the means of a syringe and a right-angled needle. The Perspex box was then transferred into the Biospherix incubator and the central rod connected to the actuator. The outermost constructs represented control specimens which, due to the weight of the pins, were subjected to an equivalent tare strain of 0.2% throughout the test protocol. On the other hand, the innermost constructs were subjected to intermittent compression under unconfined conditions, with a profile of 10 min compression followed by

a 5 hour 50 min unstrained period for 48 hours, as previously described. The *ex-vivo* conditions had been previously reported to be optimal when measuring the production of inflammatory mediators and protein synthesis (Parker et al., 2013, Raveenthiran & Chowdhury, 2009, Chowdhury, Bader and Lee, 2001). The dynamic compression regime was applied at a strain amplitude of 0-15 % using a sinusoidal waveform at a frequency of 1 Hz, resulting in a total of 4800 duty cycles during the 48 hour culture period.

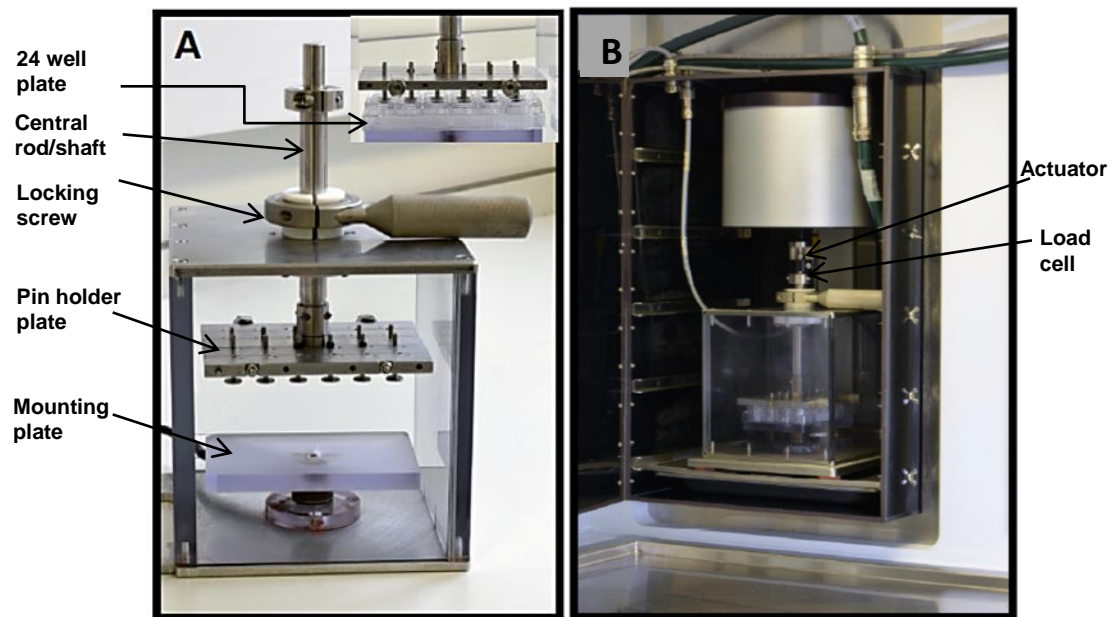


Figure 2.4. The *ex vivo* 3D/bioreactor system. Bose bioreactor cell straining apparatus (A) integrated with the Biospherix (B). Inset in (A) shows custom designed compressive mounting plate with loading pins positioned above a 24-well culture plate.

2.5 Biochemical analysis

2.5.1 DNA quantification

The DNA content in each chondrocyte/agarose construct was quantified using the fluorometric dye, Hoechst 33258 as a means of assessing cell proliferation (Kim et al., 1988). The DNA-specific stain binds to contiguous adenine-thymine base pairs, resulting in the emission of fluorescence at a wavelength of 460nm (Lee et al., 1997, Rao and Otto, 1992).

Initially, saline sodium citrate (SSC) was prepared by adding 44.1g of trisodium citrate and 87.65g of sodium chloride to 500ml of distilled water. The resulting solution was then adjusted to pH 7.0 with 1M of hydrochloric acid or 1M of sodium hydroxide. The buffer was then diluted by a factor of 20 and an equal volume was added to a solution of 0.01M PBS containing 0.7g of cysteine hydrochloride and 0.4g of EDTA, resulting in a ratio of 1:1. A serial dilution of calf thymus type XV DNA (all reagents supplied by Sigma-Aldrich, Poole, UK) was then prepared in the SSC/PBS buffer to generate concentrations ranging between 0 and 20 μ g/ml (0, 0.31, 0.62, 1.25, 2.5, 5, 10 and 20 μ g/ml). 100 μ l of each concentration of DNA was then pipetted the wells of a 96-well plate in triplicates, along with an equal volume of each digested chondrocyte/agarose construct. A volume of 100 μ l of 1 μ g/ml Hoechst 33258 (in digest buffer) was then added to all the samples and standards. Finally, using a fluorometer (FLUOstar, BMG Labtech Ltd., Aylesbury, UK), fluorescence was then measured at an excitation wavelength of 355nm and an emission wavelength of 460nm, which corresponded to the total DNA content per chondrocyte/agarose construct, using the standard curve as shown in figure 2.5.

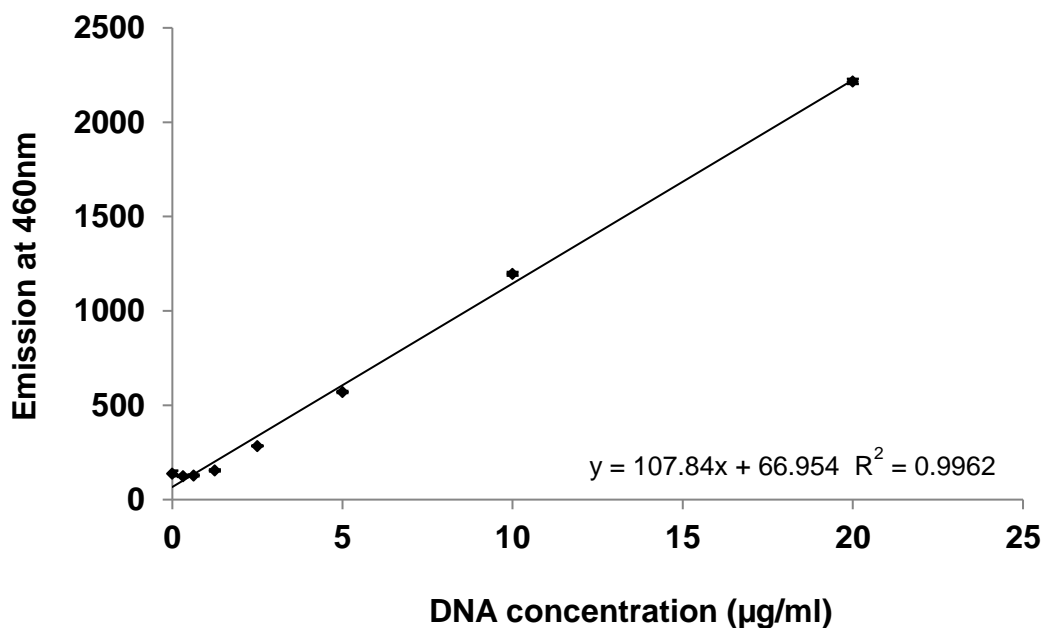


Figure 2.5. DNA standard curve obtained from fluorometer at an emission and excitation wavelength of 355nm and 460nm, respectively, which was then used to determine the concentration of DNA in each chondrocyte/agarose construct (Error bars represent SD of 3 replicates).

Results from the Hoechst 33258 standards were plotted as DNA concentration versus fluorescence with a linear trendline fitted to the data. The graph was then used to calculate the absolute concentrations of DNA in each sample. The total DNA content derived from the fluorometric assay was subsequently used to normalise GAG synthesis. Additionally, the cell number within each construct was determined by dividing the total quantity of DNA by the average amount of DNA present in a single primary bovine chondrocyte, typically 7.7pg (Kim et al., 1988).

2.5.2 Quantification of GAG synthesis

Proteoglycan aggrecan is one of the major matrix macromolecules present in articular cartilage and has a great impact on the healthy functioning of the tissue. It consists of a multi-domain globular core protein to which numerous sulphated GAG chains are attached (Kiani et al., 2002), as described in chapter 1. In cell culture models, an increase in proteoglycan synthesis results in the release of this proteoglycan into the culture supernatant, which can be assessed by assaying the GAG content of the culture medium. During this process, some of the GAG remains bound up with cells in the 3D scaffold, which makes it necessary for the GAG content of the scaffold to be also examined. Another factor responsible for the release of GAG into the culture supernatant in 3D cell culture models is the response of cells to damaging factors such as cytokines (Wann et al., 2010). As such, in subsequent studies a well-established spectrophotometric assay, involving the use of the 1,9-dimethylmethylene blue dye (DMMB, Sigma-Aldrich, Poole, UK) was employed for the quantification of GAG content in chondrocyte seeded agarose constructs (Farndale et al., 1982, Enobakhare et al., 1996). The binding of the cationic dye to the negatively charged carboxyl and sulphate groups of GAGs induces a metachromatic shift of the absorbance peak from 600nm to 535nm, which can be detected using a spectrophotometer. This method has proven to be a reliable and convenient means of quantifying the turnover of aggrecan and proteoglycan synthesis in cultured chondrocyte/agarose constructs.

Once chondrocyte/agarose constructs were digested with papain and agarose as previously described in section 3.2.5, both media and digested constructs were assayed for sulphated GAGs in duplicates. Initially, a stable solution of DMMB was prepared by dissolving 2g of sodium formate, 0.016g of DMMB and 5ml of ethanol in 1000ml of water, using a magnetic stirrer. The pH of the resulting solution was then adjusted to 3.0 with either 1M sodium hydroxide or 1M hydrochloric acid (all reagents supplied by Sigma-Aldrich, Poole, UK) and stored at room temperature while ensuring it was protected from light at all times. Using a 1mg/ml stock solution, a serial dilution of bovine chondroitin 4-sulphate standards were then prepared at concentrations ranging from 0 to 50µg/ml, at increments of 5µg/ml in distilled water. 40µl of each standard was then aliquoted in duplicates into each well of a 96-well plate, along with an equal volume of agarose/papain digests or the corresponding media in

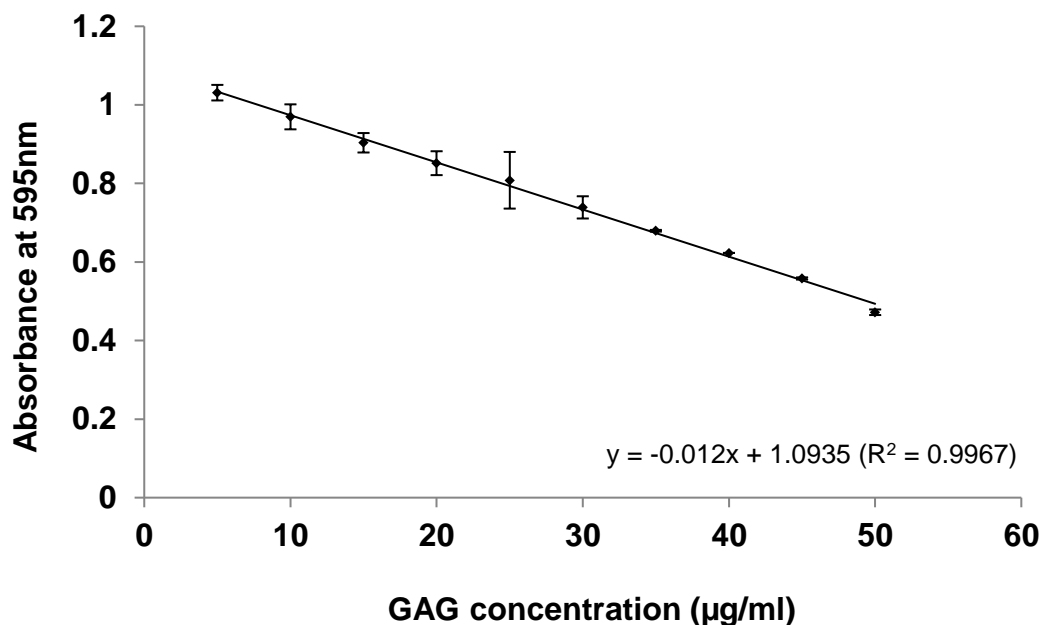


Figure 2.6. Standard curve for chondroitin 4-sulphate complexed with DMB and measured at an absorbance of 595nm (Error bars represent SD of 2 replicates).

separate wells. A volume of 250µl of DMMB (100µg/ml) was then added to all samples and standards, followed by the immediate measurement of absorbance using a spectrophotometer (FLUOstar, BMG Labtech Ltd., Aylesbury, UK), at a wavelength of 595nm. This resulted in the generation a standard curve as shown in figure 2.6.

Results from the chondroitin 4-sulphate standards were plotted as GAG concentration versus absorbance with a linear trendline fitted to the data. The graph was then used to calculate the absolute concentrations of sulphated GAG in each sample. Total GAG synthesis in each digest and its corresponding medium was then calculated and normalised to its DNA concentration as shown in equation 3.1.

$$[GAG_{synth}] = \frac{\{[cGAG] + [mGAG]\}}{[cDNA]} \quad \text{Equation 2.1}$$

Where:

[GAG_{synth}] = Total GAG synthesis

[cGAG] = GAG measured in agarose construct

[mGAG] = GAG measured in the corresponding medium

[cDNA] = DNA measured in agarose construct

2.5.3 Quantification of nitric oxide release

In oxygenated solutions, nitric oxide ($\cdot\text{NO}$) is converted into nitrate (NO_3) and nitrite (NO_2). $\cdot\text{NO}$ production can be determined by quantifying its derivative NO_2 , spectrophotometrically

in the media of cultured cells. Upon reacting with Griess reagent, NO_2 can be identified at a wavelength 550nm (Gross et al., 1991). However, one of the limitations associated with this assay is the lack of sensitivity and ability to detect nitrate levels in the culture supernatant. As such, nitrate must first be converted into nitrite for total nitrite production ($\text{NO}_2 + \text{NO}_3$) to be quantified. For example, Marzinzig reduced nitrate to nitrite with the use of nitrate reductase in order to determine $\cdot\text{NO}$ production (Marzinzig et al., 1997). Nevertheless, $\cdot\text{NO}$ can form numerous nitrogen intermediates, including peroxy nitrite and nitrosothiols, which would need to be identified and measured in order to accurately quantify $\cdot\text{NO}$ production. The detection of nitrite is limited to values between 1 and $4\mu\text{M}$ and forms roughly 20% of $\cdot\text{NO}$ (Fermor et al., 2001). However, the Griess assay assumes that the ratio of nitrite to nitrate remains constant

Initially, a stock solution of $100\mu\text{M}$ sodium nitrite (NaNO_2) was diluted using phenol red deficient culture media to yield concentrations of NaNO_2 standards ranging from 0 to $50\mu\text{M}$, at increments of $5\mu\text{M}$. $50\mu\text{l}$ of each standard was then aliquoted in duplicates into each well of a 96-well plate, along with an equal volume of sample in separate wells.

85% stock solution of orthophosphoric acid was diluted to 5% in distilled water, and was used to prepare the Griess reagent which consisted of 1% (w/v) sulphanilamide and 0.01% (w/v) naphthylethylenediamine (NED) in 5% orthophosphoric acid, respectively (all reagents supplied by Sigma-Aldrich, Poole, UK). Equal volumes of these reagents were then mixed together, and $50\mu\text{l}$ of the Griess reagent was added to samples and standards in the 96-well plate. The plate was then immediately transferred onto the Ascent plate reader, which was used to measure absorbance at 550nm, followed by the generation of a standard curve, as illustrated in figure 2.7.

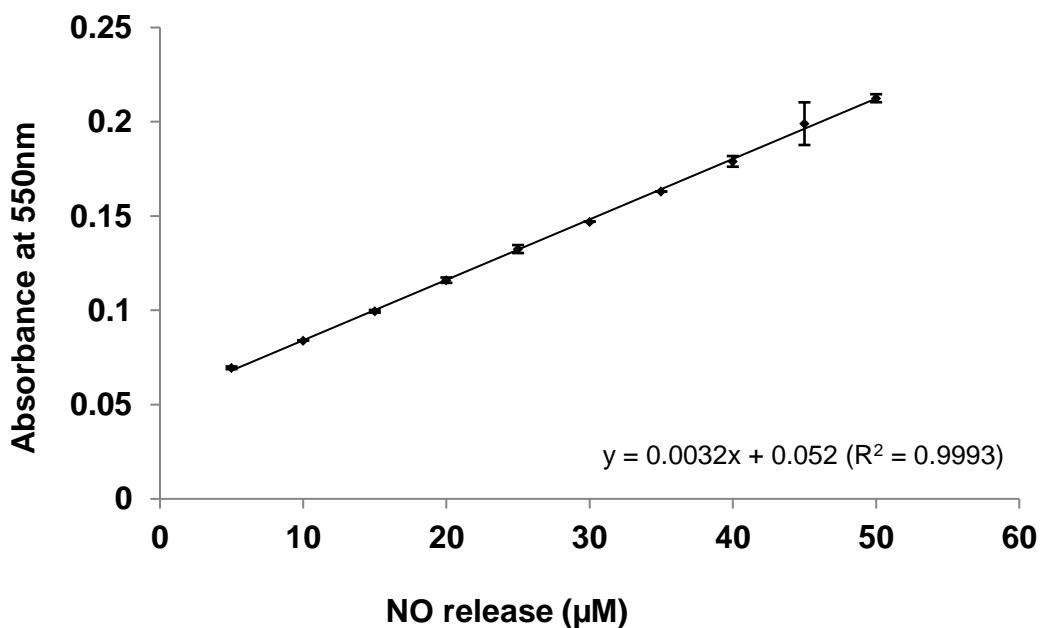


Figure 2.7. Nitrite standard curve (Error bars represent SD of 2 replicates).

The Griess reagent converts nitrite into an azo compound which has an absorbance peak at 550nm, hence permitting the precise quantification of nitrite concentration within the culture supernatant. Results from the NaNO₂ standards were plotted as nitrite concentration versus absorbance with a linear trendline fitted to the data. The graph was then used to calculate the absolute concentrations of nitrite released into the culture media of each sample.

2.5.4 Quantification of PGE₂ synthesis

Prostaglandins belong to the class of prostanoid fatty acid derivatives of arachidonic acid, which is released on the action of phospholipidases on membrane phospholipids. The arachidonic acids are then converted into PGG₂ and PGH₂ by the cyclooxygenases, COX-1 and COX-2. Finally, PGE₂ is formed when prostaglandin E₂ synthetase (PGES) acts on PGG₂ and PGH₂. PGE₂ is produced by a variety of cell types including monocytes and macrophages. COX and PGES exist in different isoforms too, which can be constitutively or inducibly activated by inflammatory stimuli. An increase in the levels of PGE₂ is observed in various pathological conditions, including inflammation, arthritis, fever, tissue injuries and a wide variety of cancers. However, PGE₂ synthesis can be blocked either with the use of corticosteroids which inhibit phospholipases or with the use of non-steroidal anti-inflammatory drugs (NSAIDs), which inhibit COXs.

In the present work, PGE₂ synthesis was quantified in culture supernatants, using a high sensitivity enzyme immunoassay (EIA) kit, according to manufacturer's instructions (R&D Systems, Abingdon, Oxfordshire, UK). The assay is a 3.5 hour forward sequential competitive enzyme immunoassay which involves the competition of PGE₂ present in a sample with horseradish peroxidase (HRP)-labelled PGE₂ for the limited number of binding sites on a mouse monoclonal antibody.

Prior to carrying out the assay, all frozen reagents of the PGE₂ ELISA kit were brought to room temperature (20°C), which included wash buffer concentrate, PGE₂ standard, calibrator diluent RD5-56, primary antibody solution, PGE₂ conjugate, color reagents A, color reagent B and stop solution, as shown in table 2.2.

Once the reagents were fully thawed, the wash buffer was prepared by carrying out a 1:25 dilution of the wash buffer concentrate with distilled water. The PGE₂ standard was then reconstituted with 1ml of distilled water to yield a stock solution of 25,000pg/ml. This solution along with the calibrator diluent RD5-56 was then used to prepare a serial dilution of PGE₂ standards with concentrations ranging from 0 to 2500pg/ml. In the non-specific binding (NSB) wells of the 96-well plate, 200µl of calibrator diluent RD5-56 was aliquoted in duplicates to serve as zero standards. The sample preparation process was then initiated by first pipetting 50µl of samples and standards into the remaining wells of the 96-well plate,

followed by 100µl of calibrator diluent RD5-56. 50µl of primary antibody solution was then added to all wells, excluding the NSB wells, leaving all but the NSB wells blue in colour.

Table 2.2: Composition of reagents supplied used for PGE₂ quantification.

Reagent	Composition
96-well microliter plate	Polystyrene microplate coated with goat anti-mouse polyclonal antibody
Wash buffer concentrate	A 25-fold concentrated solution of buffer surfactant.
PGE₂ standard	25,000pg of lyophilised PGE ₂ standard
PGE₂ antibody solution	Lyophilised PGE ₂ antibody diluted with 6ml of assay buffer
PGE₂ conjugate	Lyophilised PGE ₂ conjugated to horseradish peroxidase, diluted in 6ml of assay buffer
Calibrator diluent RD5-56	Buffered protein based solution
Color reagent A	Stabilised hydrogen peroxide solution
Color reagent B	Stabilised chromagen (tetramethylbenzidine) solution.
Stop solution	2N sulphuric acid

*It is worth noting that the concentrations of some of the above reagents were propriety due to the discretion of the company and as such were not provided to the author.

The 96-well plate was then securely covered with a plate sealer and incubated for 1 hour at room temperature on a horizontal orbital microplate shaker set to orbit at 0.12", at a speed of 500±50rpm. The purpose of this first incubation was to allow the PGE₂ present in samples to bind to the limited mouse monoclonal antibody. Following this, 50µl of PGE₂ conjugate was added to all wells, resulting in a colour change from blue to violet. The 96-well plate was then sealed with a coverslip and a second incubation was carried out for 2 hours on a horizontal orbital shaker set at the same conditions as the first incubation. This incubation permitted binding of the (HPR)-labelled PGE₂ present in the PGE₂ conjugate to the remaining antibody sites. Once the second incubation period was completed, all the wells of the 96-well plate were aspirated and washed using wash buffer in a squirt bottle, while ensuring the removal of all unbound materials from the wells. This process was repeated 3 times, after which the plate was blotted against clean paper towels in order to remove any remaining wash buffer from the wells. A light sensitive substrate solution was then prepared by mixing equal volumes of color reagents A and B, 200µl of which was then added to all wells of the 96-well plate in order to determine the bound enzyme activity. A further 30 minutes incubation of the samples was then carried out on a bench top, at room temperature, while ensuring that the plate was protected from light at all times. Finally, 100µl of the stop solution provided was added to all wells to stop the colour development, which resulted in a colour change of the wells from blue to yellow. The optical density (OD) of each

well, was then determined with the use of the Ascent spectrophotometer, at a wavelength of 450nm, within 30 minutes of adding the stop solution. On processing the 96-well plate using the plate reader, the mean OD of the NSB wells were then subtracted from that of each PGE₂ standard as shown in equation 3.2. A standard curve was then constructed by plotting these values (Final OD) on a linear y-axis versus PGE₂ concentration in a logarithmic form, as shown in figure 2.8. A best fit curve was then drawn through the points on the graph and used to calculate the final PGE₂ concentration of each sample in the 96-well plate. The sensitivity of the assay was equivalent to 30.9pg/ml.

$$\text{Final OD} = \text{Standard OD} - \text{NSB OD}$$

Equation 2.2

Where:

[Standard OD] = Mean optical density of each PGE₂ standard

[NSB OD] = Mean optical density of NSB wells

[Final OD] = Final optical density

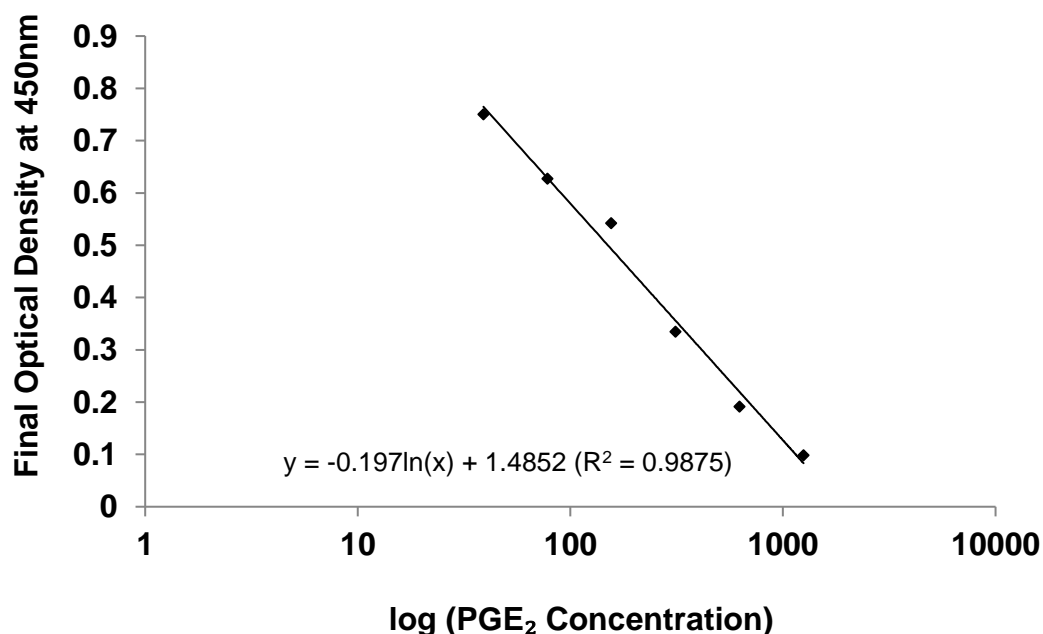


Figure 2.8. PGE₂ standard curve ranging from 39 to 1250pg/ml.

2.5.5 Total MMP activity measurement using fluorogenic substrate

In the study, MMP activity was kinetically assayed by employing the fluorogenic peptide substrate, Dnp-Pro- β -cyclohexyl-Ala-Gly-Cys(Me)-His-Ala-Lys(Nma)-NH₂ (Dnp=2, 4-dinitrophenyl; Nma=N-Me-2-aminobenzoyl; N-Me=anthranilic acid; Enzo Life Sciences, Exeter, UK), which can measure the activity of MMP-1, -3, -7, -8, -9, -11, -12, -13 and -14. The peptide is also capable of detecting MMP-2 activity but only to a relatively lower extent compared to the aforementioned MMPs. On the introduction of an active protease to the fluorogenic peptide substrate, cleavage of the bond which exists between Gly-Cys (Me) (fluorophore) occurs, resulting in an increase in fluorescence by Nma (quencher) at 440nm, once it is separated from the aromatic Dnp moiety. This increase in fluorescence can be detected by a fluorometer in the form of a kinetic profile as shown in figure 2.9. The gradient of the linear region of the graph is then calculated, which corresponds to the amount of active protease activity present per sample (Mohan et al., 2002, Fields, 2000).

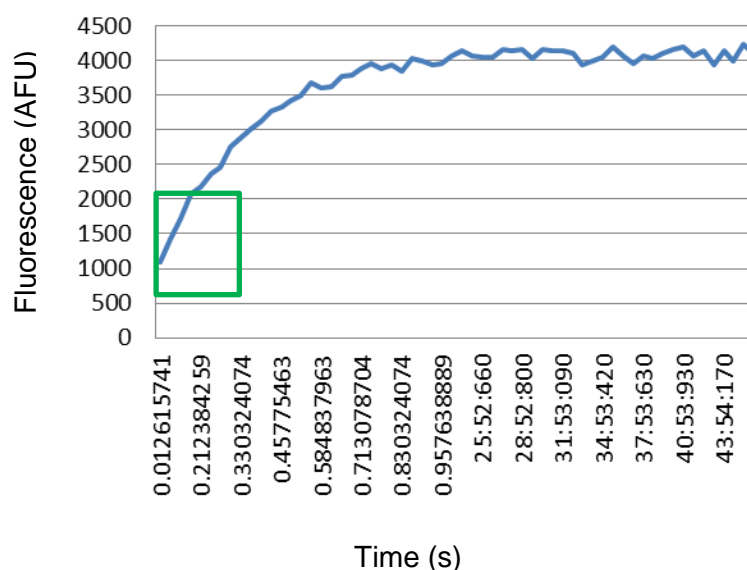


Figure 2.9. Fluorescence changes in MMP-1 activity to show kinetic performance during incubation with time (sec). Note the initial rate of hydrolysis before the reaction reached plateau. The change of fluorescence with time should be calculated from the linear part of the reaction (green square).

2.5.5.1 Established assay procedure

The following section provides a detailed description of an established assay for determining MMP activity using the fluorogenic peptide substrate. A stock solution of the Fluorogenic peptide Substrate (Dnp-PChaGCHAK(Nma), Enzo Life Sciences, Exeter, UK) was initially prepared by adding 1mg of the substrate (per vial) to the required volume of

dimethylsulfoxide (DMSO, Sigma-Aldrich, Dorset, UK) to form a peptide solution with a resultant concentration of 20mM. In order to achieve an accurate concentration of the peptide solution for each batch, the precise volume of DMSO required must be calculated by taking the specific purity and content of the peptide into account. A sample calculation for the volume of DMSO required to achieve 20mM of stock solution from a fluorogenic peptide substrate with a purity of 97% and content of 86.4% is as follows:

Equation 2.3:

$$\left(\frac{mol}{1077.2g}\right) \times \left(\frac{1 \times 10^3 mmol}{mol}\right) \times \left(\frac{L}{20 mmol}\right) \times \left(\frac{1 \times 10^6}{L} \mu l\right) \times \left(\frac{g}{1 \times 10^3 mg}\right) \times (0.864 \times 1 mg) \times (0.97) = 38.9 \mu l \text{ DMSO}$$

It should be noted that the fluorogenic MMP substrate is light sensitive and, as such, must always be light protected, even during stock preparation. The resulting stock solution was then divided into 4 μ l aliquots and stored at -20 $^{\circ}$ C.

Following this, a 10X assay buffer was prepared by adding the reagents (all purchased from Sigma-Aldrich, Dorset, UK) listed in Table 2.3 into a 150ml universal container (Sterilin, Caerphilly, UK). A magnetic stirrer was then used to ensure that all solutes were completely dissolved. The pH of the resulting solution was then adjusted to 7 with either formic acid or sodium hydroxide (NaOH).

Table 2.3: Reagents required for the preparation of 10X substrate assay buffer.

Reagents	Final Concentration	Amount of reagent
HEPES buffer	500mM	100ml
Calcium chloride (CaCl₂)	100mM	1.1098g
Brij-32	0.5%	1.67ml

In order to detect the activity of MMP-2, the 10X substrate assay buffer was modified by adding 100 μ M of zinc chloride (ZnCl₂).

Since this assay was light sensitive in nature, a white, opaque, flat-bottomed, uncoated 96-well plate (ThermoFisher Scientific, UK) was required to run the test in order to determine the total MMP activity in the culture supernatant of each chondrocyte/agarose constructs. On the completion of each experiment, 20 μ l of culture supernatant was pipetted into each well of the 96-well plate in duplicate and sealed with a cover slip before storing the plate at 4 $^{\circ}$ C. The 1x substrate assay buffer was prepared using the reagents listed in Table 2.4, such that the MMP substrate stock solution was used at a final concentration of 10 μ M. Since a 96-well plate was used, sufficient amounts of 1x substrate assay buffer was prepared for >96 wells or reactions (100 reactions, Table 2.4), ensuring that all of the 96-well plates were utilized.

Table 2.4: Reagents required for the preparation of 1x substrate assay buffer.

Reagents	Volume of reagents per reaction (μl)	Volume of reagents per 100 reactions (μl)
10x substrate assay buffer	7	700
20mM fluorogenic MMP substrate	0.035	3.5
Distilled water	43	4300

Once the 1x substrate assay buffer was prepared, the 96-well plate was removed from 4°C, followed by pipetting 50 μl of the prepared 1x substrate assay buffer to 20 μl of culture supernatant in each well. In order to run a negative control, at least 2 wells contained only 50 μl of 1x substrate assay buffer. The plate was then quickly transferred to the FLUOstar (BMG Labtech Ltd, Aylesbury, UK), followed by the selection of plate reader settings listed in Table 2.5 and the fluorometer was used at excitation wavelength of 340nm and an emission wavelength of 460nm. Figure 2.10 illustrates the kinetic profile obtained from running the described assay.

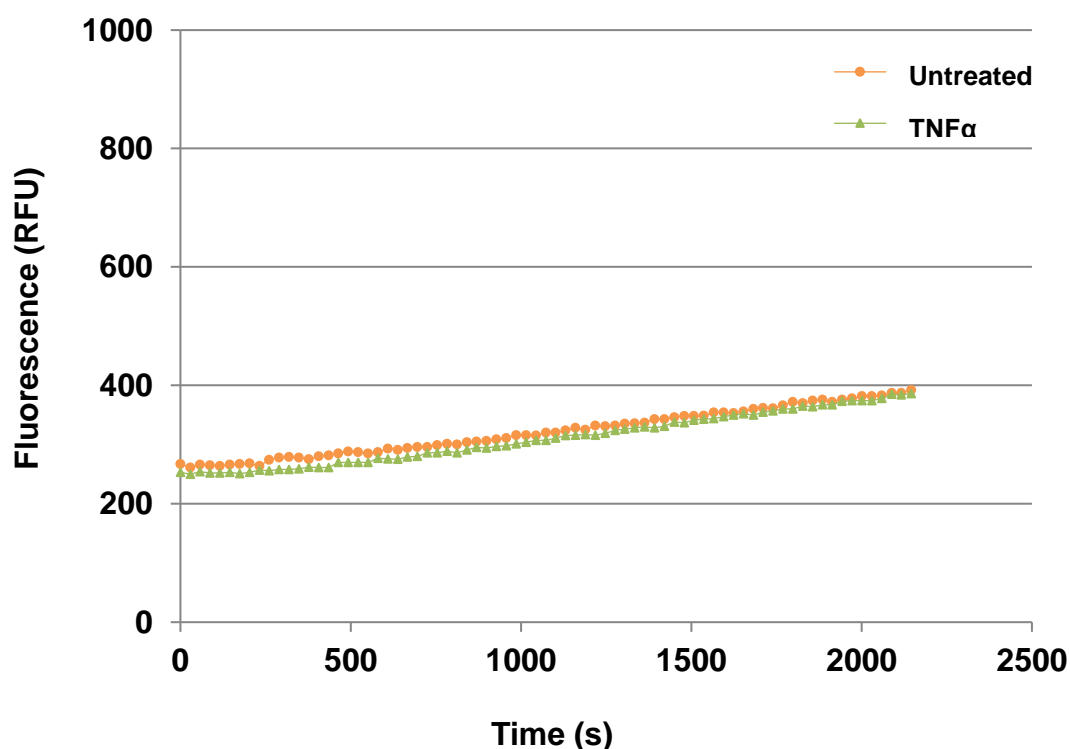


Figure 2.10. Kinetic profile obtained from performing the established fluorogenic substrate peptide assay on culture supernatants obtained from treating chondrocyte/agarose constructs with 0 or 10ng/ml of TNF α for 48 hours. RFU = Relative fluorescence unit.

Figure 2.10 shows the kinetic profile obtained from performing the established fluorogenic substrate peptide assay on culture supernatants obtained from treating chondrocyte/agarose

constructs with 0 or 10ng/ml of TNF α for 48 hours. It was observed that only a marginal increase in fluorescence with time was obtained from performing the established assay on both samples. Instead, constant fluorescence was observed with time. Also, the kinetic profile generated was incomplete and did not plateau to confirm the completion of hydrolysis of the fluorogenic substrate. Failure to acquire the standard kinetic profile (Fig. 2.9) may have been due to a number of factors, which will be discussed in the optimization section below (section 2.5.5.2). Figure 2.11 illustrates the trial and error steps taken in optimizing the MMP fluorogenic substrate assay, starting from the established assay described above.

Table 2.5: Plate reader settings for fluorogenic MMP substrate assay.

Plate reader settings	Measurement
Plate mode	Kinetic, fluorescence
Microplate	Nunc maxisorp 96
N° of cycles	25
N° of flashes	20
Positioning delay	0.5s
Reading direction	Horizontal reading
Cycle time	110s
N° of multichromatics	1
Excitation filter	340nm
Emission filter	460nm
Gain	64
Temperature	25°C
Start reading	1s

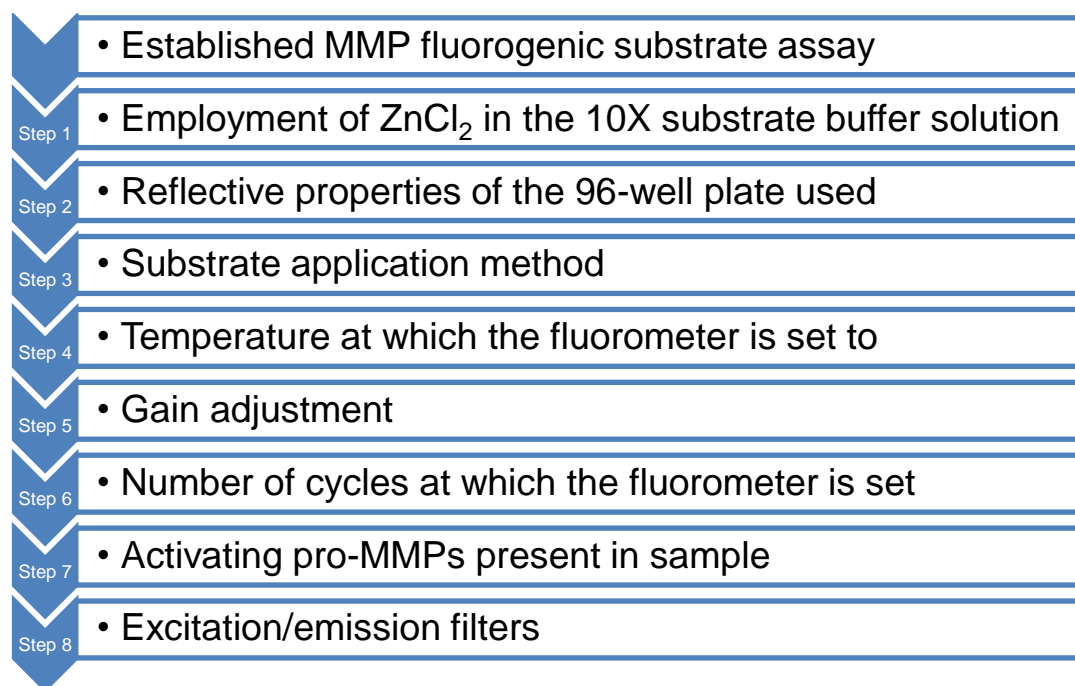


Figure 2.11. Flow chart illustrating the trial and error steps taken in optimizing the MMP fluorogenic substrate assay, starting from the established assay.

2.5.5.2 MMP Optimization

I. $ZnCl_2$ supplement

On addition of $ZnCl_2$ to the 10X substrate buffer solution in order to detect the activity of MMP-2 (Fields, 2000, Enzo Life Sciences, Exeter, UK), less fluorescence was observed when compared to buffers which were not supplemented with $ZnCl_2$ (Fig. 2.12). As such, 10X substrate assay buffer prepared for subsequent steps of the optimization process of the assay were not supplemented with $ZnCl_2$, as shown in Table 2.6.

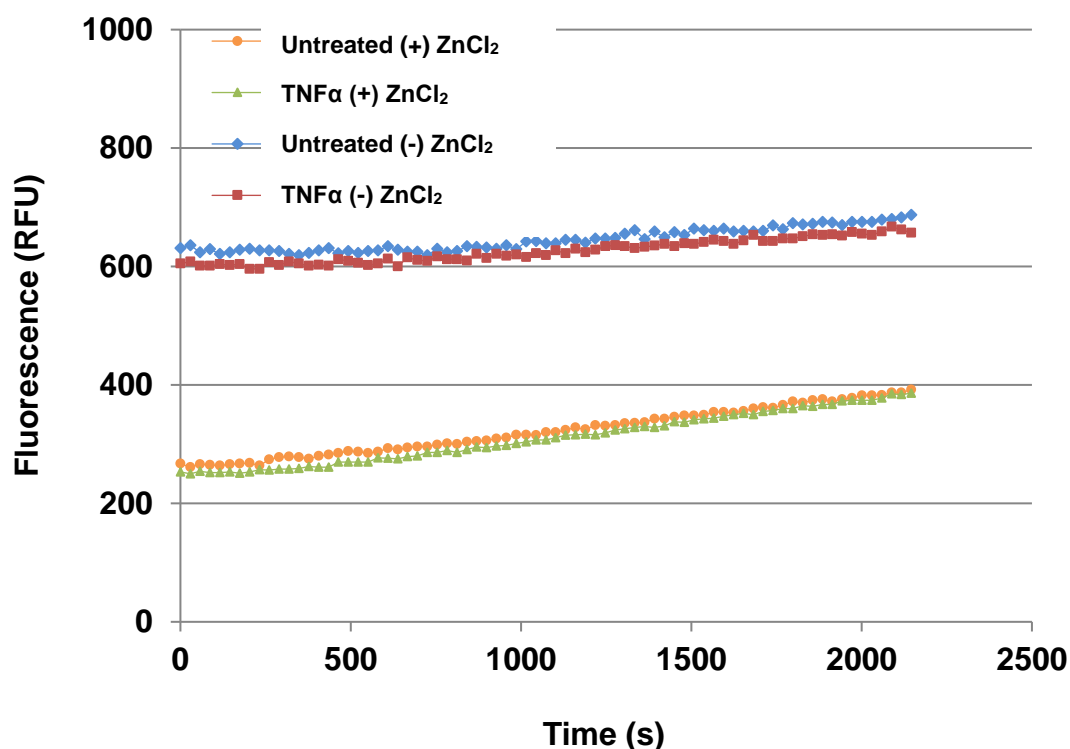


Figure 2.12. Kinetic profile obtained from performing the established fluorogenic substrate peptide assay on culture supernatants obtained from chondrocyte/agarose constructs cultured with 0 or 10ng/ml of TNF α for 48 hours in the presence and absence of $ZnCl_2$. RFU = Relative fluorescence unit.

II. Reflective properties of 96-well plate

Due to the employment of the fluorogenic peptide substrate, the assay was considered to be light-sensitive, implying that the use of opaque 96-well plates were essential in carrying out the entire assay. As such, either black or white flat bottomed, uncoated 96-well plates could be employed. In our initial MMP assay, a white, flat-bottomed, uncoated 96-well plate was used (Thermo Fisher Scientific, UK), which resulted in the measurement of fluorescence readings which remained constant throughout (Fig. 2.10). The primary difference between white and black plates is their reflective properties. While white plates reflect light and maximize the light output signal, black plates absorb light and reduce background

fluorescence and crosstalk. For these reasons, white plates are commonly used for luminescent assays and black plates are used for fluorescent assays, particularly those which employ fluorophores with short half-lives. However, time-resolved fluorescence assays usually use longer half-life fluorophores and can use either white or black plates (Promega, Southampton, UK). For these reasons, a black, flat-bottomed, uncoated 96-well plate (Thermo Fisher Scientific, UK) was employed in order to test this theory and further optimise the assay. The use of black plates however (Fig. 2.13), did not lead to any differences in the results obtained from performing the fluorogenic substrate assay in white plates, where samples were treated without $ZnCl_2$. As such, subsequent optimization steps were performed with the use of white, flat-bottomed, uncoated 96-well plates.

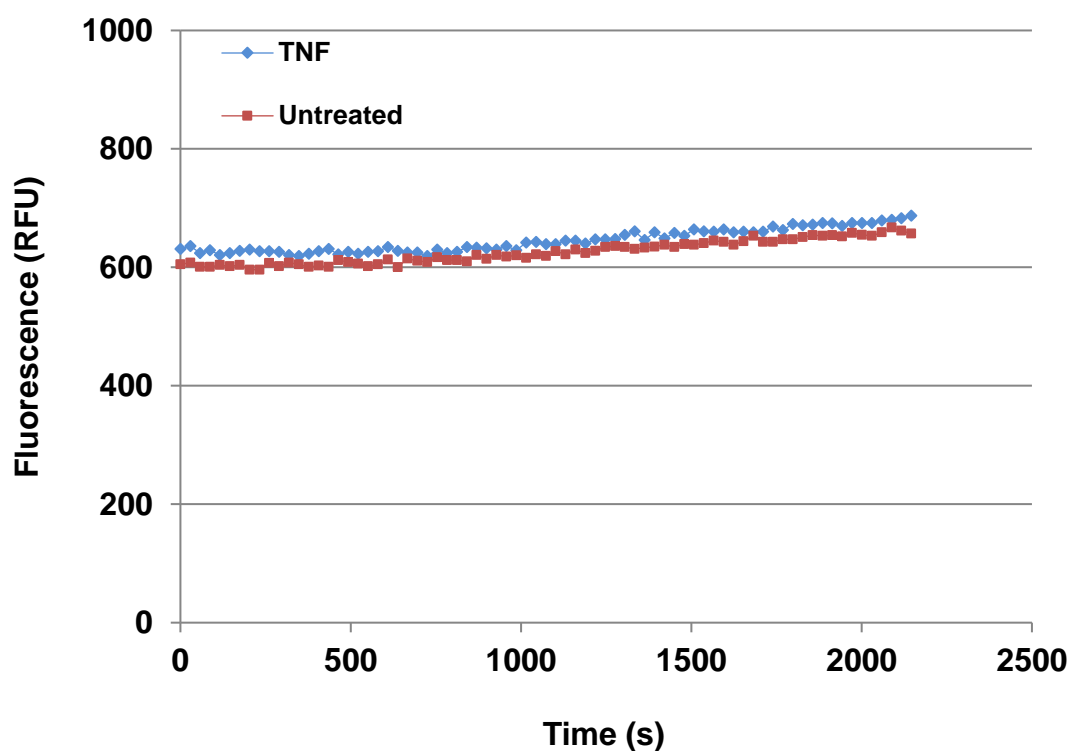


Figure 2.13. Kinetic profile obtained from employing black, flat-bottomed, uncoated 96-well plates to perform the fluorogenic substrate peptide assay on culture supernatants obtained from chondrocyte/agarose constructs cultured with 0 or 10ng/ml of $TNF\alpha$ for 48 hours, in the presence of $ZnCl_2$. RFU = Relative fluorescence unit.

Table 2.6: Parameters altered throughout the optimization process of the fluorogenic peptide substrate assay.

	Original Protocol	Step 1.	Step 2.	Step 3.	Step 4.	Step 5.	Step 6.
Optimization parameters	Amount						
ZnCl ₂	(+)	(-)	(-)	(-)	(-)	(-)	(-)
Fluorogenic peptide substrate	10µM	10µM	10µM	10µM	0, 5, 10µM	10µM	10µM
APMA	(-)	(-)	(-)	(-)	(-)	(-)	(-)
Standard curve	(-)	(-)	(-)	(-)	(-)	(-)	(-)
Substrate application method	Pipetting	Pipetting	Pipetting	Injection system	Pipetting	Pipetting	Pipetting
Plate reader settings	Measurement						
Microplate	white	white	White, black	white	white	white	white
Plate mode	✓	✓	✓	x	✓	✓	✓
N° of cycles	25	25	25	25	25	25	25
Cycle time (s)	110	110	110	110	110	110	x
Well mode	x	x	x	✓	x	x	x
N° of intervals	x	x	x	20	x	x	x
Interval time	x	x	x	1.5	x	x	x
Total measurement time/well (s) (5-7min max.)	x	x	x	300	x	x	x
N° of flashes	20	20	20	20	20	20	20
Positioning delay	0.5s	0.5s	0.5s	1s	0.5s	0.5s	0.5s
Reading direction	Horizontal reading	Horizontal reading	Horizontal reading	Horizontal reading	Horizontal reading	Horizontal reading	Horizontal reading
N° of multichromatics	1	1	1	1	1	1	1
Excitation filter	340nm	340nm	340nm	340nm	340nm	340nm	340nm
Emission filter	460nm	460nm	460nm	460nm	460nm	460nm	460nm
Gain (%)	10	10	10	10	10	10	10-60
Temperature (°C)	25	25	25	25	25	37	25
Start reading (s)	1	1	1	1	1	1	1

	Original Protocol	Step 7.	Step 8.	9. Optimized Protocol
Optimization parameters	Amount			
ZnCl ₂	(+)	(-)	(-)	(-)
Fluorogenic peptide substrate	10µM	10µM	10µM	10µM
APMA	(-)	(-)	(+)	(+)
Standard curve	(-)	(-)	(-)	(-)
Substrate application method	Pipetting	Pipetting	Pipetting	Pipetting
Plate reader settings	Measurement			
Microplate	white	white	white	white
Plate mode	✓	✓	✓	✓
N° of cycles (200 max. or 250)	25	200	200	250
Cycle time (s)	110	110	110	120
Well mode	x	x	x	x
N° of intervals	x	x	x	x
Interval time	x	x	x	x
Total measurement time/well (s) (5-7min max.)	x	x	x	x
N° of flashes	20	20	20	20
Positioning delay	0.5s	0.5s	0.5s	0.5s
Reading direction	Horizontal reading	Horizontal reading	Horizontal reading	Horizontal reading
N° of multichromatics	1	1	1	1
Excitation filter	340nm	340nm	340nm	355nm
Emission filter	460nm	460nm	460nm	460nm
Gain (%)	50	50	50	24.5
Temperature (°C)	25	25	25	25
Start reading (s)	1	1	1	1

III. Substrate application method

The time point at which fluorescence measurements were taken, following the addition of the 1x substrate assay buffer to the sample was another possible factor responsible for obtaining constant fluorescence over time. The change in fluorescence resulting from a low concentration and activity of MMPs takes place over a very short time period, following the addition of the fluorogenic substrate to the sample. By contrast, at high activity of MMP, fluorescent changes occur over an extended time period. Assuming that all the samples had significantly enhanced activities of MMPs on treatment with TNF α , it was essential that the plate reader was sensitive over the time course during which the change in fluorescence occurred. However, the addition of the substrate to individual wells using a single-channel Gilson pipette, prior to transferring the plate to the fluorometer may significantly reduce this sensitivity. Since the fluorescence value obtained from running the fluorogenic substrate assay was significant, when compared to the minimum fluorescence which can be read by the fluorometer (Fig.2.12 and 2.13), it was suggested that the initial rate of hydrolysis may have been missed, resulting in only the plateaued region (or constant) of the kinetic profile being recorded (Giricz, Lauer and Fields, 2011). This risk can be minimized by the following methods:

- Using a multichannel pipette (8 tips), instead of a single-channel Gilson pipette to add the 1x substrate assay buffer into 8 wells simultaneously, immediately after which the plate is transferred onto the plate reader for the acquisition of fluorescence measurements
- Using the injection system associated with the fluorometer for the application of the substrate assay buffer into a single well, immediately followed by taking fluorescence measurements from the filled well. Subsequent wells could then be monitored in a similar fashion (ThermoFisher Scientific, Loughborough, UK).

From the two application methods, the injection system was considered to be the most efficient in minimizing the time between the addition of substrate into the wells and the initiation of fluorescence measurements, as it did not require the 96-well plate to be transferred onto the plate reader, once the substrate was added to the wells. Unlike pipetting using a single or multichannel pipette, the process of substrate application to the wells and fluorescent measurements each took place while the plate was already in the fluorometer. As such, the injection system was used to optimize the assay.

Before the 1x substrate buffer was added into the wells of the 96-well plate, the injection system was required to be primed using 0.1M sodium hydroxide (NaOH) in 0.1%

ethylenediaminetetraacetic acid (EDTA). This was achieved by placing a beaker containing NaOH+EDTA solution in the injection chamber of the fluorometer, from which a maximum volume of 4500 μ l of the solution was circulated at a speed of 310 μ l/s, throughout the pumps of the injector system, into an empty beaker within the same chamber. A further beaker containing distilled water was transferred into the injection chamber, which was used to rinse out any traces NaOH+EDTA solution. This was followed by priming the pumps again, but without immersing the end pipe to any solution, such that all traces of liquid were eliminated (ThermoFisher Scientific, Loughborough, UK).

The use of the injector system does not allow 'plate mode' to be activated. As such, the fluorometer was set to 'well mode', such that the fluorescence measurements were taken from individual wells of the 96-well plate one at a time, before the addition of substrate into subsequent wells for the acquisition of consequent fluorescence readings. The injection system was then set to add 50 μ l of substrate buffer solution containing the fluorogenic peptide into each well. The rest of the fluorometer settings were adjusted as shown in table 2.6 under step 4 of the optimization process. However, employing the injection system for the application of the fluorogenic substrate to samples in the 96-well plate did not result in any differences in the data obtained from performing the last optimization step. This suggested that the method of substrate application was not a contributing factor to the results obtained in figure 2.13. As such, a single-channel Gilson pipette was employed for the addition of the 1x substrate assay buffer into individual wells for subsequent optimization steps.

An alternative strategy for increasing the sensitivity of the reading for samples with enhanced MMP activity involves diluting the sample, such that enough time is provided for recording the initial rate of hydrolysis. However, since the concentration of active MMPs per sample was known, this method was not used.

IV. Substrate concentration

Substrate concentration was another possible factor responsible for the development of an incomplete kinetic profile on incubating untreated and cytokine-treated samples with the fluorogenic peptide substrate. Indeed the optimal concentration of substrate required for all the active MMPs present in a sample to hydrolyse the fluorogenic substrate was unknown. Obtaining a constant fluorescence value over time (Fig. 2.13) may be due to insufficient substrate available to react with active MMPs in a sample. According to manufacturer's instructions, the range of peptide concentration to be used is between 0 and 10 μ M, depending on the application, enzyme and other factors. This should result in a linear relationship between the initial rate of cleavage of the peptide and the concentration of MMPs. Since the fluorogenic peptide was used at a final concentration of 10 μ M in the

previous optimization steps, the effects of using the peptide at a lower concentration of 5 μ M was examined. This concentration was also chosen, as it had been previously documented to be the optimum concentration required to attain the standard kinetic profile illustrated in figure 2.9, in the identification of MMP activity (Giricz, Lauer and Fields, 2011). However, employing 5 μ M of the fluorogenic substrate did not result in any differences in the fluorescence readings obtained from using 10 μ M of the substrate. These results suggested that substrate concentration was not a contributing factor to the results obtained in figure 2.13.

V. Temperature

The temperature of the plate reader chamber was also a potential factor in optimizing the assay. According to manufacturer's instructions, the suggested range of temperature at which the assay should be run was 25-37°C. Since the initial test was run at the lowest temperature of 25°C, it could be presumed that this temperature was too low for MMPs to hydrolyse the peptide substrate. As such, the temperature at which the plate reader was set to was increased from 25 to 37°C. However this factor did not alter the results obtained in figure 2.13. As such, subsequent optimization steps were carried out at 25°C.

VI. Gain

Gain was also a possible factor in obtaining a constant recording as opposed to the changing kinetic profile. Indeed this might have been due to setting a too high gain (Giricz, Lauer and Fields, 2011, Tokmina-Roszyk, Tokmina-Roszyk and Fields, 2013). As such, the optimum value of gain at which the fluorometer must be set was determined by testing various gains starting from 10% of the maximum fluorescence that can be recorded by the fluorometer, up to 60%, in increments of 10%. It is worth noting that the maximum fluorescence which can be measured by the fluorometer was approximately 70,000 RFU at an emission/excitation wavelength of 340/460nm.

A significant increase in fluorescence was observed each time the gain was increased by a factor of 10, starting from 10% gain as shown in figure 2.13. However, each of the kinetic profiles obtained from increasing the gain did not reveal the plateau region present in a standard kinetic profile obtained from carrying out the fluorometric substrate assay. These results suggested that hydrolysis of the fluorogenic substrate by MMPs was incomplete. The gain at which the fluorometer was set, was not increased above 60%, since the fluorescence values obtained from setting the fluorometer at 60% gain were very close to the maximum fluorescence which can be read by the fluorometer. Increasing the gain above 60% would have resulted in a constant fluorescence reading being obtained.

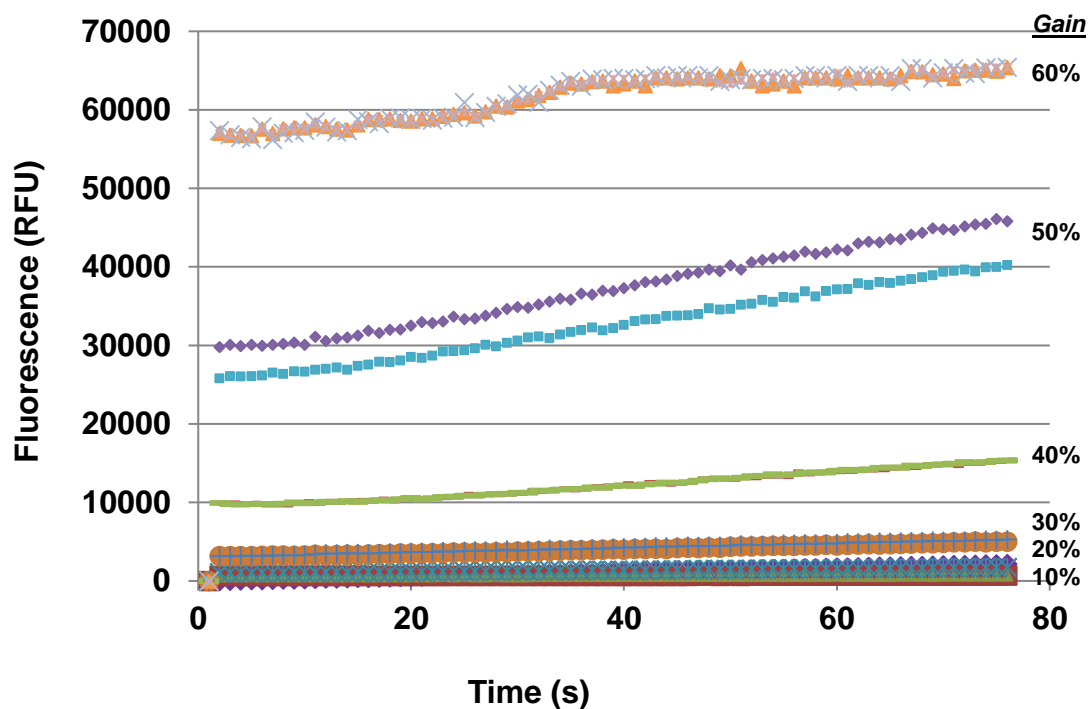


Figure 2.14. Black, flat-bottomed, 96-well plates were employed to perform the fluorogenic substrate assay on culture supernatants obtained from culturing chondrocyte/agarose constructs for 48 hours with 0 or 10ng/ml of TNF α . The gain at which the fluorometer was set was increased from 10%, at increments of 10, up to 60% gain and the effects were observed on the kinetic profiles. RFU = Relative fluorescence unit.

VII. Number of cycles

The number of cycles at which the fluorometer is set, demonstrates the number of time points at which fluorescence measurements are taken to develop a kinetic profile. Thus an increase in the cycle number will result in an increase in the number of time points at which measurements are taken. Since the kinetic profiles generated from increasing the gain were incomplete (Fig. 2.14), insufficient number of cycles was considered as a possible factor in observing such results. As such, the assay was repeated by increasing the number of cycles on the fluorometer from 25 to 200 cycles, while maintaining a gain of 50% as shown in figure 2.15.

On performing the assay at 200 cycles, an increase in the number of time points at which fluorescence readings were measured was observed. In order to ensure that fluorescence readings were not missed, the fluorometer was set to record measurements at the maximum number of cycles, 200 cycles. From this, the plateau region of the kinetic profile was revealed, ensuring that complete hydrolysis of the fluorogenic substrate by MMPs occurred. This was in correlation to the standard kinetic profile observed on performing fluorogenic substrate assays, shown in figure 2.9. As such, subsequent optimization steps were carried out by setting the fluorometer at 200 cycles.

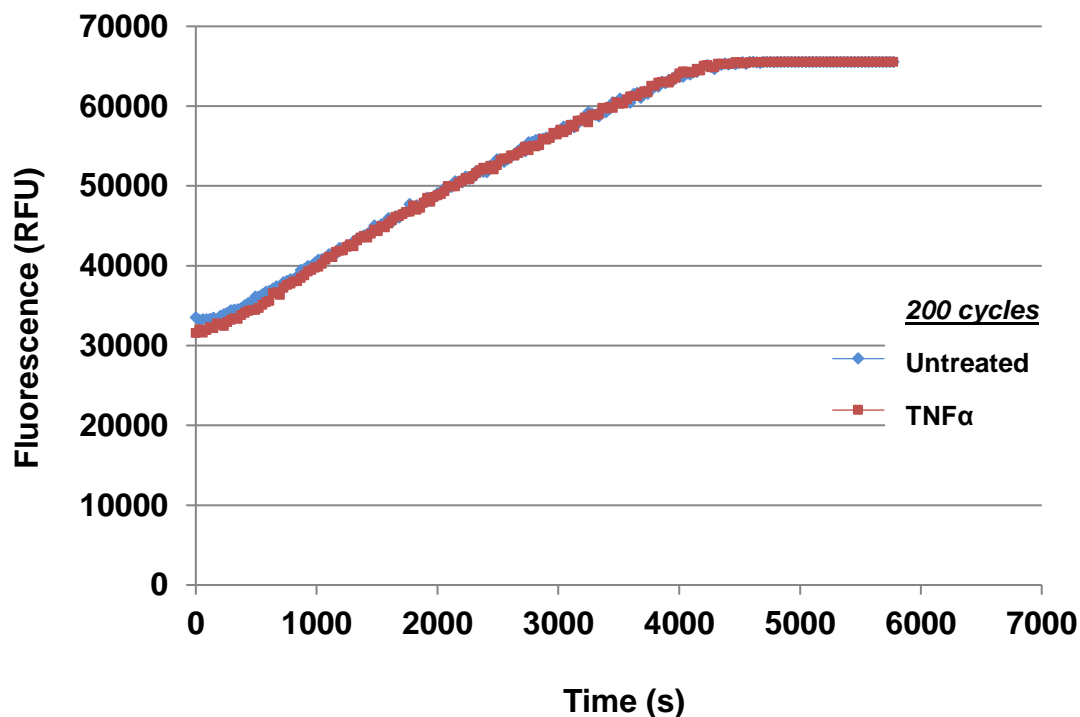


Figure 2.15. Black, flat-bottomed, 96-well plates were employed to perform the fluorogenic substrate assay on culture supernatants obtained from culturing chondrocyte/agarose constructs for 48 hours with 0 or 10ng/ml of TNF α . The cycle number was set to 200 cycles and the effects were observed on the kinetic profiles. RFU = Relative fluorescence unit.

VIII. Active versus pro-MMPs

Another factor responsible for obtaining an incomplete kinetic profile is the presence of pro-MMPs in the culture supernatant, incapable of hydrolysing the fluorogenic peptide substrate, unlike active MMPs. Additionally, freeze/thaw cycles of the culture supernatant, may influence the activities of both forms of the protease (Souza-Tarla et al., 2005). Although the kinetic profile obtained from the previous optimization step plateaued towards the end of the reaction, further optimization was carried out which involved introducing 4-Aminophenylmercuric acetate (APMA, Sigma-Aldrich, UK) into the x1 substrate assay buffer at a final concentration of 2.5mM. This step ensured that pro-MMPs which might have been present in the culture supernatant were activated, such that maximum fluorescence output was achieved from each sample (Forsyth, Pulai, and Loeser, 2002) as follows.

A stock solution of 0.5M of AMPA was initially prepared in DMSO in the fume hood, ensuring that a protective mask and gloves were used, due to the high toxicity of the reagent. The resulting solution was then stored in a 5ml bijoux tube at 4°C.

According to manufacturer's instructions, 5 μ l of 0.5M APMA was added to 1ml of culture supernatant. The resulting solution was then incubated at 37°C for 1 hour, after which 20 μ l

of it was added to each well of a 96-well plate, using a single-channel Gilson pipette. The plate was then transferred onto the plate reader, followed by the addition of 1x substrate assay buffer which resulted in a final concentration of 0.7mM APMA. Fluorescence measurements were then carried out on each well using the settings listed in table 2.6, under step 7 of the optimization process.

However, Forsyth et al. (2002) used APMA at a final concentration of 2.5mM to activate pro-MMPs when measuring MMP production. As such, an alternative method was used to treat culture supernatant with APMA, such that a final concentration of 2.5mM of APMA was achieved after the addition of all the components of the assay, including the addition of the x1 substrate assay buffer, as follows. Additionally, freeze/thaw cycles of the sample were completely eliminated by using freshly obtained culture supernatants. 25 μ l of culture supernatant was initially pipetted into each well of a 96-well plate and covered using a cover slip, after which the plate was stored at 4°C until ready. A new solution, substrate buffer A, was then prepared as shown in table 2.7. 25 μ l of this solution was then added to the 96-well plate, re-covered using a coverslip and allowed to incubate in a fume hood for 1 hour at room temperature. Meanwhile, another solution, substrate buffer B, was prepared as shown in table 2.7, while ensuring that it was protected from light at all times.

Table 2.7: Components of substrate assay buffer A and B.

Substrate assay buffer A	Substrate assay buffer B
10X substrate assay buffer = 350 μ l	10X substrate assay buffer = 350 μ l
Distilled water = 2,150 μ l	Distilled water = 2,150 μ l
APMA = 2.5mM	Fluorogenic peptide substrate = 10 μ M

Once samples in the 96-well plate were completely incubated for 1 hour, 25 μ l of substrate buffer B was pipetted using a single-channel Gilson pipette into each well. The 96-well plate was then immediately transferred into the FLUOstar, followed by the adjustment of plate reader settings as listed in Table 2.6 as 'step 7'.

Upon introducing APMA into the culture supernatant, a significant increase in fluorescence was observed with time in samples treated with 10ng/ml of TNF α and untreated controls, as shown in figure 2.16. These results suggest the presence of pro-MMPs in the culture supernatant, which were then activated by introducing APMA. Activated MMPs were then able to successfully hydrolyse the fluorogenic substrate, further enhancing the fluorescence output. As such, 2.5mM of APMA was introduced into culture supernatants used for subsequent fluorogenic substrate assays.

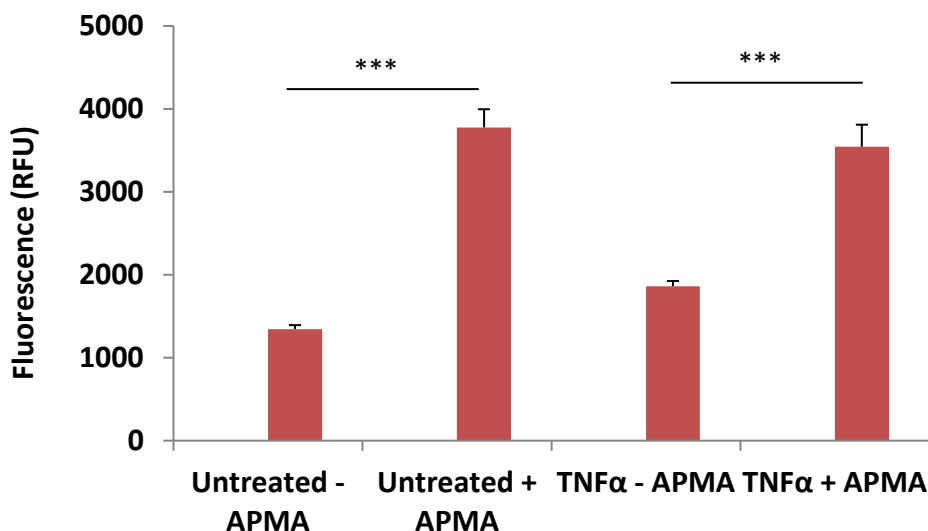


Figure 2.16. Kinetic profile obtained from carrying out the fluorogenic substrate assay on culture supernatants obtained from culturing chondrocyte/agarose constructs for 48 hours with TNF α , using excitation/emission filters with values 355nm/440nm. RFU = Relative fluorescence unit. (***) = $p < 0.001$

IX. Fluorometer filter

Although reactions between the fluorogenic peptide substrate and proteases were monitored using excitation/emission filters with values of 340nm/440nm, manufacturer's instructions suggest that the reactions can also be observed using excitation/emission filters of the following values: 360, 365/450, 460nm. Accordingly, excitation/emission filters with values of 355nm/460nm were evaluated as part of the optimization process (Fig. 2.17). It was observed that employment of these filters resulted in higher fluorescence values when compared to those obtained from using filters with values of 340nm/440nm. This was because, altering the filters led to an increase in the value of the maximum fluorescence capable of being measured by the fluorometer. Additionally, the gain of the fluorometer was automatically set to 24.5% of the maximum fluorescence which can be measured by the fluorometer, further contributing to these changes in fluorescence.

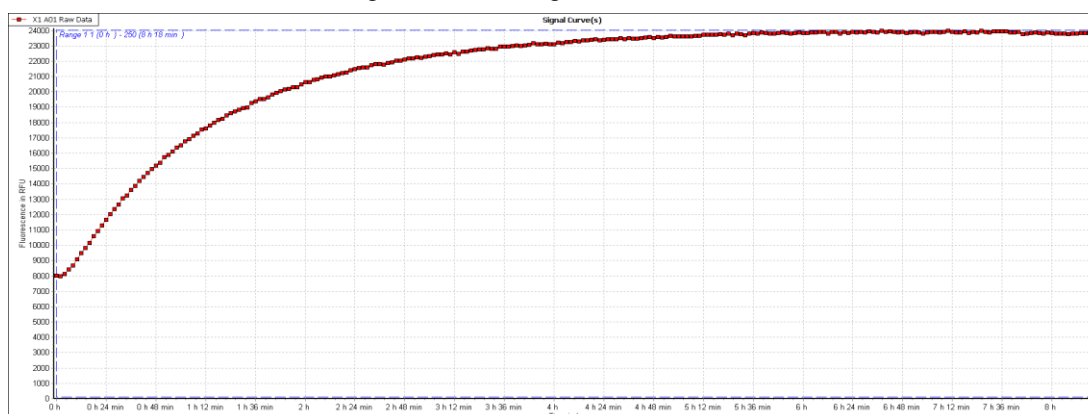


Figure 2.17. Kinetic profile obtained from carrying out the fluorogenic substrate assay on culture supernatants obtained from culturing chondrocyte/agarose constructs for 48 hours with TNF α , using excitation/emission filters with values 355nm/440nm. RFU = Relative fluorescence unit.

2.5.6 TNF α synthesis quantification

The concentration of TNF α in culture supernatants was measured by ELISA, using reagents from National Institute for Biological Standards and Control (NIBSC, Hertfordshire, UK and Sigma-Aldrich Ltd-Aldrich, UK). Briefly, Nunc maxisorp plates (Thermo scientific) were initially coated overnight at 4°C with anti-TNF α [monoclonal antibody (MAb) clone 357-101-4, NIBSC]. Plates were then blocked with 1% bovine serum albumin (BSA), followed by the addition of 50 μ l of culture supernatant or the World Health Organisation International Standards (2nd WHO Internal Standard for TNF- α NIBSC 88/786). 50 μ l of polyclonal anti-TNF α biotinylated detecting antibody (H91, NIBSC) was then added to the wells and incubated overnight at 4°C. A streptavidin-HRP conjugate (Jackson) diluted at 1/30,000 and o-Phenylenediamine dihydrochloride (OPD) (Sigma-Aldrich Ltd-Aldrich, UK) were then used to develop plates. Using 1M of sulphuric acid (Sigma-Aldrich Ltd-Aldrich, UK), the reaction was stopped and colorimetric measurements were recorded using a Spectramax plate reader (Molecular Device, USA) at an absorbance of 490nm. It is worth noting that the absorbance values recorded were also referred at as optical density (OD) values. A standard curve was then prepared, as shown in figure 2.18, using TNF α standards at concentrations ranging between 0 and 6000pg/ml.

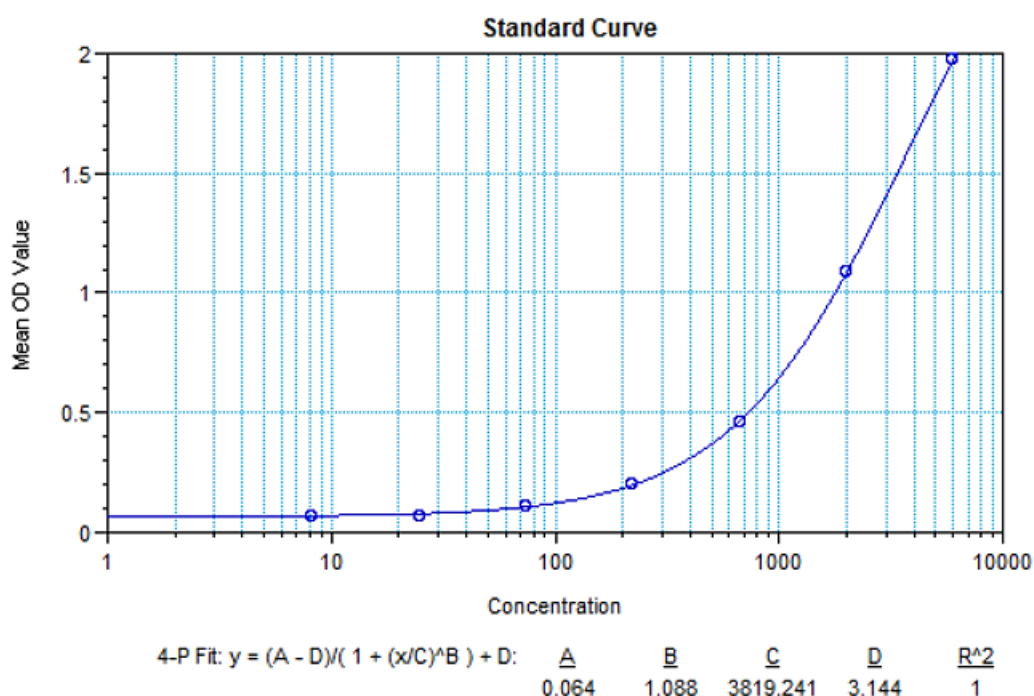


Figure 2.18. TNF α standard curve ranging from 0 to 6000pg/ml (n=2).

2.6 Statistics

For free-swelling studies, data represent the mean and SEM values for 6-18 replicates from 3-4 separate experiments. For the *ex-vivo* bioreactor experiments, data represent the mean and SEM values of 8-12 replicates from two separate experiments. Statistical analysis was performed by a two-way analysis of variance (ANOVA) and the multiple post hoc Bonferroni-corrected t-tests to compare differences between the various treatment groups as indicated in each figure legend. In all cases, a level of 5% was considered statistically significant ($p < 0.05$).

Chapter 3 – Low oxygen tension
increases the pro-inflammatory
effects induced by TNF α in
chondrocytes

3.1 Introduction

Although IL-1 β is generally considered to be the principal cytokine known to drive catabolic events in chondrocytes during the OA disease process, TNF α also contributes to the pro-inflammatory process (Kapoor et al., 2011, Kobayashi et al., 2005, Gilbert, Duance and Mason, 2002, Goodstone and Hardingham, 2002). Several *in vitro* studies have demonstrated that treatment of chondrocytes with TNF α increases production of NO, PGE₂ and MMP enzymes in human, rabbit, canine or bovine chondrocytes cultured in monolayer, explant or 3D alginate models, resulting in proteoglycan depletion (Kobayashi et al., 2005, Gilbert, Duance and Mason, 2002, Goodstone and Hardingham, 2002, Blain, 2007, Kuroki, Stoker and Cook, 2005, Sabatini et al., 2001, Schuerwegh et al., 2003, Little et al., 1999, Sabatini et al., 2000, Lefebvre, Peeters-Joris and Vaes, 1990, Reginato et al., 1993, Campbell et al., 1990). Additionally, oxygen tension has implications on the pro-inflammatory response induced by cytokines (Martin et al., 2004, Mathy-Hartert et al., 2005, Cernanec et al., 2002, Lawyer, Tucci and Benghuzzi, 2012, Grimshaw and Mason, 2000). However, very little is known about the effects of TNF α on triggering the pro-inflammatory events at low oxygen tension in chondrocytes. The present study therefore examined whether oxygen tensions at 21% and 5% could influence the effects of TNF α on catabolic activity (NO, PGE₂, MMP) and tissue remodelling (GAG synthesis and loss) in chondrocyte/agarose constructs.

3.2 Materials and methods

3.2.1 Dose response effect of TNF α on the production of catabolic and anabolic mediators in chondrocyte/agarose constructs cultured at 21 and 5% oxygen tension

Chondrocyte/agarose constructs were prepared using a well-established model as described in section 2.2. Constructs were equilibrated in culture under free-swelling conditions at 21 and 5% oxygen tensions for 72 hours. The glove-box style workspace integrated within a Biospherix incubator ensured that the experimental conditions during set-up and experimentation were uninterrupted, as previously described (Parker et al., 2013). Following the equilibration period, constructs were cultured for a further 48 hours with DMEM + 20% FCS supplemented with TNF α (Peprotech EC Ltd, London, UK) at concentrations ranging from 0.1 to 100ng/ml in the presence or absence of 1mM L-N-(1-iminoethyl)-ornithine (L-NIO). This range of TNF α concentration was selected, since a dose-dependent increase in the production of catabolic mediators, such as enhanced NO, PGE₂ and MMPs, has been demonstrated in previous *in vitro* studies, leading to the inhibition of matrix synthesis and induction of cartilage degradation (Goodstone and Hardingham, 2002; Kuroki, Stoker and Cook, 2005, Reginato et al., 1993). Additionally, these *in vitro* results are in concert with animal studies which reported a reduction in the biomechanical abnormalities and inflammatory symptoms upon selectively inhibiting iNOS in OA joints (Pelletier et al., 1996, 1999, Kammermann et al., 1996). L-NIO inhibits all isoforms of the nitric oxide synthase enzymes (Merck Chemicals, Nottingham, UK).

3.2.2 Temporal effect of exogenous TNF α on cell-free and chondrocyte seeded agarose constructs cultured at 21 and 5% oxygen tension

In a separate study, agarose constructs prepared with and without chondrocytes were equilibrated in culture under free-swelling conditions in the Biospherix incubator at both 21 and 5% oxygen tensions for 72 hours. Constructs were then cultured for a further 48 hours with DMEM + 20% FCS supplemented with 0 or 10ng/ml of TNF α (Peprotech EC Ltd, London, UK).

3.3 Results

Throughout this thesis, no change was observed in the number of chondrocytes achieved per construct. This was validated by achieving an average DNA concentration of 3.5µg/ml per construct, which remained constant throughout the thesis.

3.3.1 Dose response effect of TNFα on catabolic and anabolic mediators in chondrocyte/agarose constructs cultured at 21 and 5% oxygen tensions

The dose-dependent effects of TNFα at 21 and 5% oxygen tension on nitrite production, PGE₂ release, MMP activity, GAG synthesis and GAG loss were compared. Each mediator will be discussed separately.

3.3.1.1 Nitrite release

At both oxygen tensions, the levels of nitrite release were enhanced by the presence of TNFα, with a significant increase at 1, 10 and 100ng/ml, when compared to untreated controls (all $p < 0.001$; Fig. 3.1A, B). Co-incubation with the NOS inhibitor significantly abolished cytokine-induced nitrite release with levels returning to basal values at both 21% and 5% oxygen. For each TNFα concentration, the mean percentage differences in nitrite release between oxygen tensions of 21% and 5% ranged between 11% and 75% with no systematic trend. The corresponding range in the presence of L-NIO was -23% and 72%.

3.3.1.2 PGE₂ release

At 1, 10 and 100ng/ml, TNFα increased PGE₂ release at both oxygen tension when compared to untreated controls (all $p < 0.001$; Fig. 3.2A, B). Co-incubation with the NOS inhibitor partially reversed this effect in TNFα treated constructs cultured at both 21% and 5% oxygen. On comparing the mean percentage differences in PGE₂ release between cultures at 21 and 5% oxygen tensions, values ranging between 16% and 1833% were obtained for each concentration of TNFα, with no systematic trend. Co-incubation with the NOS inhibitor resulted in corresponding values which ranged between 19% and 1196%.

3.3.1.3 MMP activity

At TNFα concentrations greater than 1ng/ml, the cytokine increased MMP activity in a dose-dependent manner at both oxygen tensions when compared to untreated controls (Fig.

3.3A, B). Co-incubation with the NOS inhibitor partially reversed this effect in TNF α treated constructs cultured at either 21% or 5% oxygen. Values ranging between -27% and 79% were obtained for each concentration of TNF α , upon comparing the percentage differences between constructs cultured at 21% and 5% oxygen tensions. In the presence of L-NIO, corresponding values ranging between -47% and 138% were obtained.

3.3.1.4 GAG synthesis

In the absence of the cytokine, GAG synthesis was greater at 21% oxygen when compared to 5% ($p < 0.001$; Fig. 3.4A, B). The presence of TNF α did not significantly influence GAG synthesis at a low cytokine concentration (0.1ng/ml) when compared to untreated controls cultured at either 21% or 5% oxygen. However, at the elevated TNF α concentrations of 1-100ng/ml, the cytokine induced a downregulation in GAG synthesis ($p < 0.05$). This response was not significantly influenced by the NOS inhibitor, except at the highest concentration of TNF α (Fig. 3.4A, B). At all TNF α concentration, the percentage differences in GAG synthesis between 21 and 5% oxygen tensions ranged between -22% and 3%, with no systematic trend. The corresponding range in the presence of the NOS inhibitor was -25% and 15%.

3.3.1.5 GAG loss

In the absence of the cytokine, GAG loss was inhibited with L-NIO at both 21% and 5% oxygen ($p < 0.01$ and $p < 0.001$ respectively; Fig. 3.5A, B). At the higher TNF α concentrations of 10-100ng/ml, the cytokine increased GAG loss ($p < 0.05$), and this response was reversed with the NOS inhibitor. On comparing the percentage differences in GAG loss between cultures at 21 and 5% oxygen tension, values ranging between -4% and 10% were obtained for each concentration of TNF α , with no systematic trend. Co-incubation with L-NIO resulted in corresponding values which ranged between -45% and 79%.

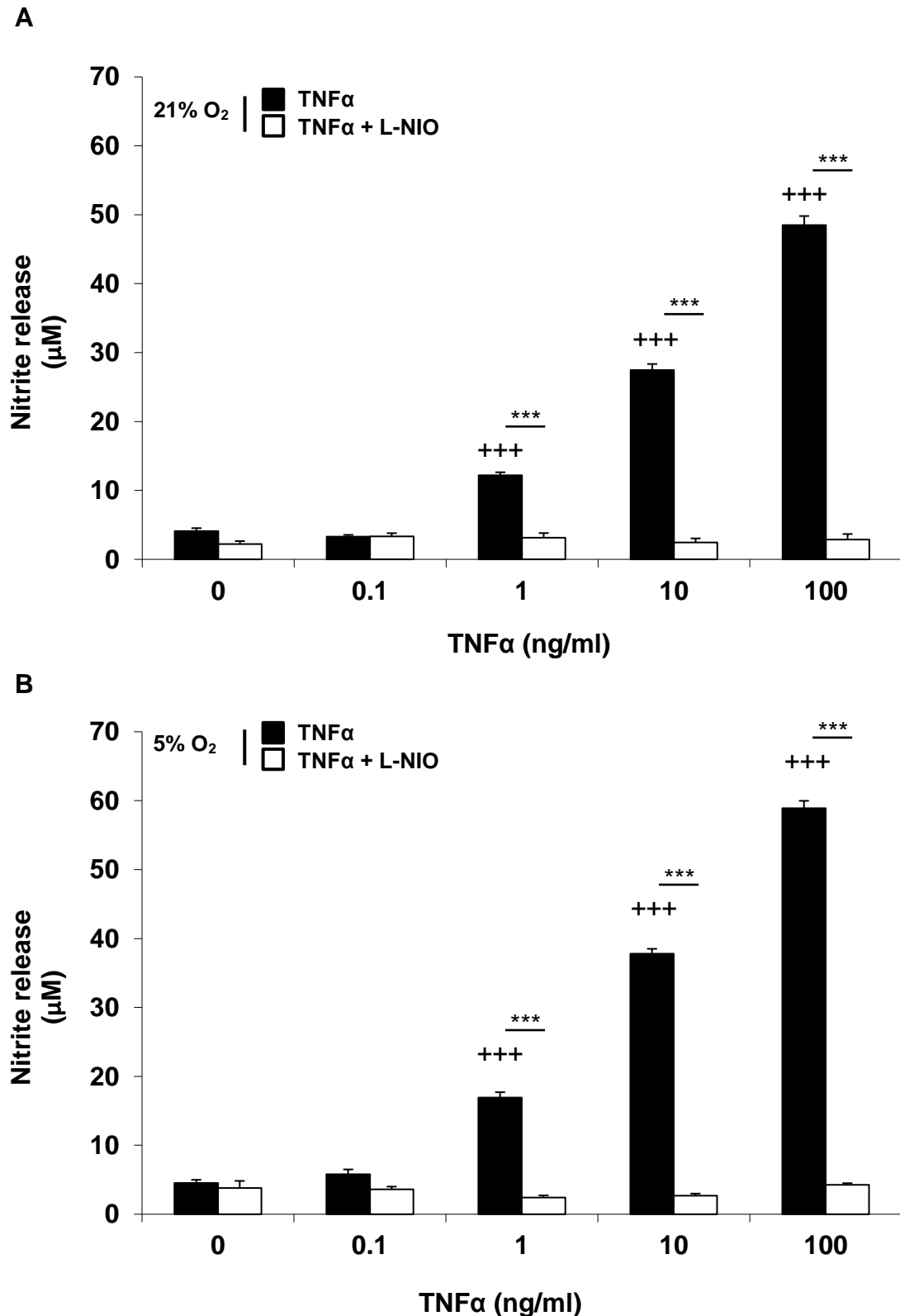


Figure 3.1. Effect of 21 and 5% oxygen tension on nitrite release in chondrocytes treated with varying concentrations of TNF α . Chondrocyte/agarose constructs were cultured for 48 hours with varying concentrations of TNF α (0.1 to 100ng/ml) and/or L-NIO (1mM) and the effects of 21% (A) and 5% (B) oxygen tension were examined on nitrite release. Error bars represent the mean and SEM values for 6-18 replicates from four separate experiments. (+++) indicates significant comparisons between untreated and cytokine treated constructs cultured at 21% and 5% oxygen tension; (***) indicates significant comparisons between TNF α and TNF α + L-NIO.

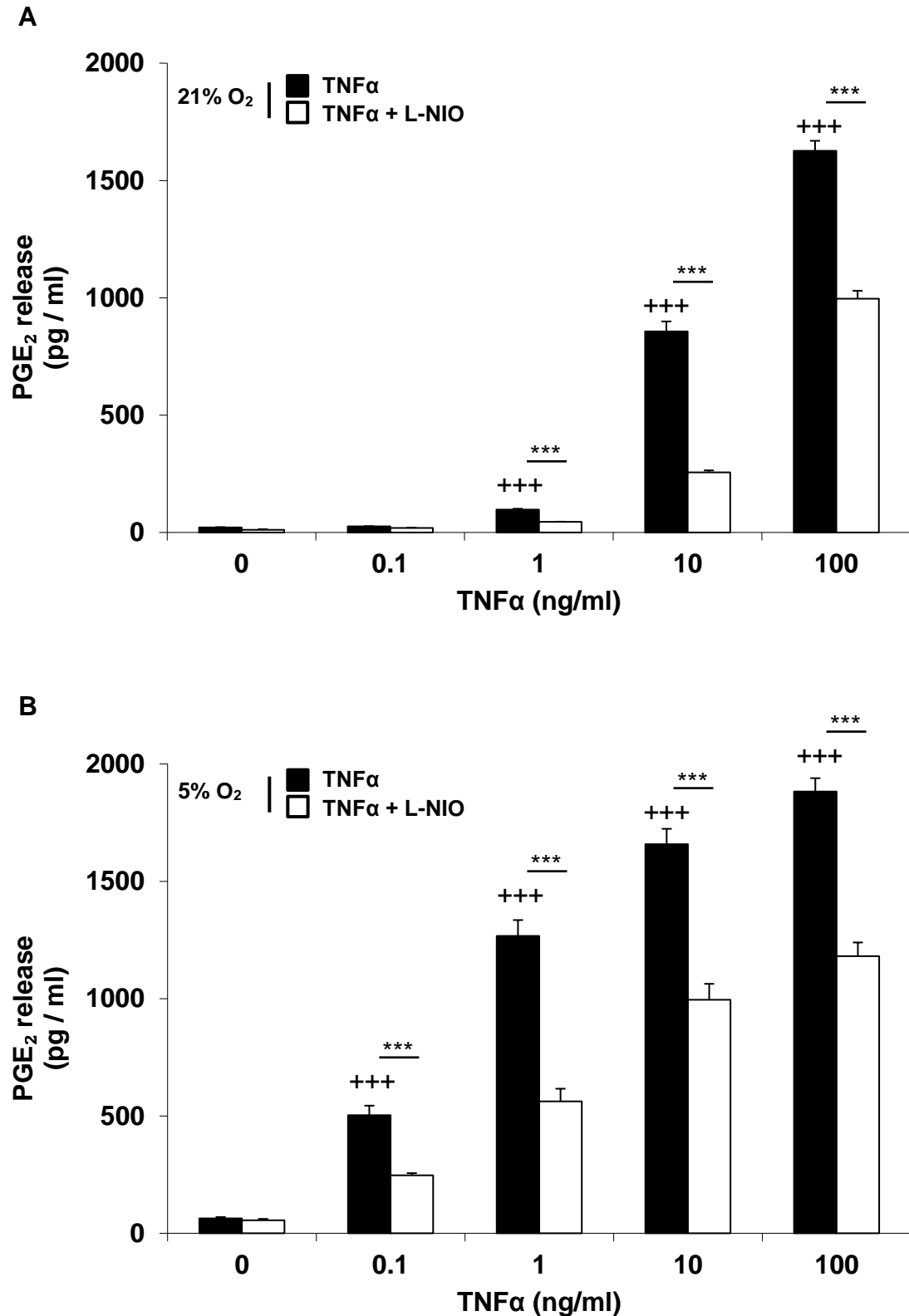


Figure 3.2. Effect of 21 and 5% oxygen tension on PGE₂ release in chondrocytes treated with varying concentrations of TNF α . Chondrocyte/agarose constructs were cultured for 48 hours with varying concentrations of TNF α (0.1 to 100ng/ml) and/or L-NIO (1mM) and the effects of 21% (A) and 5% (B) oxygen tension were examined on PGE₂ release. Error bars represent the mean and SEM values for 6-18 replicates from four separate experiments. (+++) indicates significant comparisons between untreated and cytokine treated constructs cultured at 21% and 5% oxygen tension; (***) indicates significant comparisons between TNF α and TNF α + L-NIO.

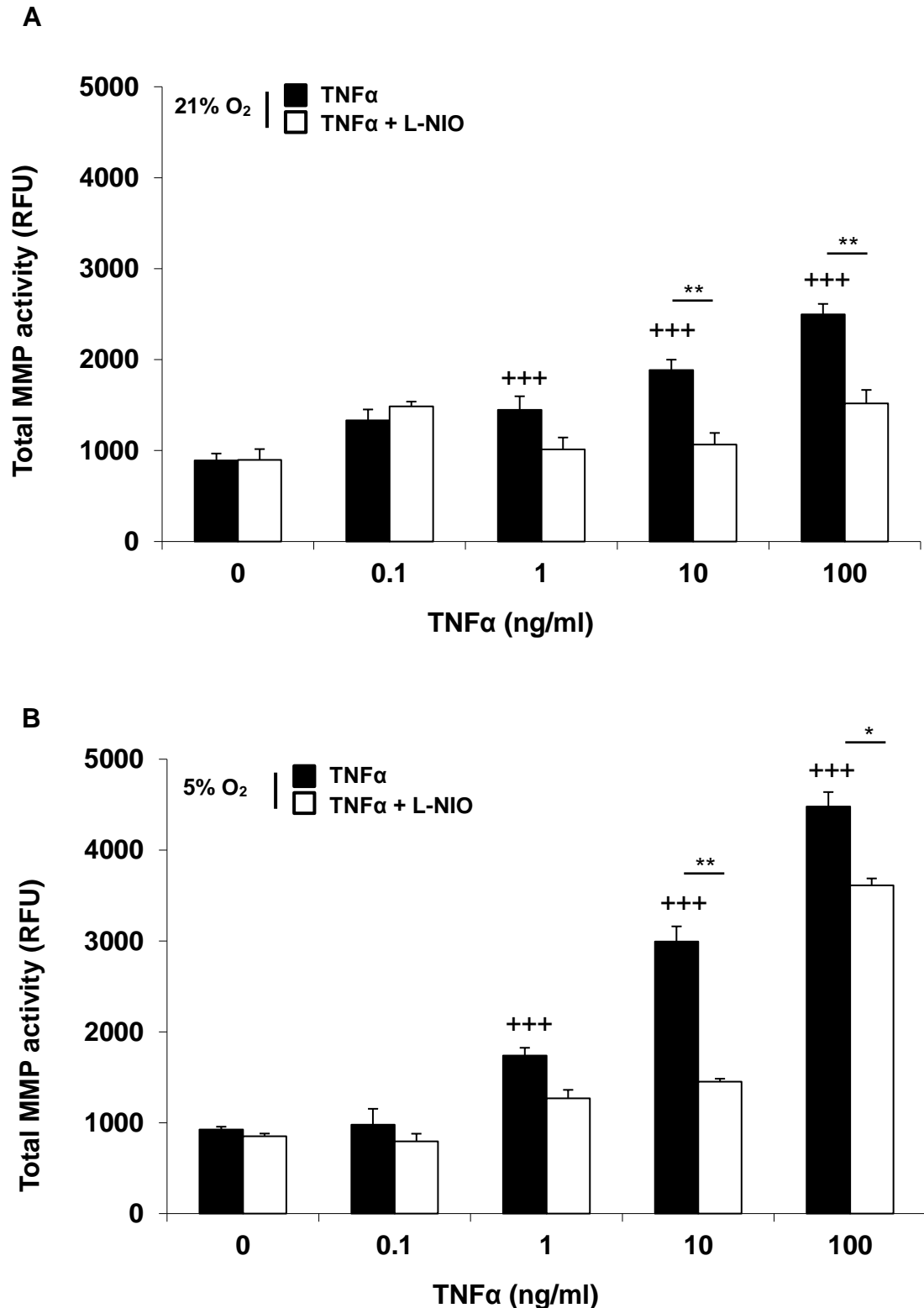


Figure 3.3. Effect of 21 and 5% oxygen tension on MMP activity in chondrocytes treated with varying concentrations of TNF α . Chondrocyte/agarose constructs were cultured for 48 hours with varying concentrations of TNF α (0.1 to 100ng/ml) and/or L-NIO (1mM) and the effects of 21% (A) and 5% (B) oxygen tension were examined on MMP activity. Error bars represent the mean and SEM values for 6-18 replicates from four separate experiments. (+++) indicates significant comparisons between untreated and cytokine treated constructs cultured at 21% and 5% oxygen tension; (* or **) indicates significant comparisons between TNF α and TNF α + L-NIO.

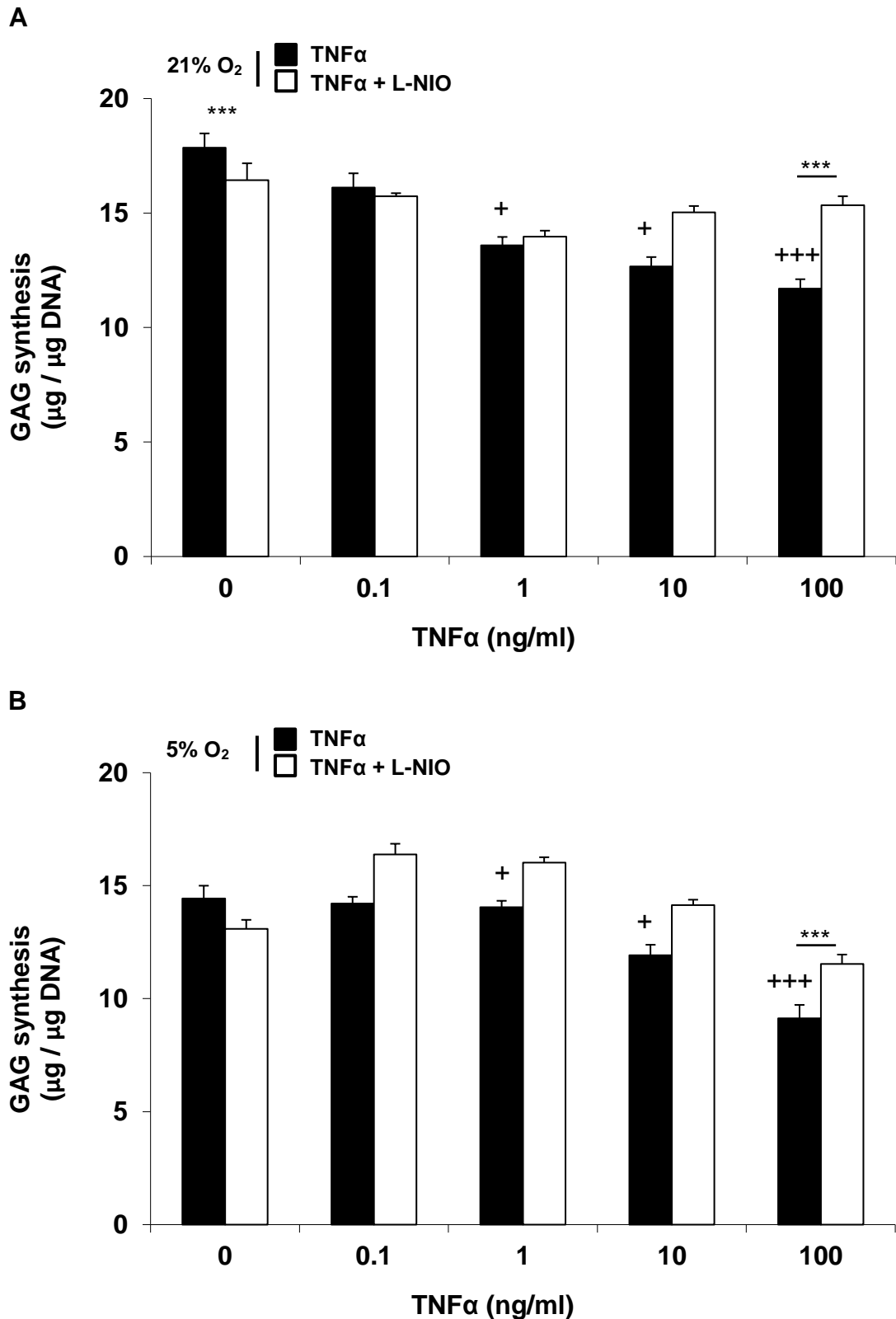


Figure 3.4. Dose-dependent effects of TNF α on matrix synthesis at 21 and 5% oxygen tension. Chondrocyte/agarose constructs were cultured with varying concentrations of TNF α (0.1 to 100ng/ml) and/or L-NIO (1mM) for 48 hours and the effects of 21% (A) and 5% (B) oxygen tension were examined on GAG synthesis. Error bars represent the mean and SEM values for 6-18 replicates from four separate experiments. (+ or +++) indicates significant comparisons between untreated and cytokine treated constructs cultured at both oxygen tensions; (***) indicates significant comparisons between TNF α and TNF α + L-NIO at both oxygen tensions.

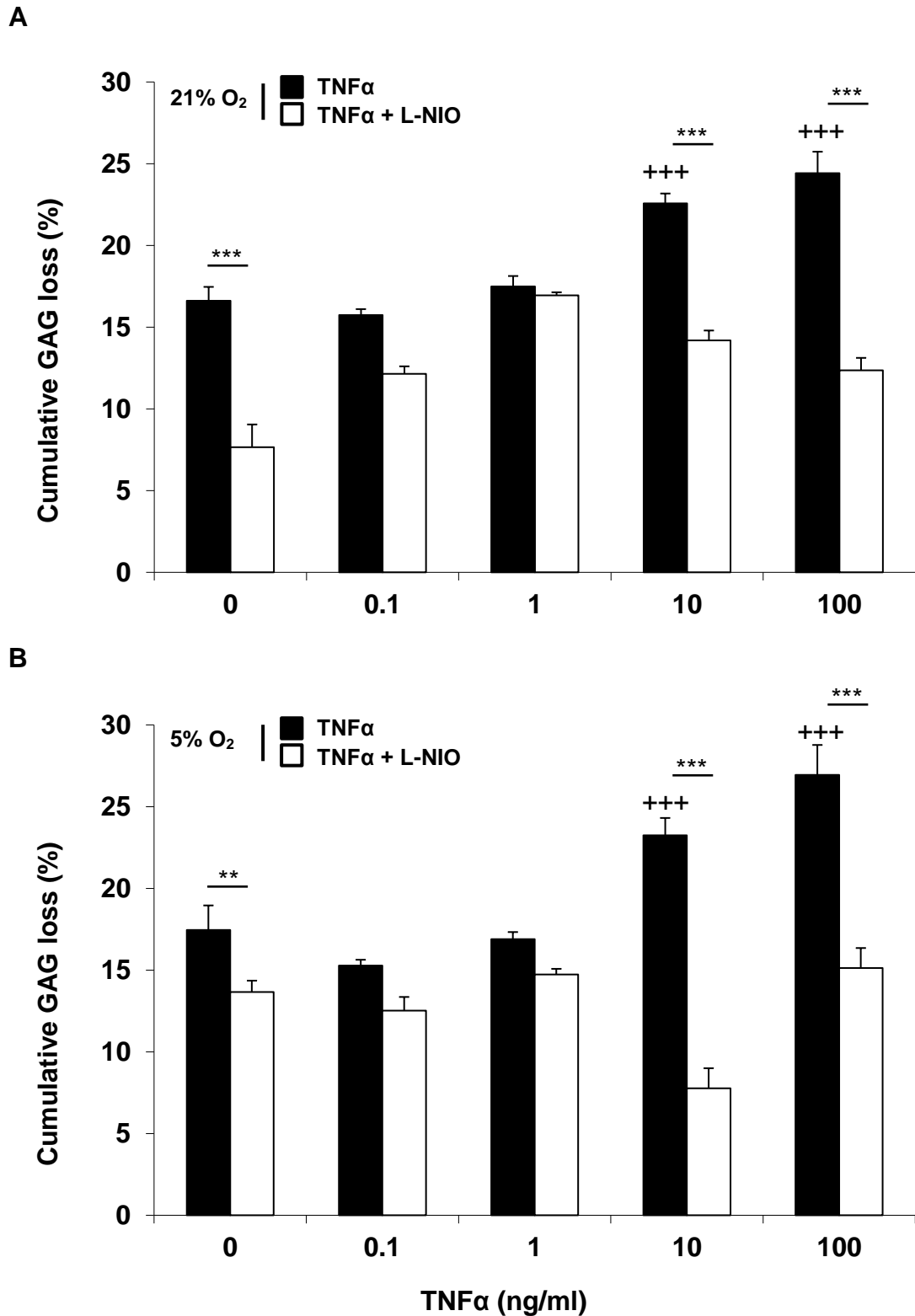


Figure 3.5. Dose-dependent effects of TNF α on matrix degradation at 21 and 5% oxygen tension. Chondrocyte/agarose constructs were cultured with varying concentrations of TNF α (0.1 to 100ng/ml) and/or L-NIO (1mM) for 48 hours and the effects of 21% (A) and 5% (B) oxygen tension were examined on GAG loss. Error bars represent the mean and SEM values for 6-18 replicates from four separate experiments. (+++) indicates significant comparisons between untreated and cytokine treated constructs cultured at both oxygen tensions; (***) indicates significant comparisons between TNF α and TNF α + L-NIO at both oxygen tensions.

3.3.1.6 Summary of catabolic and anabolic mediators

In order to examine the significance of the differences between both oxygen tensions, an ANOVA with post-hoc Bonferroni-corrected t-tests were employed, as described in section 2.6. The results for the combination of anabolic and catabolic mediators are summarised in Table 3.1.

At TNF α concentrations of both 10ng/ml and 100ng/ml, the upregulation of the catabolic mediators, i.e nitrite, PGE₂ release and MMP activity were statistically significantly greater ($p < 0.001$) at 5% oxygen tension (Table 3.1). These differences were also statistically significant for lower concentrations of TNF α for PGE₂ release alone. By contrast, at the highest TNF α concentration i.e 100ng/ml, the anabolic mediator, GAG synthesis, was significantly greater at 21% oxygen tension.

Table 3.1: Statistical level of differences between cultures at 21% and 5% oxygen tensions, stimulated with different concentrations of TNF α with respect to five catabolic and anabolic mediators in the unstrained condition.

TNFα (ng/ml)	Nitrite release	PGE₂ release	MMP activity	GAG synthesis	GAG loss
0	NS	NS	NS	NS	NS
0.1	NS	(\uparrow) ***	NS	NS	NS
1.0	NS	(\uparrow) ***	NS	NS	NS
10	(\uparrow) ***	(\uparrow) ***	(\uparrow) ***	NS	NS
100	(\uparrow) ***	(\uparrow) ***	(\uparrow) ***	(\downarrow) **	(\uparrow) **

Where:

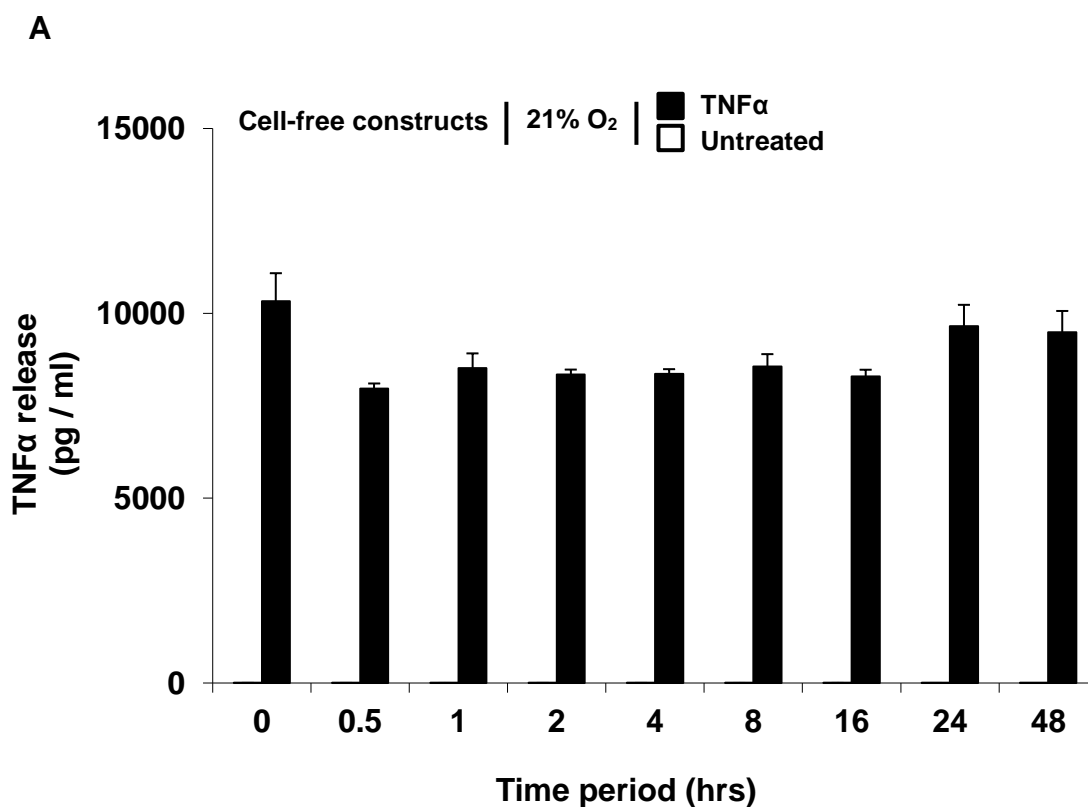
$P < 0.05$ * ; $P < 0.01$ ** ; $P < 0.001$ ***; $P > 0.001$ NS;

(\uparrow) indicates 5% > 21% effects

(\downarrow) indicates 5% < 21% effects

3.3.2 Temporal effect of exogenous TNF α on TNF α release in cell-free and chondrocyte seeded agarose constructs cultured at 21 and 5% oxygen tensions

On treating chondrocyte/agarose constructs with 10ng/ml of exogenous TNF α , a significant increase in TNF α release was observed in cell-free and chondrocyte seeded agarose constructs when compared to untreated controls at both 21% and 5% oxygen tensions ($p > 0.001$; Fig. 3.6A, B and C). Following initial stimulation, the concentration of TNF α present in both cell-free and chondrocyte seeded agarose constructs cultured at 21% oxygen tension remained constant throughout the 48 hour culture period (Fig. 3.6A and B). A similar response was observed in TNF α -treated chondrocyte/agarose constructs cultured at 5% oxygen tension, in which a significant increase in TNF α was observed when compared to untreated controls. Furthermore, the concentration of TNF α in these constructs remained constant for a period of 24 hours, after which a significant increase in TNF α was revealed at 48 hours of culture (Fig. 3.6C).



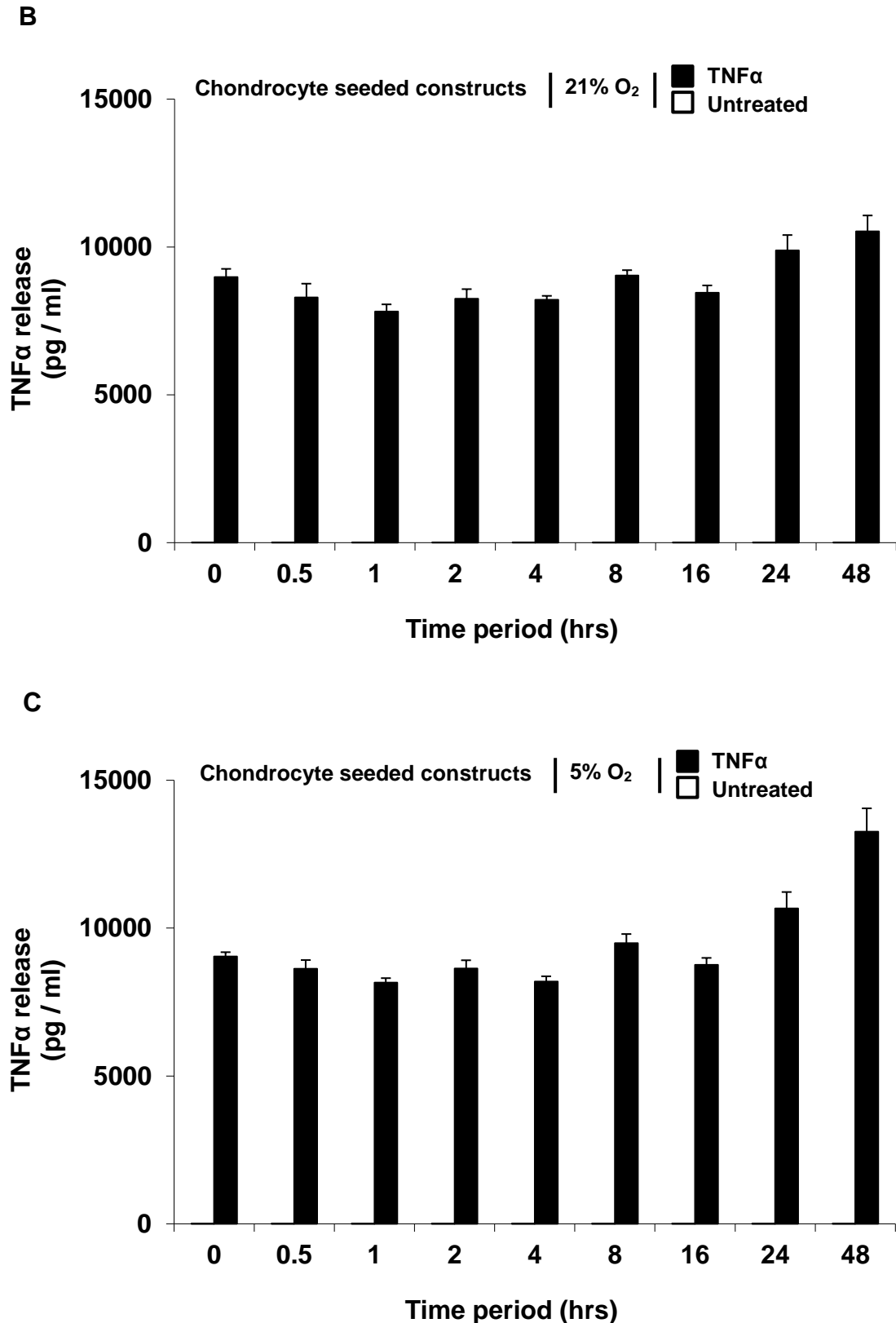


Figure 3.6. Temporal effect of exogenous TNF α . Cell-free and chondrocyte seeded agarose constructs were treated with 10ng/ml of TNF α for 48 hours at 21% (A, B) and 5% (C) oxygen tension and the temporal effect of the cytokine was examined on TNF α release in the culture supernatant. Error bars represent the mean and SEM values for 4-11 replicates from three separate experiments. (*) $p < 0.05$ indicates significant comparison between cytokine treated constructs cultured at 0 hours and those cultured for 48 hours at 5% oxygen tension.

3.4 Summary of results

- TNF α dose-dependently increased nitrite, PGE₂ and total MMP activity, changes which were associated with an inhibition in both the synthesis and loss of GAG, particularly at the highest cytokine concentration.
- At a reduced oxygen tension of 5%, the effects induced by TNF α were enhanced, with a greater induction in the levels of nitrite, PGE₂ and total MMP activity, which also correlated with an inhibition in the synthesis and loss of GAG.

3.5 Discussion

TNF α is well known to stimulate the production of catabolic mediators, such as NO and PGE₂ which inhibit matrix synthesis and induce cartilage degradation (Goodstone and Hardingham, 2002, Kuroki, Stoker and Cook, 2005, Sabatini et al., 2001, Schuerwegh et al., 2003, Little et al., 1999, Sabatini et al., 2000, Lefebvre, Peeters-Joris and Vaes, 1990, Reginato et al., 1993, Campbell et al., 1990). The present *in vitro* studies correlate with previous animal studies which showed that selective inhibition of iNOS, reduced the symptoms of inflammation and biomechanical abnormalities in osteoarthritic joints (Pelletier et al., 1996, Pelletier et al., 1999, Kammermann et al., 1996). However, the overproduction of cytokines in response to different levels of oxygen tension is less clear. Indeed, the levels of oxygen tension in the diseased joint will have a significant impact on metabolic processes, with the potential to trigger pathways induced by TNF α . The interactions between cytokines, oxygen tension and mechanical loading are therefore complex and thus remain the motivation of the present study.

In *ex-vivo* studies, we observed dose-dependent increases in nitrite, PGE₂ and MMPs, that was paralleled with an inhibition of matrix synthesis and loss at the highest cytokine concentration. Reduced oxygen tension at 5% was observed to enhance the inflammatory response with increased levels of nitrite, PGE₂ and MMP activity that also favours the inhibition of matrix synthesis and loss. In a previous study, bovine chondrocytes stimulated with IL-1 β in suspension culture exhibited a similar response, with greater levels of NO and PGE₂ production at 5% when compared to 21% oxygen tension (Mathy-Hartert et al., 2005). The enhanced production of inflammatory mediators under hypoxic conditions can contribute to the production of reactive oxygen species (ROS) that amplifies the catabolic response (Henrotin, Kurz and Aigner, 2005). Furthermore, the p55 TNF α receptor is highly expressed in human chondrocytes from OA cartilage and is particularly susceptible to degradative stimuli (Westacott et al., 1994). Activation of p55 by TNF α was shown to increase synthesis of NO, PGE₂, MMPs and cytokines such as IL-6, IL-8 that degrade collagen type II, IX and XI and inhibit matrix synthesis in a concentration-dependent manner (Lefebvre, Peeters-Joris and Vaes, 1990, Reginato et al., 1993, Campbell et al., 1990, Alaaeddine et al., 1999, Fermor et al., 2005). However, studies on the effect of low oxygen tension on the inflammatory response in chondrocytes have resulted in conflicting outcomes. On the one hand, porcine explants treated with IL-1 α or TNF α increased levels of NO and PGE₂ under normoxic conditions (21%) when compared to severe hypoxic conditions, namely 1% oxygen tension (Cernanec et al., 2002). In contrast, cytokine-treated chondrocytes induced a reduction in oxidative stress resulting in reduced MMP-9 levels at moderate hypoxia (6%) when compared to normoxia (21%) and stabilisation of hypoxia-inducible factor-1 α (HIF-1 α) expression (Lawyer, Tucci and Benghuzzi, 2012). Indeed, the regulation of HIF-1 α by oxygen tension may present a potential target for OA therapy, since HIF-1 α over-expression

in OA chondrocytes is known to have detrimental effects in cartilage pathophysiology. Furthermore, factors involved in the NF κ B and MAPK pathways were shown to mediate production of NO induced by the cytokine at 5% oxygen tension, presenting supplementary oxygen-sensitive mediators as potential therapeutic targets for treating OA (Mathy-Hartert et al., 2005, Cernanec et al., 2002, Lawyer, Tucci and Benuhuzzi, 2012, Grimshaw and Mason, 2000). Collectively, these studies emphasise the oxygen-dependency of the inflammatory response in chondrocytes and suggest that further studies should examine the interplay of the cytokine-induced pathways with oxygen tension.

Furthermore, since TNF α has been previously reported to have a very short half-life (Aderka et al., 1992, Zahn and Greischel, 1989), the culture period of treating chondrocyte/agarose constructs with TNF α was validated by culturing both cell-free agarose constructs and chondrocyte seeded agarose constructs with or without 10ng/ml of TNF α at 21 and 5% oxygen tensions, at intervals of 0.5, 1, 2, 4, 8, 16, 24 and 48 hours, under free swelling conditions. Following initial stimulation, the constant levels of TNF α observed throughout the 48 hour culture period, in both cell-free and cell-seeded constructs cultured at 21% oxygen tension, suggest that the cytokine was not degraded over the entire culture period and that the catabolic activities induced in chondrocyte-seeded constructs were a direct result of the presence of the cytokine. However, at 48 hours of culture, a significant increase in TNF α was observed in chondrocyte/agarose constructs cultured at 5% oxygen tension, due to the implications of low oxygen tension on the inflammatory conditions induced by the cytokine (Martin et al., 2004, Mathy-Hartert et al., 2005, Cernanec et al., 2002, Lawyer, Tucci and Benuhuzzi, 2012, Grimshaw and Mason, 2000).

Chapter 4 – Dynamic compression
and oxygen tension modulates the
effects of TNF α on protein synthesis
in chondrocytes.

4.1 Introduction

Inflammatory mechanisms are known to be influenced by biomechanical signals which affect synthetic activity, and contribute to changes in tissue remodelling (Bader, Salter, Chowdhury, 2011, Felson, 2013, Blain, 2007). In addition, the oxygen tension in cartilage is altered during OA disease progression and will additionally influence the inflammatory process (Fermor et al., 2007, Henrotin, Kurz, Aigner, 2005, Stevens et al., 1991). However, little is known on how biomechanical signals regulate the inflammatory signalling events induced by the combined effects of oxygen tension and TNF α .

Oxygen tension was recently reported to influence the production of inflammatory mediators in response to biomechanical signals. For example in the chondrocyte/agarose model, a reduced oxygen tension of 5% enhanced the production of NO and PGE₂ in constructs cultured with IL-1 β when compared to 21% oxygen tension and this response was abolished by dynamic compression (Parker et al., 2013). As such, the present study uses the well characterised chondrocyte/agarose model, described in Chapter 2 to test the hypothesis that stimulation with dynamic compression will interfere with the response of TNF α to oxygen tension.

4.2 Materials and methods

Effect of dynamic compression on TNF α stimulated chondrocyte/agarose constructs cultured at 21 and 5% oxygen tension.

A novel *ex-vivo* bioreactor (Bose ElectroForce, Gillingham, UK) was used to apply dynamic compression to constructs cultured at 21% or 5% oxygen tension, as previously described in Chapter 2 (Parker et al., 2013). Constructs were transferred into individual wells of a 24-well culture plate (Costar, High Wycombe, UK) and mounted within the bioreactor system that is integrated within the Biospherix incubator. The medium was supplemented with either 0 or 10ng/ml TNF α in the presence and absence of 1mM L-NIO and the experimental conditions during set-up and culture were uninterrupted. A concentration of 10ng/ml of TNF α was employed in this study, since this concentration of the cytokine was observed to induce the maximum catabolic effects in the chondrocyte/agarose model, when compared to 0.1, 1 and 100ng/ml of TNF α , as shown in Chapter 3. Constructs were then subjected to intermittent compression under unconfined conditions, with a profile of 10 min compression followed by a 5 hour 50 min unstrained period for a culture period of 48 hours, as previously described (Parker et al., 2013). The *ex-vivo* conditions were found to be optimal when measuring protein synthesis at this time point (Parker et al., 2013). The compression regime was applied in a dynamic manner with a strain amplitude of 0-15%, using a sinusoidal waveform at a frequency of 1Hz and resulted in 4800 duty cycles for the 48 hour culture period. Control constructs were maintained in an unstrained state in the bioreactor system and cultured for the same time period. At the end of the experiment, the constructs and corresponding media were stored at -20°C prior to analysis.

4.3 Results

4.3.1 Effect of dynamic compression on catabolic and anabolic mediators in TNF α stimulated chondrocyte/agarose constructs cultured at 21 and 5% oxygen tension.

The effect of dynamic compression on nitrite production, PGE₂ release, MMP activity, TNF α release, GAG synthesis and GAG loss in TNF α -stimulated chondrocyte/agarose constructs cultured at 21 and 5% oxygen tension were compared. Each mediator will be discussed separately.

4.3.1.1 Nitrite release

Figure 4.1 reveals that in the absence of the cytokine, dynamic compression did not significantly influence nitrite release at either 21% or 5% oxygen tension. In untrained constructs, TNF α enhanced nitrite production when compared to untreated controls ($p < 0.001$), with a mean percentage difference of 46% obtained in nitrite release between oxygen tensions of 21% and 5%. Upon stimulation with dynamic compression, the response was reduced at both oxygen tensions (both $p < 0.001$; Fig. 4.1A, B), resulting in a mean percentage difference of 20% between cultures at 21% and 5% oxygen tension. The inhibitory effect was then abolished upon co-stimulation with the NOS inhibitor at both oxygen tensions, such that a mean percentage difference of 113% was achieved between oxygen tensions of 21% and 5%.

4.3.1.2 PGE₂ release

In the absence of the cytokine, dynamic compression did not significantly influence PGE₂ release at either oxygen tension (Fig. 4.2A, B). In unstrained constructs, TNF α increased PGE₂ release when compared to untreated controls ($p < 0.001$), with a mean percentage difference of 91% in PGE₂ release achieved between cultures at 21% and 5% oxygen tensions. Stimulation with dynamic compression reduced cytokine-induced PGE₂ release (all $p < 0.001$) such that a mean percentage difference of 34% was achieved in PGE₂ release between cultures at 21% and 5% oxygen tension. Co-stimulation with both compression and L-NIO induced a further reduction in PGE₂ release (all $p < 0.001$), such that a mean percentage difference of -6% was obtained between cultures at 21% and 5% oxygen tension.

4.3.1.3 MMP activity

In the absence of the cytokine, dynamic compression did not significantly influence MMP activity at either oxygen tension (Fig. 4.3A, B). In unstrained constructs, the cytokine increased MMP activity when compared to untreated controls ($p < 0.001$), with values marginally greater at 5% than 21%

oxygen ($p < 0.001$), such that a mean percentage difference of 23% in MMP activity was obtained between cultures at 21% and 5% oxygen tensions. Stimulation with dynamic compression or the NOS inhibitor reduced cytokine-induced MMP activity (all $p < 0.001$), such mean percentage differences of -15% and 27% were achieved respectively between cultures at 21% and 5% oxygen tension. In the presence of TNF α , co-stimulation with compression and L-NIO reduced MMP activity (all $p < 0.001$) with a mean percentage difference of 14% in MMP activity obtained between oxygen tensions of 21% and 5%.

4.3.1.4 TNF α synthesis

The effect of TNF α , compression and oxygen tension on the release of endogenous TNF α into the culture supernatant was then examined (Fig. 4.4A, B). In unstrained constructs cultured at 21% oxygen tension, the cytokine significantly increased TNF α production when compared to untreated constructs ($p < 0.001$). This effect was further enhanced on culturing chondrocyte/agarose constructs at 5% oxygen tension when compared to 21% oxygen, such that a mean percentage difference of 29% was obtained in TNF α release between cultures at 21% and 5% oxygen tension. In contrast, on subjecting constructs to dynamic compression, cytokine-induced TNF α production was reduced, such that a percentage difference of 42% was achieved between cultures at 21% and 5% oxygen tension. Co-stimulation with compression and L-NIO, in the presence of the cytokine reduced cytokine production in an oxygen-independent manner.

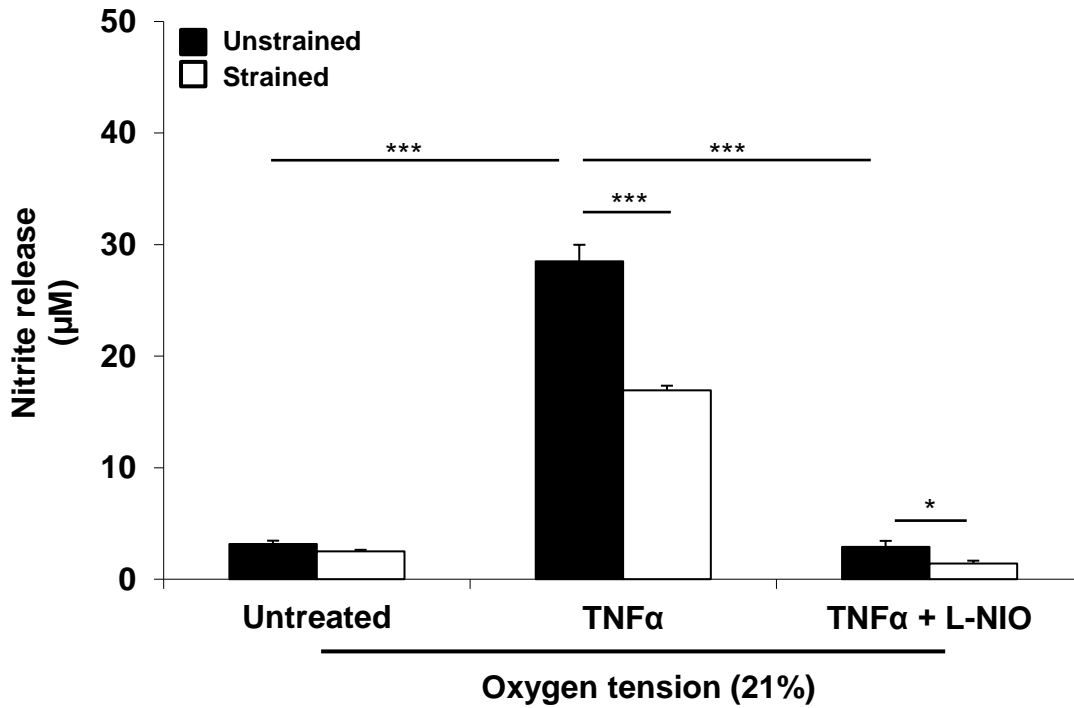
4.3.1.5 GAG synthesis

GAG synthesis was enhanced by dynamic compression when compared to unstrained controls (all $p < 0.001$; Fig. 4.5) with a greater magnitude in stimulation for constructs cultured at 21% oxygen than 5%. At both oxygen tensions, TNF α reduced GAG synthesis (all $p < 0.01$; Fig. 4.5A, B), such that a mean percentage difference in GAG synthesis between cultures at 21% and 5% oxygen tension was -3%. Dynamic compression increased GAG synthesis in cytokine treated constructs (both $p < 0.001$), with a mean percentage difference of -25% achieved between oxygen tensions of 21% and 5%. Co-stimulation with dynamic compression and L-NIO increased GAG synthesis ($p < 0.001$, Fig. 4.5A, B) with the magnitude of stimulation by dynamic compression greater at 5% oxygen than 21%, such that a mean percentage difference of -6% was achieved in GAG synthesis between cultures at 21% and 5% oxygen tension.

4.3.1.6 GAG loss

GAG loss was not influenced by compression at either oxygen tension (Fig. 4.6).

A



B

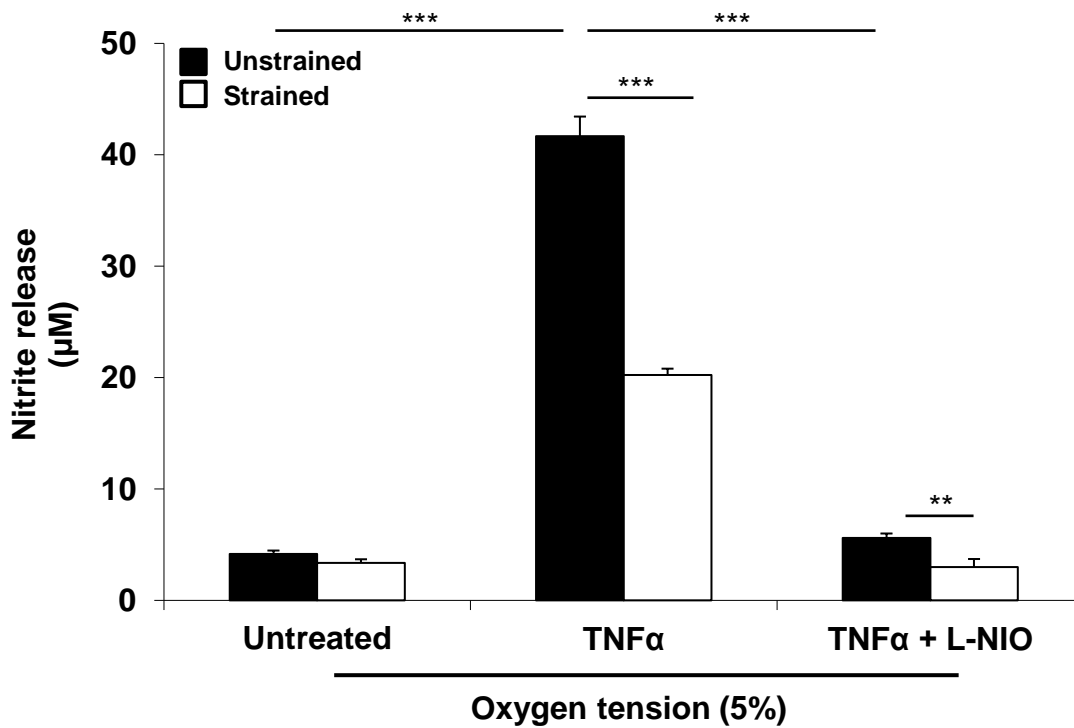


Figure 4.1. Effect of dynamic compression (15%, 1Hz) on nitrite release in chondrocyte/agarose constructs treated with TNFα (0 or 10ng/ml) and/or L-NIO (1mM) at 21% (A) and 5% (B) oxygen tension for 48 hours. Error bars represent the mean and SEM values for 8-12 replicates from four separate experiments. (** or ***) indicates significant comparisons between the different treatment conditions. All other comparisons were not significant (not indicated).

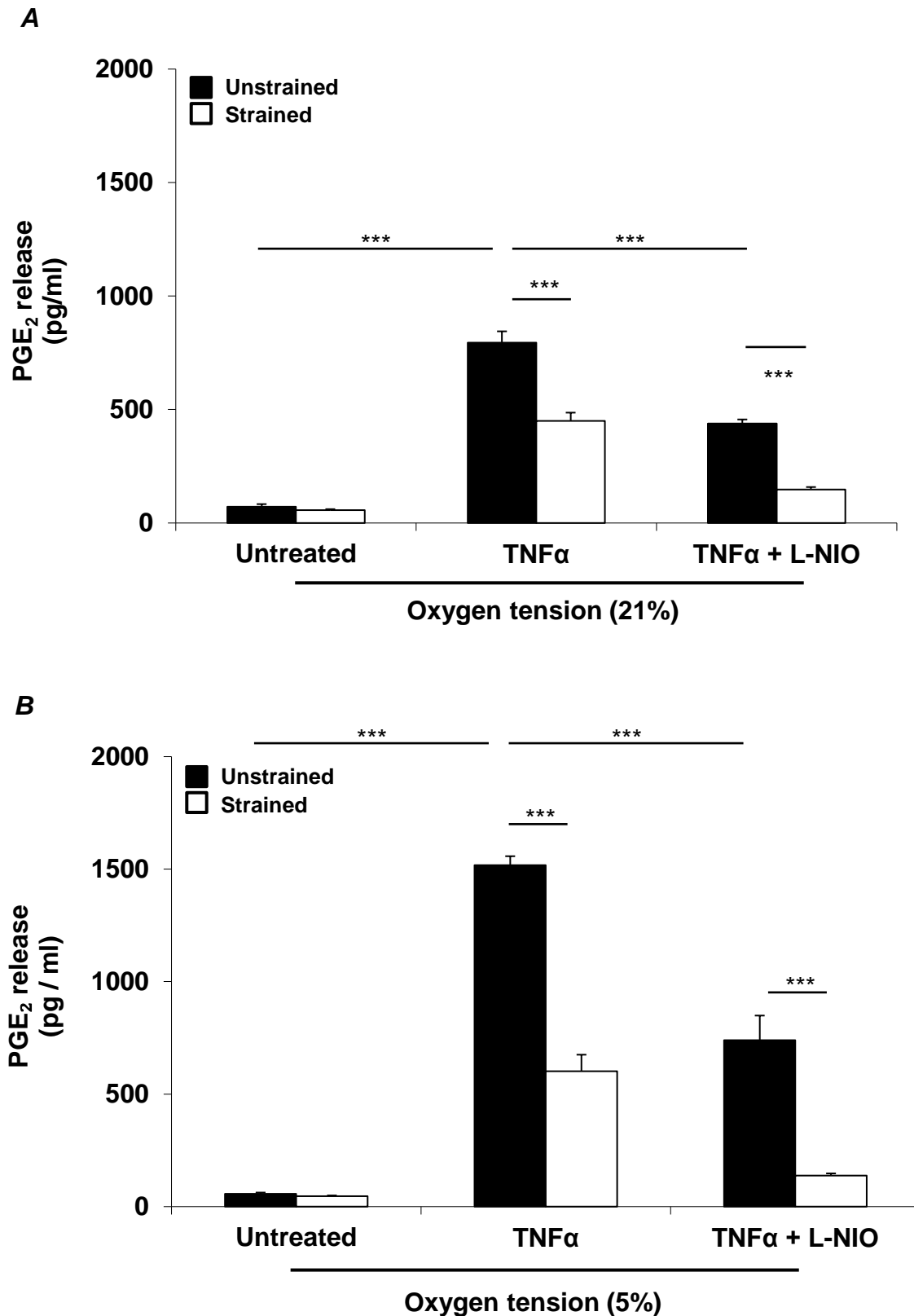


Figure 4.2. Effect of dynamic compression (15%, 1Hz) on PGE₂ release in chondrocyte/agarose constructs treated with TNF α (0 or 10ng/ml) and/or L-NIO (1mM) at 21% (A) and 5% (B) oxygen tension for 48 hours. Error bars represent the mean and SEM values for 8-12 replicates from four separate experiments. (***) indicates significant comparisons between the different treatment conditions. All other comparisons were not significant (not indicated).

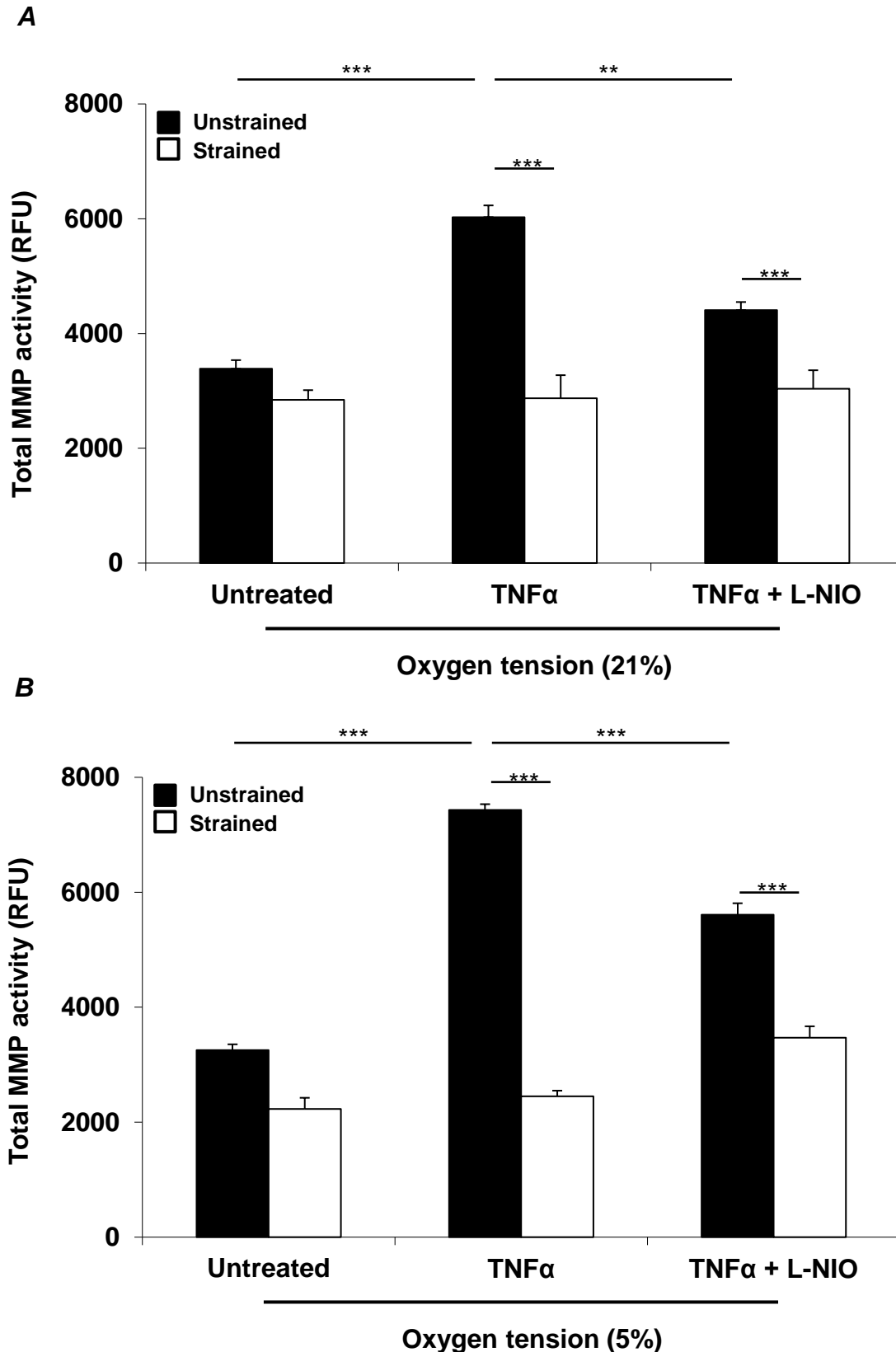


Figure 4.3. Effect of dynamic compression (15%, 1Hz) on MMP activity in chondrocyte/agarose constructs treated with TNF α (0 or 10ng/ml) and/or L-NIO (1mM) at 21% (A) and 5% (B) oxygen tension for 48 hours. Error bars represent the mean and SEM values for 8-12 replicates from four separate experiments. (***) indicates significant comparisons between the different treatment conditions. All other comparisons were not significant (not indicated).

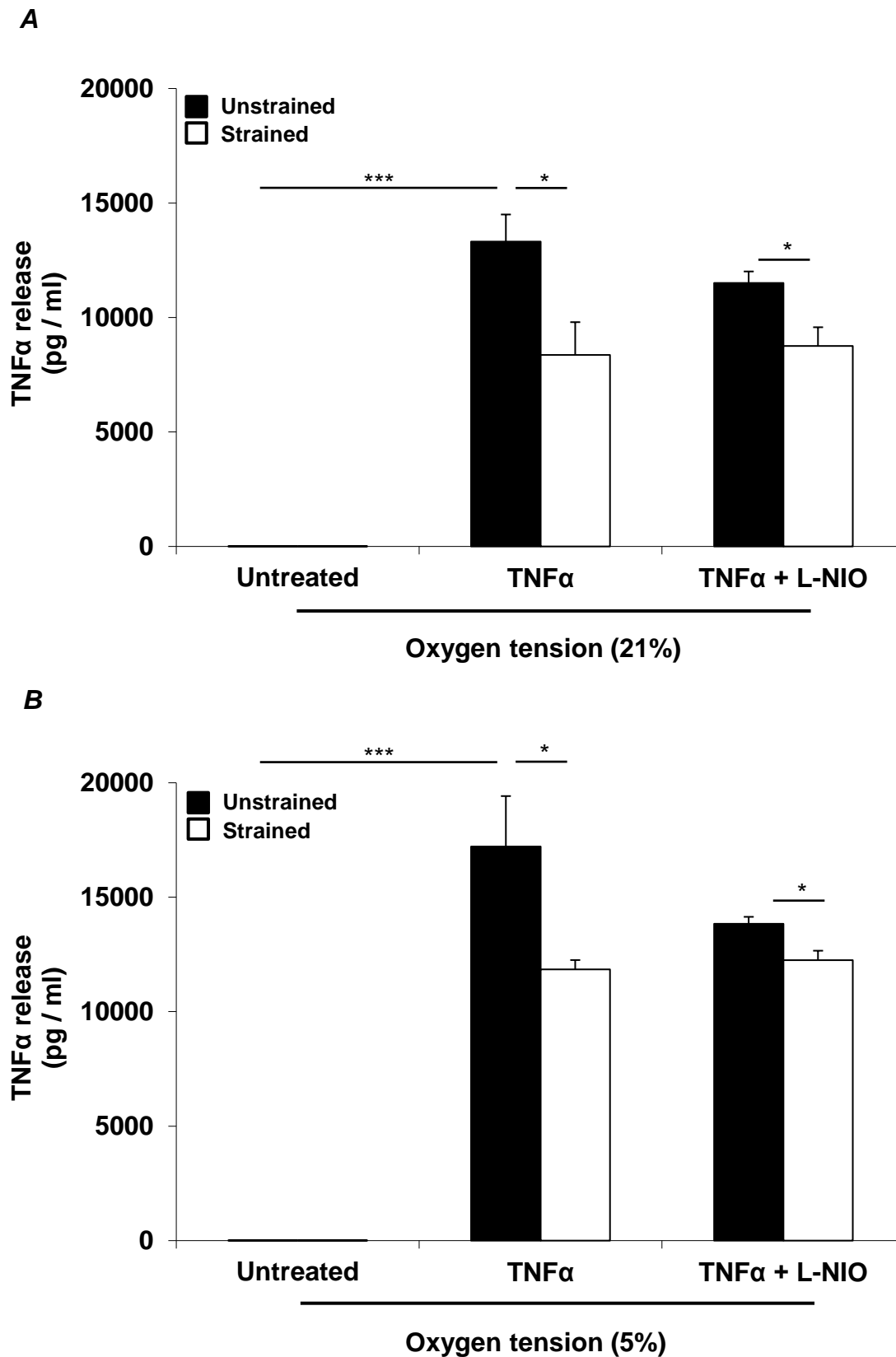


Figure 4.4. Effect of dynamic compression (15%, 1Hz) on TNF α release in chondrocyte/agarose constructs treated with TNF α (0 or 10ng/ml) and/or L-NIO (1mM) at 21% (A) and 5% (B) oxygen tension for 48 hours. Error bars represent the mean and SEM values for 6-8 replicates from two separate experiments. (*or ***) indicates significant comparisons between the different treatment conditions. All other comparisons were not significant (not indicated).

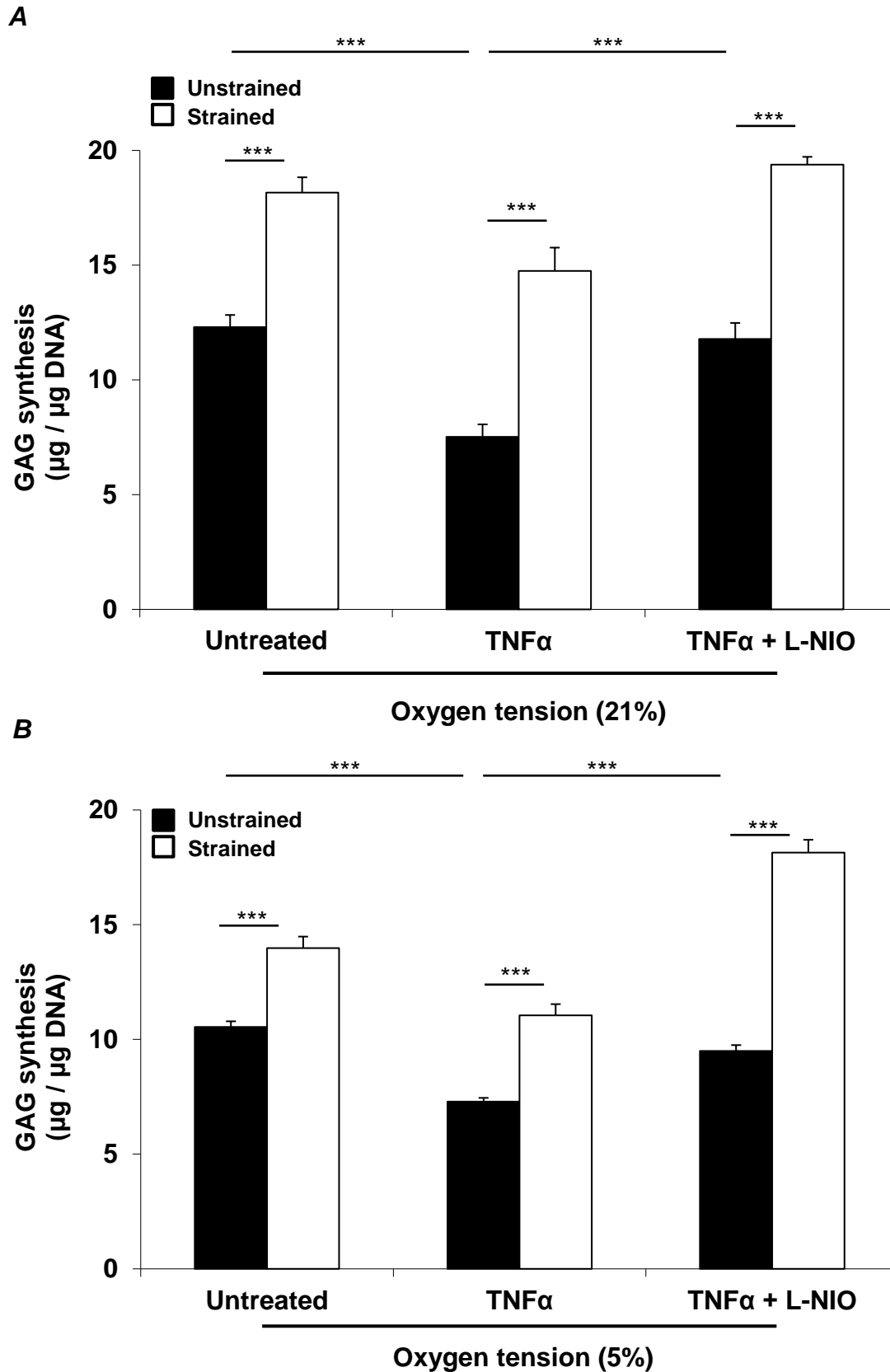


Figure 4.5. Effect of dynamic compression (15%, 1Hz) on GAG synthesis in chondrocyte/agarose constructs treated with TNF α (0 or 10ng/ml) and/or L-NIO (1mM) at 21% (A) and 5% (B) oxygen tension for 48 hours. Error bars represent the mean and SEM values for 8 replicates from two separate experiments. (***) indicates significant comparisons between the different treatment conditions. All other comparisons were not significant (not indicated).

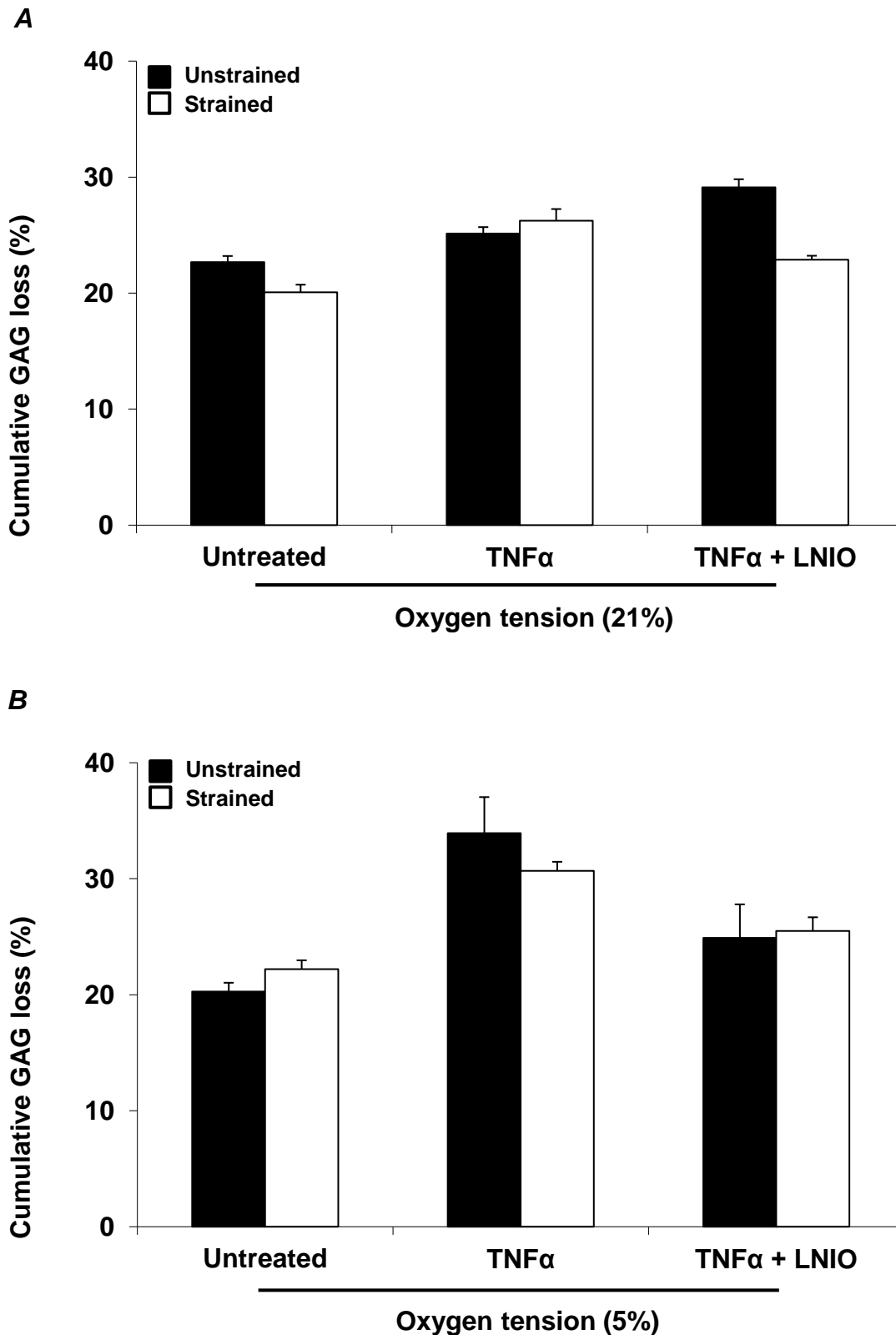


Figure 4.6. Effect of dynamic compression (15%, 1Hz) on GAG loss in chondrocyte/agarose constructs treated with TNF α (0 or 10ng/ml) and/or L-NIO (1mM) at 21% (A) and 5% (B) oxygen tension for 48 hours. Error bars represent the mean and SEM values for 8 replicates from two separate experiments. (***) indicates significant comparisons between the different treatment conditions. All other comparisons were not significant (not indicated).

Table 4.1. The effects of oxygen tension and dynamic compression on catabolic/remodelling activities in chondrocyte/agarose constructs treated with TNF α .

	Nitrite release		PGE ₂ release		MMP activity		GAG synthesis		TNF α release		GAG loss	
	21%	5%	21%	5%	21%	5%	21%	5%	21%	5%	21%	5%
Untreated	-20.6 (\pm 4.4)	-19.9 (\pm 8.3)	-20.8 (\pm 4.7)	-17.0 (\pm 7.6)	-16.1 (\pm 4.9)	-34.4 (\pm 7.3)	47.9 (\pm 3.1)	32.9 (\pm 5.5)	-32.5 (\pm 4.9)	-67.1 (\pm 3.3)	-12.07 (\pm 5.1)	8.89 (\pm 4.0)
TNFα	-39.9 (\pm 2.1)	-50.7 (\pm 2.1)	-43.8 (\pm 3.3)	-60.3 (\pm 4.8)	-43.8 (\pm 6.6)	-67.1 (\pm 5.1)	106.7 (\pm 24.2)	82.3 (\pm 7.2)	-35.1 (\pm 7.5)	-28.6 (\pm 2.5)	10.30 (\pm 5.4)	-5.12 (\pm 7.3)
TNFα + L-NIO	-45.3 (\pm 8.9)	-47.6 (\pm 14.6)	-66.2 (\pm 2.6)	-79.9 (\pm 2.5)	-66.2 (\pm 7.3)	-38.1 (\pm 5.9)	64.4 (\pm 2.9)	90.9 (\pm 5.9)	-21.7 (\pm 3.4)	-11.4 (\pm 1.3)	-22.31 (\pm 3.5)	0.89 (\pm 14.6)

Note. Chondrocyte/agarose constructs were subjected to dynamic compression in the presence and absence of TNF α and/or L-NIO at 21 and 5% oxygen tension for 48 hours. Values were expressed as a percentage change from unstrained control samples (%) where numbers in brackets represent \pm SEM values for n=8-12 from four separate experiments.

4.3.1.7 Summary of catabolic and anabolic mediators

In order to examine the significance of the differences between both oxygen tensions, an ANOVA with post-hoc Bonferroni corrected t-tests were employed, as described in section 2.6. The results for the combination of anabolic and catabolic mediators are summarised in Table 4.2.

It is most convenient to describe these results separately in terms of loading state. In the unstrained condition, there was a statistically significant increase in both nitrite and PGE₂ release at 5% oxygen tension for all three test conditions, which included untreated, TNF α and TNF α +L-NIO treated constructs. By contrast, the GAG synthesis was significantly decreased at 5% oxygen tension ($p < 0.05$) for the untreated and TNF α +L-NIO conditions (Table 4.2).

In the strained condition, the only differences which were statistically significant corresponded to nitrite release and TNF α synthesis, which was generally higher at 5% oxygen tension, and GAG synthesis which was generally higher at 21% oxygen tension.

Table 4.2: Statistical level of differences between cultures at 21% and 5% oxygen tensions stimulated with 10ng/ml of TNF α , with respect to six catabolic and anabolic mediators in both strained and unstrained conditions.

		Nitrite release	PGE₂ release	MMP activity	GAG synthesis	GAG loss	TNFα synthesis
Unstrained	<i>Untreated</i>	(↑) *	(↑) *	NS	(↓) *	(↑) *	NS
	<i>TNFα</i>	(↑) ***	(↑) ***	(↑) **	NS	(↑) *	NS
	<i>TNFα + L-NIO</i>	(↑) ***	(↑) *	(↑) **	(↓) *	NS	(↑) **
Strained	<i>Untreated</i>	(↑) *	NS	NS	(↓) ***	NS	NS
	<i>TNFα</i>	(↑) ***	NS	NS	(↓) **	(↑) *	NS
	<i>TNFα + L-NIO</i>	NS	NS	NS	NS	NS	(↑) **

Where:

$P < 0.05$ * ; $P < 0.01$ ** ; $P < 0.001$ *** ; $P > 0.001$ NS

(↑) represents 5% > 21% effects

(↓) represents 5% < 21% effects

4.4 Summary of results

- Dynamic compression reduced the production of nitrite, PGE₂ and MMP activity in response to TNF α and this response was abolished when dynamic compression was coupled with the NOS inhibitor.
- Differences in the loading-induced response were observed, such that the magnitude of inhibition was greater at 5% oxygen tension when compared to 21%.
- The stimulation of GAG synthesis by dynamic compression was greater at 21% oxygen tension when compared to 5%, although this difference was not apparent with TNF α in the presence of L-NIO.

4.5 Discussion

In *ex-vivo* bioreactor studies, dynamic compression reduced the production of inflammatory mediators in response to TNF α , and this response was abolished when dynamic compression was coupled with the NOS inhibitor. We observed differences in the loading-induced response such that the magnitude of inhibition was greater at 5% oxygen tension than 21%. In addition, the beneficial response was paralleled with anabolic activities as typified by increased matrix synthesis that was greater at 21% oxygen tension than 5%. The literature is sparse with respect to the combined effect of TNF α and dynamic compression at low oxygen tensions in chondrocytes. However, the effect of oxygen tension and mechanical stress in the absence of cytokines is well characterized (Fermor et al., 2007, Fermor et al., 2005, Wernike et al., 2008). Matrix synthesis was increased and chondrogenic gene expression was stabilised by long-term mechanical loading at 5% oxygen tension when compared to 21% in a chondrocyte/polyurethane model (Wernike et al., 2008). Conversely in porcine cartilage explants, mechanical loading enhanced NO production at 5 and 20% oxygen tension and the response was reduced at 1% oxygen tension (Fermor et al., 2007, Fermor et al., 2005).

A similar effect was observed in the alginate model which reported a greater production of GAG synthesis at 5% oxygen tension compared to 20% (Wernike, Alini and Grad, 2008). The differences observed in the present study are due to the type of model system used, for example, cell type, 2D versus 3D model, primary versus passage cells, free-swelling culture versus mechanical loading, uninterrupted oxygen tension using the Biospherix system versus oxygen controlled incubators (Meyer et al., 2010, Markway et al., 2016).

However, the manner in which cytokine-induced inflammatory pathways are influenced by oxygen tension and biomechanical signals are unclear. Further studies are needed to unravel the distinct pathways induced by oxygen tension, biomechanical signals and TNF α , which will help in identifying key targets and potential therapies for OA.

In summary, the present study demonstrates that exogenous TNF α combined with low oxygen tension enhanced the production of inflammatory mediators, which are reduced with biomechanical signals or the presence of the NOS inhibitor in an oxygen-dependent manner. The inflammatory environment attempts to assist with tissue remodelling but the response was influenced by biomechanical signals leading to restoration of matrix synthesis. Although selective inhibition of NOS and stimulation with biomechanical signals leads to chondroprotection, further studies are needed to unravel the distinct pathways induced by oxygen tension, biomechanical signals and TNF α . This will help to identify key targets and potential therapies for OA treatments.

Chapter 5 – Optimization of qRT-PCR techniques to examine the combined effects of oxygen tension and TNF α on gene expression in compressed chondrocytes

5.1 Introduction

From chapter 4, it was observed that biomechanical signals regulated the inflammatory signalling events induced by the combined effects of oxygen tension and TNF α . In order to further elucidate the manner in which oxygen tension influences the intracellular pathways activated by TNF α in dynamically stimulated chondrocytes, the present study employed the well characterised chondrocyte/agarose model, described in Chapter 2, to examine the combined effects of oxygen tension and TNF α on gene expression. This approach permits analysis at the molecular level to be performed such that alterations in mRNA expression levels of target genes in agarose construct can be detected (Chowdhury et al., 2008, Akanji et al., 2009, Raveenthiran and Chowdhury, 2009). The employment of such methods will ultimately prove to be useful in the identification of key targets in the development of therapeutic agents for osteoarthritis treatment.

5.2 Materials and methods

5.2.1 Effect of dynamic compression on the gene expression of TNF α stimulated chondrocyte/agarose constructs cultured at 21 and 5% oxygen tension.

For the application of dynamic compression to constructs cultured at 21% and 5% oxygen tensions, the novel *ex-vivo* bioreactor system (Bose ElectroForce, Gillingham, UK) described in Chapter 2 was used in a similar manner (Parker et al., 2013). Briefly, constructs were transferred into individual wells of a 24-well culture plate (Costar, High Wycombe, UK) and mounted within the bioreactor system that is integrated within the Biospherix incubator. The medium was supplemented with either 0 or 10ng/ml TNF α in the presence and absence of 1mM L-NIO and the experimental conditions during set-up and culture were uninterrupted. Constructs were then subjected to intermittent compression under unconfined conditions, with a profile of 10 min compression followed by a 5 hour 50 min unstrained period for a culture period of 6 hours, as previously described (Parker et al., 2013). In a previous study in the host laboratory these *ex-vivo* conditions were found to be optimal when measuring gene expression (Parker et al., 2013). The compression regime was applied in a dynamic manner with a strain amplitude of 0-15%, using a sinusoidal waveform at a frequency of 1Hz and resulted in 600 duty cycles over the 6 hour culture period. Control constructs were maintained in an unstrained state in the bioreactor system and cultured for the same time period. At the end of the experiment, the constructs and corresponding media were stored at -80°C prior to analysis.

5.2.2 Gene expression levels

In this study, real-time quantitative PCR (qPCR) was used to quantify basal levels of gene expression in response to the different treatment conditions stated in section 5.2.1.

5.2.2.1 RNA isolation

Prior to extracting RNA from each chondrocyte/agarose construct, the bench surface was thoroughly sprayed with RNaseZAP in order to remove RNase from the working area, which would be capable of degrading any RNA present in the samples. Each chondrocyte/agarose construct was then defrosted from -80°C by incubating it with 750 μ l of buffer QG in a 1ml microcentrifuge tube at 42°C for 10mins, using a heat block. During this step, the agarose construct was also digested, while compromising the cell membrane of chondrocytes present in the sample due to the action of the QG buffer. The tubes were then removed from

the heat block and placed on a dry rack on the bench, after which 125µl of isopropanol was added to each sample and mixed in order to increase the RNA yield. 800µl of the resulting solution was then added onto an RNeasy® spin column and centrifuged using a conventional table-top microfuge at 8000g for 15 seconds at room temperature. The flow-through was then discarded and the remaining mixture was loaded onto the column and centrifuged as above. 500µl of QG buffer was then loaded onto the same RNeasy® spin column in order to remove any remaining agarose and centrifuged again at 8000g for 15 seconds at room temperature. The flow-through was then discarded, followed by the addition of 700µl of buffer RW1 to the RNeasy® spin column in order to remove any proteins, which may have been present in the sample. Centrifugation was then carried out at the same conditions outlined previously. Buffer RPE was then diluted by the addition of 44ml of 100% ultra-pure ethanol to the RPE container provided in the QIAquick Spin gel extraction and RNeasy® kit. 500µl of this solution was then added to the RNeasy® spin column, after the flow-through from the previous centrifugation step was discarded. Centrifugation was then repeated at the same conditions described previously, followed by the elimination of the resulting flow-through. The empty RNeasy® spin column was then centrifuged again at 8000g for 1 minute at room temperature to ensure the removal of any excess solution present in the column. Using a fresh 2ml collection tube, 40µl of RNase-free water was added to the RNeasy® spin column and centrifuged at 8000g for 1 minute, after which the flow-through was discarded. The eluted RNA sample was then immediately transferred onto ice to avoid degradation.

DNase treatment was then carried out by adding 1µl of DNase I enzyme and 10x DNase buffer to the RNase sample and incubating it for 20 minutes at 37°C. Another incubation period then followed for 2 minutes at room temperature, after adding 4µl of DNase inactivating reagent to the tube. This resulted in the production of slurry by the DNase inactivating agent, which was pelleted by carrying out centrifugation at 14000g for 1 minute at 4°C. The RNA containing solution was then transferred into a new microfuge tube and kept on ice or stored at -70°C prior to RNA quantification.

The NanoDrop ND-1000 spectrophotometer (LabTech, East Sussex, UK) was used to quantify the amount of RNA present in each sample as follows. Initially, the sample pedestal of the spectrophotometer was cleaned and loaded with 1µl of RNase-free water, in order to blank the NanoDrop system. This was then followed by replacing the water on the pedestal with 1µl of RNA sample, after which RNA absorbance was measured. In each microlitre of sample, the NanoDrop system was capable of automatically measuring RNA concentrations at 260/280nm, to yield values ranging between 2 to 3000ng/µl (Qiagen, West Sussex, UK) (Parker et al., 2013, Lee et al., 2011).

At this stage, RNA samples could be stored at -80°C. However, it was advisable to carry out the reverse transcription process for the conversion of RNA to cDNA before storage, since samples are more stable in this form. Indeed cDNA samples can then be stored at 4°C for up to 1 week.

5.2.2.2 Reverse transcription and cDNA synthesis

In order to perform reverse transcription for the conversion of RNA samples into cDNA, the Enhanced Avian RT First Strand cDNA synthesis kit (Sigma Genosys, Cambridge, UK) was employed which consisted of the following components: oligo (dT)₂₃ primer, deoxynucleotide mix (dNTP), reverse transcriptase (RT), 10X buffer and RNA inhibitor (RNAi). Initially, the volume of RNA sample required to prepare a reaction mixture of 10µl was calculated using equation 6.1 for the conversion of 200ng of RNA sample into cDNA.

$$RNA \text{ volume } (\mu l) = \frac{200ng \text{ of RNA}}{RNA \text{ concentration from NanoDrop } (ng/\mu l)} \quad \text{Equation 5.1}$$

Each RNA sample was then prepared for reverse transcription in microfuge tubes placed on ice, according to manufacturer's instructions, using the reagents listed in reaction 1, in an ordered manner.

Reaction 1:

RNAse-free water	variable (µl)
Oligo (dT) ₂₃ primer	0.5µl
RNA volume per sample	variable (µl)
Total volume	5µl

Each microfuge tube was then centrifuged using a manual table-top microcentrifuge for 5 seconds, before being transferred onto a thermal cycler, where they were allowed to incubate for 10 minutes at 70°C to permit denaturation of the RNA secondary structure for more efficient reverse transcription.

In a separate 1.5ml microfuge tube placed on ice, a master mix solution was then prepared using the reagents listed in reaction 2 in an ordered fashion, according to manufacturer's instructions.

Reaction 2:

RNAse-free water	2.5µl
10x buffer	1µl
dNTP	0.5µl
RNAi	0.5µl
RT	0.5µl
Total volume	5µl

Note: The volumes of reagents listed in reaction 2 are for the preparation of master mix for one RNA sample. These volumes would be multiplied by the number of RNA samples required for reverse transcription to cDNA.

The master mix solution was then thoroughly spun using a manual table-top centrifuge for 5 seconds. Once incubation of the RNA samples was completed on the thermo cycler for 10 minutes, a volume of 5 μ l of the prepared master mix solution was then added to each RNA sample such that a final volume of 10 μ l of reaction mixture was generated per sample. Each sample was then spun again for 5 seconds using a manual table-top centrifuge, after which they were allowed to incubate for 1 hour at 42°C in a thermo cycler. The first-strand cDNA synthesis reactions were then snap-cooled on ice for 5 minutes, prior to performing qRT-PCR. Alternatively, for long-term storage, reactions can be stored for up to 6 months.

5.2.2.3 Real-time quantitative PCR

Real-time quantitative PCR was used to measure alterations in gene expressions in first-strand cDNA synthesis reactions using syber-green PCR. Syber-green is a fluorescent dye which specifically binds to double stranded DNA (dsDNA) and has an excitation/emission spectra of 494/521nm. By measuring the increase in fluorescence at a wavelength of 521nm, it is capable of quantifying the PCR product accumulated during the annealing and extension phases of the PCR reaction during qRT-PCR. The cycle number at which this increase in fluorescence is exponential is recorded and termed the Ct value (threshold cycle) and defined as the number of cycles required for the fluorescence signal to exceed the background fluorescence and an arbitrary threshold line. Although syber-green PCR is cost effective compared to other probe-based techniques, it is associated with one limitation, which is the ability of the fluorescent dye to bind to any dsDNA, regardless of its specificity. As such, primers designed such that their sequences are specific to the region of DNA required to be copied, are employed.

In order to perform qRT-PCR on 200ng of RNA (Sigma Genosys, Cambridge, UK), SYBR® Green JumpStart™ Taq ReadyMix™ (with MgCl₂ in buffer; Sigma Genosys, Cambridge, UK, D4438) was employed. Each PCR reaction consisted of the components listed in reaction 3, to achieve a final reaction volume of 10 μ l.

Reaction 3: qRT-PCR reaction:

Template cDNA	2.5 μ l
Primer (0.5 μ M)	2.5 μ l
2X SYBR green 1 Master Mix	
Jumpstart (Sigma D4438)	5 μ l
Total volume	10μl

Additionally, in order to distinguish between background contamination and actual gene expression, nuclease-free PCR-grade water (Sigma Genosys, Cambridge, UK) was used in place of template cDNA, as a standard negative control, termed 'no template control' (NTC).

The following specific primer sequences were used:

- ADAMTS-5 (NM_001166515) Forward: 5'-GCCCTGCCAGCTAACGGTA-3', Reverse: 5'-CCCCGGACACACACGGAA-3'
- MMP-13 (NM_174389.2) Forward: 5'-CCCTTGATGCCATAACCAGT-3', Reverse 5'-GCCCAAATTTTCTGCCTCT-3' and
- 18S (NR_036642.1) Forward: 5'-GCAATTATCCCATGAACG-3', Reverse: 5'-GGCCTCACTAAACCATCAA-3'.

All reactions were carried out at an annealing temperature of 60°C, except MMP-13, which was carried out at a temperature of 58°C. PCR efficiencies for optimal primer pair concentrations were derived from standard curves as described in the PCR optimization section (section 5.4). Each sample was run in duplicates on the 96-well thermal system of the Mx3000P quantitative PCR instrument (Stratagene, Amsterdam, The Netherlands). A three-step thermal cycling programme was incorporated which comprised of the following thermocycling conditions:

Segment 1 (1 cycle): Activation: 3 minutes at 95°C,

Segment 2 (40 cycles): Denaturation: 30 seconds at 95°C,
Annealing: 1 minute at 55 or 60°C and
Extension: 1 minute 72°C

Segment 3 (1 cycle): Melt curve: 1 minute at 95°C,
30 seconds at 55°C and
30 seconds at 95°C.

Fluorescence data were collected during the annealing stage of amplification, and data were analysed on the MxPro qPCR software (version 3, Stratagene). Baselines and threshold values were automatically prescribed by the RG-3000 qPCR software and used after manual inspection. The cycle threshold (Ct) value for each duplicate reaction was expressed as the mean value, and the results were exported into Microsoft Excel for subsequent statistical analysis. The Ct values for 18S remained stable, with no changes detected under all culture conditions, suggesting its suitability as a reference gene. Relative quantifications of ADAMTS-5 and MMP-13 signals were estimated by normalizing each target to the reference gene, 18S, and to the calibrator sample by a comparative Ct approach. For each sample, the ratio of target Δ Ct and reference Δ Ct was calculated, as previously described (Lee et al., 2011, Pfaffl, Horgan and Dempfle, 2002). Ratios were expressed on a logarithmic scale (base 10, arbitrary units).

5.3 Statistics

For the *ex-vivo* bioreactor experiments, data represent the mean and SEM values of 4 replicates from two separate experiments. Statistical analysis was performed using a two-way analysis of variance (ANOVA) and the multiple post hoc Bonferroni-corrected t-tests to compare differences between the various treatment groups as indicated in the figure legend. In all cases, a level of 5% was considered statistically significant ($p < 0.05$).

5.4 qRT-PCR optimization

5.4.1 Introduction

Even though it is not standard to optimize qRT-PCR, it has been shown that well-designed assays may benefit from some degree of basic optimisation. This will not only result in an improvement in the reproducibility of replicates, but also increase the efficiency of the assay. qRT-PCR can be optimized by a variety of strategies. In this thesis, qRT-PCR was optimized by first selecting a standard set of conditions for the assay, as described in section 5.2.2.3 and then examining whether the constant criteria for performance were met by the assay. The main criteria for this assay was to attain an amplification efficiency ranging between 95 and 105%, with a correlation coefficient > 0.98 after performing a 1:5 or a 1:10 cDNA dilution series with 3 replicates. Based on the results obtained from the standard set of conditions, the assay conditions were altered to achieve the ideal performance.

5.4.2 Primer binding efficiency

The optimal hybridisation of primers is an essential factor in optimising PCR efficiency, which can be manipulated by either altering primer concentration or temperature of the PCR reaction. Since most qPCR systems lack a temperature variable block, capable of ensuring extremely precise thermal uniformity, PCR reactions were optimised in this thesis by adjusting the primer concentration, which is generally considered to be the more accepted strategy. Since the primers employed in this thesis were previously optimised to be used at a concentration of $0.5\mu\text{M}$ in bovine chondrocyte samples treated with IL-1 α (Blain, Ali and Duance, 2010), optimization of primer concentration was performed at the same concentration. As such, the next step of calculating the amplification efficiency was carried out in order to integrate the selected primer concentration to the treatment conditions used for the samples. To achieve this, a 5-fold serial dilution of cDNA from sample that represented the untreated control at 21% oxygen tension was performed to yield four different concentrations of cDNA, labelled '4' to '1', with the former representing the highest concentration of cDNA sample. Each concentration of cDNA sample was then run in triplicates at the thermocycling conditions set in section 5.2.2.3, using the Mx3000P quantitative PCR instrument (Stratagene, Amsterdam, The Netherlands). It is also worth noting that each PCR reaction consisted of the components listed in reaction 3, to achieve a final reaction volume of $10\mu\text{l}$. Results from the serial dilution of cDNA were plotted as cDNA dilution series (1:5) versus the average Ct value of each corresponding cDNA concentration, with a linear model fitted to the data, as shown in figure 5.1.

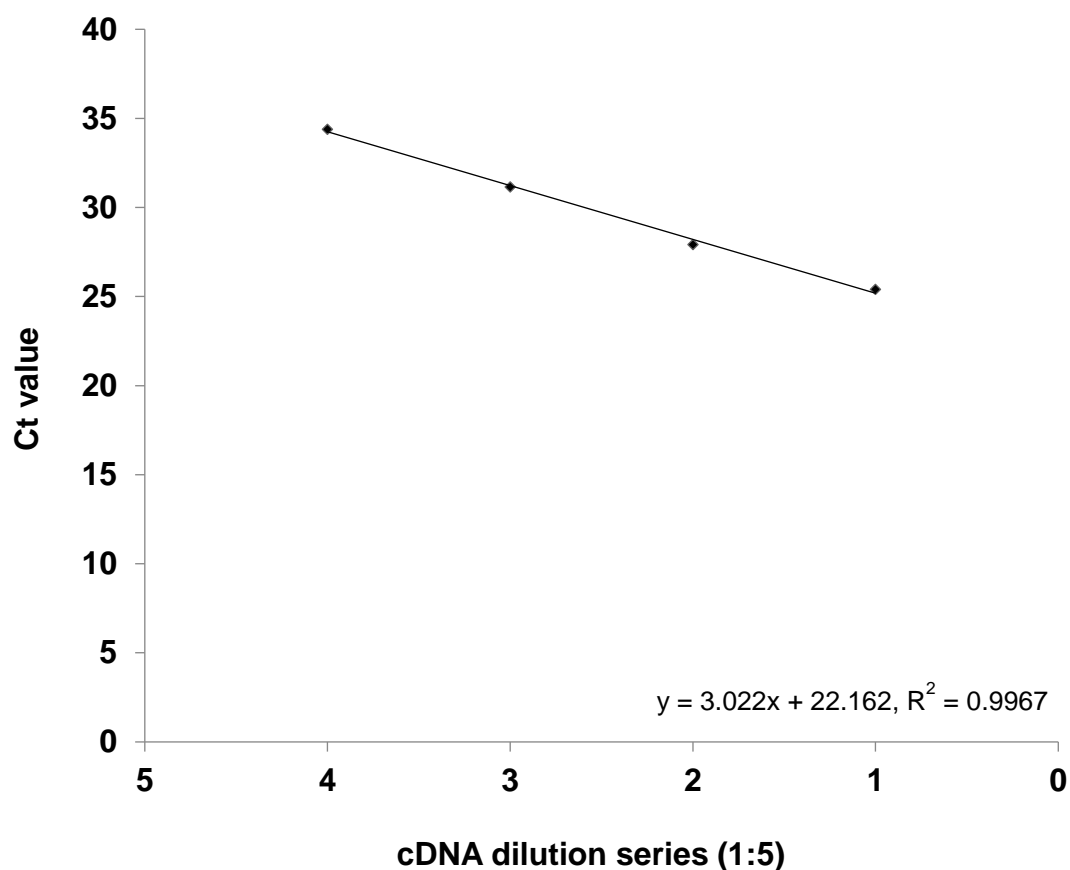


Figure 5.1. Standard curve obtained from 1:5 serial dilution of cDNA sample using 18S primers at a concentration of 500nM.

The real-time PCR efficiency (E) of amplification for each target was then defined according to the relation,

$$E = 10[-1/\text{slope}] \quad \text{Equation 5.2}$$

Similarly, standard curves were plotted for ADAMTS-5 and MMP-13 primers as shown in figure 5.2 and 5.3, respectively. The R^2 value of the standard curves exceeded 0.99 and revealed efficiency values ranging from 1.94 to 2.03.

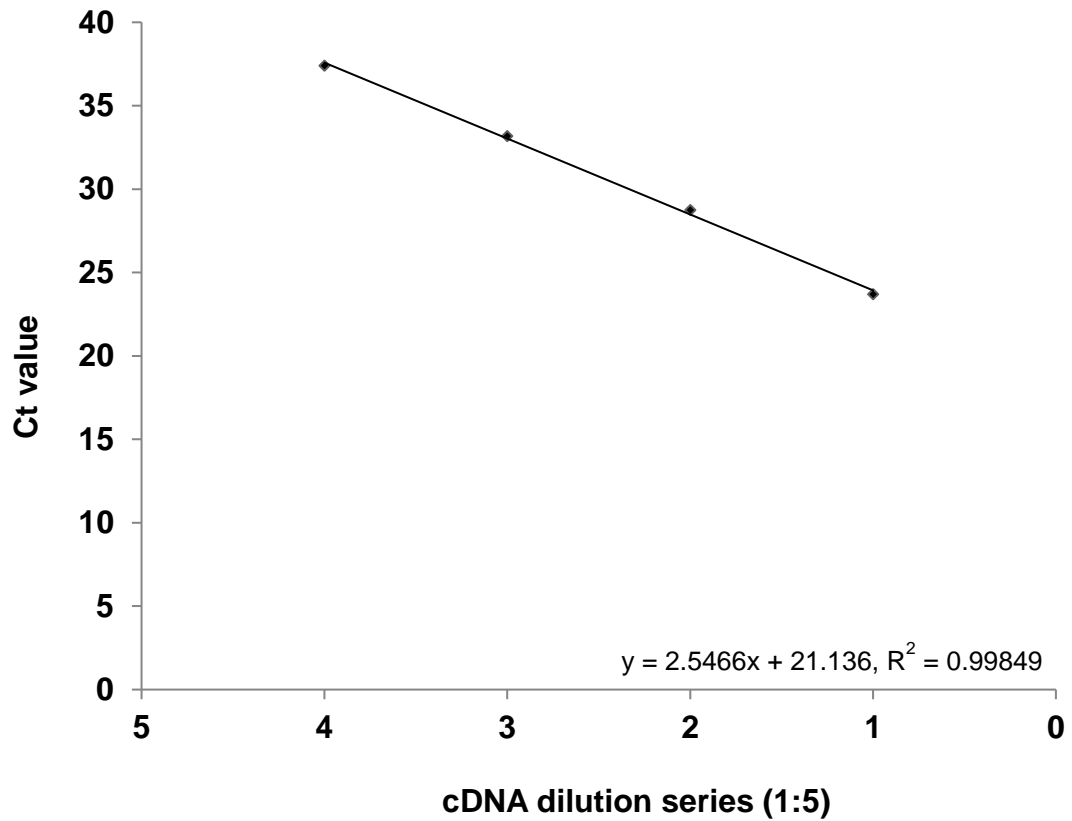


Figure 5.2. Standard curve obtained from 1:5 serial dilution of cDNA sample using ADAMTS-5 primers at a concentration of 500nM.

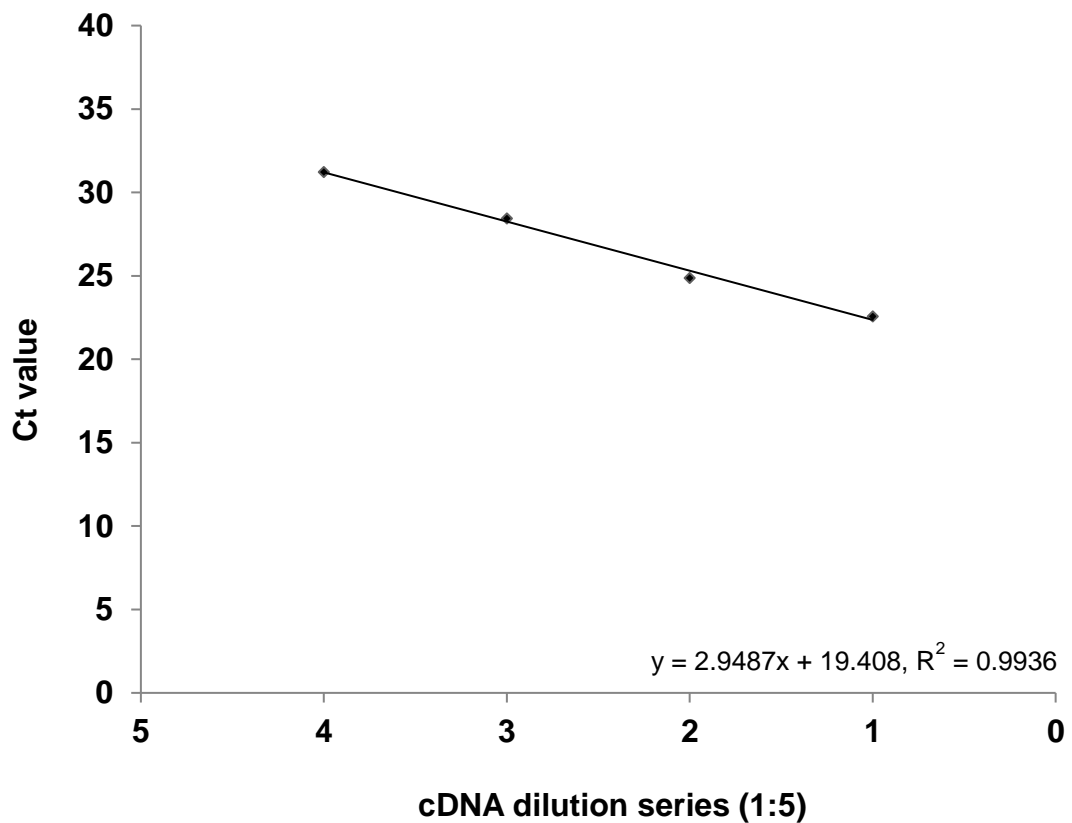


Figure 5.3. Standard curve obtained from 1:5 serial dilution of cDNA sample using MMP-13 primers at a concentration of 500nM.

5.4.3 Minimizing well evaporation

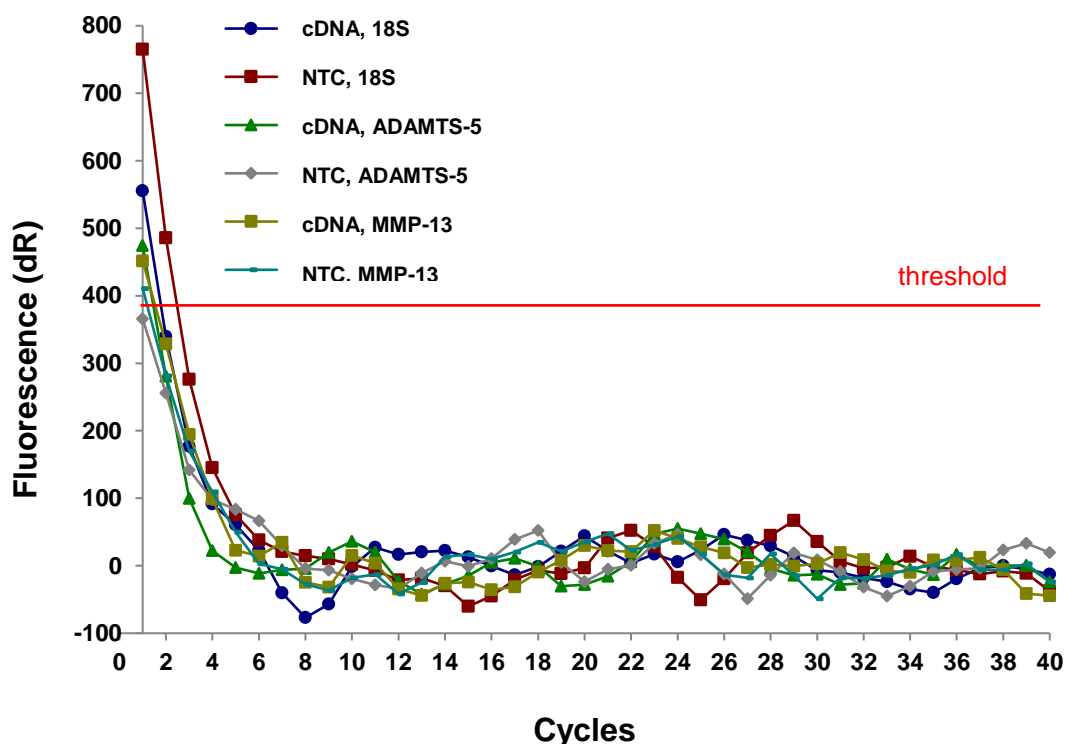


Figure 5.4. Amplification curves obtained on carrying out qRT-PCR on nuclease-free PCR-grade water and cDNA samples, using 18S, MMP-13 and ADAMTS-5 primers in a three-step thermal cycling programme, according to the standard conditions stated in section 5.2.2.3.

Initially, the standard set of conditions for qRT-PCR listed in section 5.2.2.3 were tested on cDNA samples as well as nuclease-free PCR-grade water, using the primers 18S, MMP-13 and ADAMTS-5, in order to check whether the constant criteria for performance were met by these stated conditions of the assay. It was observed that irregular fluorescence readings were obtained for each cDNA/water sample, as shown in the amplification plot in figure 5.4. There was no increase in fluorescence above the threshold line, set at 370dR and, as a result, no Ct values were recorded on the MxPro qPCR software. On inspecting the 96-well plate, it was observed that at the end of the three-step thermal cycling protocol, all wells containing 10 μ l of PCR reaction mix were completely dried out due to evaporation resulting from:

- the use of an ineffective cover slip on the 96-well plate
- carrying out a three-step thermal cycling protocol which subjects samples to high temperatures for a longer period of time instead of a three-step thermal cycling protocol
- the use of an insufficient volume of PCR reaction mix - 10 μ l

To test the first factor, the cover slip used to seal the 96-well plate was changed to a new batch of an adhesive PCR polyester film (Thermo Fisher Scientific, Loughborough, UK, AB0558). This material was capable of withstanding temperatures of up to 120°C during thermal cycling, while preventing evaporation. Since the highest temperature to which samples were subjected was 95°C, this plate sealant was deemed ideal for the specific application.

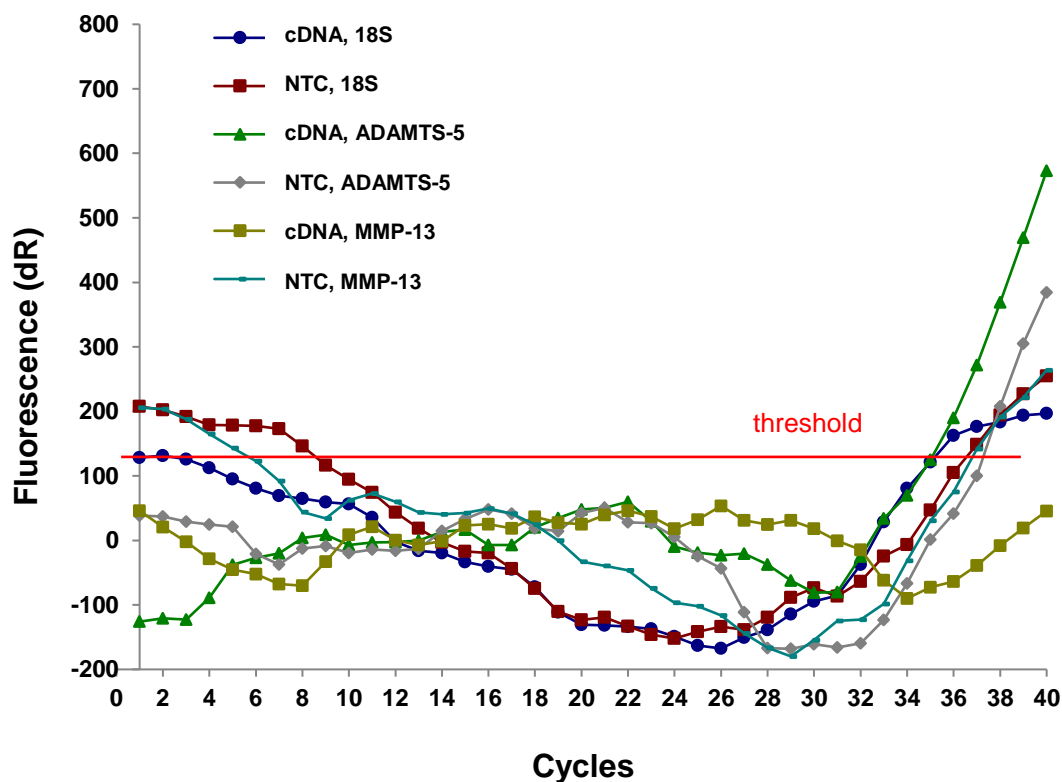


Figure 5.5. Amplification curves obtained on employing a new batch of plate sealer for qRT-PCR on nuclease-free PCR-grade water and cDNA samples, using 18S, MMP-13 and ADAMTS-5 primers in a three-step thermal cycling programme, according to the standard conditions stated in section 5.2.2.3.

Using the new cover slip, the PCR process was repeated on cDNA samples as well as nuclease-free PCR-grade water, using the primers 18S, MMP-13 and ADAMTS-5, while keeping all other assay conditions constant. On inspecting the 96-well plate on completion of the PCR process, it was observed that evaporation of the wells was successfully prevented. As such, it was unnecessary to reduce the three-step PCR reaction to a two-step thermal cycling protocol. It is worth noting that although increasing the volume of PCR reaction mix may have been an alternative solution to minimizing well evaporation, there was limited availability of cDNA samples.

On employing the new batch of plate sealants, the fluorescent readings obtained for each cDNA/water sample were still irregular and below the threshold line, until at least the 34th cycle of the PCR reaction, as shown from the amplification plot in figure 5.5. Additionally, these fluorescence curves did not plateau, which is required to ensure the completion of the PCR reaction.

Since all the other set of conditions stated in section 5.2.2.3 were in place and incapable of creating such irregular fluorescence readings, the only possible contributing factor to such signals was the type of syber-green used in the assay. Subsequently, the reagent was changed from SYBR® Green JumpStart™ Taq ReadyMix™ (with MgCl₂ in buffer; Sigma Genosys, Cambridge, UK, D4438) to Kapa SYBR® FAST Universal qPCR Master Mix (2X) containing KAPA SYBR® and Green 1 dye (Kapa Biosystems, Wilmington, Massachusetts, USA). Using the new syber-green, qRT-PCR was then carried out on cDNA samples as well as nuclease-free PCR-grade water, using only MMP-13 primer pairs, while keeping all other assay conditions constant. This resulted in a PCR reaction with the constituents listed in reaction 4. Only one primer pair was tested in this optimization step since testing one primer pair was sufficient to determine the efficacy of KAPA syber-green, without the use of the other primer pairs. Furthermore, using only one primer pair minimized the waste of cDNA and other resources. It was essential to include nuclease-free PCR-grade water in this optimization step to identify contamination of reagents and false amplification, as described previously.

Reaction 4:

Template cDNA	2.5µl
Primer (0.5µM)	2.5µl
KAPA master mix	5µl
Total volume	10µl

Figure 5.6 illustrates the amplification plot obtained from running a three-step thermal cycling qRT-PCR programme on cDNA and water samples, using MMP-13 primer pairs and KAPA master mix.

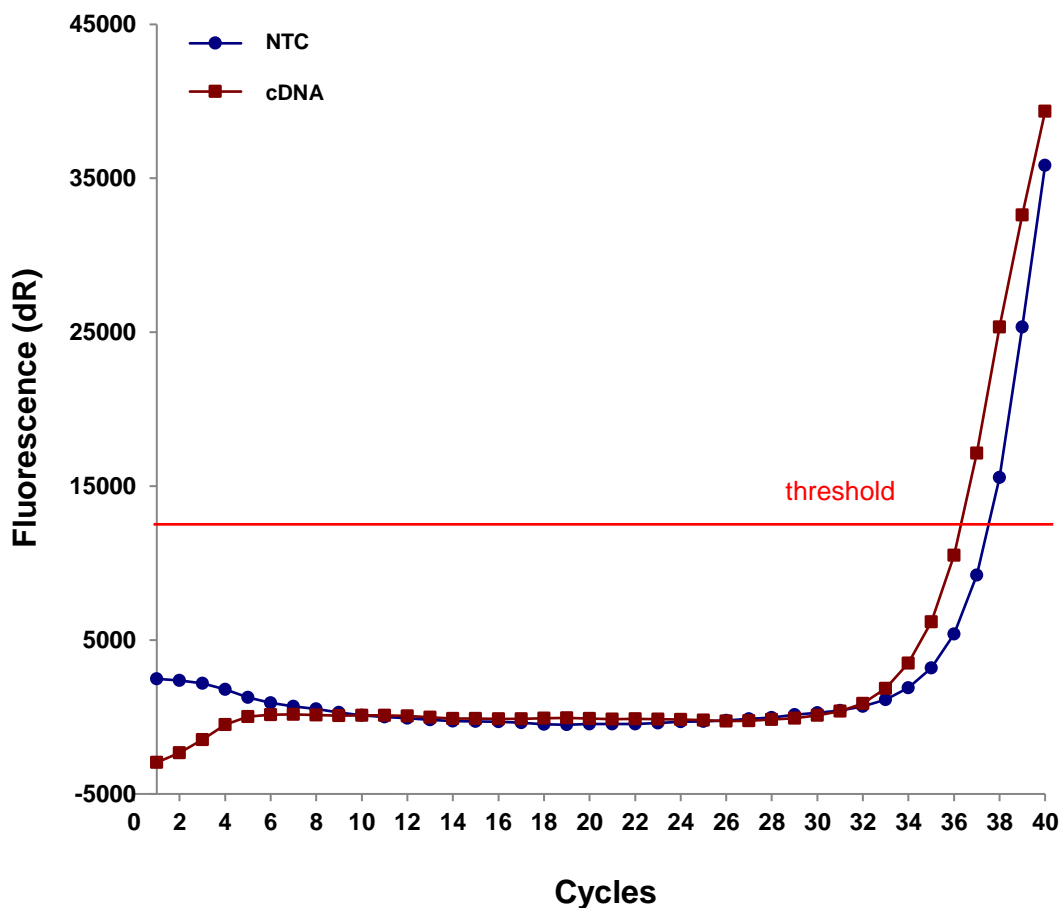


Figure 5.6. Amplification curves obtained on employing KAPA master mix for qRT-PCR on nuclease-free PCR-grade water and cDNA samples, using MMP-13 primer pairs in a three-step thermal cycling programme.

It was evident that the employment of the KAPA master mix successfully prevented the production of irregular fluorescent readings and noise. The amplification plots obtained for both cDNA and water samples, using MMP-13 primer pairs were similar to that of a standard qRT-PCR amplification plot. There was an exponential increase in fluorescence for both cDNA and NTC samples above the threshold line, such that Ct values of 36.2 and 37.6 were obtained for cDNA and NTC samples respectively. As the PCR reaction proceeded, there was a steady increase in fluorescence for both samples up to the 40th cycle of the reaction, hence creating the linear region of the PCR reaction. However, following this region, the expected plateau stage was not established, which may have been due to limitations such as a loss in specificity. Additionally, the difference in Ct values between that of the cDNA and NTC values was less than minimal, accounting for the presence of reagent contamination or false amplification. As such, magnesium chloride (MgCl₂) was incorporated, into the PCR reaction to improve the stringency of the reaction. qRT-PCR was performed on both cDNA and NTC samples in duplicates, using MMP-13 primer pairs under a three-step thermal cycling programme with and without the employment of MgCl₂, as shown in reactions 5A and 5B:

Reaction 5A (+MgCl₂):

Template cDNA	1.5µl
Primer (0.5µM)	2.5µl
KAPA master mix	5µl
MgCl ₂	1µl
Total volume	10µl

Reaction 5B (-MgCl₂):

Template cDNA	2.5µl
Primer (0.5µM)	2.5µl
KAPA master mix	5µl
MgCl ₂	0µl
Total volume	10µl

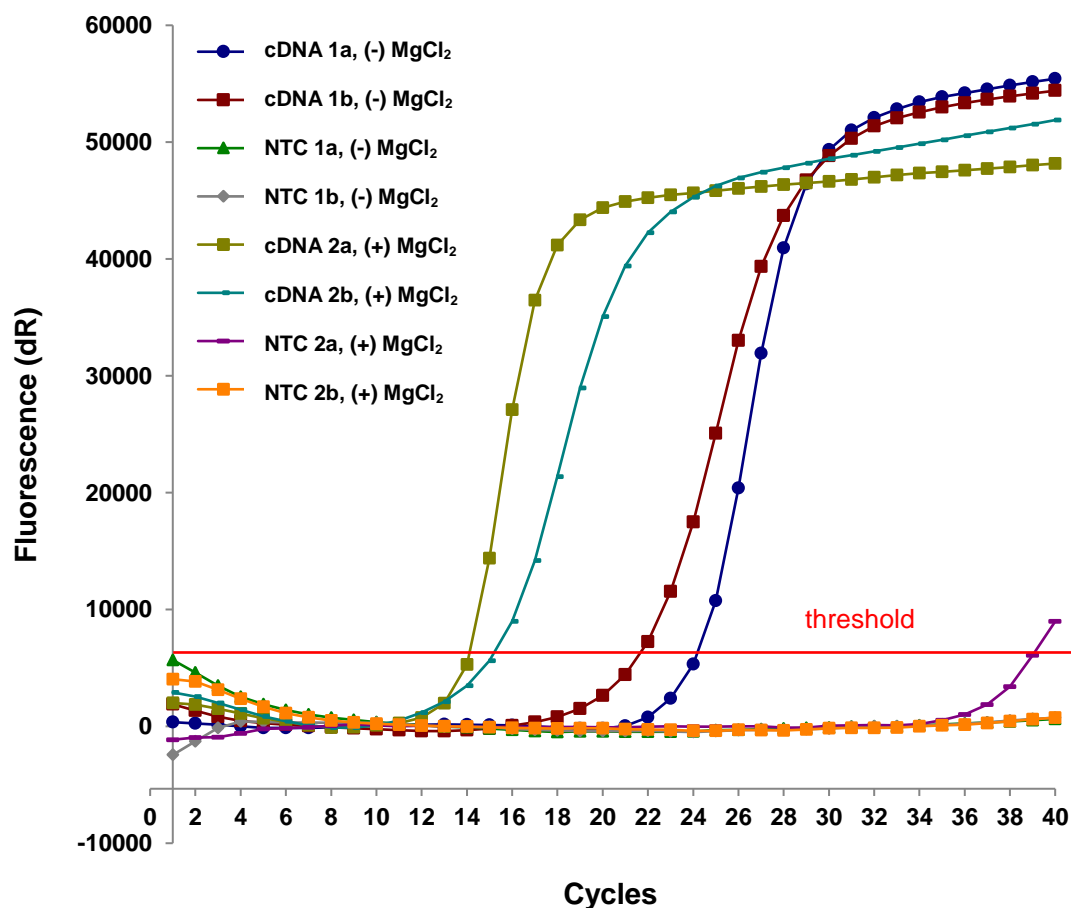


Figure 5.7. Amplification plots obtained on performing qRT-PCR on nuclease-free PCR-grade water (NTC) and cDNA samples in duplicates, using MMP-13 primer pairs in a three-step thermal cycling programme with and without MgCl₂.

On treating cDNA samples with MgCl₂, there was an earlier exponential increase in fluorescence compared to those of cDNA samples treated without MgCl₂ (Figure 5.7). As such, samples treated with MgCl₂ had lower Ct values compared to those without MgCl₂. Conversely, there was no difference in the Ct values of NTC samples treated with and/or without MgCl₂ (Table 5.1). Furthermore, figure 5.7 revealed a plateau stage for each cDNA sample, which was absent in figure 5.6, suggesting that these PCR reactions successfully reached completion, fully utilizing the cDNA template. These findings were in agreement with our hypothesis that MgCl₂ contributes to the improvement of stringency of PCR reactions. However, the Ct values obtained for each cDNA sample, following the employment of MgCl₂ were considered to be too low and similar to those of the reference gene, which might prove difficult in calculating the relative gene expressions of MMP-13, when using the comparative Ct approach. Since the amplification plots in figure 5.7 showed that the difference between the Ct values of cDNA and NTC samples treated with and without MgCl₂ was greater than 2 (Ct>2), suggesting the elimination of reagent contamination or false amplification from the PCR reactions, it was decided to remove the use of MgCl₂ in subsequent PCR reactions involving MMP-13 primer pairs.

Table 5.1: Ct values of NTC and cDNA samples, from carrying out qRT-PCR using MMP-13 primer pairs in a three-step thermal cycling programme, with and without MgCl₂.

	(-) MgCl₂	(+) MgCl₂
cDNA a	24.15	14.11
cDNA b	21.59	15.11
NTC a	No Ct	38.95
NTC b	No Ct	No Ct

Following this, the process was repeated to observe the effect of MgCl₂ in qRT-PCR reactions which included ADAMTS-5 primer pairs. qRT-PCR was performed on both cDNA and NTC samples in duplicates, using ADAMTS-5 primer pairs under a three-step thermal cycling programme with and without the employment of MgCl₂. Figure 5.8 illustrates the amplification plots obtained from this process.

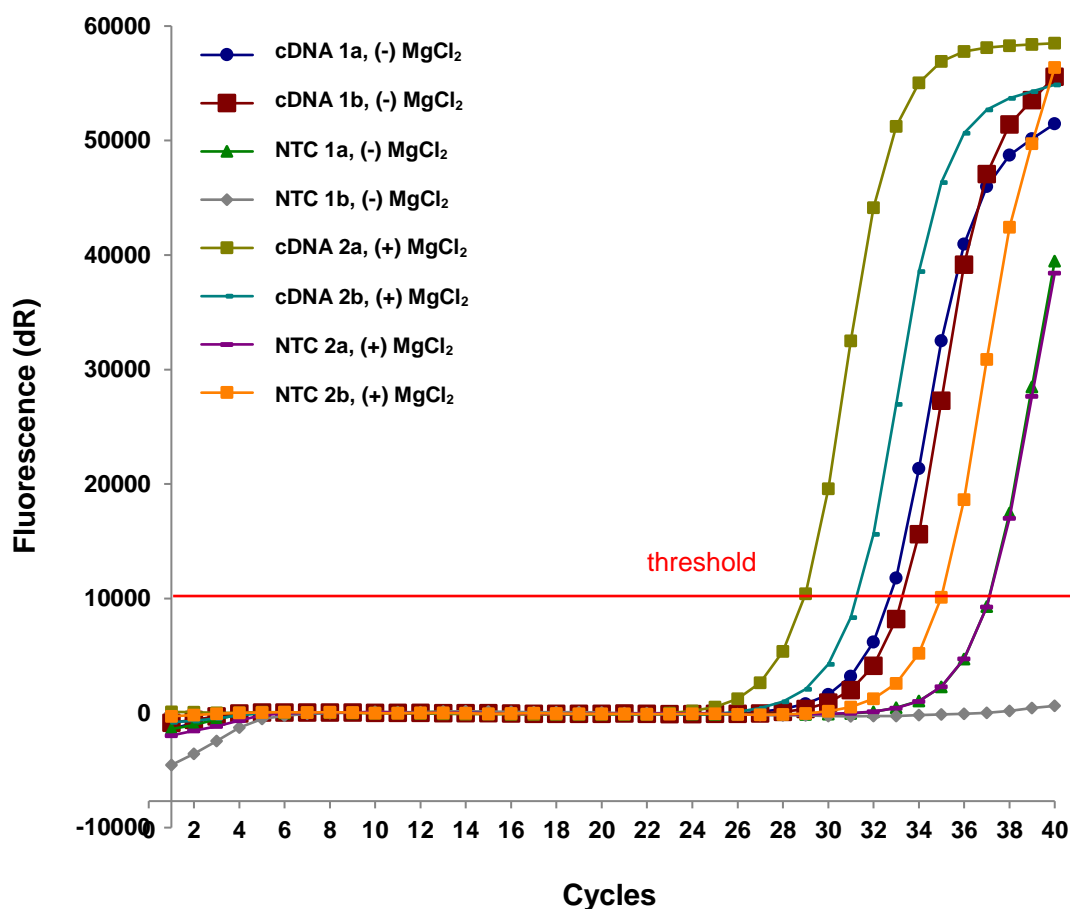


Figure 5.8. Amplification plots obtained on performing qRT-PCR on nuclease-free PCR-grade water (NTC) and cDNA samples in duplicates, using ADAMTS-5 primer pairs in a three-step thermal cycling programme with and without $MgCl_2$.

It was evident that the difference in Ct values between cDNA and NTC samples treated with and without $MgCl_2$ exceeded a Ct value of 2, which is required to confirm the abolition of reagent contamination or false amplification from the PCR reactions ($Ct > 2$). However, there was not a significant difference between the Ct values of samples treated with and without $MgCl_2$, as indicated in table 5.2. As such, subsequent optimization steps excluded the use of $MgCl_2$ in combination with ADAMTS-5 primer pairs. From the amplification plots, it was also observed that the exponential increase in fluorescence for each cDNA sample occurred at or beyond the 29th cycle of the PCR reaction, resulting in Ct values which are abnormally high for any given PCR reaction. Such findings suggested a loss of specificity to some extent in these PCR reactions, which might have been due to the type of thermal cycling programme in use, which represented the remaining qRT-PCR condition still to be tested.

Table 5.2: Ct values of NTC and cDNA samples, from carrying out qRT-PCR using ADAMTS-5 primer pairs in a three-step thermal cycling programme, with and without MgCl₂.

	(-) MgCl ₂	(+) MgCl ₂
cDNA a	32.75	28.95
cDNA b	33.32	31.30
NTC a	37.13	37.14
NTC b	No Ct	34.99

Since a three-step thermal cycling programme was used for the previous qRT-PCR optimization steps, the effect of using a two-step thermal cycling programme on ADAMTS-5 primers was examined in order to reduce the loss in specificity in the PCR reactions and to reduce the Ct values of cDNA samples such that they fell between values of 20 and 30. As such, qRT-PCR was carried out on both cDNA and NTC samples, using ADAMTS-5 primer pairs under a two-step thermal cycling programme without the employment of MgCl₂ (reaction 5B).

Figure 5.9 illustrates the amplification plots obtained from this reaction. It was evident that using a two-step thermal cycling programme on ADAMTS-5 primers reduced the Ct value of the cDNA sample to a value between 20 and 30 (Ct=24.42, Fig. 5.9). Additionally, the difference between the Ct values of cDNA and NTC samples was 3.32 (Ct>2), which is required to confirm the elimination of reagent contamination or false amplification from the PCR reaction. Furthermore, all three stages of the PCR reaction were clearly indicated in the response, namely, the exponential, linear and plateau stages. As such, the ideal conditions to carryout qRT-PCR on cDNA samples, in combination with 0.5µM of ADAMTS-5 primer pairs involve the use of a two-step thermal cycling programme. This comprised of an initial polymerase activation step at 95°C for 3 minutes, followed by denaturation of 35 cycles at 95°C for 30 seconds, annealing at 60°C for 1 minute, and extension at 72°C for 1 minute. Reaction 6 lists the proportion of components required for this PCR reaction:

Reaction 6:

Template cDNA	2.5µl
Primer (0.5µM)	2.5µl
KAPA master mix	5µl
Total volume	10µl

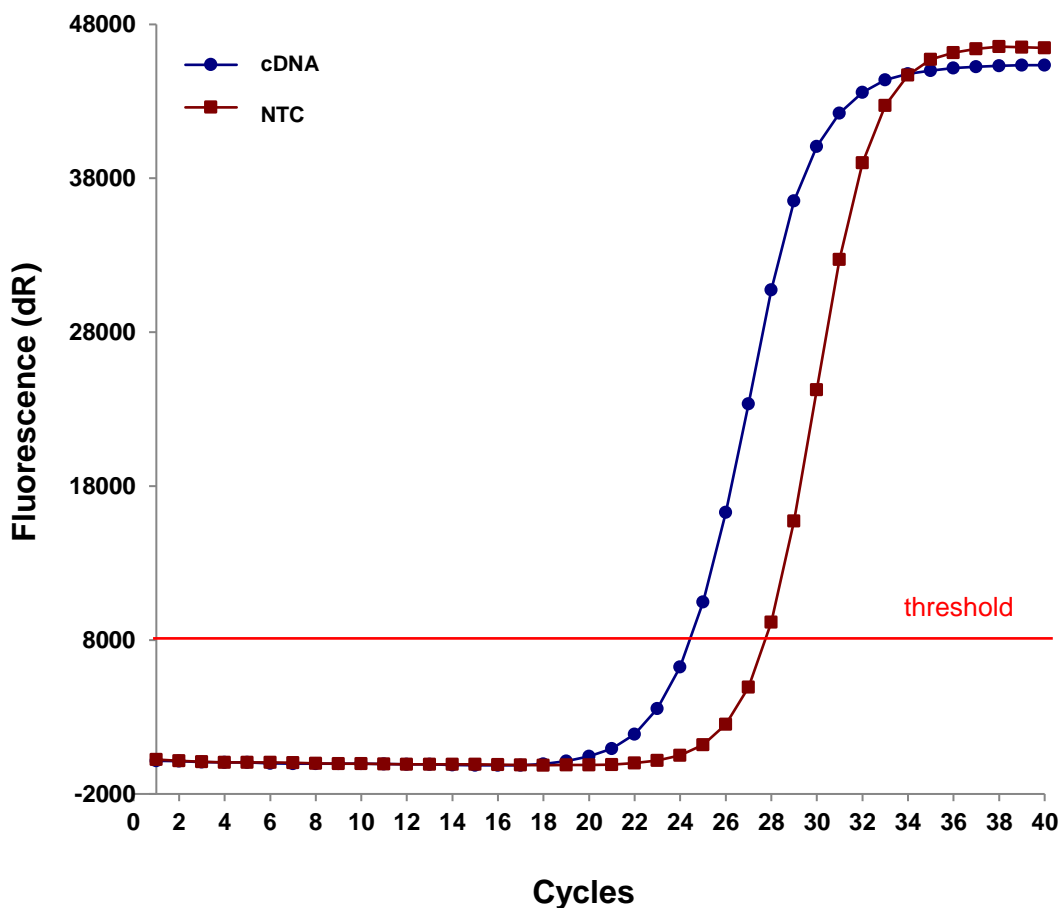


Figure 5.9. Amplification plots obtained on performing qRT-PCR on nuclease-free PCR-grade water (NTC) and cDNA samples, using ADAMTS-5 primer pairs in a two-step thermal cycling programme without $MgCl_2$.

Since a two-step thermal cycling programme dramatically improved the qRT-PCR results (Fig. 5.9), in relation to ADAMTS-5 primers, it was interesting to examine the effect of performing the equivalent programme on MMP-13 and 18-S primer pairs, as this thermal cycling programme reduces the time required to run samples on the Mx3000P quantitative PCR instrument (Stratagene, Amsterdam, The Netherlands) for approximately 1 hour. qRT-PCR was subsequently performed on both cDNA and NTC samples, using MMP-13 and 18-S primer pairs under a two-step thermal cycling programme in the absence of $MgCl_2$, following reaction 6.

This resulted in a Ct value of 25.37 for the cDNA sample, whereas no Ct value was obtained for the NTC samples, as illustrated in figure 5.10. Since the difference between these values was greater than 2, this finding confirmed the elimination of reagent contamination and false amplification. In a similar manner to the amplification plot obtained from the cDNA sample treated with ADAMTS-5, all three stages of the PCR reaction were exhibited in the amplification plot obtained from the cDNA sample in figure 5.10, ensuring that the PCR reaction was successfully completed. Additionally the Ct values obtained from cDNA samples which were subjected to a two-step thermal cycling programme were similar to those obtained from cDNA samples subjected to the three-step thermal cycling programme,

while keeping all other PCR conditions constant ($C_t=24.15$, table 5.1). Hence, performing a two-step thermal cycling programme was preferable to a three-step thermal cycling programme, as the former proved less time consuming and produced similar results to that of a three-step thermal cycling programme.

Thus, qRT-PCR involving the use of MMP-13 primer pairs was performed under the same conditions as that of ADAMTS-5 primer pairs.

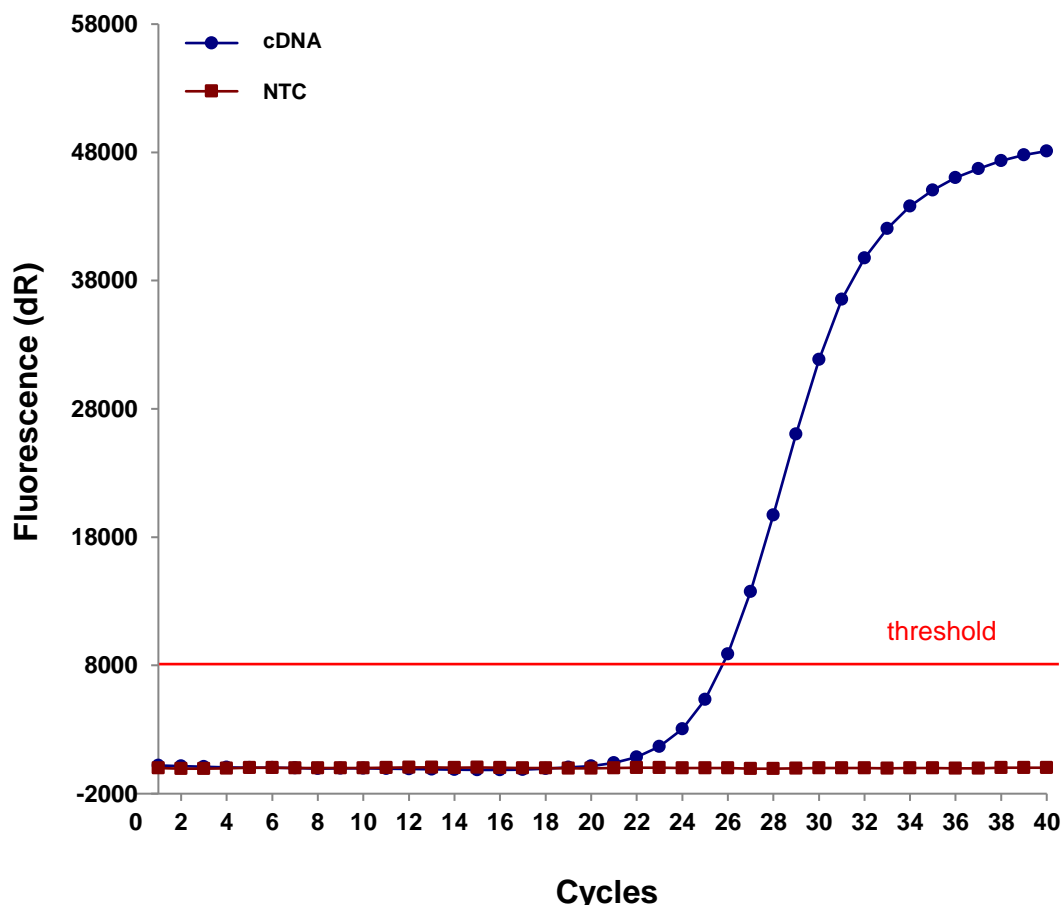


Figure 5.10. Amplification plots obtained on performing qRT-PCR on nuclease-free PCR-grade water (NTC) and cDNA samples, using MMP-13 primer pairs in a two-step thermal cycling programme without $MgCl_2$.

Figure 5.11 illustrates the amplification plots obtained from carrying out qRT-PCR on both cDNA and NTC samples, using 18-S primer pairs under a two-step thermal cycling programme in the absence of $MgCl_2$. A C_t value of 19.69 was obtained from the cDNA sample in figure 5.11, whereas no C_t value was obtained from the NTC sample. Similar to figures 5.9 and 5.10, this finding suggested the elimination of contamination and false amplification in the PCR reaction. Additionally, the first two stages of the PCR reaction, namely, the amplification and linear stages were clearly exhibited in the amplification plot obtained from the cDNA sample in figure 5.11. Thus, the ideal conditions required to carry

out qRT-PCR which involve the employment of 18-S are the same as those required to run qRT-PCR which employ ADAMTS-5 and MMP-13 primer pairs.

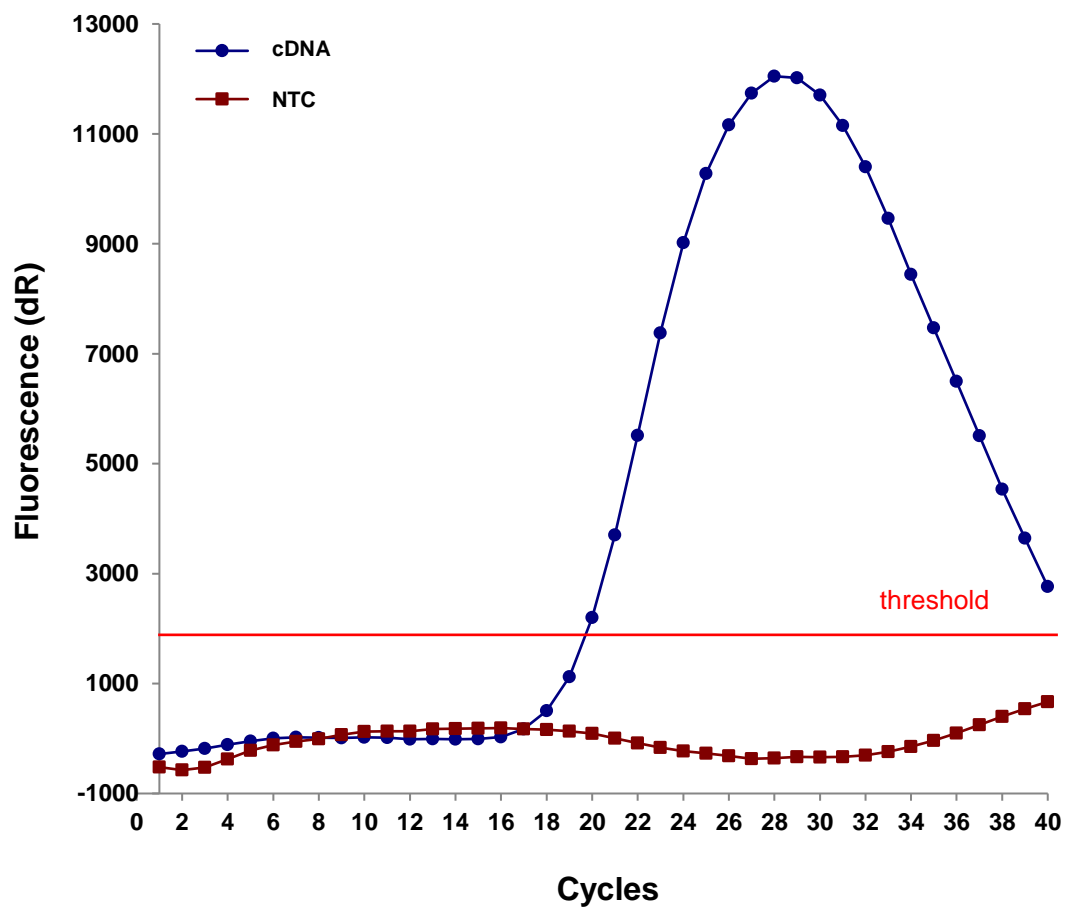


Figure 5.11. Amplification plots obtained on carrying out qRT-PCR on nuclease-free PCR-grade water (NTC) and cDNA samples, using 18-S primer pairs in a two-step thermal cycling programme without $MgCl_2$.

Consequently, cDNA samples obtained from subjecting chondrocyte/agarose constructs to dynamic loading and treated with $TNF\alpha$ in the presence and absence of L-NIO at both 5% and 21% oxygen tensions were analysed for ADAMTS-5 and MMP-13, using reaction 6, and a two-step thermal cycling programme without the employment of $MgCl_2$.

5.5 Results

Low oxygen tension increased expression of MMP-13 and ADAMTS-5 in chondrocytes treated with TNF α and the response was reduced by dynamic compression

The effect of oxygen tension on the gene expression of MMP-13 and ADAMTS-5 in chondrocytes cultured with TNF α and subjected to dynamic compression was examined in six replicates from two separate experiments. Due to the small number of repeats (n=2), inferential statistical analysis was not performed to compare differences between the various treatment groups. As such data from the two experiments were represented separately, as shown in figures 5.12 and 5.13. It is evident that for unstrained constructs, at 21% and 5% oxygen tensions, the presence of TNF α resulted in a 1-fold and 3-fold increase in ADAMTS-5 gene expression, respectively, when compared to untreated controls from experiment 1 (Figs. 5.12 A and B). From the same experiment, the presence of TNF α in chondrocyte/agarose constructs resulted in an approximate 1-fold and 2-fold change in MMP-13 gene expression when cultured at 21% and 5% oxygen tension, respectively (Figs. 5.13 A and B). Similar effects were observed in experiment 2 upon analysing the gene expression of both ADAMTS-5 and MMP-13. In unstrained constructs, greater levels of ADAMTS-5 and MMP-13 gene expression were observed at 5% oxygen tension when compared to 21% in both experiments. The induction of MMP-13 and ADAMTS-5 gene expression by TNF α at 21% and 5% oxygen tension were reduced with the NOS inhibitor and abolished completely by stimulation with dynamic compression in both experiments (Figs. 5.12 and 5.13).

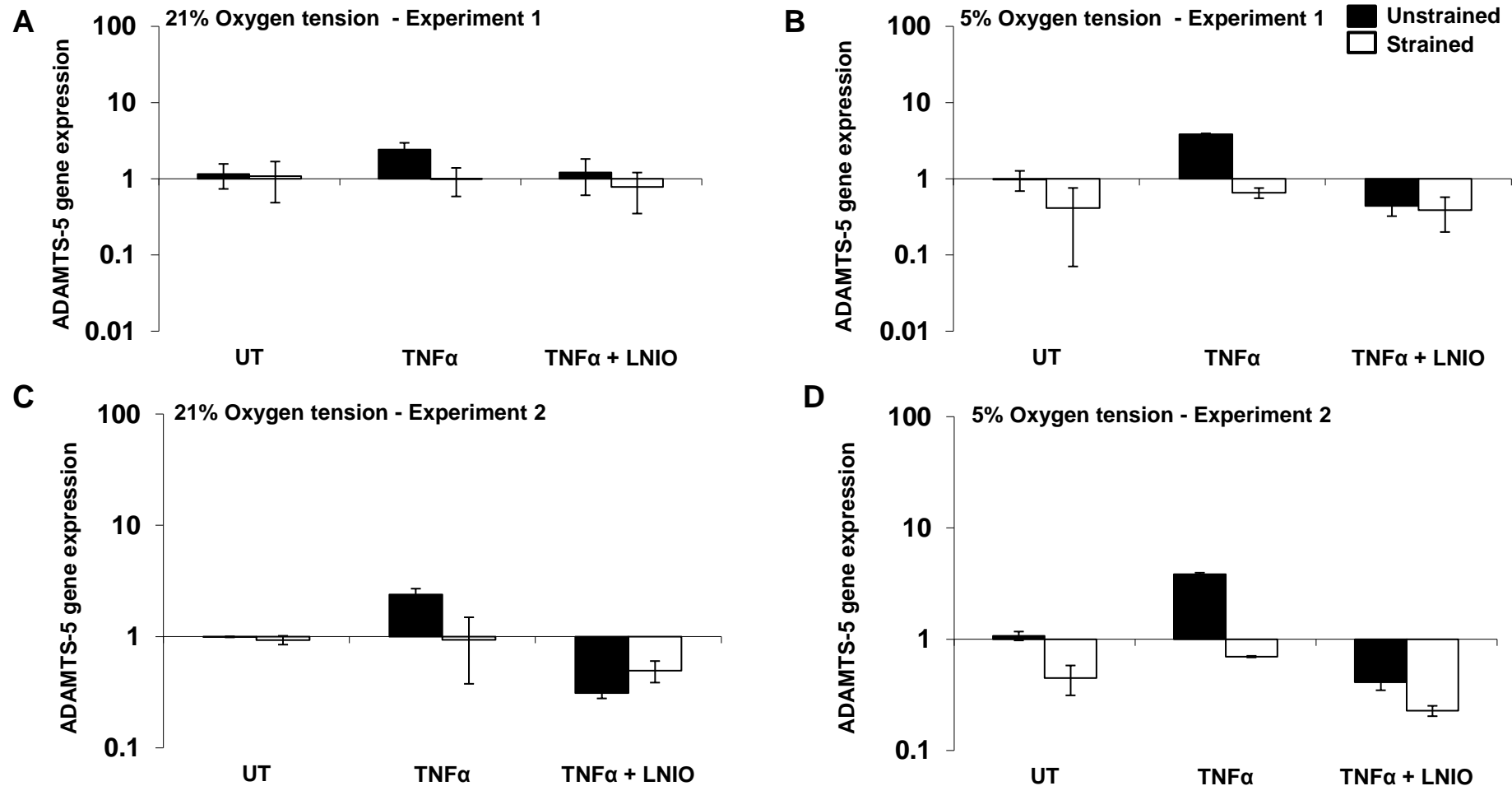


Figure 5.12. The effects of TNF α and dynamic compression on ADAMTS-5 gene expression at 21 and 5% oxygen. Data obtained from the two experiments carried out have been divided into experiment 1 (A, B) and experiment 2 (C, D) in order to determine the presence of significant differences between the two sets of experiments. Chondrocyte/agarose constructs were subjected to dynamic compression (15%, 1 Hz) in the presence or absence of TNF α (0 or 10 ng/ml) and/or L-NIO (1 mM) at 21 and 5% oxygen tension for 6 hours. Error bars represent the mean and SEM values for 3 replicates from a single experiment.

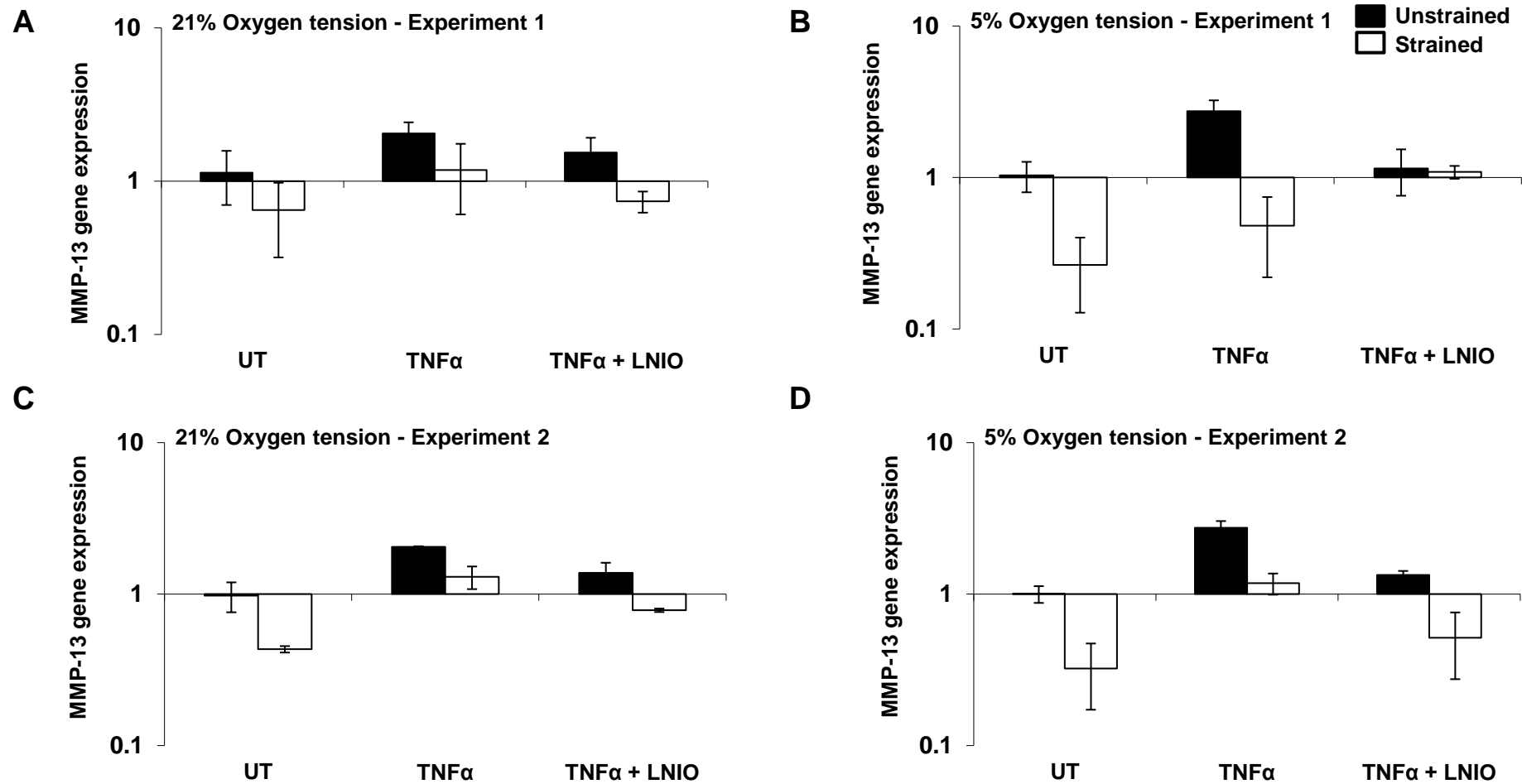


Figure 5.13. The effects of TNF α and dynamic compression on MMP-13 gene expression at 21 and 5% oxygen. Data obtained from the two experiments carried out have been divided into experiment 1 (A, B) and experiment 2 (C, D) in order to determine the presence of significant differences between the two sets of experiments. Chondrocyte/agarose constructs were subjected to dynamic compression (15%, 1 Hz) in the presence or absence of TNF α (0 or 10 ng/ml) and/or L-NIO (1 mM) at 21 and 5% oxygen tension for 6 hours. Error bars represent the mean and SEM values for 3 replicates from a single experiment.

5.6 Discussion

One of the key difficulties encountered in cartilage mechanobiology is the analysis of RT-qPCR data, to examine the mRNA expressions of the anabolic and catabolic genes of chondrocytes. Studies which particularly involve numerous experimental test conditions, such as mechanical, chemical and time-dependent factors, encounter major differences in RT-qPCR results, since data obtained predominantly depends on the selection of appropriate normalisation strategy. Insufficient normalisation of data obtained, as well as statistical errors during analysis will prove difficult in obtaining meaningful data which may not be reproducible or comparable to previously published work. Furthermore, insufficient validation and optimization of the conditions required to perform qPCR can contribute to these difficulties in analysing RT-qPCR data. The use of unreliable reference genes for each experimental test condition is also a contributing factor to these challenges. As such, the trial and error steps taken to optimise RT-qPCR techniques, for mechanotransduction studies, using the well characterized 3D chondrocyte/agarose model and Bose bioreactor system described in chapter 2, were described in the present chapter for cartilage mechanobiology studies.

In *ex-vivo* studies, reduced oxygen tension at 5% was observed to enhance the inflammatory response with greater induction of MMP-13 and ADAMTS-5 gene expression that also favours the inhibition of matrix synthesis and loss. In *ex-vivo* bioreactor studies, dynamic compression reduced the production of inflammatory mediators in response to TNF α , and this response was abolished when dynamic compression was coupled with the NOS inhibitor. We observed differences in the loading-induced response such that the magnitude of inhibition was greater at 5% oxygen tension than 21%. In addition, the beneficial response was paralleled with anabolic activities as typified by increased matrix synthesis that was greater at 21% oxygen tension than 5%. The literature is sparse with respect to the combined effect of TNF α and dynamic compression at low oxygen tensions in chondrocytes. However, the effect of oxygen tension and mechanical stress is well characterized (Fermor et al., 2007, Fermor et al., 2005, Wernike et al., 2008). Matrix synthesis was increased and chondrogenic gene expression was stabilised by long-term mechanical loading at 5% oxygen tension when compared to 21% in a chondrocyte/polyurethane model (Wernike et al., 2008). Conversely in porcine cartilage explants, mechanical loading enhanced NO production at 5 and 20% oxygen tension and the response was reduced at 1% oxygen tension (Fermor et al., 2007, Fermor et al., 2005). However, the manner in which cytokine-induced inflammatory pathways are influenced by oxygen tension and biomechanical signals are unclear. Further studies are needed to unravel the distinct pathways induced by oxygen tension, biomechanical signals and TNF α . This will help to identify key targets and potential therapies for OA.

In summary, the present study demonstrates that exogenous TNF α combined with low oxygen tension enhanced the production of inflammatory mediators, which are reduced with biomechanical signals or the presence of the NOS inhibitor in an oxygen-dependent manner. The inflammatory environment attempts to assist with tissue remodelling but the response was influenced by biomechanical signals leading to restoration of matrix synthesis. Although selective inhibition of NOS and stimulation with biomechanical signals leads to chondroprotection, further studies are needed to unravel the distinct pathways induced by oxygen tension, biomechanical signals and TNF α . This will help to identify key targets and potential therapies for OA treatments.

Chapter 6 – Extracellular matrix fragments

6.1 Introduction

It has been well documented that ECM-fs induce catabolic activities during OA disease progression and hence they are involved in the regulation of cartilage tissue remodelling. Of these matrix fragments, the 29kDa NH₂-terminal heparin binding FN-f has been proven to be the most potent, followed by Col-fs, in particular, amino and carboxyl telopeptides (Homandberg, 1998). Previous studies have shown that during OA disease progression, oxygen tension has a substantial influence on the metabolic activities of chondrocytes, hence affecting the pathways induced by extracellular matrix fragments (Parker et al., 2013). The signalling cascades induced by a combination of ECM-fs and oxygen tension are complex, providing drive for the current study to be carried out. It has been well documented that Col-fs and FN-fs ranging from 29 to 140kDa in size induce a loss in proteoglycans and an inhibition in matrix synthesis under ambient conditions (Homandberg, Meyers and Xie, 1992, Homandberg, Wen and Hui, 1998, Homandberg and Hui, 1996, Homandberg and Wen, 1998, Xie, Hui and Homandberg, 1993, Xie, Hui, Meyers and Homandberg, 1994). Also, studies incorporating 3D chondrocyte/agarose models revealed an increase in levels of NO in the presence of the highly potent 29kDa heparin binding FN-f, which was commercially available (Raveenthiran and Chowdhury, 2009, Chowdhury et al., 2010, Mosesson, Homandberg and Amrani, 1984).

In extracellular matrix proteins such as elastin and collagen, a sequence of consensus pattern, *XGXXPG* has been identified, which is known to bind to the EBP receptor, also termed SGAL. In recent studies, inhibition of the consensus pattern *XGXXPG* has been demonstrated with the incorporation of lactose. Since FN-fs are derived from the matrix protein FN, in a similar manner to which Col-fs are derived from type II collagen, and since this consensus pattern is present in collagen, the present study investigates whether the sequence of consensus pattern, *XGXXPG* is also present in FN-fs, and whether it is responsible for the mediation of catabolic activities in chondrocytes via EBP/SGAL. Additionally, the effect of hypoxia on the response of FN-fs to lactose and mechanical conditioning is also examined. Furthermore, the study also examines the effects of commercially available amino telopeptides on the metabolic activities of chondrocytes seeded in agarose constructs under varying oxygen tensions.

6.2 Materials and methods

6.2.1 Effect of NT telopeptides on the production of catabolic and anabolic mediators in chondrocyte/agarose constructs cultured at 21, 5 and 2% oxygen tension

Chondrocyte/agarose constructs were prepared using a well-established model as described in section 2.2. At this point of the study, more incubators were available in the host laboratories, which enabled the examination of an additional hypoxic condition. Thus, constructs were equilibrated in culture under free-swelling conditions at 21, 5 and 2% oxygen tensions for 72 hours. The glove-box style workspace was integrated within a Biospherix incubator to ensure that the experimental conditions during set-up and experimentation were uninterrupted, as previously described (Parker et al., 2013). Following the equilibration period, constructs were cultured for a further 48 hours with DMEM + 20% FCS supplemented with 0 or 3 μ M of N-terminal (NT) telopeptides derived from collagen type II (Laboratoire de Biotechnologie du Luxembourg S.A.) in the presence and absence of 1mM L-N-(1-iminoethyl)-ornithine (L-NIO) or 100 μ M of the COX-2 inhibitor, NS-398 for up to 48 hours at 21, 5 and 2% oxygen tensions. The synthetic peptides were 10kDa in size and were synthesized by using sequences published previously (Chowdhury et al., 2010; Lucic et al., 2003; Guo et al., 2009). More specifically, the NT peptide corresponds to the amino-terminal region of collagen type II and contains 19 amino acids (residues 182 to 212) with an additional four glycine-proline-hydroxyproline (GPX) tripeptide repeat resulting in a short 31-mer peptide (sequence: QMAGGFDEKAGGAGLGVMQQGPMGPMGPRGPP). Additionally, 10ng/ml of TNF α (Peprotech EC Ltd, London, UK) was incorporated into the experiment as a positive control, in the presence and absence of the two inhibitors at 21% oxygen tension, such that the N-terminal-induced response was compared to these constructs. L-NIO inhibits all isoforms of the nitric oxide synthase enzymes (Merck Chemicals, Nottingham, UK), whereas NS-398 is a selective inhibitor of cyclooxygenase-2.

In a separate experiment aiming at improving the N-terminal-induced response in chondrocyte/agarose constructs, the concentration of N-terminal (NT) telopeptides derived from collagen type II (LifeTein LLC, Somerset, New Jersey, US) was increased from 3 to 50 μ M. The number of variables incorporated into the experiment was also reduced by observing the effects of the NT telopeptides only in the presence and absence of L-NIO and not NS-398 at 21 and 5% oxygen tensions. Similar to the previous experiment, 10ng/ml of TNF α (Peprotech EC Ltd, London, UK) was incorporated into the experiment as a positive control, in the presence and absence of the NOS inhibitor at 21% oxygen tension. At the end of the culture period, the constructs and corresponding media were removed and immediately stored at -20°C prior to biochemical analysis. Figure 6.1 illustrates the steps

undertaken when examining the effects of NT telopeptides in chondrocyte/agarose constructs.

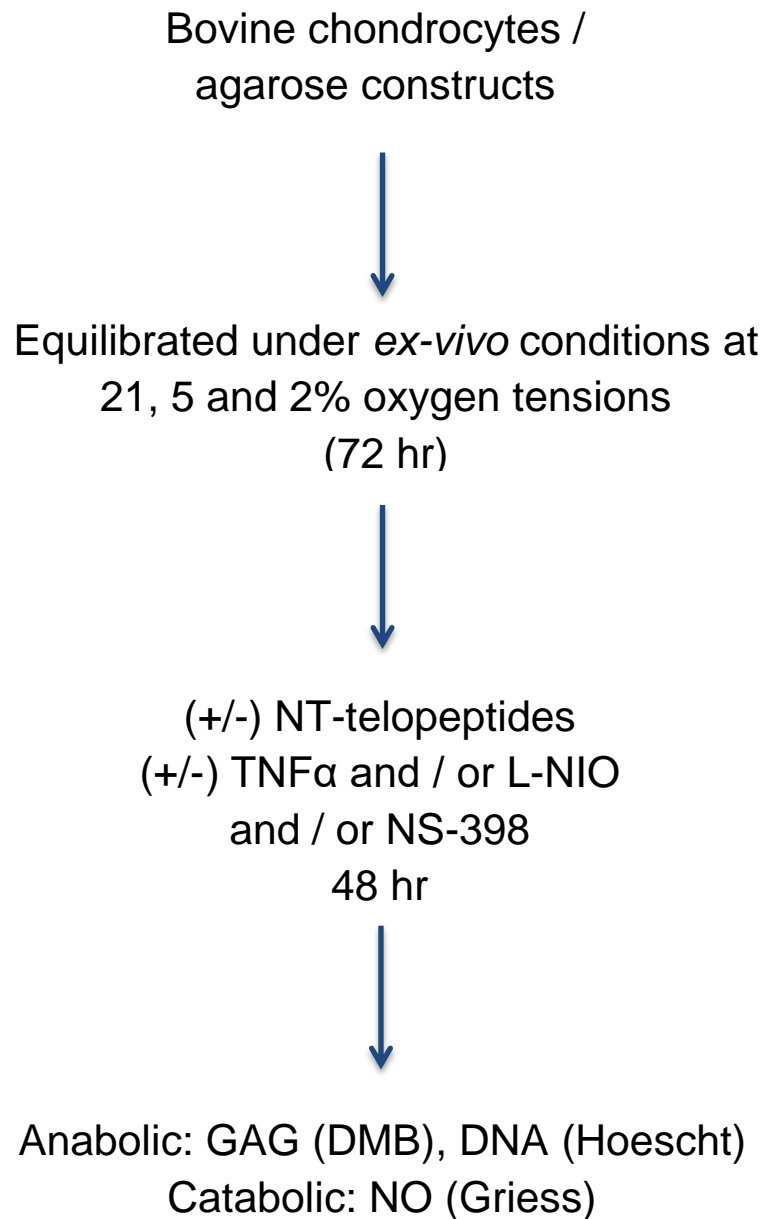


Figure 6.1. Flow chart illustrating *ex-vivo* methods and protein analysis for the investigation of the effects of N-telopeptides on chondrocyte metabolism.

6.2.2 Effect of fibronectin fragments on the production of catabolic and anabolic mediators in chondrocyte/agarose constructs cultured at 21, 5 and 2% oxygen tension

Following the preliminary study on FN-fs and lactose carried out by Drs Parker and Peake (Fig. 1.26, 1.27; unpublished), the dose response effect of lactose on FN-fs was examined. Free-swelling culture conditions of chondrocyte/agarose constructs were kept the same as those incorporated for TNF α studies in chapters 3 and 4, such that the potencies of TNF α and FN-fs can be compared from both studies. Briefly, these free-swelling studies involved equilibrating chondrocyte/agarose constructs for 72 hours, followed by 48 hours of treatment with TNF α at 37°C and 5% CO₂. Similarly, in this study, chondrocyte/agarose constructs were initially equilibrated in culture under free-swelling conditions at 21% oxygen tension for 72 hours. Following the equilibration period, constructs were cultured for a further 48 hours with DMEM + 20% FCS supplemented with either 0 or 1 μ M of 29kDa NH₂-heparin-binding FN-f (generous gift from Prof Gene Homandberg) in the presence and absence of α lactose monohydrate at increasing concentrations of 0.1, 1, 10 and 100mM (Sigma-Aldrich, Dorset, UK). It must be noted that FN-fs were isolated from cathepsin D and thrombin digests of fibronectin from plasma adsorption, as previously described (Mosesson, Homandberg and Amrani, 1984). Figure 6.2 illustrate the steps undertaken when examining the effects of FN-fs in chondrocyte/agarose constructs.

Optimization of the culture conditions required for lactose to inhibit the FN-f-induced catabolic activities was then carried out, which involved trial and error steps, starting from the standard free-swelling culture conditions stated above (section 6.2.2), with sequentially changes made based on the results obtained. Figure 6.3 is a flow chart illustrating these optimization steps incorporated.

Once the optimum culture conditions and concentrations of FN-f and lactose were established for the inhibition of FN-f-induced catabolic activities (this is protocol was further optimised as described in section 6.3.3), the effect of 21, 5 and 2% oxygen tension on the response of FN-fs to lactose was then examined. Chondrocyte/agarose constructs treated with the optimum concentration of FN-fs in the presence and absence of the optimum concentration of α lactose monohydrate (Sigma-Aldrich, Dorset, UK) were cultured under free-swelling conditions at 21, 5 and 2% oxygen tensions in a glove-box style workspace integrated within a Biospherix incubator to ensure that the experimental conditions during set-up and experimentation were uninterrupted, as previously described in section 2.2 (Parker et al., 2013).

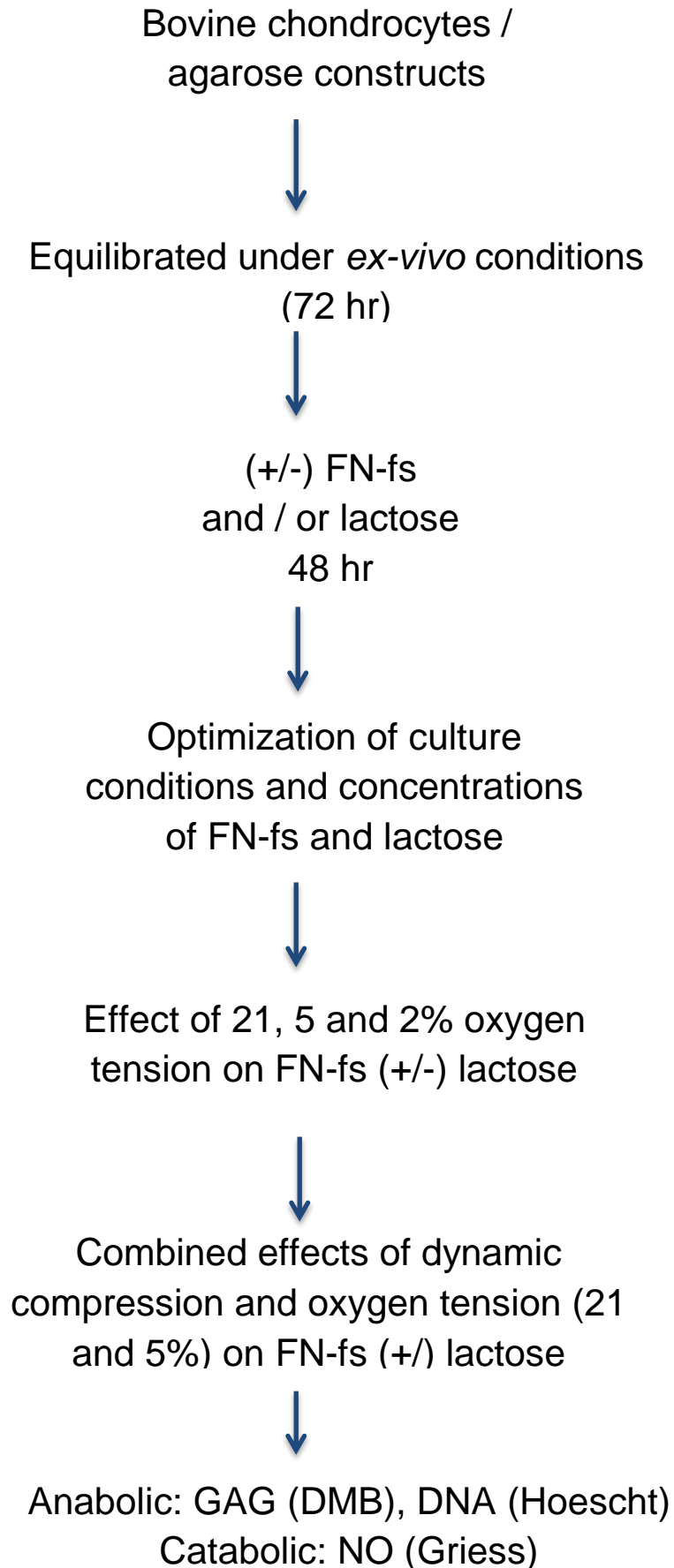


Figure 6.2. Flow chart illustrating *ex-vivo* methods and protein analysis for the investigation of the effects of FN-fs on chondrocyte metabolism.

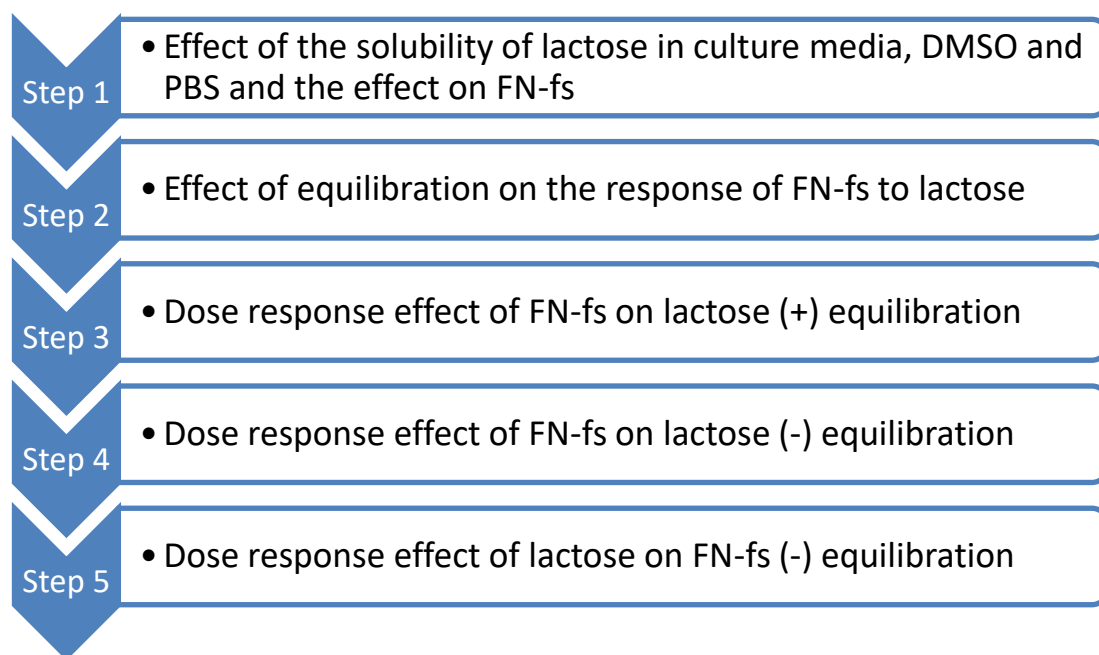


Figure 6.3. Flow chart illustrating the steps taken for the optimization of the culture conditions and concentrations required for lactose to inhibit FN-fs induced catabolic activities.

6.2.3 Effect of dynamic compression on VGVAPG peptide-stimulated chondrocyte/agarose constructs cultured at 21, 5 and 2% oxygen tensions

In a separate experiment, a novel *ex-vivo* bioreactor (Bose ElectroForce, Gillingham, UK) was used to examine the effect of α lactose monohydrate on synthesized VGVAPG peptides (Elastin Products Company, Missouri, USA) in chondrocyte/agarose constructs subjected to dynamic compression at 21% or 5% oxygen tension, as previously described in section 2.2 (Parker et al., 2013). Constructs were transferred into individual wells of a 24-well culture plate (Costar, High Wycombe, UK) and mounted within the bioreactor system that was integrated within the Biospherix incubator. The medium was supplemented with either 0 or 10 μ g/ml of VGVAPG peptide in the presence and absence of 100mM lactose and the experimental conditions during set-up and culture were uninterrupted. A concentration of 10 μ g/ml of VGVAPG peptide was employed in this study, since this concentration of peptide was mostly employed in previous studies which examined the inhibitory effects of lactose on the VGVAPG peptide. It is worth noting that the purpose of employing the VGVAPG peptide in this study was for the replacement of the catabolic activities normally induced by FN-fs, thus confirming the presence of the XGXXPG sequence in FN-fs. Constructs were subjected to intermittent compression under unconfined conditions, with a profile of 10 min compression followed by a 5 hour 50 min unstrained period for a culture period of 48 hours, as previously described (Parker et al., 2013). The *ex-vivo* conditions were found to be optimal when measuring protein synthesis at this time point (Parker et al., 2013). The

compression regime was applied in a dynamic manner with a strain amplitude of 0-15%, using a sinusoidal waveform at a frequency of 1Hz and resulted in 4800 duty cycles for the 48 hour culture period. Control constructs were maintained in an unstrained state in the bioreactor system and cultured for the same time period. The time period of 48 hours was found to be optimal when assessing nitrite release and GAG synthesis. At the end of the experiment, the constructs and corresponding media were stored at -20°C prior to analysis.

6.3 Results

6.3.1 Effect of 3 and 50 μ M NT telopeptides on nitrite release and GAG synthesis in chondrocyte/agarose constructs cultured at 21, 5 and 2% oxygen tension

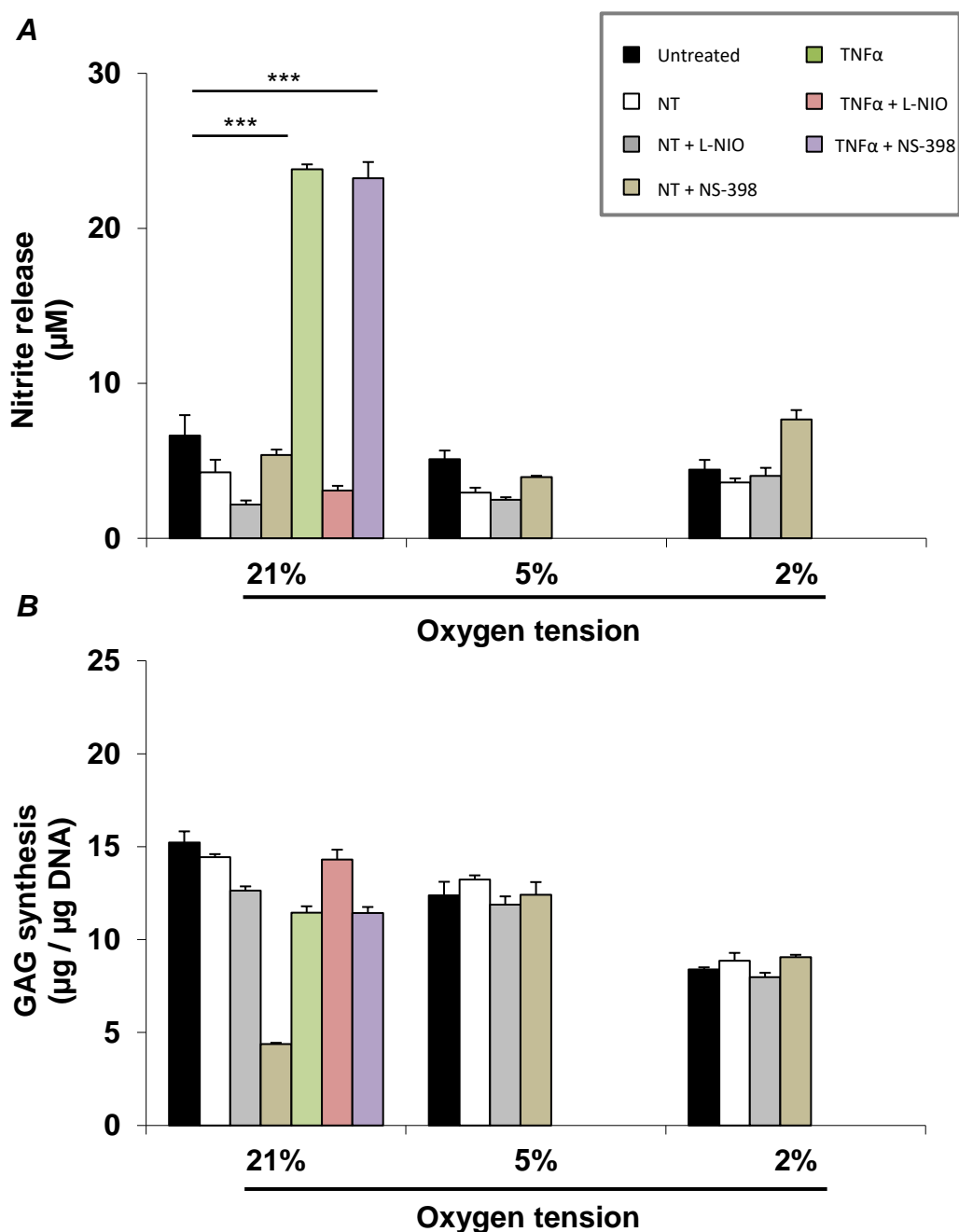


Figure 6.4. Effect of 21, 5 and 2% oxygen tension on (A) nitrite release and (B) GAG synthesis in chondrocytes treated with 3 μ M of NT telopeptides and/or L-NIO (1mM), and/or NS-398 (100mM) for 48 hours. 10ng/ml of TNF α in the presence and absence of both inhibitors represented a positive control. Error bars represent the mean and SEM values for 4 replicates from one experiment. (***) indicates significant comparisons between treatment conditions at 21%, 5% and 2% oxygen tension.

The ability of 3 μ M of the synthesized NT telopeptides (Laboratoire de Biotechnologie du Luxembourg S.A.) to influence nitrite release in chondrocyte/agarose constructs in an oxygen-dependent manner was compared to that of constructs treated with TNF α for 48 hours (Figure 6.4A). A decrease in nitrite production was observed with NT telopeptides when compared to untreated controls at all oxygen tensions, except 2% oxygen tension where no change in nitrite production was observed with the employment of NT telopeptides. Conversely, a significant increase in nitrite release was observed in TNF α -treated constructs at 21% oxygen tension when compared to untreated chondrocyte/agarose constructs. Co-incubation of NT-treated samples with L-NIO had no effect on nitrite release at both 5 and 2% oxygen tensions, unlike 21% oxygen tension which revealed a decrease in nitrite production on stimulating NT-treated constructs with L-NIO. On the other hand, co-incubating NT-treated constructs with the COX-2 inhibitor induced an increase in nitrite production at 2% oxygen tension, unlike 5 and 21% oxygen tensions, at which no change in nitrite release was observed. Similar results were identified in chondrocyte/agarose constructs treated with TNF α and NS-398, as shown in figure 6.4A

Figure 6.4B illustrates the corresponding GAG synthesis effects on culturing chondrocyte/agarose constructs, under free-swelling conditions with 3 μ M of NT telopeptides (Laboratoire de Biotechnologie du Luxembourg S.A.) in the presence or absence of the NOS inhibitor, with or without NS-398. No change in GAG synthesis was observed on treating chondrocyte/agarose constructs with NT telopeptides at 21, 5 and 2% oxygen tensions, compared to untreated controls. Similarly, at all oxygen tensions, co-incubation of NT-treated samples with L-NIO had no effect on nitrite production, when compared to untreated samples. Conversely, on stimulating chondrocyte/agarose constructs with TNF α a marginal decrease in GAG synthesis was induced, which was reversed on co-incubation with the NOS inhibitor. Co-incubation of NT-treated constructs with NS-398 resulted in no change in nitrite release at both 5 and 2% oxygen tensions, compared to untreated controls. Contrariwise, a decrease in nitrite release was observed on co-incubating NT-treated peptides with the COX-2 inhibitor. In the case of TNF α -treated samples, co-incubation with NS-398 had no effect in the restoration of GAG levels.

Conclusively, these results suggested that 3 μ M NT telopeptides synthesized by Laboratoire de Biotechnologie (Luxembourg S.A.) did not stimulate a catabolic effect in chondrocyte/agarose constructs and are not in agreement with previous studies which observed the induction of catabolic effects on employing synthetic NT telopeptides in both 2D and 3D models (Chowdhury et al., 2010; Lucic D. et al., 2003; Guo. D et al., 2009; further discussed in section 7.8). As a result, the concentration of synthetic NT-telopeptides incorporated was increased from 3 to 50 μ M in order to induce a catabolic response.

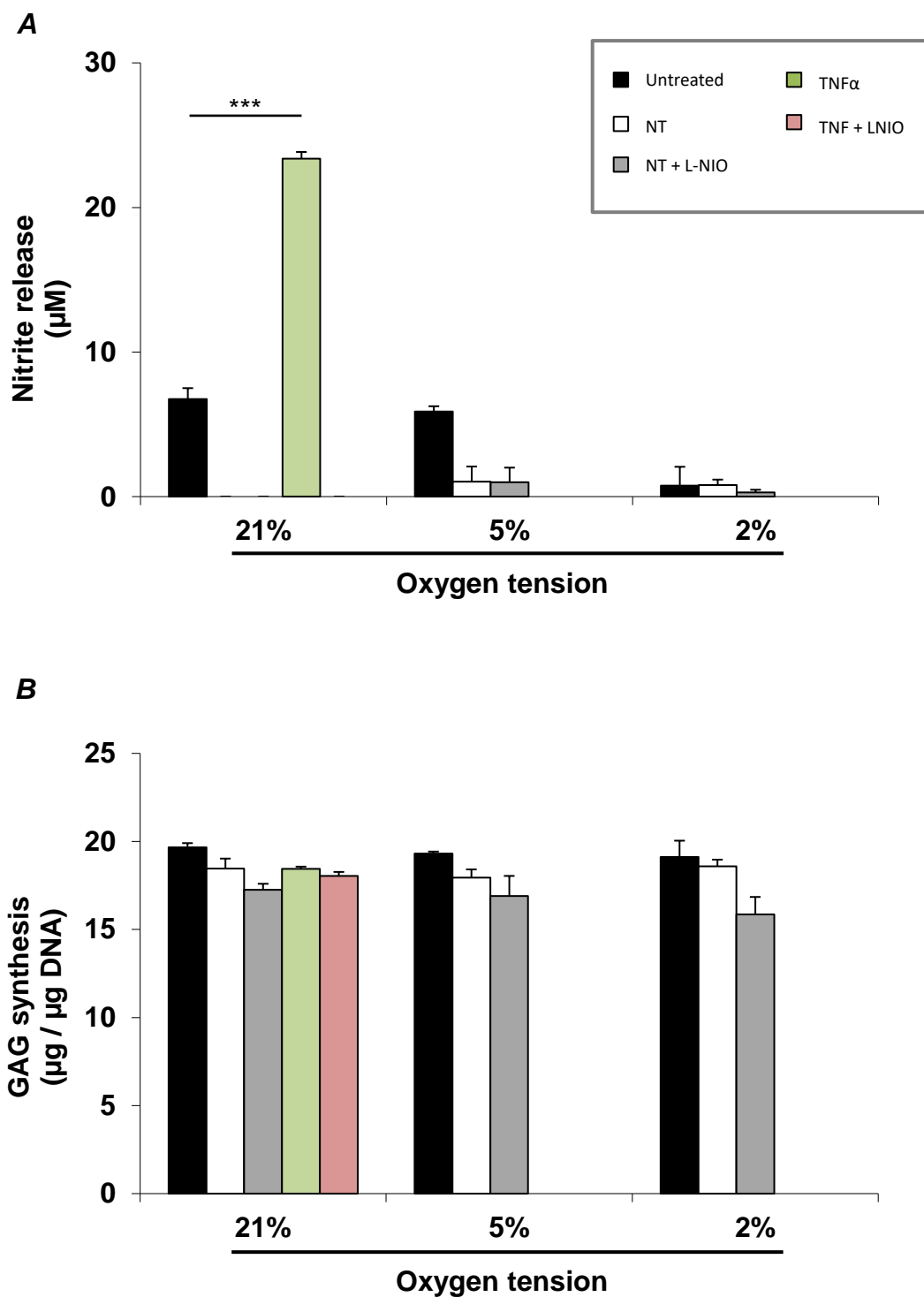


Figure 6.5. Effect of 21, 5 and 2% oxygen tension on (A) nitrite release and (B) GAG synthesis in chondrocytes treated with 50µM of NT telopeptides and/or L-NIO (1mM) for 48 hours. 10ng/ml of TNFα in the presence and absence of both inhibitors represented a positive control. Error bars represent the mean and SEM values for 4 replicates from one experiments. (***) indicates significant comparisons between treatment conditions at 21%, 5% and 2% oxygen tension.

Figures 6.5A and 6.5B represent nitrite release and GAG synthesis effects on culturing chondrocyte/agarose constructs, under free-swelling conditions with an increased concentration of 50 μ M of NT telopeptides synthesized by LifeTein (LLC, Somerset, New Jersey, US) in the presence or absence of the NOS inhibitor. In this experiment, chondrocyte/agarose constructs were also cultured with TNF α with and without L-NIO to act as a positive control. On culturing constructs with TNF α , a significant increase in nitrite release was observed which was decreased to basal levels on co-incubation with L-NIO at 21% oxygen tension (Fig. 6.5A). Constructs treated with 50 μ M of NT-telopeptides at 21, 5 and 2% oxygen tension did not stimulate a catabolic effect in chondrocytes. Instead, a decrease in nitrite release was observed at 21 and 5% oxygen tension on employing the synthetic telopeptide, whereas no change was exhibited at 2% oxygen tension, when compared to untreated controls. Similarly, co-incubation of NT telopeptide-treated constructs with the NOS inhibitor did not induce any changes in nitrite release at 21, 5 and 2% oxygen tension.

GAG synthesis data (fig. 6.5B) revealed that treating chondrocyte/agarose constructs with TNF α or NT telopeptides did not have any effect on GAG synthesis when compared to untreated controls at 21, 5 and 2% oxygen tension and co-incubation with L-NIO also showed similar results at all three oxygen tensions.

Hence, the above results suggested that increasing the concentration of NT-telopeptides from 3 to 50 μ M did not induce any catabolic activity in chondrocyte/agarose constructs and were not consistent with previous studies which examined the effect of various concentrations of the synthetic NT-telopeptide in both 2D and 3D model systems (Chowdhury et al., 2010; Lucic D. et al., 2003; Guo. D et al., 2009).

6.3.2 Dose response effect of lactose on FN-fs-induced NO release and GAG synthesis in chondrocyte/agarose constructs cultured under free-swelling conditions

The dose response effect of lactose on the nitrite production of chondrocyte/agarose constructs treated with 1 μ M FN-f is shown in figure 6.6. A significant increase in nitrite production was observed on treating constructs with 1 μ M of FN-fs ($p < 0.001$) or 10ng/ml of TNF α ($p < 0.001$), when compared to untreated controls. The increase in nitrite production was significantly greater in FN-fs-treated constructs when compared to constructs treated with TNF α ($p < 0.001$). However, co-incubation of FN-fs-treated samples with 0.1, 1, 10 or 100mM of lactose did not reverse this effect at all ($p > 0.05$ at all concentrations of lactose).

A decrease in GAG synthesis was observed on treating chondrocyte/agarose constructs with FN-fs ($p > 0.001$) when compared to untreated controls, unlike treating samples with TNF α ($p > 0.05$). On co-incubating FN-f-treated constructs with any of the aforementioned concentrations of lactose, this catabolic effect was not reversed ($p > 0.05$).

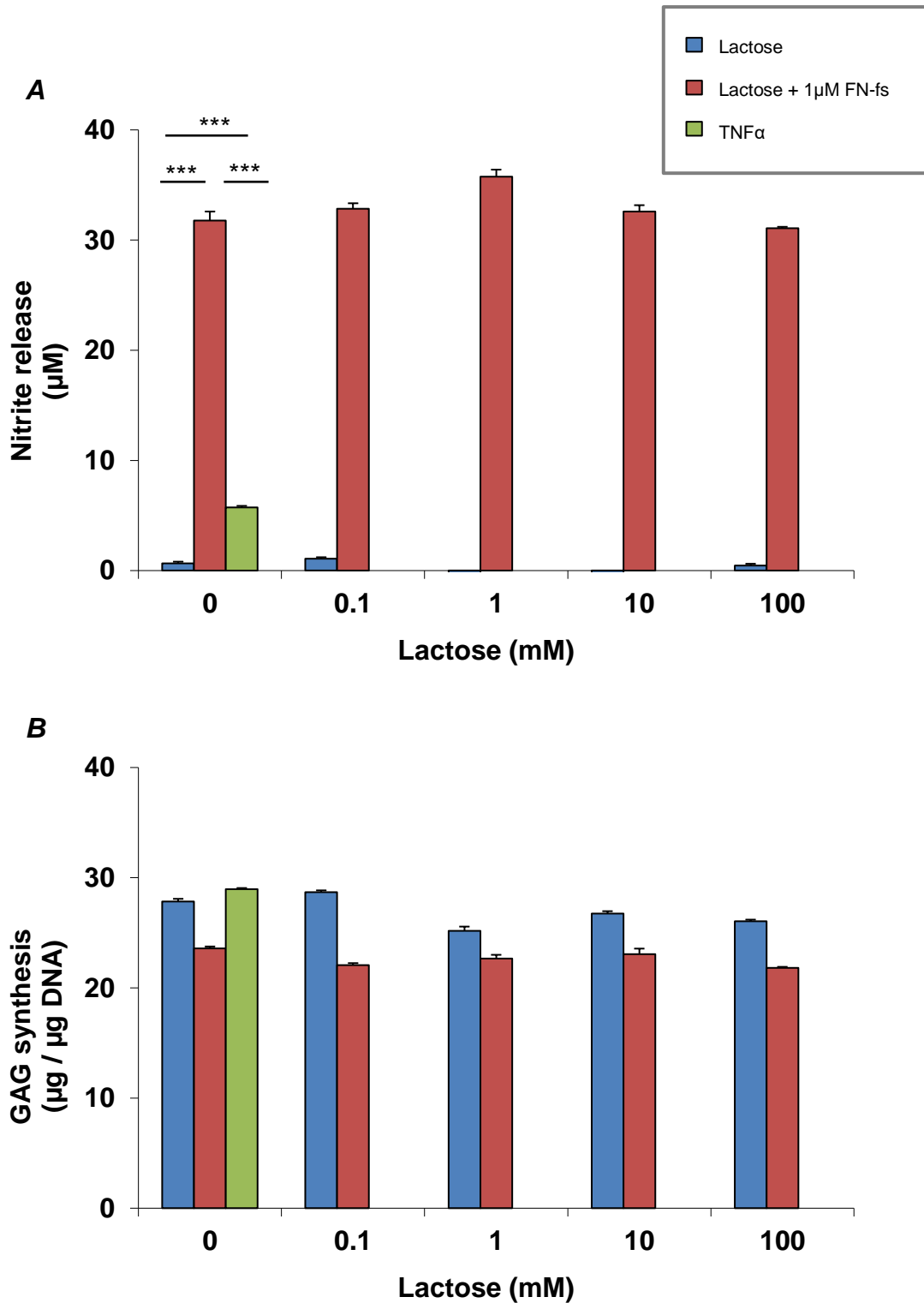


Figure 6.6. Effect of varying concentrations of lactose on (A) nitrite release and (B) GAG synthesis in chondrocytes treated with 1µM FN-f. Chondrocyte/agarose constructs were cultured for 48 hours with varying concentrations of lactose (0.1 to 100 mM) and/or FN-fs (1µM) and the effects were examined on (A) nitrite release and (B) GAG synthesis. TNFα was used as a positive control. Error bars represent the mean and SEM values for 4 replicates from one experiment. (***) $p < 0.001$ indicate significant comparisons between treatment conditions.

The inability of lactose to inhibit FN-f-induced nitrite production in figure 6.6, was assumed to be a result of the difficulties encountered when preparing lactose solutions at concentrations ranging from 0.1 to 100mM, using DMEM supplemented with 20% FCS. When preparing these lactose solutions, saturation was observed at all concentrations, especially at the highest concentration of lactose solution, 100mM. This inability of lactose to completely solubilize in DMEM + 20% FCS (culture media) may have prevented lactose molecules from diffusing into the 3D chondrocyte/agarose model, hence stopping them from interacting with the cell surface to induce an anabolic effect on chondrocytes. Nevertheless, lactose solutions were prepared in the same manner as those from the preliminary study carried out by Drs Parker and Peake (Fig. 7.12, 7.13; unpublished), in which a 40% decrease in FN-f-induced nitrite production was observed with 100mM lactose. Additionally, the culture media used in this study composed of the same constituents as that of Dr Parker's (unpublished); also described in Chapter 2. According to manufacturer's instructions, the solubility of lactose in water is approximately 278mM (MW=360.31g/mol, Sigma). This suggested that even though the concentrations of lactose solutions prepared did not exceed its maximum solubility limit, the solvent used in this case, culture media, may have interfered with the solubility of lactose. As such, the following study examined whether the use of alternative solvents, namely: DMSO and PBS (Sigma), improved the solubility of lactose when compared to culture media in preparing the maximum concentration of lactose solution required to inhibit FN-fs (100mM). 100mM lactose was selected as the maximum concentration of lactose required to perform a dose response study since previous studies which examined the inhibitory effects of lactose incorporated concentrations ranging from 5mM to 200mM (Hinek and Rabinovitch, 1994, Hinek et al., 1988, 1991, 1993, Hinek and Wilson, 2000, Wachi et al., 2004, Mecham et al., 1989a, 1989b, 1991, Privitera et al., 1998, Blanchevoye et al., 2013).

6.3.3 Optimization of the culture conditions required for lactose to induce anabolic effects in FN-f-treated constructs

6.3.3.1 Effect of the solubility of lactose in culture media versus DMSO and PBS

To determine whether the employment of DMSO or PBS improved the solubility of lactose when compared to culture media, 100mM of lactose solution was prepared using the 3 solvents, while keeping all other culture conditions constant. Each lactose solution was then incubated on rollers at 37°C for 30mins. Following this, chondrocyte/agarose constructs were treated with 1 μ M FN-fs in the presence and absence of the prepared lactose solutions to examine whether a well dissolved lactose solution had an effect of FN-f-treated chondrocytes (figure 6.7).

On mixing lactose powder with DMSO and PBS, it was observed that lactose was completely insoluble in both solvents, when compared to culture media. Yet, minor traces of saturation were observed when lactose was mixed with culture media. In order to eliminate this, each lactose solution was incubated at 37°C for 30mins in order to increase its rate of solubility (Fox, 1985, Zadow, 1992). From this step, complete solubility of lactose was achieved with culture media unlike DMSO and PBS. As such lactose in DMSO or PBS was discarded from being tested with chondrocytes. On the other hand, chondrocyte/agarose constructs were treated with FN-fs in the presence and absence of lactose, in order to examine the effects of lactose on FN-fs, as shown in figure 6.7. It is worth noting that all subsequent experiments involve preparing lactose in culture media.

A significant increase in nitrite release was observed on treating chondrocyte/agarose constructs with 1 μ M FN-fs, when compared to untreated controls ($p < 0.001$), as shown in figure 6.7A. However, co-incubation with 100mM of lactose solution, prepared in culture media did not reverse this catabolic effect ($p > 0.05$). Figure 6.7B shows that a marginal decrease in GAG synthesis was observed on treating chondrocyte/agarose constructs with FN-fs when compared to untreated constructs ($p < 0.05$). On co-incubating these samples with lactose, a significant increase in GAG synthesis was not revealed ($p > 0.05$).

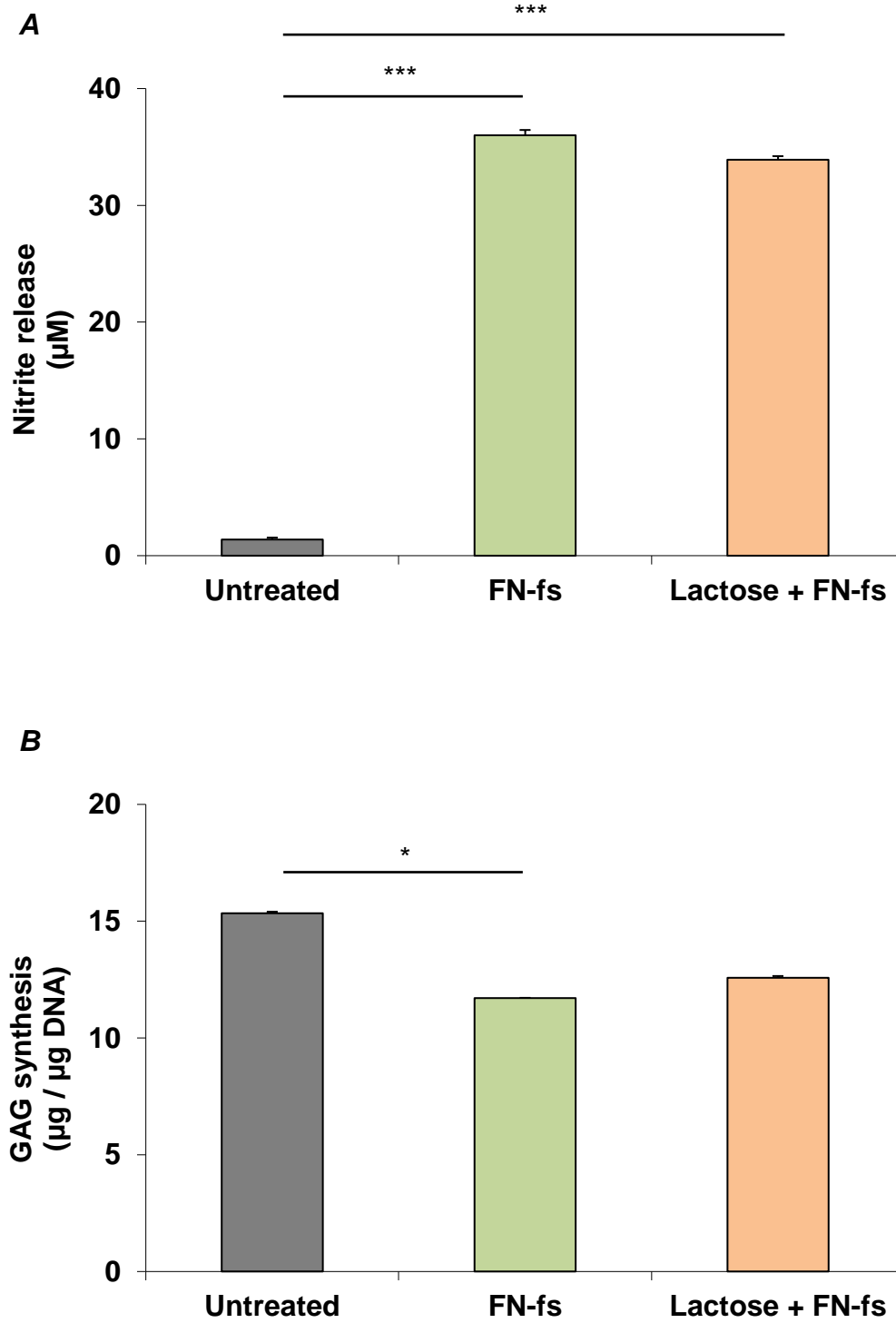


Figure 6.7. Effect of lactose prepared in culture media on (A) nitrite release and (B) GAG synthesis in chondrocytes treated with $1\mu\text{M}$ FN-f. Chondrocyte/agarose constructs were cultured for 48 hours with 100mM lactose and/or $1\mu\text{M}$ of FN-fs and the effects were examined on (A) nitrite release and (B) GAG synthesis. Error bars represent the mean and SEM values for 4 replicates from one experiment. (*) $p < 0.05$ and (***) $p < 0.001$, indicate significant comparisons between treatment conditions.

The absence of a significant reduction in FN-f-induced nitrite release with lactose in figure 6.7A, may have been due to the incorporation of a 72 hour equilibration period, prior to treatment with FN-fs and/or lactose for 48 hours. This is because, on comparing the present study to that which revealed a successful reduction in FN-fs-induced nitrite production (figure 1.27), it was observed that the only difference in the culture conditions between the two studies was that chondrocyte/agarose constructs were not equilibrated prior to treatment with FN-fs in the preliminary study. This difference in culture conditions may be a contributing factor in the changes observed in the effects of lactose between the two studies. In order to confirm this, the following study was performed (section 6.3.3.2).

6.3.3.2 Effect of equilibration on the response of FN-fs to lactose in chondrocyte/agarose constructs

Chondrocyte/agarose constructs were subjected to either 0 hours of equilibration or 72 hours of equilibration, followed by treatment with 1 μ M FN-fs in the presence or absence of 100mM lactose for 48 hours as shown below in figure 6.8. All other culture conditions remained constant.

On treating chondrocyte/agarose constructs with FN-fs, following 0 or 72 hours of equilibration, a significant increase in nitrite release was observed when compared to untreated controls ($p < 0.001$, Fig. 6.8A, B). However, constructs subjected to 72 hours of equilibration followed by FN-f treatment revealed higher levels of nitrite release (39.59 μ M), compared to those which did not undergo equilibration (15.66 μ M, $p < 0.001$). Co-incubation with lactose did not significantly reduce this catabolic effect in both equilibrated and non-equilibrated samples ($p > 0.05$, Fig. 6.8A, B).

Unlike constructs which did not undergo equilibration, a significant decrease in GAG synthesis was observed on treating chondrocyte/agarose constructs with FN-fs, following a 72 hour equilibration period ($p < 0.01$, Fig. 6.8C). However, co-incubation of FN-f-treated constructs with lactose did not reverse these induced catabolic effects in both equilibrated samples and those which did not undergo equilibration (Fig. 6.8).

During tissue digestion, cells are subjected to extreme conditions by the addition of enzymes such as pronase and collagenase. These enzymes are capable of not only degrading proteins in the surrounding ECM, but are also capable of compromising the cell surfaces to some extent. Since FN-fs are known to bind to cell surface receptors for the induction of catabolic activities, it is essential for the cell surface to recover from enzyme action following tissue digestion. Equilibrating samples allow the cell surface to recover from these extreme conditions during enzymatic digestion and also allow cells to stabilize their metabolic activities to a state of equilibrium following cell isolation from *in vivo* conditions. As such,

samples which were equilibrated in this study allowed a high affinity of FN-f-cell surface binding, compared to non-equilibrated samples, resulting in the induction of higher levels of nitrite release when compared to non-equilibrated samples.

A possible contributing factor to the inability of lactose in inhibiting FN-f-induced catabolic activities may have been over-stimulation of the model system by incorporating an extended culture period via equilibration of samples, which resulted in higher levels of nitrite production in equilibrated constructs when compared to non-equilibrated samples (Kelly et al., 2006, Frenkel et al., 1996, Hauselmann et al., 1994, Mauck et al., 2003). At such high levels of nitrite production, it is possible that the lactose present in the culture media was rapidly used up by chondrocytes, in an attempt to initiate self-repair processes, since lactose is a sugar. As a result, only an insufficient amount of lactose might have been left to bind to FN-fs present at the cell surface for the inhibition of FN-f-induced catabolic activities. Furthermore, FN-fs do not possess a quick turnover compared to other inflammatory molecules such as TNF α . Instead, they follow a positive feedback loop in the induction of catabolic activities *in vivo*, hence allowing them to be more potent compared to inflammatory cytokines (Homandberg, Ding and Guo, 2007). As such, this further limited the ability of lactose to inhibit FN-f-induced catabolic activities within the 48 hour culture period, particularly in equilibrated constructs. In order to eliminate the above limitations and enhance the inhibitory effects of lactose, the following solutions were considered:

- Replenishing the amount of lactose provided to chondrocyte/agarose constructs over the 48 hour culture period, following the confirmation through biochemical analyses of whether lactose is indeed diminished in the culture media after 48 hours.
- Examining the dose response effect of FN-fs on chondrocyte/agarose constructs so that the optimum concentration at which the fragment still exerts sufficient catabolic activity and is inhibited by lactose can be determined. This will be the first ever study to examine the dose response effect of FN-fs (29kDa heparin binding FN-fs) derived from cathepsin D and thrombin digests of fibronectin from plasma adsorption on 3D chondrocyte/agarose constructs.
- Additionally, since significant differences in FN-f-induced nitrite production were observed between equilibrated constructs and those (figure 6.8A, B) which did not undergo equilibration, subsequent dose response studies were carried out on both equilibrated constructs and those without equilibration to examine the differences between them.

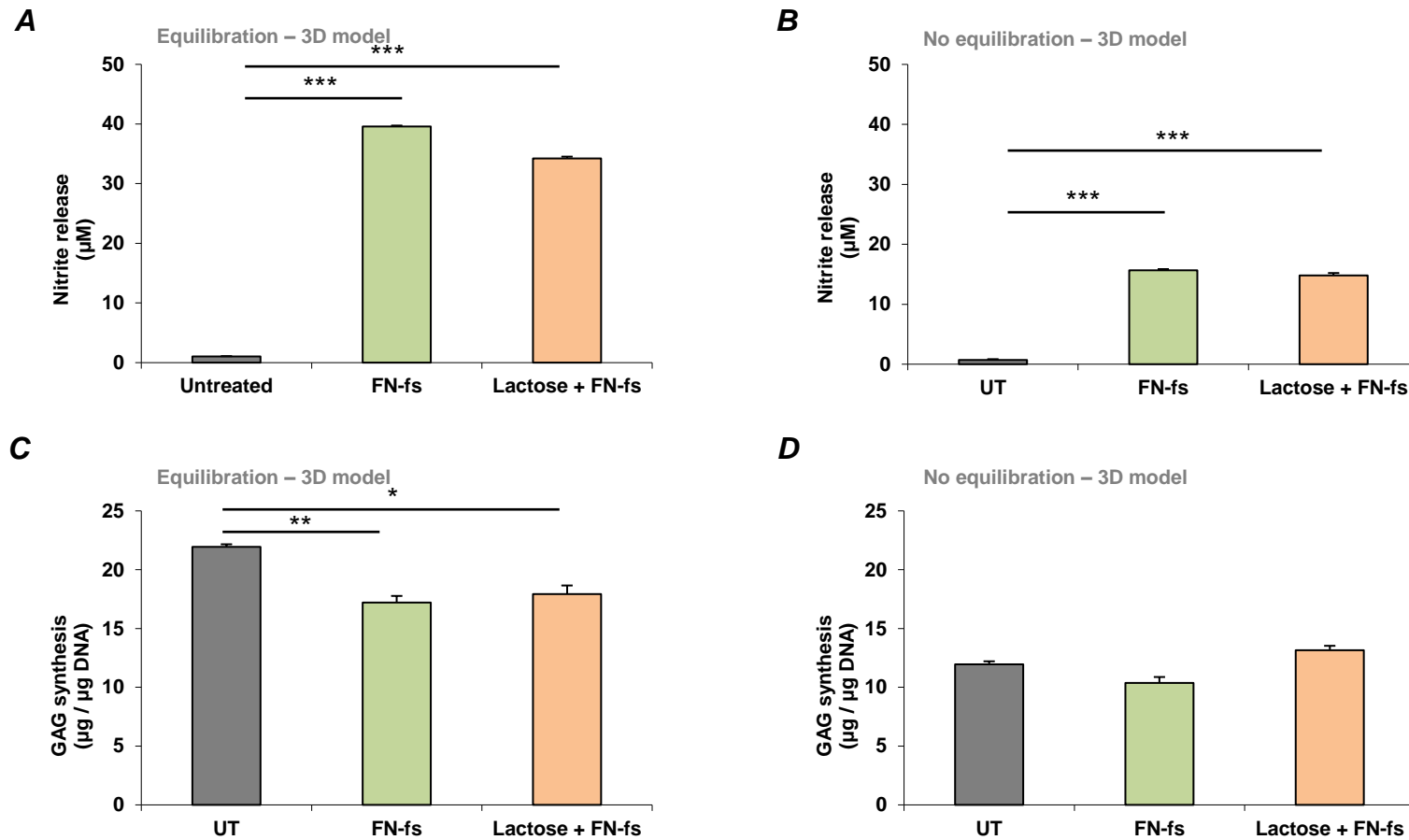


Figure 6.8. Effect of 0 or 72 hours of equilibration on (A) nitrite release and (B) GAG synthesis in chondrocytes treated with FN-f and lactose. Chondrocyte/agarose constructs were subjected to either 0 or 72 hours equilibration followed by 48 hours of culture with $1\mu\text{M}$ FN-fs in the presence or absence of 100mM lactose. The effects were then examined on (A) nitrite release and (B) GAG synthesis. Error bars represent the mean and SEM values for 4 replicates from one experiment. (*) $p < 0.05$, (**) $p < 0.01$ and (***) $p < 0.001$, indicate significant comparisons between treatment conditions.

6.3.3.3 Dose response effect of FN-fs with and without lactose in equilibrated chondrocyte/agarose constructs

Chondrocyte/agarose constructs were initially equilibrated in culture under free-swelling conditions for 72 hours. Following this, they were cultured with DMEM + 20% FCS supplemented with FN-fs at increasing concentrations of 0.25, 0.5, 1 and 2 μ M in the presence and absence of 100mM lactose for a further 48 hours. The concentration range of FN-fs incorporated to examine the dose response effects of the fragment was then altered to 0.01, 0.1 and 1 μ M, while keeping all other culture conditions constant, as shown in figure 6.9.

A significant increase in nitrite production was observed on treating chondrocyte/agarose constructs with 0.25, 0.5, 1 and 2 μ M FN-fs, when compared to untreated controls ($p < 0.001$; Fig. 6.9A). However, there were no significant differences in nitrite production between any of the FN-f-treated constructs (all $p > 0.05$; Fig. 6.9A). All of the aforementioned concentrations of FN-fs induced a marginal decrease in GAG synthesis when compared to untreated controls ($p < 0.05$, Fig. 6.9B). Similar to the trend observed in nitrite release, significant differences in GAG synthesis were not identified between each concentration of FN-f used (all $p > 0.05$; 6.9B). Since a dose-dependent effect of FN-f was not observed in figure 6.9, the concentration range of FN-fs incorporated was altered to that shown in figure 6.10.

The levels of nitrite release were enhanced in chondrocyte/agarose constructs by the presence of FN-fs, with a significant increase at 0.01, 0.1 and 1 μ M, when compared to untreated controls (all $p < 0.001$; Fig. 6.10A). A rise in nitrite release was not observed each time the concentration of FN-fs was increased by a factor of 10, starting from 0.01 μ M (all $p > 0.05$, Fig. 6.10A). The presence of FN-fs did not significantly influence GAG synthesis at any of the concentrations of FN-f used, as shown in figure 6.10B ($p < 0.05$). Co-incubation with lactose did not reverse this effect at any of the FN-f concentrations examined (all $p > 0.05$; Fig. 6.11A, B).

Although a dose-dependent effect of FN-f is observed in figure 6.10, the inability of lactose to significantly inhibit FN-f-induced catabolic activities may have been due to the excessive levels of nitrite released, from over-stimulating the system by the incorporation of extended culture periods as explained in section 6.3.3.2. Since section 6.3.3.2 revealed significant differences between FN-f-treated chondrocytes which were equilibrated and those which were not, a similar dose-response study of the effects of FN-fs in chondrocytes was carried out in constructs which did not undergo equilibration. This was carried out in order to determine whether lower levels of nitrite were induced by FN-fs without equilibrating

constructs and if so, whether a significant reduction of this effect can be achieved with lactose.

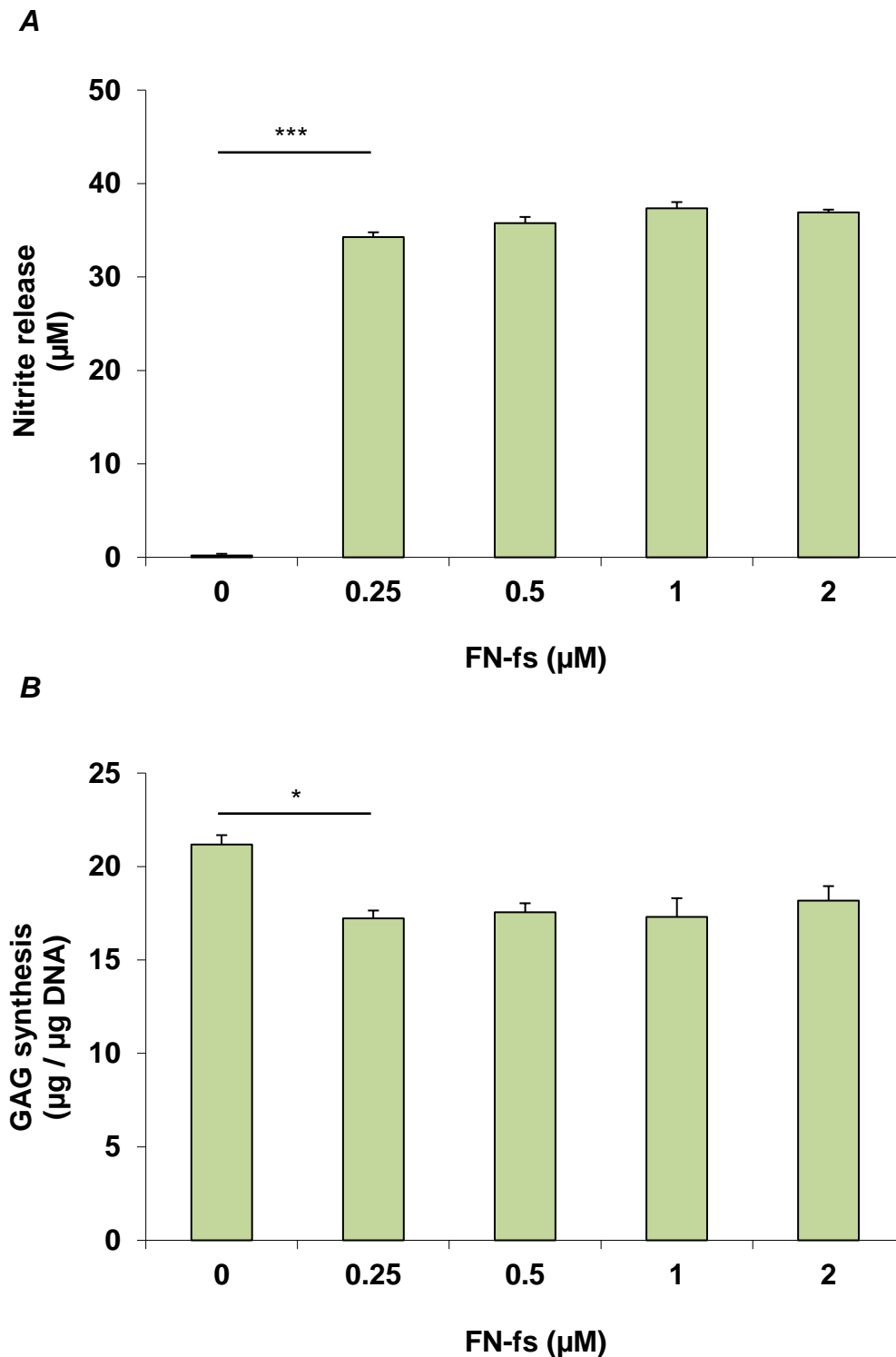


Figure 6.9. Dose response effect of FN-fs (0.25 to 2 μM) on equilibrated chondrocyte/agarose constructs. Chondrocyte/agarose constructs were subjected to 72 hours equilibration followed by 48 hours of culture with 0.25, 0.5, 1 and 2 μM FN-fs. The effects were then examined on (A) nitrite release and (B) GAG synthesis. Error bars represent the mean and SEM values for 4 replicates from one experiment. (*) $p < 0.05$ and (***) $p < 0.001$, indicate significant comparisons between treatment conditions.

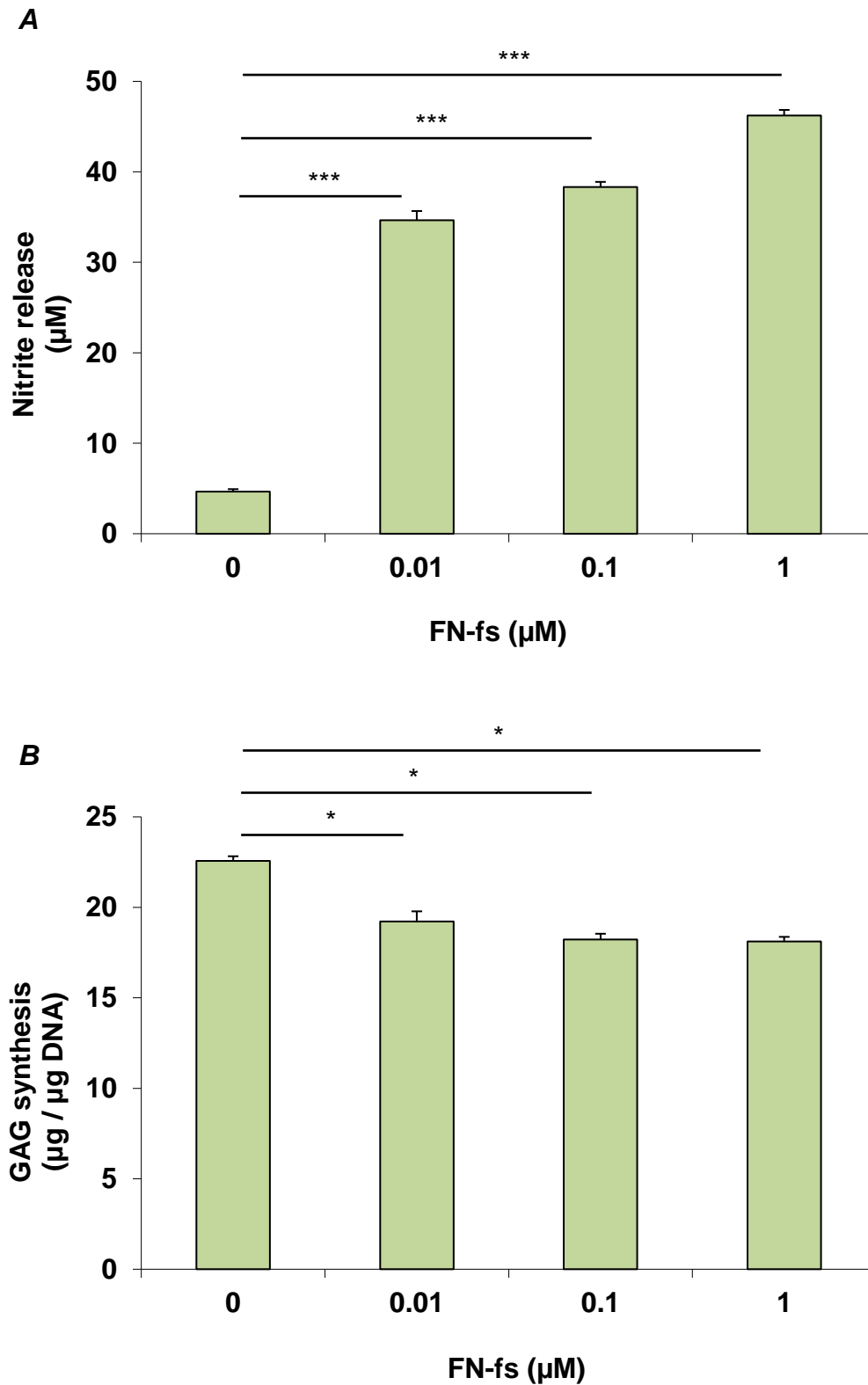


Figure 6.10. Dose response effect of FN-fs (0.01 to 1 μM) on equilibrated chondrocyte/agarose constructs. Chondrocyte/agarose constructs were subjected to 72 hours equilibration followed by 48 hours of culture with 0.25, 0.5, 1 and 2 μM FN-fs. The effects were then examined on (A) nitrite release and (B) GAG synthesis. Error bars represent the mean and SEM values for 4 replicates from one experiment. (*) $p < 0.05$ and (***) $p < 0.001$, indicate significant comparisons between treatment conditions.

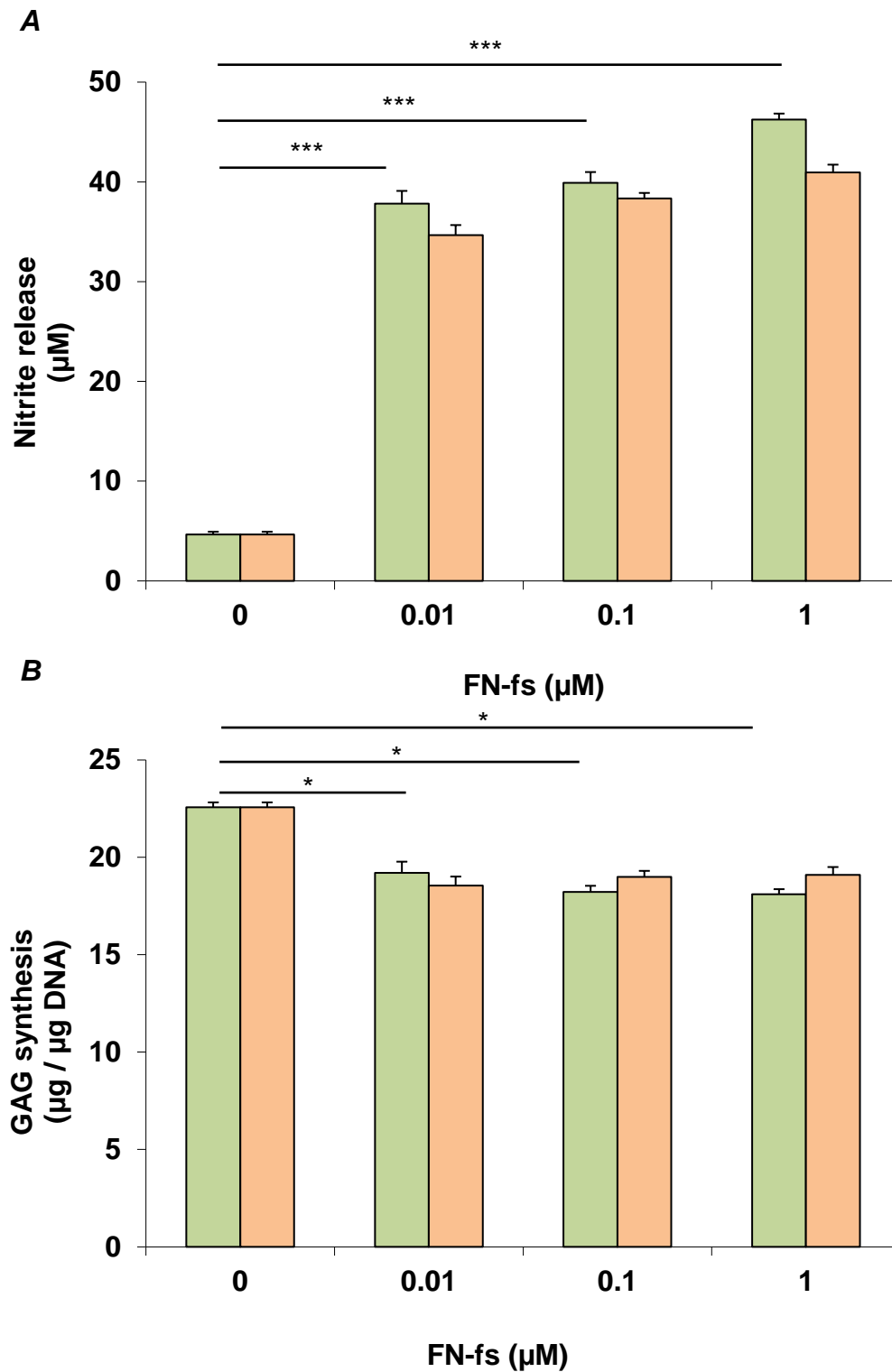


Figure 6.11. Dose response effect of FN-fs in equilibrated chondrocytes treated with lactose. Chondrocyte/agarose constructs were subjected to 72 hours of equilibration, followed by 48 hours of culture with varying concentrations of FN-fs (0.01 to $1\mu\text{M}$) and/or 100mM of lactose and the effects were examined on (A) nitrite release and (B) GAG synthesis. Error bars represent the mean and SEM values for 4 replicates from one experiment. (*) $p < 0.05$ and (***) $p < 0.001$, indicate significant comparisons between treatment conditions.

6.3.3.4 Dose response effect of FN-fs in chondrocyte/agarose constructs treated with lactose without equilibration

Chondrocyte/agarose constructs were directly cultured under free-swelling conditions, without equilibration, for 48 hours with DMEM + 20% FCS, supplemented with FN-fs at increasing concentrations of 0.01, 0.1, and 1 μ M in the presence and absence of 100mM lactose, as shown in figure 6.12.

A significant increase in nitrite production was observed on treating chondrocyte/agarose constructs with 0.01, 0.1, and 1 μ M FN-fs, when compared to untreated controls ($p < 0.001$, Fig. 6.12A). A dose dependent effect of FN-fs on nitrite production was also observed, (Fig. 6.12A) such that upon increasing the concentration of FN-fs by a factor of 10, a partial increase in nitrite production was observed each time (all $p < 0.01$, Fig. 6.12A). Co-incubation with lactose reversed FN-f-induced nitrite production at each concentration of FN-f examined, with maximum inhibition observed at 0.01 μ M ($p < 0.001$, 43.83%) when compared to 0.1 or 1 μ M FN-fs (both $p < 0.01$, 36.64% and 32.23% respectively; Fig. 6.12A). The presence of FN-fs significantly reduced GAG synthesis at all of the concentrations of FN-f examined ($p < 0.01$; 6.12B).

The inhibition of FN-f-induced nitrite production with lactose at all the concentrations of FN-f examined (Fig. 6.12) was in correlation with the decrease in nitrite release observed (>30% inhibition) in chondrocyte/agarose constructs treated with FN-fs in the presence of 100mM lactose (Fig. 1.27, Drs Parker and Peake; unpublished). Based on nitrite release and GAG synthesis observed in figure 6.12, 0.01 μ M was considered the optimum concentration required for FN-fs to induce catabolic activities in chondrocyte/agarose constructs. At this concentration, a significant increase in nitrite release was observed when compared to untreated controls (Fig. 6.12). Additionally, 0.01 μ M did not induce any anabolic activities, evident from the GAG synthesis, as shown in figure 6.12B. This observation however, does not correlate with previous studies which examined the dose-response effect of FN-fs on the anabolic and catabolic activities of chondrocytes in cartilage explants (Homandberg et al., 1994, 1996, 1997, 1998, 2007). It is worth noting that the range of concentrations of FN-fs employed in these studies was similar to one another. 1 μ M of FN-fs was initially used in this experiment, since previous studies which examined the dose response effects of these FN-fs in cartilage explants revealed that concentrations less than 1 μ M induced anabolic or delayed catabolic responses which were later reversed to catabolic effects (Homandberg and Hui, 1994, Homandberg and Wen, 1998, Homandberg et al., 1996, Homandberg et al., 1997). Also, studies which employed synthetic 30kDa NH₂-heparin-binding FN-fs (Sigma-Aldrich, Poole, UK) to induce catabolic effects in 3D porcine chondrocyte/agarose constructs, similar to the one described in this thesis, employed 1 μ M of FN-fs (Chowdhury et al., 2010).

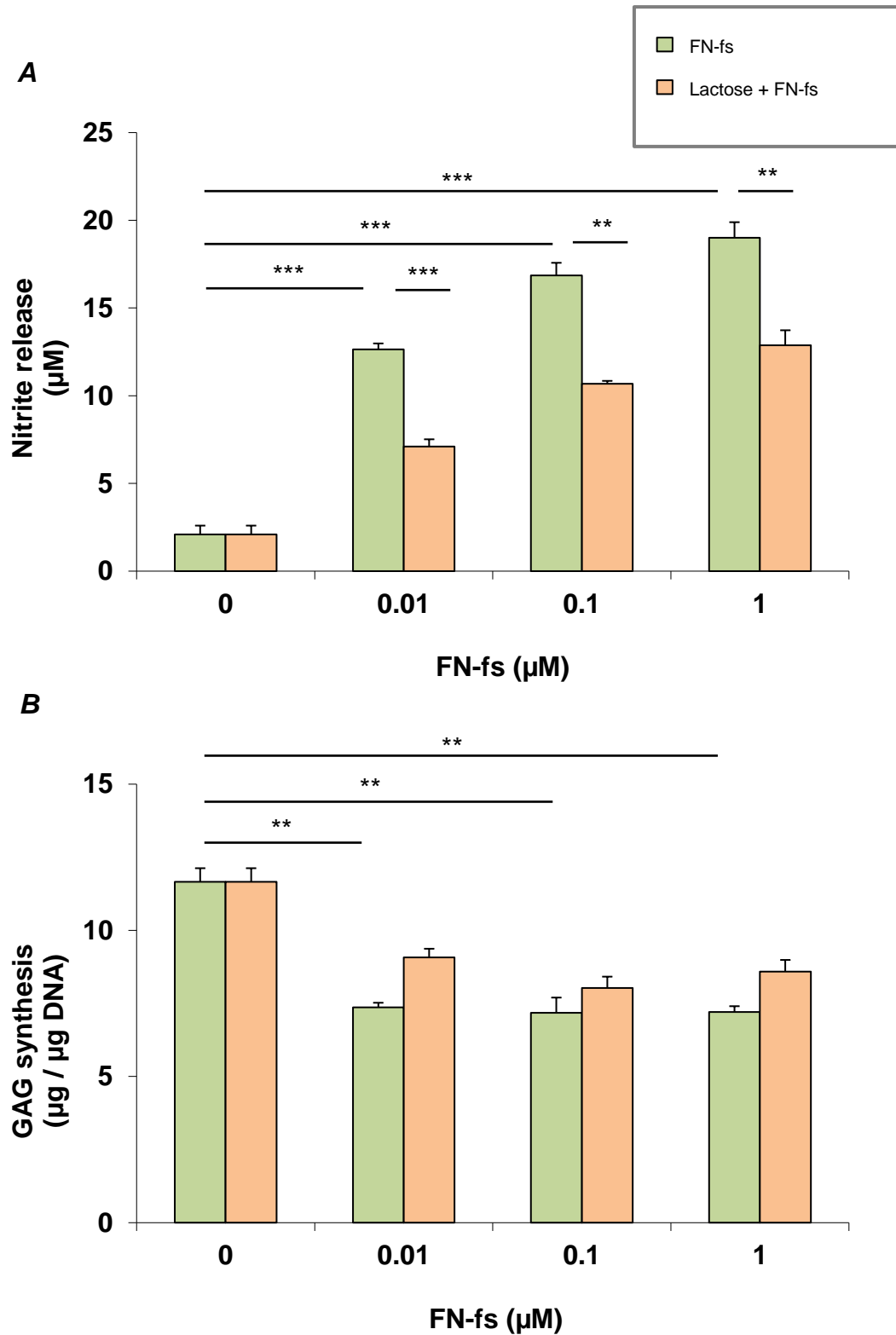


Figure 6.12. Dose response effect of FN-fs in chondrocytes treated with lactose without equilibration. Chondrocyte/agarose constructs were subjected to 0 hours of equilibration, followed by 48 hours of culture with varying concentrations of FN-fs (0.01 to 1µM) and/or 100mM of lactose and the effects were examined on (A) nitrite release and (B) GAG synthesis. Error bars represent the mean and SEM values for 4 replicates from one experiment. (*) $p < 0.05$, (**) $p < 0.01$ and (***) $p < 0.001$, indicate significant comparisons between treatment conditions.

Furthermore, a study which incorporated a 3D bovine chondrocyte/agarose model identical to the one used in this thesis, together with FN-fs from the same source (derived from cathepsin D and thrombin digests) used 1 μ M of FN-fs to stimulate a catabolic effect in chondrocytes (Parker et al., 2013). However, it is worth noting that the latter study which incorporated 3D chondrocyte/agarose models did not examine the dose response effect of these FN-fs in the 3D model, suggesting that the effects of using concentrations of FN-fs less than or greater than 1 μ M in the 3D cell-seeded models were still unknown, unlike cartilage explants (Homandberg et al., 1994, 1996, 1997, 1998). The importance of investigating the dose response effect instead of completely relying on the observations obtained from cartilage explant models is because the findings from explant model systems and those from 3D biomaterial constructs may differ, as both models are associated with different limitations. For example, in explant models it is problematic to separate the contribution of multiple physiochemical and mechanical alterations present in the model which regulate cell function and intracellular pathways, unlike 3D biomaterial model systems (Bader et al., 2011). Furthermore, differences in the source of FN-fs may contribute to variations in results obtained.

Furthermore, on comparing the dose response effects of FN-fs in chondrocyte/agarose constructs which were equilibrated for 72 hours (Fig. 6.10, 6.11) to those which were not (Fig. 6.12), it was observed that these results were in correlation, suggesting that equilibrating chondrocyte/agarose constructs has a significant impact on the effects of lactose on FN-f. The partial inhibition of FN-f-induced nitrite production with lactose in equilibrated samples (Fig. 6.12) when compared those which were not, may have been due to the reduced levels of nitrite released observed in equilibrated samples, by eliminating the equilibration of constructs (Kelly et al., 2006, Frenkel et al., 1996, Hauselmann et al., 1994), as explained in section 6.3.3.2. As such subsequent experiments examining the effects of lactose on FN-fs was carried out without the equilibration of chondrocyte/agarose constructs.

The partial inhibition of FN-f-induced catabolic effects with the employment of lactose suggests the presence of SGAL/EBP signalling, since lactose is a known inhibitor of the sequence XGXXPG, binding to the SGAL receptor or EBP (Hinek and Rabinovitch, 1994, Hinek et al., 1988, 1991, 1993, Hinek and Wilson, 2000, Wachi et al., 2004, Mecham et al., 1989a, 1989b, 1991, Privitera et al., 1998, Blanchevoye et al., 2013). Data from figure 6.12 also suggests that FN-fs induce signalling cascades through the SGAL receptor or EBP. In order to investigate whether FN-f-induced SGAL signalling pathway in chondrocytes is influenced by the inherent low oxygen tension of articular cartilage, the effects of oxygen tension on the response of FN-fs to lactose in chondrocyte/agarose constructs was examined, as detailed in section 6.3.4. However, prior to this, a dose response study on the effects of lactose on FN-fs in chondrocytes was carried out in order to optimize the

concentration of lactose required to inhibit FN-f-induced catabolic activities, as explained in the following section.

6.3.3.5 Dose response effect of lactose in FN-f-treated chondrocyte/agarose constructs

Upon establishing the optimum culture conditions and concentration of FN-fs required to induce catabolic activities in chondrocyte/agarose constructs (Fig. 6.12), the dose response effect of lactose on chondrocyte/agarose constructs treated with 0.01 μ M of FN-fs was examined, in order to determine whether a lower concentration of lactose can be used to induce anabolic responses similar to those induced by 100mM of lactose.

Chondrocyte/agarose constructs were directly cultured under free-swelling conditions, without equilibration for 48 hours with DMEM + 20% FCS, supplemented with lactose at increasing concentrations of 1, 10 and 100mM in the presence and absence of 0.01 μ M of FN-fs, as shown in figure 6.13.

Enhanced levels of nitrite production were observed in chondrocyte/agarose constructs treated with 0.01 μ M FN-fs when compared to untreated controls ($p < 0.001$), as shown in figure 6.13A. Co-incubation with lactose did induce a significant inhibition in FN-f-induced nitrite release at any of the concentrations of lactose examined ($p > 0.05$). However, when compared to 1 and 10mM of lactose, 100mM of lactose induced the most inhibition in nitrite release stimulated by FN-fs. Also, the presence of FN-fs did not induce significant effects on GAG synthesis ($p > 0.05$; Fig. 6.13B).

These results suggest that the optimum concentration of lactose required for the inhibition of FN-f-induced catabolic activities is 100mM. As such, subsequent studies examining the effects of lactose in chondrocyte/agarose constructs employed 100mM of the solution to inhibit 0.01 μ M FN-fs in chondrocyte/agarose constructs which were not subjected to equilibration.

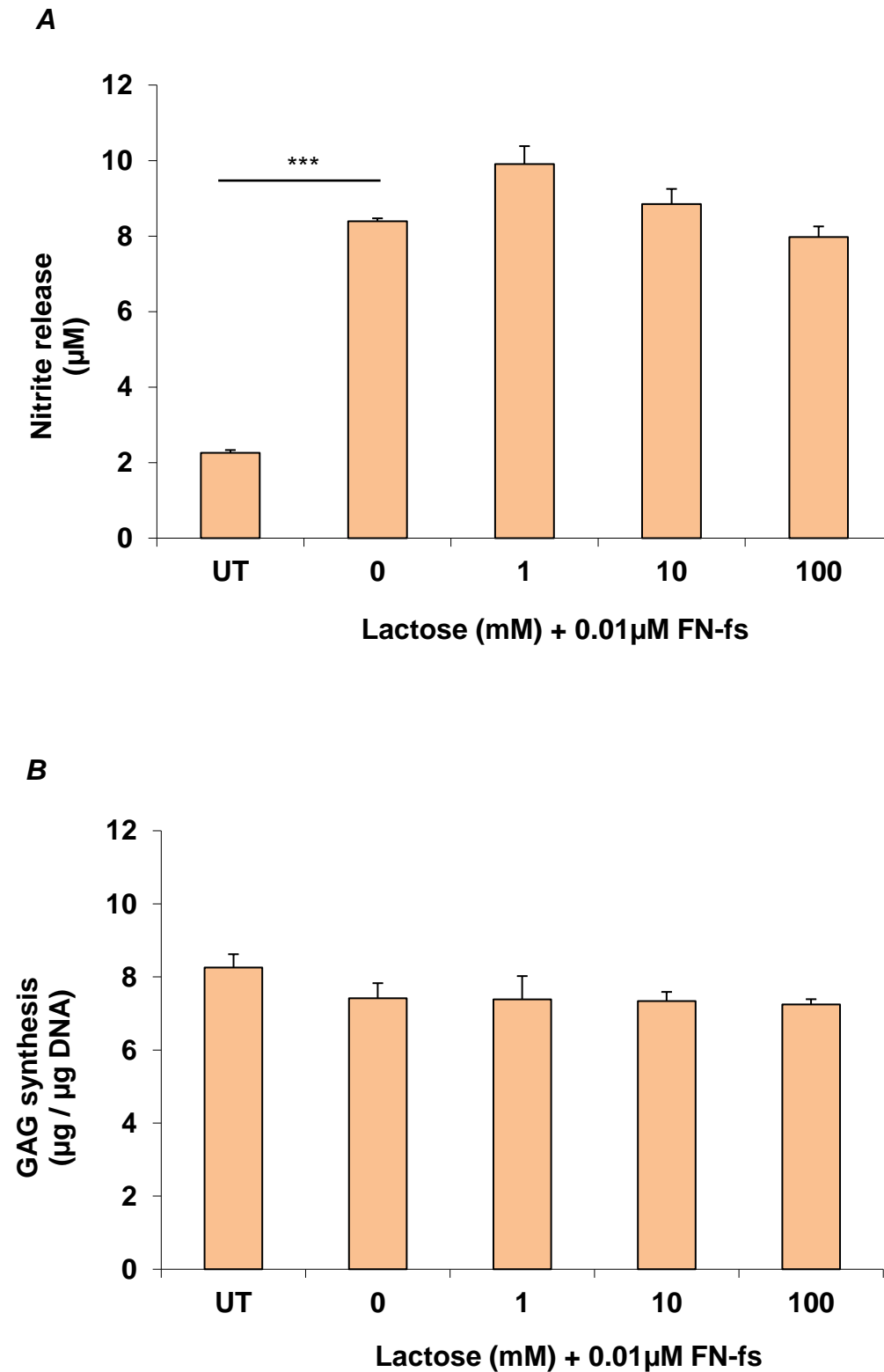


Figure 6.13. Effect of varying concentrations of lactose on (A) nitrite release and (B) GAG synthesis in chondrocytes treated with 0.01µM FN-f. Chondrocyte/agarose constructs were subjected to 0 hours of equilibration, followed by 48 hours of culture with varying concentrations of lactose (1 to 100 mM) and/or FN-fs (1µM) and the effects were examined on (A) nitrite release and (B) GAG synthesis. Error bars represent the mean and SEM values for 4 replicates from one experiment. (***) $p < 0.001$, indicate significant comparisons between treatment conditions.

6.3.4 Effect of 21, 5 and 2% oxygen tension on the response of FN-fs to lactose

Upon establishing the optimum culture conditions and the optimum concentration of FN-fs and lactose required for the induction of FN-f-induced catabolic activities in chondrocyte/agarose constructs, the effect of hypoxia on the response of FN-fs to lactose was examined.

Chondrocyte/agarose constructs treated with 0.01 μ M of FN-fs in the presence and absence of 100mM of lactose under free-swelling conditions at 21, 5 and 2% oxygen tensions in a glove-box style workspace integrated within a Biospherix incubator to ensure that the experimental conditions during set-up and experimentation were uninterrupted, as previously described (Parker et al., 2013).

Figure 6.14 shows the nitrite release and GAG synthesis in chondrocyte/agarose constructs when treated with 0.01 μ M FN-fs in the presence and absence of 100mM lactose at 21, 5 and 2% oxygen tensions. A significant increase in nitrite release was observed in chondrocyte/agarose constructs treated with FN-fs, when compared to untreated controls, at 21, 5 and 2% oxygen tensions (Fig. 6.14A). Co-incubation with lactose resulted in a marginal decrease of this effect at 21 and 2% oxygen tensions, with maximum inhibition of FN-f-induced nitrite production observed at 5% oxygen tension. The presence of FN-fs had no significant effect on GAG synthesis as shown in figure 6.14B.

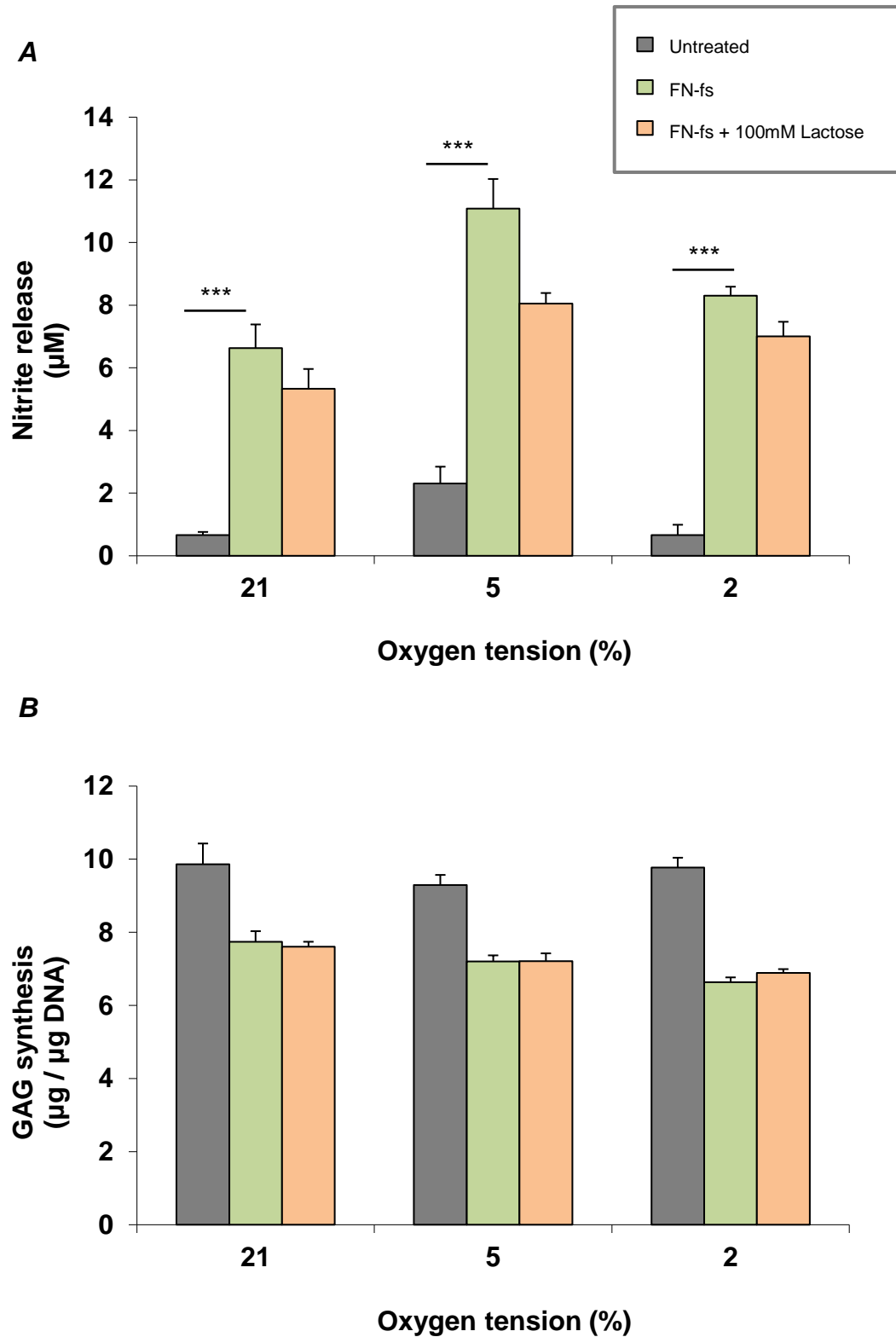


Figure 6.14. Effect of hypoxia on the response of FN-fs to lactose. Chondrocyte/agarose constructs were cultured for 48 hours with $0.01\mu\text{M}$ of FN-fs in the presence or absence of 100mM lactose at 21, 5 and 2% oxygen tensions and the effects were examined on (A) nitrite release and (B) GAG synthesis. Error bars represent the mean and SEM values for 4 replicates from one experiment. (*) $p < 0.05$, (**) $p < 0.01$ and (***) $p < 0.001$, indicate significant comparisons between treatment conditions.

6.3.5 Effect of dynamic compression on the response of the VGVAPG peptide to lactose at 21 and 5% oxygen tensions

Since FN-fs enhanced nitrite production with a greater effect at 5% oxygen tension when compared to 2% oxygen tension, 5% oxygen tension was considered to be the optimum oxygen tension for FN-fs to induce significant catabolic activities in chondrocyte/agarose constructs. As such, in order to determine whether the response of chondrocytes to VGVAPG peptides and biomechanical signals will be influenced by oxygen tension, the present study examined the effects of dynamic compression (15%, 1Hz) on the response of 10µg/ml of VGVAPG peptides to 100mM lactose at 21 and 5% oxygen tensions in chondrocyte/agarose constructs.

Figure 6.15 shows the nitrite production (A) and GAG synthesis (B) in chondrocyte/agarose constructs subjected to dynamic compression and treated with the VGVAPG peptide in the presence and absence of lactose at 21 and 5% oxygen tensions. In the absence of the VGVAPG peptide, dynamic compression significantly reduced NO production at both 21% and 5% oxygen tensions. In unstrained constructs, the VGVAPG peptide enhanced nitrite production with a marginally greater effect at 5% oxygen tension, when compared to 21% oxygen tension and this response was significantly reduced with dynamic compression.

GAG synthesis was increased by dynamic compression when compared to unstrained controls. The magnitude of GAG synthesis was relatively similar at both 5% and 21% oxygen tensions on the application of dynamic compression. At both oxygen tensions, the VGVAPG peptide decreased GAG synthesis. Dynamic compression reversed this effect, with the magnitude of stimulation at 5% and 21% oxygen tensions being relatively similar to one another. Co-stimulation with dynamic compression and lactose increased GAG synthesis with the magnitude of stimulation by dynamic compression greater at 21% oxygen tension when compared to 5% oxygen tension.

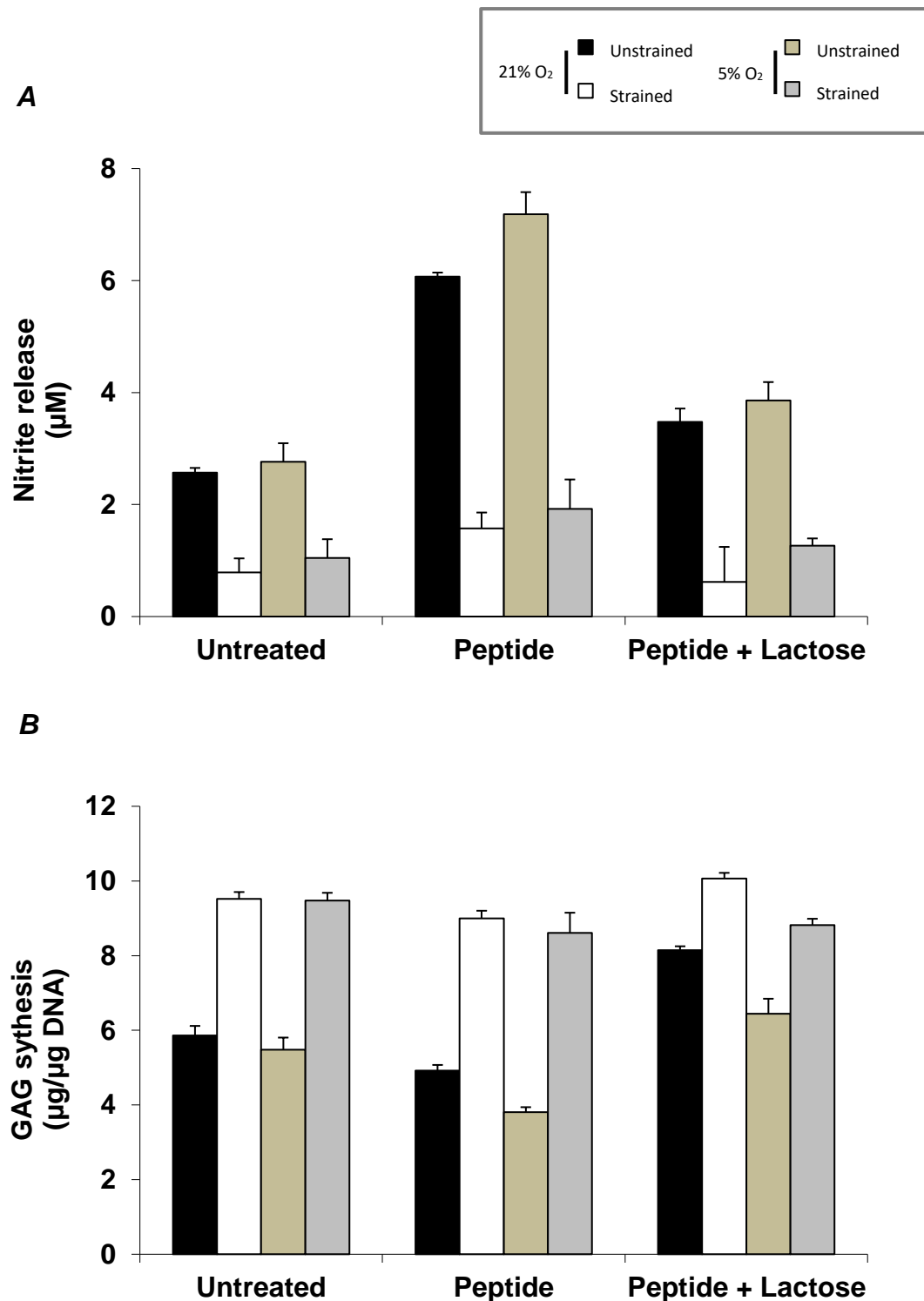


Figure 6.15. Effect of the VGVAPG peptide and lactose on chondrocyte/agarose constructs subjected to dynamic loading at 21 and 5% oxygen tensions. Dynamically loaded chondrocyte/agarose constructs were treated with 10µg/ml of the VGVAPG peptide in the presence and absence of 100mM lactose for 48 hours at 21 and 5% oxygen tensions and the effects were examined on (A) nitrite release and (B) GAG synthesis. Error bars represent the mean and SEM values for 4 replicates from one experiment. (*) $p < 0.05$, (**) $p < 0.01$ and (***) $p < 0.001$, indicate significant comparisons between treatment conditions.

6.4 Discussion

6.4.1 Effect of NT telopeptides on the production of catabolic and anabolic mediators in chondrocyte/agarose constructs cultured at 21, 5 and 2% oxygen tension

On initially treating chondrocyte/agarose constructs with 3 μ M of NT telopeptides, a catabolic response was not induced, evident from minimal levels of nitrite release as shown in figure 6.4. This was further manifested by the use of the positive control, TNF α , which stimulated enhanced levels of nitrite release in chondrocyte/agarose constructs when compared to untreated controls and NT telopeptide treated samples (Fig. 6.14). It was assumed that such an effect may have been due a lower concentration of NT telopeptides used, since previous studies which examined the dose response effect of synthetic NT telopeptides in agarose constructs seeded with porcine chondrocytes showed that the concentration of peptides required to induce maximum catabolic effects was 50 μ M (Chowdhury et al., 2010). 3 μ M of NT telopeptides was used since other studies which examined the dose-response effect of synthetic NT telopeptides on chondrocytes, demonstrated an induction of catabolic activities, such as enhanced proteoglycan loss, on using this concentration of the peptides. However, it is worth noting that cartilage explants and chondrocyte monolayer cultures were used in these studies, unlike the present study, which may account for differences in the results obtained (Guo, Ding and Homandberg, 2009). Additionally, studies which incorporated rabbit surgical models of OA observed an increase in the levels of collagen fragments in the synovial fluid to about 3 μ M (6 μ g/ml, Felice, Chichester and Barrach, 1999). As such, the concentration of synthetic NT telopeptides incorporated to induce a catabolic effect in chondrocyte/agarose constructs was increased from 3 μ M to 50 μ M. However, increasing the concentration of NT telopeptides used still did not induce any catabolic effects on culturing chondrocyte/agarose constructs for a 48 hour culture period. As such, attention was focused on the properties of the NT telopeptide, its method of synthesis and the 3D model used for this study, which might be contributing factors to obtaining such results. Each factor has been discussed further in the sections below:

6.4.1.1 Model system and species of chondrocytes used

The species of chondrocytes used in the present study were not a contributing factor to the inability of the synthetic NT telopeptides to induce catabolic activities. This was so because previous studies which employed synthetic NT telopeptides of the same sequence, did not encounter any differences in the effects of the peptides, with respect to the species of chondrocytes used (Jennings et al., 2001, Chowdhury et al., 2010, Guo, Ding and Homandberg, 2009).

Similarly, the model system employed in this study was also not a contributing factor to the results obtained, since a similar model system made of 3% agarose type VII, resulting in the same pore size was previously used to study the effects of the 10kDa synthetic NT telopeptides on chondrocytes (Chowdhury et al., 2010).

6.4.1.2 NT telopeptide synthesis

Lyophilised form of the NT telopeptides, of >95% purity were synthesized by Laboratoire de Biotechnologie (Luxembourg S.A), using analytical high-performance liquid chromatography (HPLC) analysis. Briefly, the technique involves the separation, identification and quantification of each component of a solvent mixture by passing pressurized liquid solvent through a column filled with adsorbent material. Based on the different properties of each component of the liquid solvent, the adsorbent material reacts differently to each component resulting in the separation of each component from different flow rates being generated through the column. The sequence chosen to carry out this study (section 6.2.1) has been well documented to correspond to the amino-terminal region of collagen type II for the stimulation of catabolic activities in chondrocytes in both 2D and 3D model systems (Jennings et al., 2001, Chowdhury et al., 2010, Lucic et al., 2003, Guo, Ding and Homandberg, 2009). Peptides were synthesized in a lyophilized form, since they are highly stable at room temperature in this form. During synthesis of the NT telopeptides, H and OH bonds were also added to the N- and COOH-terminals of the peptide respectively, in order to further maintain the stability of the peptide in its lyophilised form, since the first amino acid in the N-terminus of our required peptide was glutamine (Q or Gln), which is normally prone to undergo cyclization, converting it to pyroglutamine together with an overall shift in mass of the peptide (ThermoFisher Scientific, Loughborough, UK; Laboratoire de Biotechnologie, Luxembourg S.A; LifeTein LLC, Somerset, New Jersey, US). To examine the effects of 50µM of the NT telopeptides, a second batch of NT telopeptides were synthesized in a similar manner by LifeTein LLC (Somerset, New Jersey, US), while keeping all specifications of peptide synthesis constant.

6.4.1.3 Peptide preparation prior to chondrocyte treatment

Since both batches of synthesized peptides were hydrophobic due to the presence of many proline (P or Pro), leucine (L or Leu) and glycine (G or Gly) amino acids, resulting in an overall zero charge, these peptides were initially dissolved in 2% DMSO, an organic solvent, followed by diluting them in PBS in a drop wise manner to achieve a final concentration of 1mg/ml, according to manufacturers' instructions (Laboratoire de Biotechnologie, Luxembourg S.A; LifeTein LLC, Somerset, New Jersey, US). Alternative organic solvents suggested for dissolving the peptides included propanol, methanol as well as

dimethylformamide (DMF) at <5% (V/V) in order to achieve 100% solubility and prevent cytotoxicity, upon treatment of chondrocytes. However, since our peptide did not have cysteine in its sequence, it was not required to be dissolved in DMF. Another essential factor which was taken into consideration during preparation of the peptides for the stimulation of chondrocytes seeded in agarose constructs was the presence of methionine in the peptide sequence, which is generally known to be prone to oxidization into methionine sulfone, which may also cause an overall mass shift of the peptide. In order to avoid this, when solubilizing the peptides, it was essential that the peptide solution was not agitated. Instead, DMSO was added to the peptides at a slow rate, in a drop wise manner (ThermoFisher Scientific, Loughborough, UK; Laboratoire de Biotechnologie, Luxembourg S.A; LifeTein LLC, Somerset, New Jersey, US). Once the lyophilised peptides were converted into 1mg/ml of DMSO/PBS solution, it was further diluted to 3 μ M or 50 μ M with DMEM + 20% FCS, for chondrocyte treatment. The resulting solution was then filtered to maintain sterility of the peptides and prevent chondrocytes from being infected upon treatment. This was done despite a >95% purity was achieved during peptide synthesis since the recommended period of culturing these peptides, without filtration was 2-3 days (Laboratoire de Biotechnologie, Luxembourg S.A). Following this, the peptide solution was then stored at -80°C.

Following manufacturer's instructions in the preparation of the NT telopeptides for chondrocyte stimulation did not result in any catabolic activities being induced, even when the concentration of peptides being employed was increased from 3 to 50 μ M. As such, authors who examined the effects of these peptides were consulted for further information. In studies performed by Guo, Ding and Homandberg (2009), preparing synthetic NT telopeptides (Sigma Genosys, St. Louis, MO) for the stimulation of catabolic activities in cartilage explants and chondrocyte monolayer cultures, involved initially dissolving these peptides in sterile 1x PBS to achieve a concentration of 10mg/ml. The dissolved peptides were then dialyzed in benzoylated dialysis tubing with a molecular weight cutoff (MWCO) of 1.2 to 2.0kDa (Sigma Genosys, St. Louis, MO) firstly against 1x PBS (V:V = 1:100) followed by DMEM (V:V = 1:100) at 4°C, over a 72 hour period. The dialysis PBS was changed twice before being switched to DMEM. The major difference between this technique of peptide preparation and that carried out in the present study was subjecting the peptides to dialysis, as dialysis removed the salts presented during peptide synthesis and equilibrated the peptide solution with culture media. It was also a necessary step to ensure that the effect on cultures was only from peptides and not from something unknown.

6.4.2 The effect of lactose on FN-fs is oxygen-sensitive and enhanced under hypoxic conditions

In this thesis studies examining the effects of the 29kDa NH₂-heparin-binding FN-fs were carried out with a low n value of 4, due to the limited availability of the fragments, which were a generous gift from the late Gene Homandberg and the insufficient expertise and resources to derive them from bovine plasma in the host laboratory. Results from figure 6.14A are in agreement with previous findings which showed the induction of greater catabolic activities at 5% oxygen tension when compared to 21% oxygen tension in the presence of FN-fs. This effect was associated with the suppression of matrix synthesis (Fig. 6.14B) which was not significantly influenced by oxygen tension. A similar response was observed in bovine chondrocyte monolayer cultures, treated with IL-1 β which resulted in enhanced levels of NO produced at 5% oxygen tension when compared to 1 or 21% oxygen tension (Mathy-Hartert et al., 2005). Although the effect of oxygen tension on FN-fs has previously been examined in chondrocytes in the presence of the NOS inhibitor, L-NIO, this is the first study to show that the effect of lactose on FN-fs is oxygen-sensitive and enhanced under hypoxic conditions. However, studies which have examined the combined effect of oxygen tension and cytokines on the metabolic activities of chondrocytes have resulted in variable outcomes. For example, porcine explants treated with TNF α or IL-1 α revealed increased levels of NO production at 20% oxygen tension when compared to 1% oxygen tension (Cernanec et al., 2002). Conversely, a decrease in MMP-9, oxidative stress and HIF-1 α was observed in chondrocytes treated with cytokines at 6% oxygen tension when compared to ambient conditions (21% oxygen tension, Lawyer, Tucci and Benghuzzi, 2012).

During OA disease process, an upregulation in the expression of HIF-1 α has been observed. It has also been shown that HIF-1 α is oxygen-sensitive and as such, possesses the potential for the development of therapeutic strategies for the treatment of OA. Examples of other oxygen-sensitive mediators which can be used as therapeutic targets for OA include MAPK and NF- κ β which have been shown to be involved in the increase of NO release in cytokine-treated samples at 5% oxygen tension (Mathy-Hartert et al., 2005, Grimshaw and Mason, 2000, Martin et al., 2004). Collectively, these studies emphasize the importance of oxygen tension in the inflammatory response of chondrocytes and that further investigations should be carried out to examine how the signalling cascades induced by FN-fs and lactose interplay with oxygen tension.

6.4.3 The effect of dynamic compression on the response of the VGVAPG peptide to lactose is oxygen-independent

From figure 6.15, it was observed that whilst lactose reduced peptide-induced nitrite production in unstrained constructs, treatment with lactose alone did not lead to the restoration of GAG synthesis. The response of dynamic loading, on the other hand, was found to be oxygen-independent, such that dynamic compression alone resulted in a greater reduction in peptide-induced catabolic effects, at both 21 and 5% oxygen tension. This effect was shown to be associated with GAG synthesis (Fig. 6.15B). This is the first study to examine the combined effects of oxygen tension and dynamic compression on the suppression of the catabolic effects induced by the VGVAPG peptide. It has been well documented that oxygen tension and mechanical loading has an implication on the inflammatory response of chondrocytes. Results from figure 6.15, suggests the presence of the *XGXXPG* sequence in FN-fs, as lactose was able to successfully inhibit the VGVAPG peptide, which correlates with a previous study which examined the inhibitory effects of lactose on the VGVAPG peptide (Blanchevoye et al., 2013). This data is also in agreement with results from Chapters 4, which showed that cytokine-induced catabolic activities were reduced on subjecting chondrocyte/agarose constructs to mechanical loading at both 21% and 5% oxygen tensions. The results from figure 6.15 are also in correlation with those from a study in which dynamically stimulated chondrocyte/agarose constructs were treated with FN-fs in the presence and absence of L-NIO, at both 21% and 5% oxygen tension. From the study, it was observed that FN-f-induced catabolic activities were reduced by dynamic compression in an oxygen independent manner (Parker et al., 2013). Collectively, these results emphasize the oxygen-dependency of the response of chondrocytes to FN-fs or its *XGXXPG* sequence and lactose, and suggest that further studies should be carried out to examine the interplay of FN-fs, lactose and oxygen tension, together with dynamic compression to identify potential targets for OA therapy.

Chapter 7 – General Discussion

7.1 Introduction

The present thesis has examined the dose response effect of TNF α in chondrocytes seeded in 3D agarose constructs, in addition to elucidating the signalling pathway through which FN-fs induce catabolic activities. The effect of hypoxia on the metabolic activities of chondrocytes, in response to these inflammatory agents was then examined, in addition to whether the induced inflammatory response was influenced by mechanical stimuli. These studies employed a well-documented loading modality to enhance matrix synthesis in *in vitro* models to interrogate the hypotheses most conveniently listed below.

- TNF α dose-dependently increases the production of catabolic mediators in chondrocytes, with effects, which are further enhanced under hypoxic conditions.
- Dynamic compression and/or L-NIO reduces TNF α -induced catabolic effects at both 21% and 5% oxygen tensions.
- Dynamic compression induces greater GAG synthesis at 21% oxygen tension when compared to that expressed at 5%.
- FN-fs induce catabolic activities in chondrocytes through SGAL/EBP receptors, due to the presence of the XGXXPG amino acid sequence, which is influenced by both hypoxia and mechanical stimuli.
- NT-telopeptides induce catabolic activities in chondrocytes, which are then reduced/abolished in the presence of NOS and COX inhibitors.

Some of the experimental methods to interrogate these hypotheses required optimisation through a series of trial and error procedures. The materials and methods employed in order to achieve the aims and objectives of the present study has been summarised in the flow chart illustrated in figure 7.1.

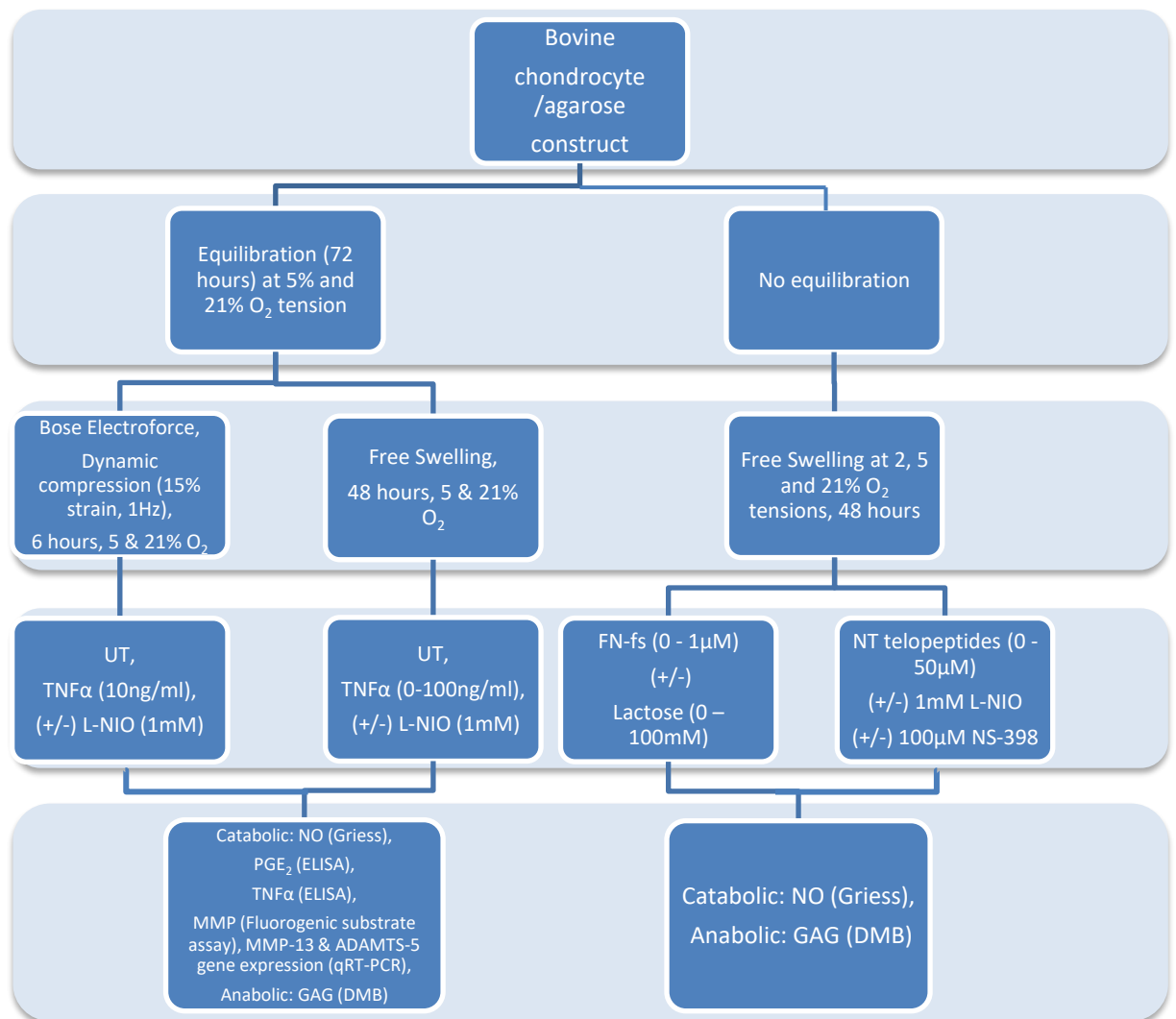


Fig. 7.1. Flow chart illustrating the test protocols employed to achieve the aims and objectives of the present study (UT denotes untreated constructs).

7.2 Model System

As a scaffold material, agarose proved to be highly appropriate for the development of the 3D model system in order to address the aims and objectives of the present study. Indeed, its pore size allowed the effective diffusion of the pro-inflammatory cytokine, $\text{TNF}\alpha$, allowing its dose response effects to be successfully examined on chondrocyte metabolism (Aydelotte et al., 1992). Similarly, the effects of the other inflammatory and inhibitory agents could be examined. These included FN-fs, NT-telopeptides, L-NIO and NS-398. However, upon examining the effects of lactose on FN-f-induced catabolic activities, difficulties were encountered in generating an inhibitory effect, which may have been as a result of the large molecular weight of lactose, that is 360Da, preventing it from effectively diffusing through the pores of the scaffold, as discussed in section 6.3.2. It is fully accepted that the homogenous agarose model differs from the complex constituents and architecture of native cartilage ECM, as discussed in section 2.1.1. Indeed the associated chondrocytes do not bind to agarose as in native ECM within the pericellular region. This will clearly influence the manner in which the mechanical signals will be transduced to the surface of chondrocytes. Nevertheless, chondrocytes seeded in 3D agarose constructs presents a robust mechanically stable system and provides an ideal model system in which the effects of discrete changes in input parameters can be examined selectively in the light of well-defined output parameters.

7.3 Test Equipment

By employing the cell straining system described in section 2.4, the effect of dynamic compression was successfully examined on the metabolic activities of chondrocytes stimulated with TNF α in agarose constructs. It is worth noting that the applied loading regimen was prescribed to be within physiological levels, with a strain amplitude of 0-15%, using a sinusoidal waveform at a frequency of 1Hz, subsequently resulting in 600 to 4800 duty cycles during a 6 to 48 hour culture period. Another benefit of the system was the design of the pin holder plate which incorporated 24 light-weight stainless steel loading pins (each pin of mass 2g), thereby allowing 24 constructs to be strained simultaneously within individual wells of a 24-well plate without damage or permanent deformation. The design also enabled individual constructs to be periodically supplemented with culture media, via the use of a syringe and right-angled needle, enabling the examination of a range of inflammatory and inhibitory reagents on chondrocyte metabolism. Additionally, the presence of a Perspex box enclosing the entire set-up allowed the maintenance of sterility throughout the 6 or 48 hour culture period.

Furthermore, the compact size of the cell straining apparatus allowed it to be integrated within the Biospherix incubator (Fig. 2.4), which permitted the effects of various oxygen tensions to be studied in chondrocyte/agarose constructs subjected to both dynamic compression and free swelling conditions. The Biospherix incubator was successfully utilized in achieving this purpose, by ensuring that experimental conditions remained uninterrupted during the setup of each experiment.

7.4 Biochemical and molecular analysis

Upon completion of the various treatment conditions, standard biochemical assays including DMB, Hoescht, Griess, PGE₂ ELISA and fluorogenic substrate assay, as well as RT-qPCR were performed in order to quantify both anabolic and catabolic markers. Although agarose has been shown to be amenable for analysing cell proliferation, GAG synthesis, nitrite and PGE₂ release, certain limitations were associated with some of these biochemical assays.

Indeed, the Griess assay estimated nitric oxide production by spectrophotometrically quantifying its derivative nitrite in the culture media. However, one of the limitations associated with this assay is the lack of sensitivity and ability to detect nitrate levels in the culture supernatant. As such, nitrate must first be converted into nitrite for total nitrite production to be quantified (Marzinzig et al., 1997). Nevertheless, nitric oxide can form numerous nitrogen intermediates, including peroxynitrite and nitrosothiols, which would need to be identified and measured in order to accurately quantify nitric oxide production. Additionally, the detection of nitrite is limited to values between 1 and 4 μM, which constitutes approximately 20% of the total nitric oxide production (Fermor et al., 2001). However, the Griess assay assumes that the ratio of nitrite to nitrate remains constant.

To the author's knowledge, this study represents the first in which MMP activity was quantified in 3D chondrocyte/agarose constructs using a fluorogenic substrate assay. As such, the assay had to be developed and optimized through a series of trial and error procedures, as described in section 2.5.5. It should be accepted, however, that the optimization of the assay was performed only on culture supernatants, according to manufacturer's instructions. Since MMPs are synthesized by chondrocytes seeded within the agarose constructs, it might be predicted that MMPs will also be present within the construct. This could have been examined following enzymatic digestion of chondrocyte/agarose constructs using agarose and papain, as described in section 2.2.5. The standard method for estimating MMP concentration would have involved developing a standard curve of fluorescence activity with time. This enables comparison of MMP activity from one study to another. However, the approach adopted in the present study did not involve the development of a standard curve, rendering it difficult to compare to other studies analysing MMP activity. This is particularly so in the case of studies which incorporate substrate buffer solutions designed to quantify the activity of different types of MMPs. Nevertheless, this proved a simple, cheaper and reliable approach. From section 5.4, it was observed that agarose may not be the ideal model system for analysing the gene expression of tissue remodelling markers using qRT-PCR, as limited protein/mRNA purity was obtained due to interference of the scaffold material. Notwithstanding this limitation, the assay was optimized through a series of incremental stages in order to enhance protein/mRNA purification for the analysis of ADAMTS-5 and MMP-13 gene expression in chondrocyte/agarose constructs.

7.5 Scientific findings

The strategies undertaken for elucidating cartilage mechanotransduction pathways over the last few decades have progressed remarkably, starting with analysing the overall response of cartilage tissue upon stimulation with mechanical loading, to incorporating 3D cell seeded model systems (Buschmann et al., 1992, 1995; Lee and Bader, 1997). Attention was particularly focused on the changes observed in chondrocyte metabolism, upon the application of external loads of varied strains and frequencies. However, more recently, interest has been diverted to examining the intracellular signalling cascades which take place upon stimulation with mechanical loading, which subsequently influence biochemical parameters such as GAG synthesis and cell proliferation. In the present work, specific biochemical and mechanotransduction pathways through which dynamic compression changes the production of catabolic and anabolic mediators have been described in the following section. Additionally, the effect of dynamic compression on the regulation of mRNA corresponding to tissue remodelling mediators at a molecular level has also been reported. The purpose of conducting this work was to provide a critical knowledge of both the intercellular and intracellular mechanisms associated with dynamic compression.

7.5.1 The effect of TNF α and the NOS inhibitor, L-NIO on NO production

The main principles associated with NOS isoforms, is that constitutively synthesized NOS (cNOS) isoforms are essential in the regulation of most physiological processes, whereas inducible NOS isoforms (iNOS) act as mediators in inflammatory environments. It has long been speculated that NO may have both beneficial and detrimental effects. For instance, while the inhibition of NO has resulted in cartilage degradation in some inflammatory models, inhibition of the free radical in other models has led to the induction of beneficial outcomes (Willoughby et al., 2000). Nevertheless, the detrimental effects of NO are only expressed when it is produced in large concentrations by iNOS (Martel-Pelletier and Pelletier, 2010). On the other hand, its beneficial outcomes are revealed, when the free radical is produced in relatively lower concentrations by cNOS. This hypothesis was examined in Chapter 3 which demonstrated a dose-dependent increase in nitrite production on stimulating chondrocyte/agarose constructs with TNF α at concentrations ranging from 0.1 to 100ng/ml (Fig. 3.1). These results were in concert with previous findings which demonstrated an upregulation in iNOS expression in chondrocytes treated with lipopolysaccharide (LPS), TNF α and IL-1 β , which led to an enhanced NO production and cell apoptosis (Maier et al., 1994, Blanco et al., 1995). Similarly, TNF α has been observed to increase NO levels as well as superoxide production in both OA synoviocytes and

chondrocytes (Ahmadzadeh et al., 1990, Maier et al., 1994). Indeed, chondrocyte alginate beads and monolayer cultures treated with TNF α revealed an upregulation in iNOS expression and NO release, with a consequent decrease in aggrecan synthesis (Goodstone and Hardingham, 2002, Schuerwegh et al., 2003, Rai et al., 2008). Chondrocyte/agarose constructs treated with a combination of TNF α , IL-1 and LPS also resulted in elevated levels of NO production (Stadler et al., 1991). On treating the constructs with L-NMA, an inhibitor of all the isoforms of NOS, an inhibition in NO production was observed. Co-stimulation with the NOS substrate, L-arginine, however, resulted in an increase in NO synthesis. Interestingly, in the absence of L-NMA, L-arginine inhibited the synthesis of NO. From this study, it was suggested that the NOS enzyme may have a high binding affinity to its substrate. Additionally, L-NMA is well known to influence the transfer of L-arginine into the cell, which may account for the inhibition in NO production by chondrocytes when co-stimulated with the NOS substrate (Forray et al., 1995). NO synthesis has also been demonstrated in a wide range of species. For example, the initial identification of NO production involved the treatment of monolayer cultures of human chondrocytes with a variety of cytokines, including TNF, IL-1 and LPS (Palmer et al., 1993). Furthermore, synthesis of the inflammatory mediator has been shown to be dependent on the concentration and type of cytokine with which cells are stimulated. Co-stimulation of chondrocytes with the NOS inhibitor, L-NIO, abolished the cytokine-induced NO production, confirming that NO was synthesised by the NOS enzyme. Similar observations were made in OA joints on the selective inhibition of iNOS, which resulted in a reduction in the symptoms of inflammation and biomechanical abnormalities (Pelletier et al., 1999, Pelletier et al., 1996).

Additionally, TNF α was shown to induce the production of PGE₂ in a dose-dependent manner (Fig. 3.2). The response was then partially inhibited upon co-stimulation with L-NIO, implying that the induction of PGE₂ was via NO production. However, PGE₂ synthesis can be enhanced directly by TNF α , without the activation of NO as a secondary messenger. Indeed NO has a very short half-life and is capable of reacting with superoxide radicals to form peroxynitrite (ONOO⁻), which could act as a mediator to further synthesize PGE₂, in the absence of NO (Asada et al., 1999, 2001, Beckman and Koppenol, 1996, Oh et al., 1998). It has also been well documented that activation of the COX-2 enzyme results in the production of PGE₂ (Murakami et al., 2000, Vane and Botting, 1998a). The present findings were in agreement with studies in which TNF α -treated OA menisci explants, chondrocyte alginate beads and monolayer cultures demonstrated an upregulation in COX-2 expression and PGE₂ production, which were associated with increased iNOS and NO synthesis (Rai et al., 2008). Similarly, elevated levels of PGE₂ synthesis were observed on stimulating human chondrocyte monolayer cultures with TNF α (Bunning & Russell, 1989, Carames et al., 2008). Similar observations were made in OA cartilage explants, in which increased levels of PGE₂ were shown to correspond with enhanced expression of COX-2 (Amin et al., 1997).

Consequently, these activities resulted in enhanced cartilage damage (Notoya et al., 2000, Pelletier et al., 2001a, Goldring and Berenbaum, 2004).

Previous studies have revealed that upstream activators, such as kinases and intracellular messenger systems, are involved in the modulation of iNOS and COX-2 expression, together with NO and PGE₂ release, in response to TNF α in a variety of model systems (Table 1.5). Indeed, activation of the transcription factor, NF- κ B, has been demonstrated in human or murine chondrocytes stimulated with TNF α in alginate beads and monolayer cultures (Yasuda, 2011, Seguin & Bernier, 2003, Mehdi et al., 2007). Similar observations were made in other cell types treated with TNF α , such as human fibrosarcoma cells, wild-type mouse embryonic fibroblasts and human OA synovial fibroblasts, which also revealed activation of the NF- κ B transcription factor (Alaaeddine et al., 1999, Varfolomeev et al., 2008). Examples of other upstream activators which have been shown to be influenced by TNF α include p38 MAPK, ERK and JNK (Badger et al., 2000, Seguin & Bernier, 2003, Zhou et al., 2007). Although, the activation of protein kinases by pro-inflammatory cytokines have been well documented, sufficient evidence has also been provided on the regulation of cytokines and other catabolic mediators by protein kinases, resulting in the formation of a positive feedback loop of sustained NF- κ B activation (Ge et al., 2011, Kapoor et al., 2011). For example, p38 MAPK and JNK have been shown to regulate the production of IL-1 and TNF α which, in turn, upregulated the expression of MMP-1, -3 and -13 (Liacini et al., 2002, Ahmed et al., 2003). In OA chondrocytes, iNOS expression and NO synthesis were also observed to be regulated by MAPK-activated protein kinase (MAPKAPK, Martel-Pelletier et al., 1999).

A dose-dependent increase in MMP activity was observed in the present study on treating chondrocyte/agarose constructs with concentrations of TNF α above 1ng/ml. The TNF α -induced response was then partially reversed upon co-stimulation with L-NIO (Fig. 3.3). Furthermore, an upregulation in the expression of MMP-13 and ADAMTS-5 was observed on stimulating constructs with the pro-inflammatory cytokine (Fig. 5.12 and 5.13). This resulted in a decrease in GAG synthesis and increase in GAG loss in constructs treated with the highest concentration of TNF α (100ng/ml, Fig. 3.4 and 3.5). Upon co-stimulation with the NOS inhibitor, the response was reversed, suggesting that endogenously synthesized NO and MMP activity influences proteoglycan synthesis. The present findings are in agreement with studies which showed that MMP expression and protein synthesis are regulated by TNF α , consequently leading to the disruption of cartilage (Malemud et al., 2003, He et al., 2002). The principal MMPs involved in OA pathogenesis include, MMP-1, -3, -8, -9 and -13, along with aggrecanases, which belong to the ADAMTS family. The matrix proteases are responsible for the degradation of ECM components such as proteoglycans, fibronectin, collagen and link protein, all of which contribute to both the integrity and function of articular cartilage (Malemud et al., 2003).

Additionally, the present findings are in concert with studies which demonstrated a downregulation in aggrecan content and an upregulation in proteoglycan release, upon treating porcine and bovine chondrocytes cultured in monolayer or explant models, with concentrations of TNF α ranging between 50 and 100ng/ml (Gilbert, Duance and Mason., 2002, Goodstone and Hardingham, 2002). Similar findings were reported with human RA synovial fibroblasts co-cultured with bovine cartilage explants in a 3D agarose embedded model, stimulated with TNF α . Furthermore, the decrease in ECM content observed in the 3D model was shown to be associated with an upregulation in MMPs (Pretzel et al., 2009). Rai et al, (2008) demonstrated similar findings in porcine chondrocyte monolayer cultures treated with TNF α , reporting an upregulation in the expression of MMP-3 and -13 and a decrease in aggrecan synthesis. Conclusively, from these findings, it can be seen that NO influences proteoglycan synthesis via multiple pathways, which have not yet been fully explored. Figure 7.2 illustrates the signalling pathways influenced by TNF α during OA disease progression.

Collectively, these studies demonstrate the importance of TNF α in cartilage degradation, a feature which is inevitable in OA disease progression (Malemud, 1999, Petterson et al., 2002, Islam et al., 2002, Greenwel et al., 2000).

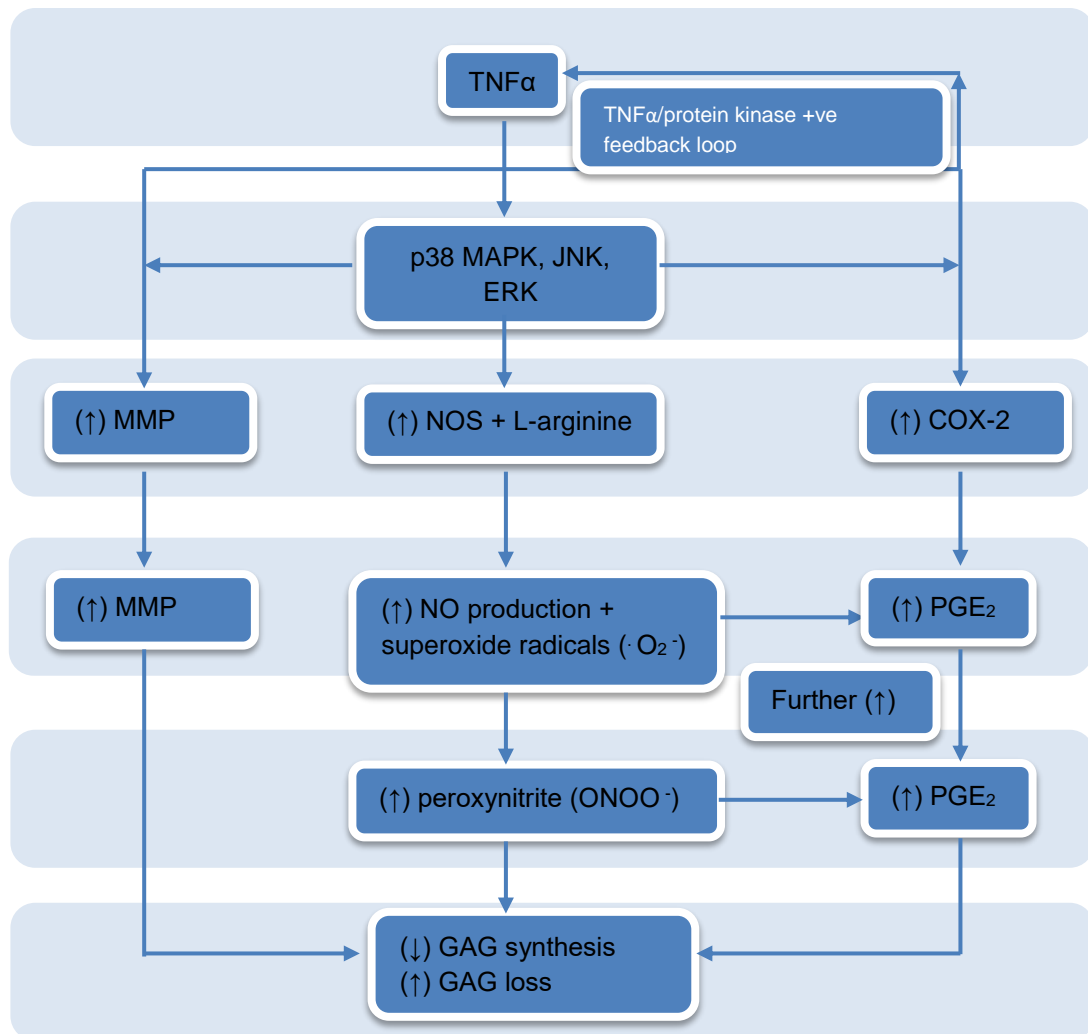


Fig. 7.2. Flow chart illustrating the signalling cascades triggered on stimulating chondrocyte/agarose constructs with TNF α .

7.5.2 The effect of dynamic compression on chondrocytes stimulated with TNF α

It has been well established that mechanical stimulation is essential for the maintenance of cartilage homeostasis. One of the objectives of the study presented, involved examining the effects of physiological mechanical loading on markers of catabolic activities and tissue remodelling in chondrocyte/agarose constructs. More specifically, the study was designed to elucidate the effects of dynamic compressive strain on nitrite, PGE₂, MMP, TNF α and GAG synthesis in the 3D agarose model system.

The present study revealed that in the absence of TNF α , dynamic compression did not significantly influence nitrite production. In unstrained constructs, the pro-inflammatory

cytokine was observed to significantly enhance nitrite production and the response was reduced with dynamic compression. Upon co-incubation with the NOS inhibitor, the response was abolished (Fig. 4.1). These findings suggest that NO is a mechanotransduction mediator, which is induced by the pro-inflammatory cytokine, TNF α , since its effects are reversed upon stimulation with dynamic compression. However, the signalling cascades through which NO is inhibited by dynamic compression in chondrocyte/agarose constructs are not fully understood.

Another intracellular molecule influenced by mechanical stimulation, in particular, fluid flow, is calcium (D'Andrea et al., 2000). Calcium is an upstream activator of mechanotransduction pathways, which is known to be regulated by calcium-sensitive stretch-activated (SA) ion channels, capable of influencing the activation of cNOS. Indeed, a decrease in shear-induced intracellular calcium was observed upon employing inhibitors of extracellular calcium and its admission into the cell via mechanosensitive ion channels. In a separate study, the effect of 20% gross compressive strain on intracellular calcium was observed in chondrocyte/agarose constructs, which demonstrated an increase in the number of cells responding to mechanical simulation. This effect was evident from the upregulation of intracellular calcium (Roberts et al., 2001). Figure 7.3 illustrates the activation of calcium ions on the application of dynamic compression.

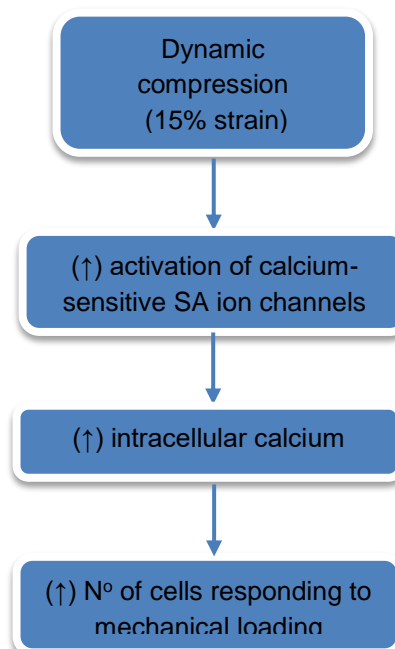


Fig. 7.3. Flow chart illustrating the activation of calcium ions upon stimulating chondrocyte/agarose constructs with dynamic compression.

Co-incubation with gadolinium, an inhibitor of SA ion channels, led to a decrease in intracellular calcium, implicating SA or voltage-gated ion channels in the admission of calcium ions into the cell (Guilak et al., 1999, Wright et al., 1997). Between 24 and 72 hours of culture, Knight et al. (1998) demonstrated a decrease in intracellular calcium in chondrocyte/agarose constructs subjected to compressive strain. This decrease in intracellular calcium correlated with a reduction in the number of chondrocytes responding to the mechanical stimuli which, in turn, was found to be associated with the development of pericellular matrix around the cells, hence reducing the extent of cell deformation. Furthermore, the observed increase in intracellular calcium may be associated with an upregulation in the expression of cNOS, thereby enhancing NO production. It is also worth noting that the response of calcium to mechanical stimulation is time delayed by approximately 3 minutes. Although the signalling cascades responsible for this delayed effect is unknown, the activation of Na⁺ and K⁺ ions may be related to it (Walev et al., 2000).

In previous studies, the effects of different types of compression regimens on chondrocyte metabolism have also been investigated. For example, both an increase in NOS expression and NO release was observed in porcine cartilage explants, following the application of either static or intermittent compression (Fermor et al., 2001). However these findings are not in agreement with those from the present study which examined the effects of dynamic compression on nitrite production. The differences observed between both studies may be as a result of the different model systems employed, which also include different chondrocyte species. Furthermore, NO production has been found to be particularly significant within the first 48 hours of culture, which may be due to the culture conditions to which the cells are subjected, as opposed to the loading modality employed (Stefanovic-Racic et al., 1997).

In the present study, dynamic compression did not significantly influence PGE₂ release in the absence of TNF α (Fig. 4.2). However, in the presence of the cytokine, a decrease in the inflammatory mediator was observed upon stimulation with either dynamic compression or the NOS inhibitor. Co-stimulation with both compression and the NOS inhibitor induced a further reduction in PGE₂ release (Fig. 4.2). These findings suggest that PGE₂ may directly be influenced by TNF α , in the absence of NO.

Bovine chondrocyte/agarose constructs subjected to dynamic compression previously demonstrated poor correlation between NO production and GAG synthesis, in the presence of the pro-inflammatory cytokine, IL-1b (Chowdhury, Bader and Lee, 2001). In contrast, the present study demonstrated enhanced GAG synthesis in TNF α -treated chondrocyte/agarose constructs in response to dynamic compression, although there were differences in the temporal compression regimens (Fig. 4.5). The effect was further enhanced upon co-incubation with the NOS inhibitor. In a separate study, cyclic tensile strain demonstrated an

inhibition in proteoglycan synthesis in IL-1 β -treated rabbit chondrocyte monolayer cultures (Gassner et al., 1999). Additionally, Taskiran et al., (1994) observed a decrease in GAG synthesis in rabbit chondrocytes treated with IL-1 β .

7.5.3 The effect of oxygen tension in chondrocytes stimulated with TNF α

The effects of 21 and 5% oxygen tension on the anabolic and catabolic activities of TNF α -treated chondrocyte/agarose constructs were examined in the present study. 5% oxygen tension was used for investigating the effects of hypoxia on chondrocyte metabolism, since it represents the approximate mean oxygen tension within human cartilage *in vivo*. Additionally, this concentration of oxygen is mostly used in studies comparing the effects of both hypoxia and normoxia in cartilage biology. It has been well-established that oxygen is required for the production of NO and PGE₂. As such, it is expected that oxygen has an influence on the production of these inflammatory mediators, when induced by TNF α -treated chondrocytes or untreated controls.

In untreated constructs, the levels of nitrite production in chondrocytes cultured at 5% oxygen tension were fairly similar to those cultured at 21% oxygen tension (Fig. 3.1). Similar results were obtained in untreated chondrocyte/agarose constructs cultured at both oxygen tensions (Fig. 3.1). The data suggest that chondrocytes were well equipped with sufficient oxygen in order to maintain basal levels of the inflammatory mediators. These findings were in concert with those from previous studies which demonstrated similar levels of NO and PGE₂ upon culturing porcine and bovine chondrocytes under hypoxic and normoxic conditions (Cernanec et al., 2002, Mathy-Hartert et al., 2005).

In the presence of TNF α , the present study revealed an increase in nitrite production, with a greater effect at 5% oxygen tension when compared to 21% (Fig. 3.1). Similar findings were apparent in PGE₂ production, when TNF α -stimulated constructs were cultured at both oxygen tensions (Fig. 3.1 and 3.2). This effect however, cannot be attributed to cell number, as this factor was not influenced by changes in oxygen tension, as evident from the constant DNA content obtained from all treatment conditions. Accordingly, the present data suggests that oxygen tension plays a key role in the progression of OA. Indeed, a correlation has been reported between the severity of RA and the partial pressure of oxygen (pO₂), such that the lower pO₂ values in the synovial fluid are associated with more serious disease conditions (Mathy-Hartert et al., 2005). Based on this hypothesis and given the fact that PGE₂ production was enhanced in response to TNF α at 5% oxygen tension, it can be concluded that the inflammatory mediator plays an essential role in synovitis pathogenesis. NO on the other hand, is known to significantly contribute to tissue degradation, with the

help of other reactive nitrogen species (Veihelmann et al., 2001). As such, it can be suggested that the inflammatory effects of hypoxia are further enhanced via increased NO production. Nevertheless, the array of signalling cascades by which hypoxia elevates NO and PGE₂ production is still not fully understood.

7.5.4 The effect of lactose on FN-fs

It has been well documented that ECM-fs induce catabolic activities during OA disease progression and hence they are involved in the regulation of cartilage tissue remodelling (Fig. 6.1). Of these matrix fragments, the 29kDa NH₂-terminal heparin binding FN-f has been proven to be the most potent, followed by Col-fs (Homandberg, 1998). Despite the fact that several types of Col-fs are produced from type II collagen during OA, the most significant types are the amino and carboxyl telopeptides (Reijman et al., 2004), which have been shown to induce increased levels of cytokines, NO release and inhibit GAG synthesis in porcine chondrocyte/agarose constructs (Chowdhury et al., 2010).

Indeed, upon binding to the pericellular matrix, FN-fs have been shown to induce a series of catabolic activities, including an increase in the production of matrix proteases, such as MMP-1,-3 and -13, together with enhanced levels of pro-inflammatory cytokine such as IL-1 and TNF α , consequently leading to cartilage breakdown and progression of tissue lesions (Mehraban et al., 1998, Xie and Homandberg, 1993, Homandberg et al., 1992). These studies suggest that FN-fs are involved upstream of the OA disease process, when compared to pro-inflammatory cytokines and, as such, are more potent in nature. Furthermore, FN-fs have been shown to induce enhanced levels of NO and PGE₂ production in human and bovine chondrocytes cultured in monolayer, explant and 3D agarose models (Pichika and Homandberg, 2004, Homandberg and Hui, 1996, Homandberg, Wen and Hui, 1998, Homandberg, Meyers and Xie, 1992, Homandberg et al., 1997). These signalling cascades have been shown to be mediated by MAPK and NF- κ B, subsequently leading to the inhibition of proteoglycan synthesis and increase in proteoglycan loss (Forsyth, Pulai and Loeser, 2002, Pulai et al., 2005). Additionally, co-stimulation of cartilage explants with a NOS inhibitor revealed a reduction in FN-f-induced catabolic activities (Homandberg and Hui, 1996). Although FN-fs have been shown to influence the multiple aforementioned signalling pathways, the specific receptor(s) to which the matrix fragment binds for the induction of these catabolic processes remains unknown. Nevertheless, numerous receptors have been suggested to bind to FN-fs, including:

- TLR4 receptor which has been shown to bind to HA and heparin sulphate,
- CD44 receptor
- $\alpha_5\beta_1$ receptor implemented in the mediation of biomechanical signals.

However, upon examining the effects of inhibiting these receptors on NO production in FN-f-treated chondrocytes in the host laboratory, it was observed that a significant inhibition in NO production was only observed upon inhibiting the SGAL receptor with α -lactose monohydrate (Fig. 1.26, 1.27). The SGAL receptor was targeted as it represents the primary receptor of elastin, which is known to be rich in the VGVAPG motif. Similarly, the sequence of consensus pattern, XGXXPG, is present in most matrix proteins, including collagen (Hinek and Rabinovitch, 1994, Hinek et al., 1988, 1991, 1993, Hinek and Wilson, 2000, Wachi et al., 2004, Mecham et al., 1989a, 1989b, 1991, Privitera et al., 1998, Blanchevoye et al., 2013). Accordingly, it was suggested that the XGXXPG sequence may also be present in FN-fs, through which the matrix fragment induces catabolic activities. Therefore, the present study investigated the dose-response effect of lactose on nitrite production and GAG synthesis in chondrocyte/agarose constructs stimulated with $1\mu\text{M}$ of the 29kDa heparin binding FN-f. It was observed that FN-fs successfully induced an increase in nitrite release and a decrease in GAG synthesis, when compared to untreated controls (Fig. 6.6). This data was in agreement with previous findings which demonstrated increased levels of NO and a decrease in GAG synthesis in human and bovine chondrocytes treated with FN-fs in 2D and 3D models (Pichika and Homandberg, 2004, Homandberg and Hui, 1996, Homandberg, Wen and Hui, 1998, Homandberg, Meyers and Xie, 1992, Homandberg et al., 1997). However, co-incubation of the chondrocyte/agarose constructs with lactose at concentrations ranging from 0.1 to 100mM did not inhibit FN-f-induced nitrite production, nor did it restore GAG synthesis (Fig. 6.6). Upon optimizing the culture conditions required for the highest concentration of lactose i.e.100mM to inhibit FN-f-induced catabolic activities, it was observed that a 72 hour equilibration period, prior to the stimulation of chondrocytes with FN-fs was unfavourable (Fig. 6.8). Equilibrating samples may have created a high affinity of FN-f-cell surface binding, compared to non-equilibrated samples in which a higher proportion of cell surfaces may have been compromised from enzymatic action, during cell isolation. Additionally, equilibrating samples may have led to the over-stimulation of the model system, evident by the higher levels of nitrite being produced when compared to non-equilibrated samples (Kelly et al., 2006, Frenkel et al., 1996, Hauselmann et al., 1994, Mauck et al., 2003). At such high levels of nitrite production, it is possible that the lactose present in the culture media was rapidly used up by chondrocytes, in an attempt to initiate self-repair processes, since lactose is a sugar. As a result, only a limited amount of lactose might have been available to bind to FN-fs present at the cell surface for the inhibition of FN-f-induced catabolic activities. Furthermore, FN-fs do not possess a rapid turnover compared with other inflammatory molecules such as TNF α . Instead, they follow a positive feedback loop (Fig. 7.4) in the induction of catabolic activities *in vivo*, hence allowing them to be more potent compared to inflammatory cytokines (Homandberg, Ding and Guo, 2007). As such, this further limited the ability of lactose to inhibit FN-f-induced catabolic activities within the 48 hour culture period, particularly in equilibrated constructs.

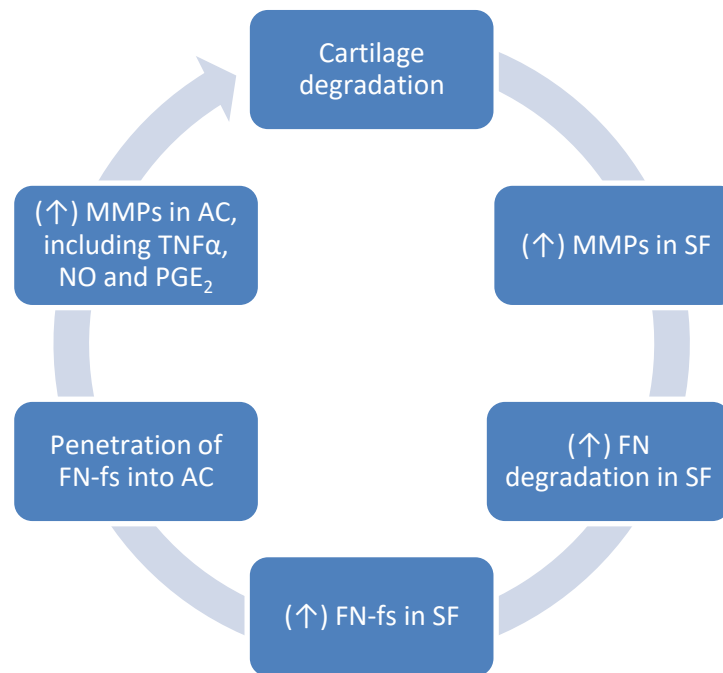


Fig. 7.4. Flow chart illustrating the positive feedback loop of catabolic events induced by FN-fs and MMPs. SF = synovial fluid and AC = articular cartilage.

Furthermore it was interesting to note from the dose-response study of FN-fs in the 3D model system that concentrations of FN-fs below $1\mu\text{M}$ did not induce an anabolic response, evident from the consistent levels in GAG production at each concentration of FN-f used (Fig. 6.12). This finding contradicted those in previous studies, which demonstrated anabolic or delayed catabolic responses upon treating cartilage explants with concentrations of FN-fs less than $1\mu\text{M}$ (Homandberg and Hui, 1994, Homandberg and Wen, 1998, Homandberg et al., 1996, 1997). Co-incubation of these constructs with lactose led to a significant inhibition of FN-f-induced catabolic activities. This is the first study to demonstrate that FN-fs induce catabolic activities in chondrocyte/agarose constructs via the EBP/SGAL signalling pathway. Studies in the host laboratory have demonstrated that biomechanical signals will influence the inflammatory response induced by matrix fragments. Indeed, intermittent dynamic compression was shown to inhibit FN-f-induced NO and PGE_2 production and restore GAG synthesis in chondrocyte/agarose constructs. The study was extended by co-stimulating constructs with the NOS inhibitor, which revealed a further inhibition in the catabolic effects induced by FN-fs (Raveenthiran and Chowdhury, 2009).

Furthermore, the signalling pathways induced by the inherent low oxygen tension within cartilage will interact with those induced by matrix fragments and biomechanical signals. As such, the present study examined the effects of lactose on FN-f-treated chondrocyte/agarose constructs cultured at 21, 5 and 2% oxygen tensions. From figure

6.11), it was observed that FN-f-induced catabolic activities were enhanced at 5% oxygen tension when compared to either 2% or 21% oxygen tensions. These findings are in concert with previous studies, which have demonstrated an increase in the catabolic activities induced by FN-fs under hypoxic conditions (Parker et al., 2013). The present study was then extended to examine the combined effects of dynamic compression and hypoxia on the anabolic and catabolic activities of chondrocyte/agarose constructs treated with lactose and the synthetic VGVAPG peptide. The synthetic VGVAPG peptide was incorporated to replace the effects of the FN-fs and to confirm that the catabolic activities induced by the FN-fs are via the EBP/SGAL signalling pathway. An increase in nitrite production was observed upon treating constructs with the VGVAPG peptide, when compared to untreated controls (Fig. 6.12), suggesting that they induce equivalent catabolic effects as FN-fs. The catabolic effects induced by the peptides were further enhanced by culturing constructs at 5% oxygen tension, when compared to 21% oxygen tension. This effect was also similar to those induced by FN-fs under hypoxic conditions. The application of dynamic compression reduced the VGVAPG peptide-induced nitrite production and restored GAG synthesis in an oxygen-independent manner (Fig. 6.12). Co-incubation with lactose led to a further decrease in nitrite production, which correlated with a further increase in GAG synthesis. The results from Figure 6.12, suggests the presence of the *XGXXPG* sequence in FN-fs, as lactose was able to successfully inhibit the VGVAPG peptide, which correlates with a recent study, which examined the inhibitory effects of lactose on the VGVAPG peptide (Blanchevoye et al., 2013). This data is also in agreement with results from Chapter 4, which showed that cytokine-induced catabolic activities were reduced on subjecting chondrocyte/agarose constructs to mechanical loading at both 21% and 5% oxygen tensions. The results from Figure 6.12 are also in correlation with those from a study in which dynamically stimulated chondrocyte/agarose constructs were treated with FN-fs in the presence and absence of L-NIO, at both 21% and 5% oxygen tension. From the study, it was observed that FN-f-induced catabolic activities were reduced by dynamic compression in an oxygen independent manner (Parker et al., 2013). Collectively, these results emphasize the oxygen-dependency of the response of chondrocytes to FN-fs and the importance of lactose and biophysical loading in the suppression of the inflammatory processes. Accordingly, further studies are required to examine the interplay of FN-fs, lactose and oxygen tension, in conjunction with dynamic compression to identify potential targets for OA therapy.

7.5.5 The effect of NT telopeptides on chondrocyte metabolism

In the present study, synthetic NT terminal telopeptides, with a sequence corresponding to that of the amino-terminal region of type II collagen, were used to induce catabolic activities in chondrocyte/agarose constructs, similar to those observed in OA *in vivo* and *in vitro* models (Jennings et al., 2001, Chowdhury et al., 2010, Lucic et al., 2003, Guo, Ding and Homandberg, 2009). On treating constructs with 3 μ M of the synthetic peptides (Laboratoire de Biotechnologie, Luxembourg, S.A), a catabolic response was not induced at 21, 5 or 2% oxygen tension (Fig. 6.4). This may be a direct result of employing lower concentration of the peptides when compared to other studies, which demonstrated the induction of maximum catabolic activities upon stimulating similar 3D porcine chondrocyte/agarose models with a synthetic peptides at a concentration of 50 μ M (Chowdhury et a., 2010). In contrast, studies which examined the dose response effect of synthetic NT terminal telopeptides in chondrocyte monolayer cultures or cartilage explants reported the induction of maximum catabolic activities, such as enhanced proteoglycan loss, only at a specific peptide concentration of 3 μ M (Guo, Ding and Homandberg, 2009). As such, the concentration of NT telopeptides used to induce catabolic activities in chondrocyte/agarose constructs was increased from 3 μ M to 50 μ M. Nevertheless, increasing the peptide concentration of the peptides did not induce any catabolic effects on culturing constructs at either 21 or 5% oxygen tension (Fig. 6.5). Possible contributing factors to this finding were considered, including the nature of the 3D model system, the properties of the synthesized peptides and any require preparation of the peptides prior to treatment. The species of chondrocytes employed in the present study were not a contributing factor, since previous studies did not encounter any differences in the effects induced by the peptides on using chondrocytes from different animal species (Jennings et al., 2001, Chowdhury et al., 2010, Guo, Ding and Homandberg, 2009). Similarly, the differences observed in the present study upon stimulating constructs with 50 μ M NT telopeptides were not a result of the model system employed. Indeed, studies which have examined the effects of NT telopeptides on chondrocyte metabolism in similar 3D porcine/agarose constructs, of the same pore size have demonstrated a significant increase in catabolic activities upon incorporating the same concentration of the peptides (Chowdhury et al., 2010).

The stability of the synthesized NT telopeptides was another possible contributing factor to the inability of the peptide to induce catabolic activities in chondrocyte/agarose constructs, since it was synthesized with glutamine (Q or Gln) as the first amino acid in the N-terminus of the peptide. Glutamine is normally prone to undergo cyclization and convert into pyroglutamine, resulting in an overall shift in mass of the telopeptide (ThermoFisher Scientific, Loughborough, UK; Laboratoire de Biotechnologie, Luxembourg S.A; LifeTein LLC, Somerset, New Jersey, US). However, keeping this limitation in mind, the lyophilised peptide was formed using analytical HPLC with <95% purity. Additionally, H and OH bonds

were added to the N- and COOH- terminals of the peptide in order to further stabilize its structure at room temperature, confirming that the stability of the NT telopeptides did not contribute to its inability to induce inflammatory effects in chondrocytes.

Attention was then focused on the method of preparation of the telopeptides to stimulate chondrocytes, since information on this was not provided in previous publications. Due to the hydrophobic nature of the lyophilized telopeptides, 2% DMSO/PBS solution was used to prepare a 1mg/ml stock solution of the peptides, followed by diluting it in DMEM +20% FCS to prepare a working concentration of 3 μ M or 50 μ M, according to manufacturer's instructions (ThermoFisher Scientific, Loughborough, UK; Laboratoire de Biotechnologie, Luxembourg S.A; LifeTein LLC, Somerset, New Jersey, US). Although this method ensured complete solubility of the peptides, while maintaining minimum cytotoxicity levels, the solution failed to stimulate chondrocytes. Upon close examination and consultation with author's of previous publications, it was then brought to attention that for chondrocytes to be stimulated by these synthetically developed telopeptides, the peptides must be subjected to dialysis, initially with PBS, followed by DMEM. This stage is of utmost importance as it ensures the removal of unwanted salts present during peptide synthesis, which prevent chondrocytes from being activated (Guo, Ding and Homandberg 2009).

7.6 Clinical Implications

OA is a progressive, degenerative joint disease, which demands effective long-term solutions to improve the quality of life of those affected individuals. Although the currently available drugs assist in controlling or reducing joint pain, they are incapable of inhibiting the progression of the disease. As such, measures involving early diagnosis, in combination with biophysical and biochemical interventions are considered to be essential in halting the progression of the disease. However, a number of factors have restricted progress on the development of therapeutic strategies for OA treatment. These include the use of a wide variety of model systems making comparisons difficult and the limited ability of simultaneously incorporating the essential factors involved in regulating OA pathophysiology *in vivo*, such as inflammatory agents, biomechanical stimuli and hypoxia. Accordingly the understanding of the mechanisms which occur during the early stages of the disease process remains incomplete. In particular, the manner in which pro-inflammatory cytokines, matrix fragments, in combination with mechanical stimuli influence chondrocyte metabolism under hypoxic conditions is complex and requires further investigation. As such, the present study examined whether low oxygen tension at 5% could influence the response of chondrocytes to TNF α /matrix fragments and dynamic compression. The findings demonstrated that exogenous TNF α enhanced the production of inflammatory mediators, including nitrite, PGE $_2$ and MMP activity, with an enhanced effect observed under hypoxic conditions. These data suggest that oxygen tension in the diseased joint will have a significant impact on the metabolic processes of chondrocytes, with a potential to trigger pathways induced by TNF α . Accordingly, future therapeutics for OA should involve the development of oxygen-sensitive antagonists, aimed at interfering with TNF α -induced pathways involving oxygen-sensitive mediators, such as NO, PGE $_2$ and NF- κ B.

The application of biomechanical signals or the presence of the NOS inhibitor reduced the effects of TNF α , in an oxygen-dependent manner, leading to the restoration of matrix synthesis. The present findings confirm that dynamic compression induces chondroprotective effects, hence providing vital insights for the development of approaches for OA treatment. This includes subjecting the joint to moderate physiological exercise which counteracts the inflammatory processes and restores anabolic activities, subsequently maintaining normal tissue remodelling and cartilage health.

7.7 Future work

- Heterogeneous mixtures of chondrocytes isolated from full depth slices of articular cartilage were incorporated in the development of the 3D chondrocyte/agarose model used throughout the present study. Consequently, the effect of oxygen tension was not observed on sub-populations of chondrocytes obtained from the different zones of articular cartilage. Since the oxygen tension in healthy articular cartilage varies from approximately 8% in the superficial zone to approximately 1% in the deep zone, *in vivo*, it would be interesting to examine the effects of oxygen tension on sub-populations of chondrocytes (Falchuk, Goetzl, Kulka, 1970, Brighton & Heppenstall, 1971). Indeed, a previous study in the host laboratory reported distinct responses for these chondrocyte sub-populations when subjected to dynamic compression (Lee et al., 1998).
- Upon examining the effects of the NOS inhibitor in chondrocyte/agarose constructs stimulated with TNF α , it was observed that L-NIO only partially inhibited PGE₂ release when compared to nitrite release, as L-NIO is an inhibitor of all the isoforms of NOS. Additionally, since NO is known to influence COX-2 and PGE₂ release in various *in vivo* and *in vitro* models of OA, incorporating the COX-2 inhibitor, NS-398, in addition to L-NIO would provide additional information related to the reparative activities.
- In the present study, MMP activity was only analysed in culture supernatants. Since MMPs are synthesized by the chondrocytes seeded within the agarose constructs, it is highly likely that MMPs will be present within chondrocyte/agarose constructs. As such, it will be of value to analyse the MMP activity in both chondrocyte/agarose constructs and the corresponding culture supernatants.
- From chapter 6, it was shown that lactose had an inhibitory effect on FN-f-induced catabolic activities, due to the presence of the XGXXPG repeating sequence in FN-fs (Fig. 6.12). In order to further confirm that this inhibition was specific to lactose alone, the study should be expanded to include a negative control, typically sucrose, a sugar made of a combination of fructose and glucose.
- In order to confirm that lactose inhibited FN-fs- or VGVAPG-induced catabolic activities, via the SGAL/EBP signalling pathway, qRT-PCR must be performed to specifically detect the expression of SGAL receptor. Additionally, this method will reveal whether the SGAL signalling pathway is influenced by mechanical loading

and/or oxygen tension in compressed chondrocytes cultured under both normoxic and hypoxic conditions.

- There is still a major requirement to clarify the temporal influence of each of the exogenous factors. Accordingly, a temporal study is required to examine the effects of hypoxia on TNF α -treated constructs subjected to dynamic compression, using a series of time points over a 48 hour culture period, typically 0.5, 1.0, 2.0, 4.0, 8.0, 24 and 48 hours.

References

Ackermann, B. and J. Steinmeyer (2005). "Collagen biosynthesis of mechanically loaded articular cartilage explants." *Osteoarthritis Cartilage* 13(10): 906-914.

Aderka, D., H. Engelmann, Y. Maor, C. Brakebusch and D. Wallach (1992). "Stabilization of the bioactivity of tumor necrosis factor by its soluble receptors." *J Exp Med* 175(2): 323-329.

Agarwal, S., J. Deschner, P. Long, A. Verma, C. Hofman, C. H. Evans and N. Piesco (2004). "Role of NF-kappaB transcription factors in antiinflammatory and proinflammatory actions of mechanical signals." *Arthritis Rheum* 50(11): 3541-3548.

Ahmadzadeh, N., M. Shingu and M. Nobunaga (1990). "The effect of recombinant tumor necrosis factor-alpha on superoxide and metalloproteinase production by synovial cells and chondrocytes." *Clin Exp Rheumatol* 8(4): 387-391.

Ahmed, S., A. Rahman, A. Hasnain, V. M. Goldberg and T. M. Haqqi (2003). "Phenyl N-tert-butyl nitro down-regulates interleukin-1 beta-stimulated matrix metalloproteinase-13 gene expression in human chondrocytes: suppression of c-Jun NH2-terminal kinase, p38-mitogen-activated protein kinase and activating protein-1." *J Pharmacol Exp Ther* 305(3): 981-988.

Aigner, T. and J. Stove (2003). "Collagens--major component of the physiological cartilage matrix, major target of cartilage degeneration, major tool in cartilage repair." *Adv Drug Deliv Rev* 55(12): 1569-1593.

Aigner, T., U. Dietz, H. Stoss and K. von der Mark (1995). "Differential expression of collagen types I, II, III, and X in human osteophytes." *Lab Invest* 73(2): 236-243.

Akanji, O. O., D. A. Lee and D. A. Bader (2008). "The effects of direct current stimulation on isolated chondrocytes seeded in 3D agarose constructs." *Biorheology* 45(3-4): 229-243.

Akanji, O. O., P. Sakthithasan, D. M. Salter and T. T. Chowdhury (2010). "Dynamic compression alters NFkappaB activation and IkappaB-alpha expression in IL-1beta-stimulated chondrocyte/agarose constructs." *Inflamm Res* 59(1): 41-52.

Alaaeddine, N., J. A. Di Battista, J. P. Pelletier, K. Kiansa, J. M. Cloutier and J. Martel-Pelletier (1999). "Differential effects of IL-8, LIF (pro-inflammatory) and IL-11 (anti-inflammatory) on TNF-alpha-induced PGE(2) release and on signalling pathways in human OA synovial fibroblasts." *Cytokine* 11(12): 1020-1030.

- Amin, A. R., M. Attur, R. N. Patel, G. D. Thakker, P. J. Marshall, J. Rediske, S. A. Stuchin, I. R. Patel and S. B. Abramson (1997). "Superinduction of cyclooxygenase-2 activity in human osteoarthritis-affected cartilage. Influence of nitric oxide." *J Clin Invest* 99(6): 1231-1237.
- Amin, A. R., P. E. Di Cesare, P. Vyas, M. Attur, E. Tzeng, T. R. Billiar, S. A. Stuchin and S. B. Abramson (1995). "The expression and regulation of nitric oxide synthase in human osteoarthritis-affected chondrocytes: evidence for up-regulated neuronal nitric oxide synthase." *J Exp Med* 182(6): 2097-2102.
- An, Y.H., K.L. Martin (2003)." *Handbook Of Histology Methods For Bone and Cartilage.*" Humana Press 45-51.
- Anderson, C. E. (1962). "The structure and function of cartilage." *J Bone Joint Surg Am* 44-A: 777-786.
- Arden, N. and M. C. Nevitt (2006). "Osteoarthritis: epidemiology." *Best Pract Res Clin Rheumatol* 20(1): 3-25.
- Asada, S., K. Fukuda, F. Nishisaka, M. Matsukawa and C. Hamanisi (2001). "Hydrogen peroxide induces apoptosis of chondrocytes; involvement of calcium ion and extracellular signal-regulated protein kinase." *Inflamm Res* 50(1): 19-23.
- Asada, S., K. Fukuda, M. Oh, C. Hamanishi and S. Tanaka (1999). "Effect of hydrogen peroxide on the metabolism of articular chondrocytes." *Inflamm Res* 48(7): 399-403.
- Ateshian, G. A., W. H. Warden, J. J. Kim, R. P. Grelsamer and V. C. Mow (1997). "Finite deformation biphasic material properties of bovine articular cartilage from confined compression experiments." *J Biomech* 30(11-12): 1157-1164.
- Attur, M. G., M. Dave, M. Akamatsu, M. Katoh and A. R. Amin (2002). "Osteoarthritis or osteoarthrosis: the definition of inflammation becomes a semantic issue in the genomic era of molecular medicine." *Osteoarthritis Cartilage* 10(1): 1-4.
- Attur, M., H. E. Al-Mussawir, J. Patel, A. Kitay, M. Dave, G. Palmer, M. H. Pillinger and S. B. Abramson (2008). "Prostaglandin E2 exerts catabolic effects in osteoarthritis cartilage: evidence for signaling via the EP4 receptor." *J Immunol* 181(7): 5082-5088.
- Aydelotte, M. B., R. R. Greenhill and K. E. Kuettner (1988). "Differences between subpopulations of cultured bovine articular chondrocytes. II. Proteoglycan metabolism." *Connect Tissue Res* 18(3): 223-234.
- Aydelotte, M.B., B.L. Schumacher, K.E. Kuettner (1992). "Heterogeneity of articular cartilage. In: *Articular cartilage and osteoarthritis.*" Raven Press, New York 237-249.

- Bader, D. L., D. M. Salter and T. T. Chowdhury (2011). "Biomechanical influence of cartilage homeostasis in health and disease." *Arthritis* 2011: 979032.
- Badger, A. M., D. E. Griswold, R. Kapadia, S. Blake, B. A. Swift, S. J. Hoffman, G. B. Stroup, E. Webb, D. J. Rieman, M. Gowen, J. C. Boehm, J. L. Adams and J. C. Lee (2000). "Disease-modifying activity of SB 242235, a selective inhibitor of p38 mitogen-activated protein kinase, in rat adjuvant-induced arthritis." *Arthritis Rheum* 43(1): 175-183.
- Badger, A. M., M. N. Cook, M. W. Lark, T. M. Newman-Tarr, B. A. Swift, A. H. Nelson, F. C. Barone and S. Kumar (1998). "SB 203580 inhibits p38 mitogen-activated protein kinase, nitric oxide production, and inducible nitric oxide synthase in bovine cartilage-derived chondrocytes." *J Immunol* 161(1): 467-473.
- Barakat, A. F., C. J. Elson and C. I. Westacott (2002). "Susceptibility to physiological concentrations of IL-1beta varies in cartilage at different anatomical locations on human osteoarthritic knee joints." *Osteoarthritis Cartilage* 10(4): 264-269.
- Beckman, J. S. and W. H. Koppenol (1996). "Nitric oxide, superoxide, and peroxynitrite: the good, the bad, and ugly." *Am J Physiol* 271(5 Pt 1): C1424-1437.
- Bergstrom, G., A. Bjelle, L. B. Sorensen, V. Sundh and A. Svanborg (1986). "Prevalence of rheumatoid arthritis, osteoarthritis, chondrocalcinosis and gouty arthritis at age 79." *J Rheumatol* 13(3): 527-534.
- Bertrand, J., C. Cromme, D. Umlauf, S. Frank and T. Pap (2010). "Molecular mechanisms of cartilage remodelling in osteoarthritis." *Int J Biochem Cell Biol* 42(10): 1594-1601.
- Bewsey, K. E., C. Wen, C. Purple and G. A. Homandberg (1996). "Fibronectin fragments induce the expression of stromelysin-1 mRNA and protein in bovine chondrocytes in monolayer culture." *Biochim Biophys Acta* 1317(1): 55-64.
- Bigg, H. F., Y. E. Shi, Y. E. Liu, B. Steffensen and C. M. Overall (1997). "Specific, high affinity binding of tissue inhibitor of metalloproteinases-4 (TIMP-4) to the COOH-terminal hemopexin-like domain of human gelatinase A. TIMP-4 binds progelatinase A and the COOH-terminal domain in a similar manner to TIMP-2." *J Biol Chem* 272(24): 15496-15500.
- Billinghurst, R.C., L. Dahlberg, M. Lonescu, A. Reiner, R. Bourne, C. Rosbeck, P. Mitchell, J. Hambor, O. Dickmann, H. Tschesche, J. Chen, H. Van Wart, A.R. Pool (1987). "Enhanced cleavage of type II collagen by collagenases in osteoarthritic articular cartilage." *J. Clin Invest* 99: 1534-1545.
- Bird, J. L., S. May and M. T. Bayliss (2000). "Nitric oxide inhibits aggrecan degradation in explant cultures of equine articular cartilage." *Equine Vet J* 32(2): 133-139.

- Blain, E. J. (2007). "Mechanical regulation of matrix metalloproteinases." *Front Biosci* 12: 507-527.
- Blain, E. J., A. Y. Ali and V. C. Duance (2010). "Boswellia frereana (frankincense) suppresses cytokine-induced matrix metalloproteinase expression and production of pro-inflammatory molecules in articular cartilage." *Phytother Res* 24(6): 905-912.
- Blanchevoye, C., N. Floquet, A. Scandolera, S. Baud, P. Maurice, O. Bocquet, S. Blaise, C. Ghoneim, B. Cantarelli, F. Delacoux, M. Dauchez, R. G. Efremov, L. Martiny, L. Duca and L. Debelle (2013). "Interaction between the elastin peptide VGVAPG and human elastin binding protein." *J Biol Chem* 288(2): 1317-1328.
- Blanco, F. J., R. L. Ochs, H. Schwarz and M. Lotz (1995). "Chondrocyte apoptosis induced by nitric oxide." *Am J Pathol* 146(1): 75-85.
- Blanco, F., I. Rego, C. Ruiz-Romero (2011). "The role of mitochondria in osteoarthritis." *Nature Reviews Rheumatology* 7(3): 161-169.
- Boileau, C., J. Martel-Pelletier, H. Fahmi, F. Mineau, M. Boily and J. P. Pelletier (2007). "The peroxisome proliferator-activated receptor gamma agonist pioglitazone reduces the development of cartilage lesions in an experimental dog model of osteoarthritis: in vivo protective effects mediated through the inhibition of key signaling and catabolic pathways." *Arthritis Rheum* 56(7): 2288-2298.
- Brew, C. J., P. D. Clegg, R. P. Boot-Handford, J. G. Andrew and T. Hardingham (2010). "Gene expression in human chondrocytes in late osteoarthritis is changed in both fibrillated and intact cartilage without evidence of generalised chondrocyte hypertrophy." *Ann Rheum Dis* 69(1): 234-240.
- Brighton, C. T. and R. B. Heppenstall (1971). "Oxygen tension in zones of the epiphyseal plate, the metaphysis and diaphysis. An in vitro and in vivo study in rats and rabbits." *J Bone Joint Surg Am* 53(4): 719-728.
- Brown, R.A., K. Jones (1992). "Fibronectin synthesis and release in normal and osteoarthritic human articular cartilage." *Eur J Exp Musculoskel Res* 1: 25-32.
- Buckwalter, J., L. Rosenberg, R. Coutts, E. Hunziker, A.H. Reddi, V. Mow (1987). "Articular Cartilage: Injury And Repair. In: Injury And Repair Of The Musculoskeletal Soft Tissue." ed By Woo S And Buckwalter JA. American Academy, Illinois 405-425.
- Buckwalter, J. A. (1995). "Osteoarthritis and articular cartilage use, disuse, and abuse: experimental studies." *J Rheumatol Suppl* 43: 13-15.
- Bunning, R. A. and R. G. Russell (1989). "The effect of tumor necrosis factor alpha and gamma-interferon on the resorption of human articular cartilage and on the production of

prostaglandin E and of caseinase activity by human articular chondrocytes." *Arthritis Rheum* 32(6): 780-784.

Burton-Wurster, N., G. Lust and J. N. Macleod (1997). "Cartilage fibronectin isoforms: in search of functions for a special population of matrix glycoproteins." *Matrix Biol* 15(7): 441-454.

Burton-Wurster, N., M. Butler, S. Harter, C. Colombo, J. Quintavalla, D. Swartzendurber, C. Arsenis and G. Lust (1986). "Presence of fibronectin in articular cartilage in two animal models of osteoarthritis." *J Rheumatol* 13(1): 175-182.

Burton-Wuster, N., G. Lust (1985). "Deposition of fibronectin in articular cartilage of canine osteoarthritic joints." *Am. J. Vet. Res* 46 2542-2545.

Buschmann, M. D., Y. A. Gluzband, A. J. Grodzinsky and E. B. Hunziker (1995). "Mechanical compression modulates matrix biosynthesis in chondrocyte/agarose culture." *J Cell Sci* 108 (Pt 4): 1497-1508.

Buschmann, M. D., Y. A. Gluzband, A. J. Grodzinsky, J. H. Kimura and E. B. Hunziker (1992). "Chondrocytes in agarose culture synthesize a mechanically functional extracellular matrix." *J Orthop Res* 10(6): 745-758.

Byers, P. D., A. Maroudase, F. Oztop, R. A. Stockwell and M. F. Venn (1977). "Histological and biochemical studies on cartilage from osteoarthrotic femoral heads with special reference to surface characteristics." *Connect Tissue Res* 5(1): 41-49.

Cameron, M. L., F. H. Fu, H. H. Paessler, M. Schneider and C. H. Evans (1994). "Synovial fluid cytokine concentrations as possible prognostic indicators in the ACL-deficient knee." *Knee Surg Sports Traumatol Arthrosc* 2(1): 38-44.

Campbell, I. K., D. S. Piccoli, M. J. Roberts, K. D. Muirden and J. A. Hamilton (1990). "Effects of tumor necrosis factor alpha and beta on resorption of human articular cartilage and production of plasminogen activator by human articular chondrocytes." *Arthritis Rheum* 33(4): 542-552.

Carames, B., M. J. Lopez-Armada, B. Cillero-Pastor, M. Lires-Dean, C. Vaamonde, F. Galdo and F. J. Blanco (2008). "Differential effects of tumor necrosis factor-alpha and interleukin-1beta on cell death in human articular chondrocytes." *Osteoarthritis Cartilage* 16(6): 715-722.

Carnemolla, B., M. Cutolo, P. Castellani, E. Balza, S. Raffanti and L. Zardi (1984). "Characterization of synovial fluid fibronectin from patients with rheumatic inflammatory diseases and healthy subjects." *Arthritis Rheum* 27(8): 913-921.

- Caron, J. P., J. C. Fernandes, J. Martel-Pelletier, G. Tardif, F. Mineau, C. Geng and J. P. Pelletier (1996). "Chondroprotective effect of intraarticular injections of interleukin-1 receptor antagonist in experimental osteoarthritis. Suppression of collagenase-1 expression." *Arthritis Rheum* 39(9): 1535-1544.
- Cernanec, J., F. Guilak, J. B. Weinberg, D. S. Pisetsky and B. Fermor (2002). "Influence of hypoxia and reoxygenation on cytokine-induced production of proinflammatory mediators in articular cartilage." *Arthritis Rheum* 46(4): 968-975.
- Chandrasekhar, S., A. K. Harvey, J. D. Higginbotham and W. E. Horton (1990). "Interleukin-1-induced suppression of type II collagen gene transcription involves DNA regulatory elements." *Exp Cell Res* 191(1): 105-114.
- Chang, J. and C. A. Poole (1996). "Sequestration of type VI collagen in the pericellular microenvironment of adult chondrocytes cultured in agarose." *Osteoarthritis Cartilage* 4(4): 275-285.
- Chevalier, X., P. Goupille, A. D. Beaulieu, F. X. Burch, W. G. Bensen, T. Conrozier, D. Loeuille, A. J. Kivitz, D. Silver and B. E. Appleton (2009). "Intraarticular injection of anakinra in osteoarthritis of the knee: a multicenter, randomized, double-blind, placebo-controlled study." *Arthritis Rheum* 61(3): 344-352.
- Chowdhury, T. T., D. L. Bader and D. A. Lee (2001). "Dynamic compression inhibits the synthesis of nitric oxide and PGE(2) by IL-1beta-stimulated chondrocytes cultured in agarose constructs." *Biochem Biophys Res Commun* 285(5): 1168-1174.
- Chowdhury, T. T., D. L. Bader, J. C. Shelton and D. A. Lee (2003). "Temporal regulation of chondrocyte metabolism in agarose constructs subjected to dynamic compression." *Arch Biochem Biophys* 417(1): 105-111.
- Chowdhury, T. T., D. M. Salter, D. L. Bader and D. A. Lee (2008). "Signal transduction pathways involving p38 MAPK, JNK, NFkappaB and AP-1 influences the response of chondrocytes cultured in agarose constructs to IL-1beta and dynamic compression." *Inflamm Res* 57(7): 306-313.
- Chowdhury, T. T., R. M. Schulz, S. S. Rai, C. B. Thuemmler, N. Wuestneck, A. Bader and G. A. Homandberg (2010). "Biomechanical modulation of collagen fragment-induced anabolic and catabolic activities in chondrocyte/agarose constructs." *Arthritis Res Ther* 12(3): R82.
- Chowdhury, T. T., S. Arghandawi, J. Brand, O. O. Akanji, D. L. Bader, D. M. Salter and D. A. Lee (2008). "Dynamic compression counteracts IL-1beta induced inducible nitric oxide synthase and cyclo-oxygenase-2 expression in chondrocyte/agarose constructs." *Arthritis Res Ther* 10(2): R35.

- Chung, C. and J. A. Burdick (2008). "Engineering cartilage tissue." *Adv Drug Deliv Rev* 60(2): 243-262.
- Claassen, H., R. Steffen, J. Hassenpflug, D. Varoga, C. J. Wruck, L. O. Brandenburg and T. Pufe (2010). "17beta-estradiol reduces expression of MMP-1, -3, and -13 in human primary articular chondrocytes from female patients cultured in a three dimensional alginate system." *Cell Tissue Res* 342(2): 283-293.
- Clancy, R. M., P. F. Gomez and S. B. Abramson (2004). "Nitric oxide sustains nuclear factor kappaB activation in cytokine-stimulated chondrocytes." *Osteoarthritis Cartilage* 12(7): 552-558.
- Clarke, I. C. (1971). "Articular cartilage: a review and scanning electron microscope study. 1. The interterritorial fibrillar architecture." *J Bone Joint Surg Br* 53(4): 732-750.
- Clements, K. M., J. S. Price, M. G. Chambers, D. M. Visco, A. R. Poole and R. M. Mason (2003). "Gene deletion of either interleukin-1beta, interleukin-1beta-converting enzyme, inducible nitric oxide synthase, or stromelysin 1 accelerates the development of knee osteoarthritis in mice after surgical transection of the medial collateral ligament and partial medial meniscectomy." *Arthritis Rheum* 48(12): 3452-3463.
- Clemmensen, I. and R. B. Andersen (1982). "Different molecular forms of fibronectin in rheumatoid synovial fluid." *Arthritis Rheum* 25(1): 25-31.
- Coimbra, I. B., S. A. Jimenez, D. F. Hawkins, S. Piera-Velazquez and D. G. Stokes (2004). "Hypoxia inducible factor-1 alpha expression in human normal and osteoarthritic chondrocytes." *Osteoarthritis Cartilage* 12(4): 336-345.
- Cramer, T., E. Schipani, R. S. Johnson, B. Swoboda and D. Pfander (2004). "Expression of VEGF isoforms by epiphyseal chondrocytes during low-oxygen tension is HIF-1 alpha dependent." *Osteoarthritis Cartilage* 12(6): 433-439.
- Creaby, M. W., Y. Wang, K. L. Bennell, R. S. Hinman, B. R. Metcalf, K. A. Bowles and F. M. Cicuttini (2010). "Dynamic knee loading is related to cartilage defects and tibial plateau bone area in medial knee osteoarthritis." *Osteoarthritis Cartilage* 18(11): 1380-1385.
- D'Andrea, P., A. Calabrese, I. Capozzi, M. Grandolfo, R. Tonon and F. Vittur (2000). "Intercellular Ca²⁺ waves in mechanically stimulated articular chondrocytes." *Biorheology* 37(1-2): 75-83.
- Das, P., D. J. Schurman and R. L. Smith (1997). "Nitric oxide and G proteins mediate the response of bovine articular chondrocytes to fluid-induced shear." *J Orthop Res* 15(1): 87-93.

Day, J. S., J. C. Van Der Linden, R. A. Bank, M. Ding, I. Hvid, D. R. Sumner and H. Weinans (2004). "Adaptation of subchondral bone in osteoarthritis." *Biorheology* 41(3-4): 359-368.

De Bari, C., F. Dell'Accio and F. P. Luyten (2004). "Failure of in vitro-differentiated mesenchymal stem cells from the synovial membrane to form ectopic stable cartilage in vivo." *Arthritis Rheum* 50(1): 142-150.

de Brum-Fernandes, A. J., S. Morisset, G. Bkaily and C. Patry (1996). "Characterization of the PGE2 receptor subtype in bovine chondrocytes in culture." *Br J Pharmacol* 118(7): 1597-1604.

De Croos, J.N., S.S. Dhaliwal, M.D. Grynepas, R.M. Pilliar, R.A. Kandel (2006). "Cyclic compressive mechanical stimulation induces sequential catabolic and anabolic gene changes in chondrocytes resulting in increased extracellular matrix accumulation." *Matrix Biol* 25(6):323-31.

Deberg, M., A. Labasse, S. Christgau, P. Cloos, D. Bang Henriksen, J. P. Chapelle, B. Zegels, J. Y. Reginster and Y. Henrotin (2005). "New serum biochemical markers (Coll 2-1 and Coll 2-1 NO2) for studying oxidative-related type II collagen network degradation in patients with osteoarthritis and rheumatoid arthritis." *Osteoarthritis Cartilage* 13(3): 258-265.

Del Carlo, M., Jr. and R. F. Loeser (2002). "Nitric oxide-mediated chondrocyte cell death requires the generation of additional reactive oxygen species." *Arthritis Rheum* 46(2): 394-403.

Denisov, L. N., V. A. Nasonova, G. G. Koreshkov and N. G. Kashevarova (2010). "[Role of obesity in the development of osteoarthrosis and concomitant diseases]." *Ter Arkh* 82(10): 34-37.

DiBattista, J. A., S. Dore, N. Morin and T. Aribat (1996). "Prostaglandin E2 up-regulates insulin-like growth factor binding protein-3 expression and synthesis in human articular chondrocytes by a c-AMP-independent pathway: role of calcium and protein kinase A and C." *J Cell Biochem* 63(3): 320-333.

Ding, L., D. Guo, G.A. Homandberg (2006). "The order of cartilage damaging activities of different fibronectin fragments correlates with Map kinase and NF- κ B activation in chondrocytes." *Transactins of the Orthopaedics Research Society Meeting* 31; # 1326.

Dingle, J. T. (1979). "Heberden oration 1978. Recent studies on the control of joint damage: the contribution of the Strangeways Research Laboratory." *Ann Rheum Dis* 38(3): 201-214.

Domm, C., M. Schunke, K. Christesen and B. Kurz (2002). "Redifferentiation of dedifferentiated bovine articular chondrocytes in alginate culture under low oxygen tension." *Osteoarthritis Cartilage* 10(1): 13-22.

- Dudhia, J., C. Wheeler-Jones, M. Bayliss (2000). "Transient activation of P42/P44MAPK by IL-1alpha is enhanced by a low oxygen tension in human articular cartilage." In: Proc 46th Annual Meeting, Orthopaedic Research Society Orlando, FL, abstract 0943.
- Echtermeyer, F., J. Bertrand, R. Dreier, I. Meinecke, K. Neugebauer, M. Fuerst, Y. J. Lee, Y. W. Song, C. Herzog, G. Theilmeyer and T. Pap (2009). "Syndecan-4 regulates ADAMTS-5 activation and cartilage breakdown in osteoarthritis." *Nat Med* 15(9): 1072-1076.
- Enobakhare, B. O., D. L. Bader and D. A. Lee (1996). "Quantification of sulfated glycosaminoglycans in chondrocyte/alginate cultures, by use of 1,9-dimethylmethylene blue." *Anal Biochem* 243(1): 189-191.
- Ettinger, W. H., Jr., R. Burns, S. P. Messier, W. Applegate, W. J. Rejeski, T. Morgan, S. Shumaker, M. J. Berry, M. O'Toole, J. Monu and T. Craven (1997). "A randomized trial comparing aerobic exercise and resistance exercise with a health education program in older adults with knee osteoarthritis. The Fitness Arthritis and Seniors Trial (FAST)." *JAMA* 277(1): 25-31.
- Evans, C. H., S. C. Ghivizzani and P. D. Robbins (1998). "Blocking cytokines with genes." *J Leukoc Biol* 64(1): 55-61.
- Eyre, D. R. (1980). "Collagen: molecular diversity in the body's protein scaffold." *Science* 207(4437): 1315-1322.
- Falchuk, K. H., E. J. Goetzl and J. P. Kulka (1970). "Respiratory gases of synovial fluids. An approach to synovial tissue circulatory-metabolic imbalance in rheumatoid arthritis." *Am J Med* 49(2): 223-231.
- Farndale, R. W., C. A. Sayers and A. J. Barrett (1982). "A direct spectrophotometric microassay for sulfated glycosaminoglycans in cartilage cultures." *Connect Tissue Res* 9(4): 247-248.
- Farquhar, T., Y. Xia, K. Mann, J. Bertram, N. Burton-Wurster, L. Jelinski and G. Lust (1996). "Swelling and fibronectin accumulation in articular cartilage explants after cyclical impact." *J Orthop Res* 14(3): 417-423.
- Farrell, A. J., D. R. Blake, R. M. Palmer and S. Moncada (1992). "Increased concentrations of nitrite in synovial fluid and serum samples suggest increased nitric oxide synthesis in rheumatic diseases." *Ann Rheum Dis* 51(11): 1219-1222.
- Fattman, C. L., L. M. Schaefer and T. D. Oury (2003). "Extracellular superoxide dismutase in biology and medicine." *Free Radic Biol Med* 35(3): 236-256.
- Felice, B. R., C. O. Chichester and H. J. Barrach (1999). "Type II collagen peptide release from rabbit articular cartilage." *Ann N Y Acad Sci* 878: 590-593.

- Felson, D. T. (2013). "Osteoarthritis as a disease of mechanics." *Osteoarthritis Cartilage* 21(1): 10-15.
- Felson, D. T., A. Naimark, J. Anderson, L. Kazis, W. Castelli and R. F. Meenan (1987). "The prevalence of knee osteoarthritis in the elderly. The Framingham Osteoarthritis Study." *Arthritis Rheum* 30(8): 914-918.
- Felson, D. T., J. Niu, C. McClennan, B. Sack, P. Aliabadi, D. J. Hunter, A. Guermazi and M. Englund (2007). "Knee buckling: prevalence, risk factors, and associated limitations in function." *Ann Intern Med* 147(8): 534-540.
- Fermor, B., J. B. Weinberg, D. S. Pisetsky and F. Guilak (2005). "The influence of oxygen tension on the induction of nitric oxide and prostaglandin E2 by mechanical stress in articular cartilage." *Osteoarthritis Cartilage* 13(10): 935-941.
- Fermor, B., J. B. Weinberg, D. S. Pisetsky, M. A. Misukonis, A. J. Banes and F. Guilak (2001). "The effects of static and intermittent compression on nitric oxide production in articular cartilage explants." *J Orthop Res* 19(4): 729-737.
- Fermor, B., S. E. Christensen, I. Youn, J. M. Cernanec, C. M. Davies and J. B. Weinberg (2007). "Oxygen, nitric oxide and articular cartilage." *Eur Cell Mater* 13: 56-65; discussion 65.
- Fernandes, J. C., J. Martel-Pelletier and J. P. Pelletier (2002). "The role of cytokines in osteoarthritis pathophysiology." *Biorheology* 39(1-2): 237-246.
- Fields, G. (2000). "Methods in Molecular Biology – Using fluorogenic peptide substrates to assay matrix metalloproteinases" Totowa: Humana Press 215-237.
- Fitzgerald, J. B., M. Jin, D. Dean, D. J. Wood, M. H. Zheng and A. J. Grodzinsky (2004). "Mechanical compression of cartilage explants induces multiple time-dependent gene expression patterns and involves intracellular calcium and cyclic AMP." *J Biol Chem* 279(19): 19502-19511.
- Fleischmann, R. M., J. Schechtman, R. Bennett, M. L. Handel, G. R. Burmester, J. Tesser, D. Modafferi, J. Poulakos and G. Sun (2003). "Anakinra, a recombinant human interleukin-1 receptor antagonist (r-metHuIL-1ra), in patients with rheumatoid arthritis: A large, international, multicenter, placebo-controlled trial." *Arthritis Rheum* 48(4): 927-934.
- Forray, M. I., S. Angelo, C. A. Boyd and R. Deves (1995). "Transport of nitric oxide synthase inhibitors through cationic amino acid carriers in human erythrocytes." *Biochem Pharmacol* 50(12): 1963-1968.
- Forsyth, C. B., J. Pulai and R. F. Loeser (2002). "Fibronectin fragments and blocking antibodies to alpha2beta1 and alpha5beta1 integrins stimulate mitogen-activated protein

kinase signaling and increase collagenase 3 (matrix metalloproteinase 13) production by human articular chondrocytes." *Arthritis Rheum* 46(9): 2368-2376.

Fox, P.F. (ed.) (1985). "Developments in Dairy Chemistry – 3/ Lactose and Minor constituents". Elsevier Applied Science Publ.

Fransen, M., S. McConnell and M. Bell (2002). "Therapeutic exercise for people with osteoarthritis of the hip or knee. A systematic review." *J Rheumatol* 29(8): 1737-1745.

Fraser, A., U. Fearon, R. C. Billingham, M. Ionescu, R. Reece, T. Barwick, P. Emery, A. R. Poole and D. J. Veale (2003). "Turnover of type II collagen and aggrecan in cartilage matrix at the onset of inflammatory arthritis in humans: relationship to mediators of systemic and local inflammation." *Arthritis Rheum* 48(11): 3085-3095.

Freeman, P. M., R. N. Natarajan, J. H. Kimura and T. P. Andriacchi (1994). "Chondrocyte cells respond mechanically to compressive loads." *J Orthop Res* 12(3): 311-320.

Freemont, A. J., V. Hampson, R. Tilman, P. Goupille, Y. Taiwo and J. A. Hoyland (1997). "Gene expression of matrix metalloproteinases 1, 3, and 9 by chondrocytes in osteoarthritic human knee articular cartilage is zone and grade specific." *Ann Rheum Dis* 56(9): 542-549.

Frenkel, S. R., R. M. Clancy, J. L. Ricci, P. E. Di Cesare, J. J. Rediske and S. B. Abramson (1996). "Effects of nitric oxide on chondrocyte migration, adhesion, and cytoskeletal assembly." *Arthritis Rheum* 39(11): 1905-1912.

Galois, L., S. Etienne, L. Grossin, A. Watrin-Pinzano, C. Cournil-Henrionnet, D. Loeuille, P. Netter, D. Mainard and P. Gillet (2004). "Dose-response relationship for exercise on severity of experimental osteoarthritis in rats: a pilot study." *Osteoarthritis Cartilage* 12(10): 779-786.

Galois, L., S. Etienne, L. Grossin, C. Cournil, A. Pinzano, P. Netter, D. Mainard and P. Gillet (2003). "Moderate-impact exercise is associated with decreased severity of experimental osteoarthritis in rats." *Rheumatology (Oxford)* 42(5): 692-693; author reply 693-694.

Garrington, T. P. and G. L. Johnson (1999). "Organization and regulation of mitogen-activated protein kinase signaling pathways." *Curr Opin Cell Biol* 11(2): 211-218.

Gassner, R., M. J. Buckley, H. Georgescu, R. Studer, M. Stefanovich-Racic, N. P. Piesco, C. H. Evans and S. Agarwal (1999). "Cyclic tensile stress exerts antiinflammatory actions on chondrocytes by inhibiting inducible nitric oxide synthase." *J Immunol* 163(4): 2187-2192.

Ge, X. P., Y. H. Gan, C. G. Zhang, C. Y. Zhou, K. T. Ma, J. H. Meng and X. C. Ma (2011). "Requirement of the NF-kappaB pathway for induction of Wnt-5A by interleukin-1beta in condylar chondrocytes of the temporomandibular joint: functional crosstalk between the Wnt-5A and NF-kappaB signaling pathways." *Osteoarthritis Cartilage* 19(1): 111-117.

Gearing, A. J., P. Beckett, M. Christodoulou, M. Churchill, J. Clements, A. H. Davidson, A. H. Drummond, W. A. Galloway, R. Gilbert, J. L. Gordon and et al. (1994). "Processing of tumour necrosis factor-alpha precursor by metalloproteinases." *Nature* 370(6490): 555-557.

Geng, Y., F. J. Blanco, M. Cornelisson and M. Lotz (1995). "Regulation of cyclooxygenase-2 expression in normal human articular chondrocytes." *J Immunol* 155(2): 796-801.

Geng, Y., J. Valbracht and M. Lotz (1996). "Selective activation of the mitogen-activated protein kinase subgroups c-Jun NH2 terminal kinase and p38 by IL-1 and TNF in human articular chondrocytes." *J Clin Invest* 98(10): 2425-2430.

Geng, Y., R. Maier and M. Lotz (1995). "Tyrosine kinases are involved with the expression of inducible nitric oxide synthase in human articular chondrocytes." *J Cell Physiol* 163(3): 545-554.

Gilbert, S. J., V. C. Duance and D. J. Mason (2002). "Tumour necrosis factor alpha up-regulates protein kinase R (PKR)-activating protein (PACT) and increases phosphorylation of PKR and eukaryotic initiation factor 2-alpha in articular chondrocytes." *Biochem Soc Trans* 30(Pt 6): 886-889.

Gircz, O., J. L. Lauer and G. B. Fields (2011). "Comparison of metalloproteinase protein and activity profiling." *Anal Biochem* 409(1): 37-45.

Glasson, S. S., R. Askew, B. Sheppard, B. Carito, T. Blanchet, H. L. Ma, C. R. Flannery, D. Peluso, K. Kanki, Z. Yang, M. K. Majumdar and E. A. Morris (2005). "Deletion of active ADAMTS5 prevents cartilage degradation in a murine model of osteoarthritis." *Nature* 434(7033): 644-648.

Goldenberger, D.L., M.S. Egan, A.S. Cohen (1982). "Inflammatory synovitis in degenerative joint disease." *Journal of Rheumatology* 9: 204-209.

Goldring, M. B. (2000). "Osteoarthritis and cartilage: the role of cytokines." *Curr Rheumatol Rep* 2(6): 459-465.

Goldring, M. B. (2000). "The role of the chondrocyte in osteoarthritis." *Arthritis Rheum* 43(9): 1916-1926.

Goldring, M. B. and F. Berenbaum (2004). "The regulation of chondrocyte function by proinflammatory mediators: prostaglandins and nitric oxide." *Clin Orthop Relat Res*(427 Suppl): S37-46.

Goldring, M. B. and S. R. Goldring (2007). "Osteoarthritis." *J Cell Physiol* 213(3): 626-634.

Goldring, S. R. and M. B. Goldring (2004). "The role of cytokines in cartilage matrix degeneration in osteoarthritis." *Clin Orthop Relat Res*(427 Suppl): S27-36.

Golds, E. E. and A. R. Poole (1984). "Connective tissue antigens stimulate collagenase production in arthritic diseases." *Cell Immunol* 86(1): 190-205.

Goodstone, N. J. and T. E. Hardingham (2002). "Tumour necrosis factor alpha stimulates nitric oxide production more potently than interleukin-1beta in porcine articular chondrocytes." *Rheumatology (Oxford)* 41(8): 883-891.

Grabowski, P. S., P. K. Wright, R. J. Van 't Hof, M. H. Helfrich, H. Ohshima and S. H. Ralston (1997). "Immunolocalization of inducible nitric oxide synthase in synovium and cartilage in rheumatoid arthritis and osteoarthritis." *Br J Rheumatol* 36(6): 651-655.

Greenwel, P., S. Tanaka, D. Penkov, W. Zhang, M. Olive, J. Moll, C. Vinson, M. Di Liberto and F. Ramirez (2000). "Tumor necrosis factor alpha inhibits type I collagen synthesis through repressive CCAAT/enhancer-binding proteins." *Mol Cell Biol* 20(3): 912-918.

Griffiths, A. M., K. E. Herbert, D. Perrett and D. L. Scott (1989). "Fragmented fibronectin and other synovial fluid proteins in chronic arthritis: their relation to immune complexes." *Clin Chim Acta* 184(2): 133-146.

Grimshaw, M. J. and R. M. Mason (2000). "Bovine articular chondrocyte function in vitro depends upon oxygen tension." *Osteoarthritis Cartilage* 8(5): 386-392.

Grimshaw, M.J. , R.M. Mason (1991). "Bovine articular chondrocyte function in vitro depends upon oxygen tension. *Osteoarthritis Cartilage* 2000." 8:386e92.Stockwell.

Gross, S. S., E. A. Jaffe, R. Levi and R. G. Kilbourn (1991). "Cytokine-activated endothelial cells express an isotype of nitric oxide synthase which is tetrahydrobiopterin-dependent, calmodulin-independent and inhibited by arginine analogs with a rank-order of potency characteristic of activated macrophages." *Biochem Biophys Res Commun* 178(3): 823-829.

Gu, W. Y., W. M. Lai and V. C. Mow (1998). "A mixture theory for charged-hydrated soft tissues containing multi-electrolytes: passive transport and swelling behaviors." *J Biomech Eng* 120(2): 169-180.

Guccione, A.A. (1997). "Osteoarthritis, comorbidity, and physical disability." Baltimore, MD: The Johns Hopkins University Press 84-98.

Guerne, P. A., D. A. Carson and M. Lotz (1990). "IL-6 production by human articular chondrocytes. Modulation of its synthesis by cytokines, growth factors, and hormones in vitro." *J Immunol* 144(2): 499-505.

Guilak, F. (2011). "Biomechanical factors in osteoarthritis." *Best Pract Res Clin Rheumatol* 25(6): 815-823.

- Guilak, F., B. C. Meyer, A. Ratcliffe and V. C. Mow (1994). "The effects of matrix compression on proteoglycan metabolism in articular cartilage explants." *Osteoarthritis Cartilage* 2(2): 91-101.
- Guilak, F., B. Fermor, F. J. Keefe, V. B. Kraus, S. A. Olson, D. S. Pisetsky, L. A. Setton and J. B. Weinberg (2004). "The role of biomechanics and inflammation in cartilage injury and repair." *Clin Orthop Relat Res*(423): 17-26.
- Guilak, F., R. A. Zell, G. R. Erickson, D. A. Grande, C. T. Rubin, K. J. McLeod and H. J. Donahue (1999). "Mechanically induced calcium waves in articular chondrocytes are inhibited by gadolinium and amiloride." *J Orthop Res* 17(3): 421-429.
- Guo, D., L. Ding and G. A. Homandberg (2009). "Telopeptides of type II collagen upregulate proteinases and damage cartilage but are less effective than highly active fibronectin fragments." *Inflamm Res* 58(3): 161-169.
- Hardin, J. A., N. Cobelli and L. Santambrogio (2015). "Consequences of metabolic and oxidative modifications of cartilage tissue." *Nat Rev Rheumatol* 11(9): 521-529.
- Hashimoto, K., K. Fukuda, K. Yamazaki, N. Yamamoto, T. Matsushita, S. Hayakawa, H. Munakata and C. Hamanishi (2006). "Hypoxia-induced hyaluronan synthesis by articular chondrocytes: the role of nitric oxide." *Inflamm Res* 55(2): 72-77.
- Hauselmann, H. J., L. Oppliger, B. A. Michel, M. Stefanovic-Racic and C. H. Evans (1994). "Nitric oxide and proteoglycan biosynthesis by human articular chondrocytes in alginate culture." *FEBS Lett* 352(3): 361-364.
- Hauselmann, H. J., M. Stefanovic-Racic, B. A. Michel and C. H. Evans (1998). "Differences in nitric oxide production by superficial and deep human articular chondrocytes: implications for proteoglycan turnover in inflammatory joint diseases." *J Immunol* 160(3): 1444-1448.
- He, W., J. P. Pelletier, J. Martel-Pelletier, S. Laufer and J. A. Di Battista (2002). "Synthesis of interleukin 1beta, tumor necrosis factor-alpha, and interstitial collagenase (MMP-1) is eicosanoid dependent in human osteoarthritis synovial membrane explants: interactions with antiinflammatory cytokines." *J Rheumatol* 29(3): 546-553.
- Hedborn, E., H.J. Hauselmann (2002). "Molecular aspects of pathogenesis in osteoarthritis: the role of inflammation." *Cell Mol Life Sci* 59: 45-53.
- Helminen, H. J., M. M. Hyttinen, M. J. Lammi, J. P. Arokoski, T. Lapvetelainen, J. Jurvelin, I. Kiviranta and M. I. Tammi (2000). "Regular joint loading in youth assists in the establishment and strengthening of the collagen network of articular cartilage and contributes to the prevention of osteoarthrosis later in life: a hypothesis." *J Bone Miner Metab* 18(5): 245-257.

Henrotin, Y. E., P. Bruckner and J. P. Pujol (2003). "The role of reactive oxygen species in homeostasis and degradation of cartilage." *Osteoarthritis Cartilage* 11(10): 747-755.

Henrotin, Y., B. Kurz and T. Aigner (2005). "Oxygen and reactive oxygen species in cartilage degradation: friends or foes?" *Osteoarthritis Cartilage* 13(8): 643-654.

Hermansson, M., Y. Sawaji, M. Bolton, S. Alexander, A. Wallace, S. Begum, R. Wait and J. Saklatvala (2004). "Proteomic analysis of articular cartilage shows increased type II collagen synthesis in osteoarthritis and expression of inhibin betaA (activin A), a regulatory molecule for chondrocytes." *J Biol Chem* 279(42): 43514-43521.

Hernborg, J. and B. E. Nilsson (1973). "The relationship between osteophytes in the knee joint, osteoarthritis and aging." *Acta Orthop Scand* 44(1): 69-74.

Hess, D. T., A. Matsumoto, S. O. Kim, H. E. Marshall and J. S. Stamler (2005). "Protein S-nitrosylation: purview and parameters." *Nat Rev Mol Cell Biol* 6(2): 150-166.

Heywood, H. K., D. L. Bader and D. A. Lee (2006a). "Glucose concentration and medium volume influence cell viability and glycosaminoglycan synthesis in chondrocyte-seeded alginate constructs." *Tissue Eng* 12(12): 3487-3496.

Heywood, H. K., D. L. Bader and D. A. Lee (2006b). "Rate of oxygen consumption by isolated articular chondrocytes is sensitive to medium glucose concentration." *J Cell Physiol* 206(2): 402-410.

Heywood, H. K., P. K. Sembi, D. A. Lee and D. L. Bader (2004). "Cellular utilization determines viability and matrix distribution profiles in chondrocyte-seeded alginate constructs." *Tissue Eng* 10(9-10): 1467-1479.

Hinek, A. and M. Rabinovitch (1994). "67-kD elastin-binding protein is a protective "companion" of extracellular insoluble elastin and intracellular tropoelastin." *J Cell Biol* 126(2): 563-574.

Hinek, A. and S. E. Wilson (2000). "Impaired elastogenesis in Hurler disease: dermatan sulfate accumulation linked to deficiency in elastin-binding protein and elastic fiber assembly." *Am J Pathol* 156(3): 925-938.

Hinek, A., D. S. Wrenn, R. P. Mecham and S. H. Barondes (1988). "The elastin receptor: a galactoside-binding protein." *Science* 239(4847): 1539-1541.

Hinek, A., M. Rabinovitch, F. Keeley, Y. Okamura-Oho and J. Callahan (1993). "The 67-kD elastin/laminin-binding protein is related to an enzymatically inactive, alternatively spliced form of beta-galactosidase." *J Clin Invest* 91(3): 1198-1205.

- Hinek, A., R. P. Mecham, F. Keeley and M. Rabinovitch (1991). "Impaired elastin fiber assembly related to reduced 67-kD elastin-binding protein in fetal lamb ductus arteriosus and in cultured aortic smooth muscle cells treated with chondroitin sulfate." *J Clin Invest* 88(6): 2083-2094.
- Hino, K., S. Shiozawa, Y. Kuroki, H. Ishikawa, K. Shiozawa, K. Sekiguchi, H. Hirano, E. Sakashita, K. Miyashita and K. Chihara (1995). "EDA-containing fibronectin is synthesized from rheumatoid synovial fibroblast-like cells." *Arthritis Rheum* 38(5): 678-683.
- Holt, I., R. G. Cooper, J. Denton, A. Meager and S. J. Hopkins (1992). "Cytokine inter-relationships and their association with disease activity in arthritis." *Br J Rheumatol* 31(11): 725-733.
- Homandberg, G. A. and C. Wen (1998). "Exposure of cartilage to a fibronectin fragment amplifies catabolic processes while also enhancing anabolic processes to limit damage." *J Orthop Res* 16(2): 237-246.
- Homandberg, G. A. and F. Hui (1994). "Arg-Gly-Asp-Ser peptide analogs suppress cartilage chondrolytic activities of integrin-binding and nonbinding fibronectin fragments." *Arch Biochem Biophys* 310(1): 40-48.
- Homandberg, G. A. and F. Hui (1994). "High concentrations of fibronectin fragments cause short-term catabolic effects in cartilage tissue while lower concentrations cause continuous anabolic effects." *Arch Biochem Biophys* 311(2): 213-218.
- Homandberg, G. A. and F. Hui (1996). "Association of proteoglycan degradation with catabolic cytokine and stromelysin release from cartilage cultured with fibronectin fragments." *Arch Biochem Biophys* 334(2): 325-331.
- Homandberg, G. A., C. Wen and F. Hui (1998). "Cartilage damaging activities of fibronectin fragments derived from cartilage and synovial fluid." *Osteoarthritis Cartilage* 6(4): 231-244.
- Homandberg, G. A., D. Guo, L. M. Ray and L. Ding (2006). "Mixtures of glucosamine and chondroitin sulfate reverse fibronectin fragment mediated damage to cartilage more effectively than either agent alone." *Osteoarthritis Cartilage* 14(8): 793-806.
- Homandberg, G. A., F. Hui and C. Wen (1996). "Fibronectin fragment mediated cartilage chondrolysis. I. Suppression by anti-oxidants." *Biochim Biophys Acta* 1317(2): 134-142.
- Homandberg, G. A., F. Hui, C. Wen, C. Purple, K. Bewsey, H. Koepp, K. Huch and A. Harris (1997). "Fibronectin-fragment-induced cartilage chondrolysis is associated with release of catabolic cytokines." *Biochem J* 321 (Pt 3): 751-757.

Homandberg, G. A., G. Davis, C. Maniglia and A. Shrikhande (1997). "Cartilage chondrolysis by fibronectin fragments causes cleavage of aggrecan at the same site as found in osteoarthritic cartilage." *Osteoarthritis Cartilage* 5(6): 450-453.

Homandberg, G. A., R. Meyers and D. L. Xie (1992). "Fibronectin fragments cause chondrolysis of bovine articular cartilage slices in culture." *J Biol Chem* 267(6): 3597-3604.

Homandberg, G. A., R. Meyers and J. M. Williams (1993). "Intraarticular injection of fibronectin fragments causes severe depletion of cartilage proteoglycans in vivo." *J Rheumatol* 20(8): 1378-1382.

Homandberg, G. A., V. Costa and C. Wen (2002). "Fibronectin fragments active in chondrocytic chondrolysis can be chemically cross-linked to the alpha5 integrin receptor subunit." *Osteoarthritis Cartilage* 10(12): 938-949.

Homandberg, G. A., Y. Kang, J. Zhang, A. A. Cole and J. M. Williams (2001). "A single injection of fibronectin fragments into rabbit knee joints enhances catabolism in the articular cartilage followed by reparative responses but also induces systemic effects in the non-injected knee joints." *Osteoarthritis Cartilage* 9(8): 673-683.

Homandberg, G.A., L.B. Ding and D.B. Guo (2007). "Extracellular Matrix Fragments as Regulators of Cartilage Metabolism in Health and Disease." *CRR* 3(3), 183-196.

Huang, W., W. Q. Li, F. Dehnade and M. Zafarullah (2002). "Tissue inhibitor of metalloproteinases-4 (TIMP-4) gene expression is increased in human osteoarthritic femoral head cartilage." *J Cell Biochem* 85(2): 295-303.

Hughes, C., B. Faurholm, F. Dell'Accio, A. Manzo, M. Seed, N. Eltawil, A. Marrelli, D. Gould, C. Subang, A. Al-Kashi, C. De Bari, P. Winyard, Y. Chernajovsky and A. Nissim (2010). "Human single-chain variable fragment that specifically targets arthritic cartilage." *Arthritis Rheum* 62(4): 1007-1016.

Hulth, A., L. Lindberg and H. Telhag (1972). "Mitosis in human osteoarthritic cartilage." *Clin Orthop Relat Res* 84: 197-199.

Im, H. J., C. Pacione, S. Chubinskaya, A. J. Van Wijnen, Y. Sun and R. F. Loeser (2003). "Inhibitory effects of insulin-like growth factor-1 and osteogenic protein-1 on fibronectin fragment- and interleukin-1beta-stimulated matrix metalloproteinase-13 expression in human chondrocytes." *J Biol Chem* 278(28): 25386-25394.

Im, H. J., P. Muddasani, V. Natarajan, T. M. Schmid, J. A. Block, F. Davis, A. J. van Wijnen and R. F. Loeser (2007). "Basic fibroblast growth factor stimulates matrix metalloproteinase-13 via the molecular cross-talk between the mitogen-activated protein kinases and protein

kinase Cdelta pathways in human adult articular chondrocytes." *J Biol Chem* 282(15): 11110-11121.

Irie, K., E. Uchiyama and H. Iwaso (2003). "Intraarticular inflammatory cytokines in acute anterior cruciate ligament injured knee." *Knee* 10(1): 93-96.

Islam, N., T. M. Haqqi, K. J. Jepsen, M. Kraay, J. F. Welter, V. M. Goldberg and C. J. Malesud (2002). "Hydrostatic pressure induces apoptosis in human chondrocytes from osteoarthritic cartilage through up-regulation of tumor necrosis factor-alpha, inducible nitric oxide synthase, p53, c-myc, and bax-alpha, and suppression of bcl-2." *J Cell Biochem* 87(3): 266-278.

Iwamoto, G. K., M. M. Monick, B. D. Clark, P. E. Auron, M. F. Stinski and G. W. Hunninghake (1990). "Modulation of interleukin 1 beta gene expression by the immediate early genes of human cytomegalovirus." *J Clin Invest* 85(6): 1853-1857.

James, M. J., L. G. Cleland, A. M. Rofe and A. L. Leslie (1990). "Intraarticular pressure and the relationship between synovial perfusion and metabolic demand." *J Rheumatol* 17(4): 521-527.

Jansen, M. J., E. J. Hendriks, R. A. Oostendorp, J. Dekker and R. A. De Bie (2010). "Quality indicators indicate good adherence to the clinical practice guideline on "Osteoarthritis of the hip and knee" and few prognostic factors influence outcome indicators: a prospective cohort study." *Eur J Phys Rehabil Med* 46(3): 337-345.

Jansen, M. J., W. Viechtbauer, A. F. Lenssen, E. J. Hendriks and R. A. de Bie (2011). "Strength training alone, exercise therapy alone, and exercise therapy with passive manual mobilisation each reduce pain and disability in people with knee osteoarthritis: a systematic review." *J Physiother* 57(1): 11-20.

Jarvinen, T. A., T. Moilanen, T. L. Jarvinen and E. Moilanen (1995). "Nitric oxide mediates interleukin-1 induced inhibition of glycosaminoglycan synthesis in rat articular cartilage." *Mediators Inflamm* 4(2): 107-111.

Jennings, L., L. Wu, K. B. King, H. Hammerle, G. Cs-Szabo and J. Mollenhauer (2001). "The effects of collagen fragments on the extracellular matrix metabolism of bovine and human chondrocytes." *Connect Tissue Res* 42(1): 71-86.

Jiang, Y., H. K. Genant, I. Watt, M. Cobby, B. Bresnihan, R. Aitchison and D. McCabe (2000). "A multicenter, double-blind, dose-ranging, randomized, placebo-controlled study of recombinant human interleukin-1 receptor antagonist in patients with rheumatoid arthritis: radiologic progression and correlation of Genant and Larsen scores." *Arthritis Rheum* 43(5): 1001-1009.

- Jordan, K. M., N. K. Arden, M. Doherty, B. Bannwarth, J. W. Bijlsma, P. Dieppe, K. Gunther, H. Hauselmann, G. Herrero-Beaumont, P. Kaklamanis, S. Lohmander, B. Leeb, M. Lequesne, B. Mazieres, E. Martin-Mola, K. Pavelka, A. Pendleton, L. Punzi, U. Serni, B. Swoboda, G. Verbruggen, I. Zimmerman-Gorska, M. Dougados and E. Standing Committee for International Clinical Studies Including Therapeutic Trials (2003). "EULAR Recommendations 2003: an evidence based approach to the management of knee osteoarthritis: Report of a Task Force of the Standing Committee for International Clinical Studies Including Therapeutic Trials (ESCISIT)." *Ann Rheum Dis* 62(12): 1145-1155.
- Julkunen, P., J. Iivarinen, P. A. Brama, J. Arokoski, J. S. Jurvelin and H. J. Helminen (2010). "Maturation of collagen fibril network structure in tibial and femoral cartilage of rabbits." *Osteoarthritis Cartilage* 18(3): 406-415.
- Jung, M., S. Christgau, M. Lukoschek, D. Henriksen, W. Richter (2004). "Increased urinary concentration of collagen type II C-telopeptide fragments in patients with osteoarthritis." *Pathobiology* 71 70-76.
- Kamiya, S., T. Kawaguchi, S. Hasebe, N. Kamiya, Y. Saito, S. Miura, S. Wada, H. Yajima, T. Katayama and F. Fukai (2004). "A fibronectin fragment induces tumor necrosis factor production of rat basophilic leukemia cells." *Biochim Biophys Acta* 1675(1-3): 87-94.
- Kammermann, J. R., S. A. Kincaid, P. F. Rumph, D. K. Baird and D. M. Visco (1996). "Tumor necrosis factor-alpha (TNF-alpha) in canine osteoarthritis: Immunolocalization of TNF-alpha, stromelysin and TNF receptors in canine osteoarthritic cartilage." *Osteoarthritis Cartilage* 4(1): 23-34.
- Kang, Y., W. Eger, H. Koepp, J. M. Williams, K. E. Kuettner and G. A. Homandberg (1999). "Hyaluronan suppresses fibronectin fragment-mediated damage to human cartilage explant cultures by enhancing proteoglycan synthesis." *J Orthop Res* 17(6): 858-869.
- Kapoor, M., J. Martel-Pelletier, D. Lajeunesse, J. P. Pelletier and H. Fahmi (2011). "Role of proinflammatory cytokines in the pathophysiology of osteoarthritis." *Nat Rev Rheumatol* 7(1): 33-42.
- Karan, A., M. A. Karan, P. Vural, N. Erten, C. Tascioglu, C. Aksoy, M. Canbaz and A. Oncel (2003). "Synovial fluid nitric oxide levels in patients with knee osteoarthritis." *Clin Rheumatol* 22(6): 397-399.
- Kelly, T. A., K. W. Ng, C. C. Wang, G. A. Ateshian and C. T. Hung (2006). "Spatial and temporal development of chondrocyte-seeded agarose constructs in free-swelling and dynamically loaded cultures." *J Biomech* 39(8): 1489-1497.
- Kiani, C., L. Chen, Y. J. Wu, A. J. Yee and B. B. Yang (2002). "Structure and function of aggrecan." *Cell Res* 12(1): 19-32.

- Kim, E., F. Guilak and M. A. Haider (2008). "The dynamic mechanical environment of the chondrocyte: a biphasic finite element model of cell-matrix interactions under cyclic compressive loading." *J Biomech Eng* 130(6): 061009.
- Kim, Y. J., A. J. Grodzinsky and A. H. Plaas (1996). "Compression of cartilage results in differential effects on biosynthetic pathways for aggrecan, link protein, and hyaluronan." *Arch Biochem Biophys* 328(2): 331-340.
- Kim, Y. J., R. L. Sah, J. Y. Doong and A. J. Grodzinsky (1988). "Fluorometric assay of DNA in cartilage explants using Hoechst 33258." *Anal Biochem* 174(1): 168-176.
- Kiviranta, I., M. Tammi, J. Jurvelin, A. M. Saamanen and H. J. Helminen (1988). "Moderate running exercise augments glycosaminoglycans and thickness of articular cartilage in the knee joint of young beagle dogs." *J Orthop Res* 6(2): 188-195.
- Knight, M. M., D. A. Lee and D. L. Bader (1998). "The influence of elaborated pericellular matrix on the deformation of isolated articular chondrocytes cultured in agarose." *Biochim Biophys Acta* 1405(1-3): 67-77.
- Knight, M. M., S. A. Ghorri, D. A. Lee and D. L. Bader (1998). "Measurement of the deformation of isolated chondrocytes in agarose subjected to cyclic compression." *Med Eng Phys* 20(9): 684-688.
- Knight, M. M., T. Toyoda, D. A. Lee and D. L. Bader (2006). "Mechanical compression and hydrostatic pressure induce reversible changes in actin cytoskeletal organisation in chondrocytes in agarose." *J Biomech* 39(8): 1547-1551.
- Knudson, C. B. and W. Knudson (2001). "Cartilage proteoglycans." *Semin Cell Dev Biol* 12(2): 69-78.
- Kobayashi, M., G. R. Squires, A. Mousa, M. Tanzer, D. J. Zukor, J. Antoniou, U. Feige and A. R. Poole (2005). "Role of interleukin-1 and tumor necrosis factor alpha in matrix degradation of human osteoarthritic cartilage." *Arthritis Rheum* 52(1): 128-135.
- Koepp, H. E., K. T. Sampath, K. E. Kuettner and G. A. Homandberg (1999). "Osteogenic protein-1 (OP-1) blocks cartilage damage caused by fibronectin fragments and promotes repair by enhancing proteoglycan synthesis." *Inflamm Res* 48(4): 199-204.
- Kumar, S., J. Boehm, J.C. Lee (2003). p38 MAP kinases: key signalling molecules as therapeutic targets for inflammatory diseases. *Nat Rev Drug Discov* 2:717-726.
- Kuroki, K., A. M. Stoker and J. L. Cook (2005). "Effects of proinflammatory cytokines on canine articular chondrocytes in a three-dimensional culture." *Am J Vet Res* 66(7): 1187-1196.

- Kurz, B., A. Lemke, M. Kehn, C. Domm, P. Patwari, E. H. Frank, A. J. Grodzinsky and M. Schunke (2004). "Influence of tissue maturation and antioxidants on the apoptotic response of articular cartilage after injurious compression." *Arthritis Rheum* 50(1): 123-130.
- Kwon, N. S., C. F. Nathan, C. Gilker, O. W. Griffith, D. E. Matthews and D. J. Stuehr (1990). "L-citrulline production from L-arginine by macrophage nitric oxide synthase. The ureido oxygen derives from dioxygen." *J Biol Chem* 265(23): 13442-13445.
- Lai, W. M., J. S. Hou and V. C. Mow (1991). "A triphasic theory for the swelling and deformation behaviors of articular cartilage." *J Biomech Eng* 113(3): 245-258.
- Landínez-Parra, N., D. Garzón-Alvarado, J. Vanegas-Acosta (2012). "Mechanical Behavior of Articular Cartilage." In: N. Landínez-Parra, ed., *Injury and Skeletal Biomechanics*, InTech 1: 197-216.
- Lane Smith, R., M. C. Trindade, T. Ikenoue, M. Mohtai, P. Das, D. R. Carter, S. B. Goodman and D. J. Schurman (2000). "Effects of shear stress on articular chondrocyte metabolism." *Biorheology* 37(1-2): 95-107.
- Lane, J. M., C. T. Brighton and B. J. Menkowitz (1977). "Anaerobic and aerobic metabolism in articular cartilage." *J Rheumatol* 4(4): 334-342.
- Lark, M. W., E. K. Bayne, J. Flanagan, C. F. Harper, L. A. Hoerrner, N. I. Hutchinson, Singer, II, S. A. Donatelli, J. R. Weidner, H. R. Williams, R. A. Mumford and L. S. Lohmander (1997). "Aggrecan degradation in human cartilage. Evidence for both matrix metalloproteinase and aggrecanase activity in normal, osteoarthritic, and rheumatoid joints." *J Clin Invest* 100(1): 93-106.
- Lawrence, J. S., J. M. Bremner and F. Bier (1966). "Osteo-arthritis. Prevalence in the population and relationship between symptoms and x-ray changes." *Ann Rheum Dis* 25(1): 1-24.
- Lawyer, T. J., M. A. Tucci and H. A. Benghuzzi (2012). "Evaluation of chondrocyte growth and function subjected to 21% and 6% oxygen levels." *Biomed Sci Instrum* 48: 246-253.
- Lee, D. A. and D. L. Bader (1995). "The development and characterization of an in vitro system to study strain-induced cell deformation in isolated chondrocytes." *In Vitro Cell Dev Biol Anim* 31(11): 828-835.
- Lee, D. A. and D. L. Bader (1997). "Compressive strains at physiological frequencies influence the metabolism of chondrocytes seeded in agarose." *J Orthop Res* 15(2): 181-188.
- Lee, D. A. and M. M. Knight (2004). "Mechanical loading of chondrocytes embedded in 3D constructs: in vitro methods for assessment of morphological and metabolic response to compressive strain." *Methods Mol Med* 100: 307-324.

Lee, D. A., G. Bentley and C. W. Archer (1993). "The control of cell division in articular chondrocytes." *Osteoarthritis Cartilage* 1(2): 137-146.

Lee, D. A., J. Brand, D. Salter, O. O. Akanji and T. T. Chowdhury (2011). "Quantification of mRNA using real-time PCR and Western blot analysis of MAPK events in chondrocyte/agarose constructs." *Methods Mol Biol* 695: 77-97.

Lee, D. A., S. P. Frean, P. Lees and D. L. Bader (1998). "Dynamic mechanical compression influences nitric oxide production by articular chondrocytes seeded in agarose." *Biochem Biophys Res Commun* 251(2): 580-585.

Lee, R. B. and J. P. Urban (1997). "Evidence for a negative Pasteur effect in articular cartilage." *Biochem J* 321 (Pt 1): 95-102.

Lefebvre, V., C. Peeters-Joris and G. Vaes (1990). "Modulation by interleukin 1 and tumor necrosis factor alpha of production of collagenase, tissue inhibitor of metalloproteinases and collagen types in differentiated and dedifferentiated articular chondrocytes." *Biochim Biophys Acta* 1052(3): 366-378.

LeGrand, A., B. Fermor, C. Fink, D. S. Pisetsky, J. B. Weinberg, T. P. Vail and F. Guilak (2001). "Interleukin-1, tumor necrosis factor alpha, and interleukin-17 synergistically up-regulate nitric oxide and prostaglandin E2 production in explants of human osteoarthritic knee menisci." *Arthritis Rheum* 44(9): 2078-2083.

Liacini, A., J. Sylvester, W. Q. Li and M. Zafarullah (2002). "Inhibition of interleukin-1-stimulated MAP kinases, activating protein-1 (AP-1) and nuclear factor kappa B (NF-kappa B) transcription factors down-regulates matrix metalloproteinase gene expression in articular chondrocytes." *Matrix Biol* 21(3): 251-262.

Lim, H. and H. P. Kim (2011). "Matrix metalloproteinase-13 expression in IL-1beta-treated chondrocytes by activation of the p38 MAPK/c-Fos/AP-1 and JAK/STAT pathways." *Arch Pharm Res* 34(1): 109-117.

Lin, P. M., C. T. Chen and P. A. Torzilli (2004). "Increased stromelysin-1 (MMP-3), proteoglycan degradation (3B3- and 7D4) and collagen damage in cyclically load-injured articular cartilage." *Osteoarthritis Cartilage* 12(6): 485-496.

Lindhorst, E., L. Wachsmuth, N. Kimmig, R. Raiss, T. Aigner, L. Atley and D. Eyre (2005). "Increase in degraded collagen type II in synovial fluid early in the rabbit meniscectomy model of osteoarthritis." *Osteoarthritis Cartilage* 13(2): 139-145.

Linn, F. C. and L. Sokoloff (1965). "Movement and Composition of Interstitial Fluid of Cartilage." *Arthritis Rheum* 8: 481-494.

- Lipshitz, H., R. Etheredge, 3rd and M. J. Glimcher (1976). "Changes in the hexosamine content and swelling ratio of articular cartilage as functions of depth from the surface." *J Bone Joint Surg Am* 58(8): 1149-1153.
- Little, C. B., C. E. Hughes, C. L. Curtis, M. J. Janusz, R. Bohne, S. Wang-Weigand, Y. O. Taiwo, P. G. Mitchell, I. G. Otterness, C. R. Flannery and B. Caterson (2002). "Matrix metalloproteinases are involved in C-terminal and interglobular domain processing of cartilage aggrecan in late stage cartilage degradation." *Matrix Biol* 21(3): 271-288.
- Little, C. B., C. R. Flannery, C. E. Hughes, J. S. Mort, P. J. Roughley, C. Dent and B. Caterson (1999). "Aggrecanase versus matrix metalloproteinases in the catabolism of the interglobular domain of aggrecan in vitro." *Biochem J* 344 Pt 1: 61-68.
- Liu-Bryan, R. and R. Terkeltaub (2010). "Chondrocyte innate immune myeloid differentiation factor 88-dependent signaling drives pro-catabolic effects of the endogenous Toll-like receptor 2/Toll-like receptor 4 ligands low molecular weight hyaluronan and high mobility group box chromosomal protein 1 in mice." *Arthritis Rheum* 62(7): 2004-2012.
- Loeser, R. F. (2000). "Chondrocyte integrin expression and function." *Biorheology* 37(1-2): 109-116.
- Loeser, R. F. (2006). "Molecular mechanisms of cartilage destruction: mechanics, inflammatory mediators, and aging collide." *Arthritis Rheum* 54(5): 1357-1360.
- Lohmander, L. S., L. A. Hoerrner and M. W. Lark (1993). "Metalloproteinases, tissue inhibitor, and proteoglycan fragments in knee synovial fluid in human osteoarthritis." *Arthritis Rheum* 36(2): 181-189.
- Lohmander, L. S., L. M. Atley, T. A. Pietka and D. R. Eyre (2003). "The release of crosslinked peptides from type II collagen into human synovial fluid is increased soon after joint injury and in osteoarthritis." *Arthritis Rheum* 48(11): 3130-3139.
- Lorenz, H., W. Wenz, M. Ivancic, E. Steck and W. Richter (2005). "Early and stable upregulation of collagen type II, collagen type I and YKL40 expression levels in cartilage during early experimental osteoarthritis occurs independent of joint location and histological grading." *Arthritis Res Ther* 7(1): R156-165.
- Lorenzo, P., M. T. Bayliss and D. Heinegard (2004). "Altered patterns and synthesis of extracellular matrix macromolecules in early osteoarthritis." *Matrix Biol* 23(6): 381-391.
- Lotz, M. (2001). "Cytokines in cartilage injury and repair." *Clin Orthop Relat Res*(391 Suppl): S108-115.
- Lotz, M., S. Hashimoto and K. Kuhn (1999). "Mechanisms of chondrocyte apoptosis." *Osteoarthritis Cartilage* 7(4): 389-391.

- Lucic, D., J. Mollenhauer, K. E. Kilpatrick and A. A. Cole (2003). "N-telopeptide of type II collagen interacts with annexin V on human chondrocytes." *Connect Tissue Res* 44(5): 225-239.
- Maier, R., G. Bilbe, J. Rediske and M. Lotz (1994). "Inducible nitric oxide synthase from human articular chondrocytes: cDNA cloning and analysis of mRNA expression." *Biochim Biophys Acta* 1208(1): 145-150.
- Malemud, C. J. and V. M. Goldberg (1999). "Future directions for research and treatment of osteoarthritis." *Front Biosci* 4: D762-771.
- Malemud, C. J., N. Islam and T. M. Haqqi (2003). "Pathophysiological mechanisms in osteoarthritis lead to novel therapeutic strategies." *Cells Tissues Organs* 174(1-2): 34-48.
- Mandy, M.Y., Ho, K.W. Ng, R.L. Mauck, G.A. Ateshian, T. Clark (2003). "Hung: Gelling Temperature And Gel Concentration Effects On Tissue Development In Chondrocytes-Seeded Agarose Hydrogel." *Bioengineering* 355.
- Maneiro, E., M. J. Lopez-Armada, J. L. Fernandez-Sueiro, B. Lema, F. Galdo and F. J. Blanco (2001). "Aceclofenac increases the synthesis of interleukin 1 receptor antagonist and decreases the production of nitric oxide in human articular chondrocytes." *J Rheumatol* 28(12): 2692-2699.
- Manfield, L., D. Jang and G. A. Murrell (1996). "Nitric oxide enhances cyclooxygenase activity in articular cartilage." *Inflamm Res* 45(5): 254-258.
- Mankin, H. J. and L. Lippiello (1971). "The glycosaminoglycans of normal and arthritic cartilage." *J Clin Invest* 50(8): 1712-1719.
- Manninen, P., H. Riihimaki, M. Heliovaara and O. Suomalainen (2001). "Physical exercise and risk of severe knee osteoarthritis requiring arthroplasty." *Rheumatology (Oxford)* 40(4): 432-437.
- Marcu, K. B., M. Otero, E. Olivotto, R. M. Borzi and M. B. Goldring (2010). "NF-kappaB signaling: multiple angles to target OA." *Curr Drug Targets* 11(5): 599-613.
- Maroudas, A. (1979). "Physicochemical Properties Of Articular Cartilage." In M.A.R. Freeman (Ed.). Tunbridge Wells, England: Pitman Medical, *Adult Articular Cartilage* 2: 215-290.
- Maroudas, A. I. (1976). "Balance between swelling pressure and collagen tension in normal and degenerate cartilage." *Nature* 260(5554): 808-809.

- Maroudas, A., E. Wachtel, G. Grushko, E. P. Katz and P. Weinberg (1991). "The effect of osmotic and mechanical pressures on water partitioning in articular cartilage." *Biochim Biophys Acta* 1073(2): 285-294.
- Martel-Pelletier, J. and J. P. Pelletier (2010). "Is osteoarthritis a disease involving only cartilage or other articular tissues?" *Eklek Hastalik Cerrahisi* 21(1): 2-14.
- Martel-Pelletier, J., N. Alaaeddine and J. P. Pelletier (1999). "Cytokines and their role in the pathophysiology of osteoarthritis." *Front Biosci* 4: D694-703.
- Martel-Pelletier, J., R. McCollum, N. Fujimoto, K. Obata, J. M. Cloutier and J. P. Pelletier (1994). "Excess of metalloproteases over tissue inhibitor of metalloprotease may contribute to cartilage degradation in osteoarthritis and rheumatoid arthritis." *Lab Invest* 70(6): 807-815.
- Martin, G., R. Andriamanalijaona, S. Grassel, R. Dreier, M. Mathy-Hartert, P. Bogdanowicz, K. Boumediene, Y. Henrotin, P. Bruckner and J. P. Pujol (2004). "Effect of hypoxia and reoxygenation on gene expression and response to interleukin-1 in cultured articular chondrocytes." *Arthritis Rheum* 50(11): 3549-3560.
- Martina, M., J. W. Mozrzymas and F. Vittur (1997). "Membrane stretch activates a potassium channel in pig articular chondrocytes." *Biochim Biophys Acta* 1329(2): 205-210.
- Marzinzig, M., A. K. Nussler, J. Stadler, E. Marzinzig, W. Barthlen, N. C. Nussler, H. G. Beger, S. M. Morris, Jr. and U. B. Bruckner (1997). "Improved methods to measure end products of nitric oxide in biological fluids: nitrite, nitrate, and S-nitrosothiols." *Nitric Oxide* 1(2): 177-189.
- Mathy-Hartert, M., G. Martin, P. Devel, G. Deby-Dupont, J. P. Pujol, J. Y. Reginster and Y. Henrotin (2003). "Reactive oxygen species downregulate the expression of pro-inflammatory genes by human chondrocytes." *Inflamm Res* 52(3): 111-118.
- Mathy-Hartert, M., S. Burton, G. Deby-Dupont, P. Devel, J. Y. Reginster and Y. Henrotin (2005). "Influence of oxygen tension on nitric oxide and prostaglandin E2 synthesis by bovine chondrocytes." *Osteoarthritis Cartilage* 13(1): 74-79.
- Mauck, R. L., C. C. Wang, E. S. Oswald, G. A. Ateshian and C. T. Hung (2003). "The role of cell seeding density and nutrient supply for articular cartilage tissue engineering with deformational loading." *Osteoarthritis Cartilage* 11(12): 879-890.
- May, S. A., R. E. Hooke and P. Lees (1992). "Equine chondrocyte activation by a variety of stimuli." *Br Vet J* 148(5): 389-397.
- McTiernan, C. F., M. A. Mathier, X. Zhu, X. Xiao, E. Klein, C. H. Swan, H. Mehdi, G. Gibson, A. M. Trichel, J. C. Glorioso, A. M. Feldman, K. R. McCurry and B. London (2007).

"Myocarditis following adeno-associated viral gene expression of human soluble TNF receptor (TNFRII-Fc) in baboon hearts." *Gene Ther* 14(23): 1613-1622.

Mecham, R. P., A. Hinek, G. L. Griffin, R. M. Senior and L. A. Liotta (1989). "The elastin receptor shows structural and functional similarities to the 67-kDa tumor cell laminin receptor." *J Biol Chem* 264(28): 16652-16657.

Mecham, R. P., A. Hinek, R. Entwistle, D. S. Wrenn, G. L. Griffin and R. M. Senior (1989). "Elastin binds to a multifunctional 67-kilodalton peripheral membrane protein." *Biochemistry* 28(9): 3716-3722.

Mecham, R. P., L. Whitehouse, M. Hay, A. Hinek and M. P. Sheetz (1991). "Ligand affinity of the 67-kD elastin/laminin binding protein is modulated by the protein's lectin domain: visualization of elastin/laminin-receptor complexes with gold-tagged ligands." *J Cell Biol* 113(1): 187-194.

Mehraban, F., M. W. Lark, F. N. Ahmed, F. Xu and R. W. Moskowitz (1998). "Increased secretion and activity of matrix metalloproteinase-3 in synovial tissues and chondrocytes from experimental osteoarthritis." *Osteoarthritis Cartilage* 6(4): 286-294.

Melchiorri, C., R. Meliconi, L. Frizziero, T. Silvestri, L. Pulsatelli, I. Mazzetti, R. M. Borzi, M. Ugucioni and A. Facchini (1998). "Enhanced and coordinated in vivo expression of inflammatory cytokines and nitric oxide synthase by chondrocytes from patients with osteoarthritis." *Arthritis Rheum* 41(12): 2165-2174.

Melillo, G., L. S. Taylor, A. Brooks, G. W. Cox and L. Varesio (1996). "Regulation of inducible nitric oxide synthase expression in IFN-gamma-treated murine macrophages cultured under hypoxic conditions." *J Immunol* 157(6): 2638-2644.

Messier, S. P. (2010). "Diet and exercise for obese adults with knee osteoarthritis." *Clin Geriatr Med* 26(3): 461-477.

Miller, D. R., H. J. Mankin, H. Shoji and R. D. D'Ambrosia (1984). "Identification of fibronectin in preparations of osteoarthritic human cartilage." *Connect Tissue Res* 12(3-4): 267-275.

Millward-Sadler, S. J. and D. M. Salter (2004). "Integrin-dependent signal cascades in chondrocyte mechanotransduction." *Ann Biomed Eng* 32(3): 435-446.

Minor, M. A. (1999). "Exercise in the treatment of osteoarthritis." *Rheum Dis Clin North Am* 25(2): 397-415, viii.

Mirzayan, R. (2006). "Cartilage Injury in the athlete." Forward by Lars Peterson. Thieme.

- Miwa, M., R. Saura, S. Hirata, Y. Hayashi, K. Mizuno and H. Itoh (2000). "Induction of apoptosis in bovine articular chondrocyte by prostaglandin E(2) through cAMP-dependent pathway." *Osteoarthritis Cartilage* 8(1): 17-24.
- Mohan, M. J., T. Seaton, J. Mitchell, A. Howe, K. Blackburn, W. Burkhart, M. Moyer, I. Patel, G. M. Waitt, J. D. Becherer, M. L. Moss and M. E. Milla (2002). "The tumor necrosis factor-alpha converting enzyme (TACE): a unique metalloproteinase with highly defined substrate selectivity." *Biochemistry* 41(30): 9462-9469.
- Moos, V., S. Fickert, B. Muller, U. Weber and J. Sieper (1999). "Immunohistological analysis of cytokine expression in human osteoarthritic and healthy cartilage." *J Rheumatol* 26(4): 870-879.
- Morales, T. I. and A. B. Roberts (1992). "The interaction between retinoic acid and the transforming growth factors-beta in calf articular cartilage organ cultures." *Arch Biochem Biophys* 293(1): 79-84.
- Mosesson, M.W., G.A. Homandberg, D.L. Amrani (1984). "Human platelet fibrinogen gamma chain structure." *Blood* 63:990-995.
- Moskowitz, R.W. (1992). "Osteoarthritis-symptoms and signs." In: *Osteoarthritis, Diagnosis and Medical / Surgical Management*, ed by Moskowitz RW, Howell DS, Goldberg VM, Mankin HJ, Saunders Company, Philadelphia 2: 255-261.
- Mov V.C., A. Ratcliffe, A.R. Poole (1992). "Cartilage and Diarthrodial Joints as Paradigms for Hierarchical Materials and Structures." *Biomaterials* 13:67-97.
- Mow, V. C., C. C. Wang and C. T. Hung (1999). "The extracellular matrix, interstitial fluid and ions as a mechanical signal transducer in articular cartilage." *Osteoarthritis Cartilage* 7(1): 41-58.
- Muddasani, P., J. C. Norman, M. Ellman, A. J. van Wijnen and H. J. Im (2007). "Basic fibroblast growth factor activates the MAPK and NFkappaB pathways that converge on Elk-1 to control production of matrix metalloproteinase-13 by human adult articular chondrocytes." *J Biol Chem* 282(43): 31409-31421.
- Muir, H. (1995). "The chondrocyte, architect of cartilage. Biomechanics, structure, function and molecular biology of cartilage matrix macromolecules." *Bioessays* 17(12): 1039-1048.
- Murakami, M., Y. Nakatani, H. Kuwata and I. Kudo (2000). "Cellular components that functionally interact with signaling phospholipase A(2)s." *Biochim Biophys Acta* 1488(1-2): 159-166.
- Murrell, G. A., D. Jang and R. J. Williams (1995). "Nitric oxide activates metalloprotease enzymes in articular cartilage." *Biochem Biophys Res Commun* 206(1): 15-21.

Nalesso, G., J. Sherwood, J. Bertrand, T. Pap, M. Ramachandran, C. De Bari, C. Pitzalis and F. Dell'Accio (2011). "WNT-3A modulates articular chondrocyte phenotype by activating both canonical and noncanonical pathways." *J Cell Biol* 193(3): 551-564.

Nevo, Z., A. Beit-Or and Y. Eilam (1988). "Slowing down aging of cultured embryonal chick chondrocytes by maintenance under lowered oxygen tension." *Mech Ageing Dev* 45(2): 157-165.

Niederberger, E. and G. Geisslinger (2008). "The IKK-NF-kappaB pathway: a source for novel molecular drug targets in pain therapy?" *FASEB J* 22(10): 3432-3442.

Notoya, K., D. V. Jovanovic, P. Reboul, J. Martel-Pelletier, F. Mineau and J. P. Pelletier (2000). "The induction of cell death in human osteoarthritis chondrocytes by nitric oxide is related to the production of prostaglandin E2 via the induction of cyclooxygenase-2." *J Immunol* 165(6): 3402-3410.

Oeckinghaus, A. and S. Ghosh (2009). "The NF-kappaB family of transcription factors and its regulation." *Cold Spring Harb Perspect Biol* 1(4): a000034.

Oh, M., K. Fukuda, S. Asada, Y. Yasuda and S. Tanaka (1998). "Concurrent generation of nitric oxide and superoxide inhibits proteoglycan synthesis in bovine articular chondrocytes: involvement of peroxynitrite." *J Rheumatol* 25(11): 2169-2174.

Otte, P. (1991). "Basic cell metabolism of articular cartilage. Manometric studies." *Z Rheumatol* 50(5): 304-312.

Otterness, I. G., J. D. Eskra, M. L. Bliven, A. K. Shay, J. P. Pelletier and A. J. Milici (1998). "Exercise protects against articular cartilage degeneration in the hamster." *Arthritis Rheum* 41(11): 2068-2076.

Palmer, R. M., M. S. Hickery, I. G. Charles, S. Moncada and M. T. Bayliss (1993). "Induction of nitric oxide synthase in human chondrocytes." *Biochem Biophys Res Commun* 193(1): 398-405.

Palmer, R. M., T. Andrews, N. A. Foxwell and S. Moncada (1992). "Glucocorticoids do not affect the induction of a novel calcium-dependent nitric oxide synthase in rabbit chondrocytes." *Biochem Biophys Res Commun* 188(1): 209-215.

Parker, E., S. Vessillier, B. Pingguan-Murphy, W. Abas, D. L. Bader and T. T. Chowdhury (2013). "Low oxygen tension increased fibronectin fragment induced catabolic activities--response prevented with biomechanical signals." *Arthritis Res Ther* 15(5): R163.

Pelletier JP, Lascau-Coman V, Jovanovic D, Fernandes JC, Manning P, Connor JR, Currie MG, Martel-Pelletier J. Selective inhibition of inducible nitric oxide synthase in experimental

osteoarthritis is associated with reduction in tissue levels of catabolic factors. *J Rheumatol*. 1999;26:2002–14.

Pelletier, J. P. and J. Martel-Pelletier (1989). "Evidence for the involvement of interleukin 1 in human osteoarthritic cartilage degradation: protective effect of NSAID." *J Rheumatol Suppl* 18: 19-27.

Pelletier, J. P., F. Mineau, P. Ranger, G. Tardif and J. Martel-Pelletier (1996). "The increased synthesis of inducible nitric oxide inhibits IL-1ra synthesis by human articular chondrocytes: possible role in osteoarthritic cartilage degradation." *Osteoarthritis Cartilage* 4(1): 77-84.

Pelletier, J. P., J. A. DiBattista, P. Roughley, R. McCollum and J. Martel-Pelletier (1993). "Cytokines and inflammation in cartilage degradation." *Rheum Dis Clin North Am* 19(3): 545-568.

Pelletier, J. P., J. C. Fernandes, D. V. Jovanovic, P. Reboul and J. Martel-Pelletier (2001). "Chondrocyte death in experimental osteoarthritis is mediated by MEK 1/2 and p38 pathways: role of cyclooxygenase-2 and inducible nitric oxide synthase." *J Rheumatol* 28(11): 2509-2519.

Pelletier, J. P., J. Martel-Pelletier and S. B. Abramson (2001). "Osteoarthritis, an inflammatory disease: potential implication for the selection of new therapeutic targets." *Arthritis Rheum* 44(6): 1237-1247.

Pelletier, J. P., J. Martel-Pelletier, R. D. Altman, L. Ghandur-Mnaymneh, D. S. Howell and J. F. Woessner, Jr. (1983). "Collagenolytic activity and collagen matrix breakdown of the articular cartilage in the Pond-Nuki dog model of osteoarthritis." *Arthritis Rheum* 26(7): 866-874.

Pelletier, J., D. Jovanovic, J. C. Fernandes, P. Manning, J. R. Connor, M. G. Currie and J. Martel-Pelletier (1999). "Reduction in the structural changes of experimental osteoarthritis by a nitric oxide inhibitor." *Osteoarthritis Cartilage* 7(4): 416-418.

Perkins, D. J., E. W. St Clair, M. A. Misukonis and J. B. Weinberg (1998). "Reduction of NOS2 overexpression in rheumatoid arthritis patients treated with anti-tumor necrosis factor alpha monoclonal antibody (cA2)." *Arthritis Rheum* 41(12): 2205-2210.

Perrot, S., S. Poiraudou, M. Kabir-Ahmadi and F. Rannou (2009). "Correlates of pain intensity in men and women with hip and knee osteoarthritis. Results of a national survey: The French ARTHRIX study." *Clin J Pain* 25(9): 767-772.

Petersen, S. V., T. D. Oury, L. Ostergaard, Z. Valnickova, J. Wegrzyn, I. B. Thogersen, C. Jacobsen, R. P. Bowler, C. L. Fattman, J. D. Crapo and J. J. Enghild (2004). "Extracellular

superoxide dismutase (EC-SOD) binds to type I collagen and protects against oxidative fragmentation." *J Biol Chem* 279(14): 13705-13710.

Pettersen, I., E. Figenschau, W. Olsen (2002). "Tumor necrosis factor-related apoptosis-inducing ligand induces apoptosis in human articular chondrocytes." *Biochem Biophys Res Commun* 296: 671-6.

Pfaffl, M. W., G. W. Horgan and L. Dempfle (2002). "Relative expression software tool (REST) for group-wise comparison and statistical analysis of relative expression results in real-time PCR." *Nucleic Acids Res* 30(9): e36.

Pfander, D., T. Cramer, E. Schipani and R. S. Johnson (2003). "HIF-1 α controls extracellular matrix synthesis by epiphyseal chondrocytes." *J Cell Sci* 116(Pt 9): 1819-1826.

Pichika, R. and G. A. Homandberg (2004). "Fibronectin fragments elevate nitric oxide (NO) and inducible NO synthetase (iNOS) levels in bovine cartilage and iNOS inhibitors block fibronectin fragment mediated damage and promote repair." *Inflamm Res* 53(8): 405-412.

Pingguan-Murphy, B., M. El-Azzeh, D. L. Bader and M. M. Knight (2006). "Cyclic compression of chondrocytes modulates a purinergic calcium signalling pathway in a strain rate- and frequency-dependent manner." *J Cell Physiol* 209(2): 389-397.

Piscocya, J. L., B. Fermor, V. B. Kraus, T. V. Stabler and F. Guilak (2005). "The influence of mechanical compression on the induction of osteoarthritis-related biomarkers in articular cartilage explants." *Osteoarthritis Cartilage* 13(12): 1092-1099.

Pratta, M. A., P. A. Scherle, G. Yang, R. Q. Liu and R. C. Newton (2003). "Induction of aggrecanase 1 (ADAM-TS4) by interleukin-1 occurs through activation of constitutively produced protein." *Arthritis Rheum* 48(1): 119-133.

Pretzel, D., D. Pohlers, S. Weinert and R. W. Kinne (2009). "In vitro model for the analysis of synovial fibroblast-mediated degradation of intact cartilage." *Arthritis Res Ther* 11(1): R25.

Pritzker, K. P., S. Gay, S. A. Jimenez, K. Ostergaard, J. P. Pelletier, P. A. Revell, D. Salter and W. B. van den Berg (2006). "Osteoarthritis cartilage histopathology: grading and staging." *Osteoarthritis Cartilage* 14(1): 13-29.

Privitera, S., C. A. Prody, J. W. Callahan and A. Hinek (1998). "The 67-kDa enzymatically inactive alternatively spliced variant of beta-galactosidase is identical to the elastin/laminin-binding protein." *J Biol Chem* 273(11): 6319-6326.

Pufe, T., A. Lemke, B. Kurz, W. Petersen, B. Tillmann, A. J. Grodzinsky and R. Mentlein (2004). "Mechanical overload induces VEGF in cartilage discs via hypoxia-inducible factor." *Am J Pathol* 164(1): 185-192.

- Pulai, J. I., H. Chen, H. J. Im, S. Kumar, C. Hanning, P. S. Hegde and R. F. Loeser (2005). "NF-kappa B mediates the stimulation of cytokine and chemokine expression by human articular chondrocytes in response to fibronectin fragments." *J Immunol* 174(9): 5781-5788.
- Quinn, T. M., V. Morel and J. J. Meister (2001). "Static compression of articular cartilage can reduce solute diffusivity and partitioning: implications for the chondrocyte biological response." *J Biomech* 34(11): 1463-1469.
- Rai, M. F., P. S. Rachakonda, K. Manning, B. Vorwerk, L. Brunberg, B. Kohn and M. F. Schmidt (2008). "Quantification of cytokines and inflammatory mediators in a three-dimensional model of inflammatory arthritis." *Cytokine* 42(1): 8-17.
- Rao, J. and W. R. Otto (1992). "Fluorimetric DNA assay for cell growth estimation." *Anal Biochem* 207(1): 186-192.
- Raveenthiran, S. P. and T. T. Chowdhury (2009). "Dynamic compression inhibits fibronectin fragment induced iNOS and COX-2 expression in chondrocyte/agarose constructs." *Biomech Model Mechanobiol* 8(4): 273-283.
- Rediske, J. J., C. F. Koehne, B. Zhang and M. Lotz (1994). "The inducible production of nitric oxide by articular cell types." *Osteoarthritis Cartilage* 2(3): 199-206.
- Regan, E., J. Flannelly, R. Bowler, K. Tran, M. Nicks, B. D. Carbone, D. Glueck, H. Heijnen, R. Mason and J. Crapo (2005). "Extracellular superoxide dismutase and oxidant damage in osteoarthritis." *Arthritis Rheum* 52(11): 3479-3491.
- Reginato, A. M., C. Sanz-Rodriguez, A. Diaz, R. M. Dharmavaram and S. A. Jimenez (1993). "Transcriptional modulation of cartilage-specific collagen gene expression by interferon gamma and tumour necrosis factor alpha in cultured human chondrocytes." *Biochem J* 294 (Pt 3): 761-769.
- Reijman, M., J. M. Hazes, S. M. Bierma-Zeinstra, B. W. Koes, S. Christgau, C. Christiansen, A. G. Uitterlinden and H. A. Pols (2004). "A new marker for osteoarthritis: cross-sectional and longitudinal approach." *Arthritis Rheum* 50(8): 2471-2478.
- Relic, B., M. Bentires-Alj, C. Ribbens, N. Franchimont, P. A. Guerne, V. Benoit, M. P. Merville, V. Bours and M. G. Malaise (2002). "TNF-alpha protects human primary articular chondrocytes from nitric oxide-induced apoptosis via nuclear factor-kappaB." *Lab Invest* 82(12): 1661-1672.
- Rencic, A., A. L. Gehris, S. D. Lewis, E. L. Hume and V. D. Bennett (1995). "Splicing patterns of fibronectin mRNA from normal and osteoarthritic human articular cartilage." *Osteoarthritis Cartilage* 3(3): 187-196.

Rhee, D. K., J. Marcelino, M. Baker, Y. Gong, P. Smits, V. Lefebvre, G. D. Jay, M. Stewart, H. Wang, M. L. Warman and J. D. Carpten (2005). "The secreted glycoprotein lubricin protects cartilage surfaces and inhibits synovial cell overgrowth." *J Clin Invest* 115(3): 622-631.

Rice, A. and M. J. Banda (1995). "Neutrophil elastase processing of gelatinase A is mediated by extracellular matrix." *Biochemistry* 34(28): 9249-9256.

Ridley, S. H., S. J. Sarsfield, J. C. Lee, H. F. Bigg, T. E. Cawston, D. J. Taylor, D. L. DeWitt and J. Saklatvala (1997). "Actions of IL-1 are selectively controlled by p38 mitogen-activated protein kinase: regulation of prostaglandin H synthase-2, metalloproteinases, and IL-6 at different levels." *J Immunol* 158(7): 3165-3173.

Roach, H. I., N. Yamada, K. S. Cheung, S. Tilley, N. M. Clarke, R. O. Oreffo, S. Kokubun and F. Bronner (2005). "Association between the abnormal expression of matrix-degrading enzymes by human osteoarthritic chondrocytes and demethylation of specific CpG sites in the promoter regions." *Arthritis Rheum* 52(10): 3110-3124.

Roberts, S. R., M. M. Knight, D. A. Lee and D. L. Bader (2001). "Mechanical compression influences intracellular Ca²⁺ signaling in chondrocytes seeded in agarose constructs." *J Appl Physiol* (1985) 90(4): 1385-1391.

Roddy, E., W. Zhang and M. Doherty (2005). "Aerobic walking or strengthening exercise for osteoarthritis of the knee? A systematic review." *Ann Rheum Dis* 64(4): 544-548.

Roos, E. M. and L. Dahlberg (2005). "Positive effects of moderate exercise on glycosaminoglycan content in knee cartilage: a four-month, randomized, controlled trial in patients at risk of osteoarthritis." *Arthritis Rheum* 52(11): 3507-3514.

Rutgers, M., M. J. van Pelt, W. J. Dhert, L. B. Creemers and D. B. Saris (2010). "Evaluation of histological scoring systems for tissue-engineered, repaired and osteoarthritic cartilage." *Osteoarthritis Cartilage* 18(1): 12-23.

Saamanen, A. M., M. Tammi, I. Kiviranta, J. Jurvelin and H. J. Helminen (1987). "Maturation of proteoglycan matrix in articular cartilage under increased and decreased joint loading. A study in young rabbits." *Connect Tissue Res* 16(2): 163-175.

Sabatini, M., G. Rolland, S. Leonce, M. Thomas, C. Lesur, V. Perez, G. de Nanteuil and J. Bonnet (2000). "Effects of ceramide on apoptosis, proteoglycan degradation, and matrix metalloproteinase expression in rabbit articular cartilage." *Biochem Biophys Res Commun* 267(1): 438-444.

- Sabatini, M., M. Thomas, C. Deschamps, C. Lesur, G. Rolland, G. de Nanteuil and J. Bonnet (2001). "Effects of ceramide on aggrecanase activity in rabbit articular cartilage." *Biochem Biophys Res Commun* 283(5): 1105-1110.
- Safran, M. and W. G. Kaelin, Jr. (2003). "HIF hydroxylation and the mammalian oxygen-sensing pathway." *J Clin Invest* 111(6): 779-783.
- Sah, R. L., Y. J. Kim, J. Y. Doong, A. J. Grodzinsky, A. H. Plaas and J. D. Sandy (1989). "Biosynthetic response of cartilage explants to dynamic compression." *J Orthop Res* 7(5): 619-636.
- Saito, T., A. Fukai, A. Mabuchi, T. Ikeda, F. Yano, S. Ohba, N. Nishida, T. Akune, N. Yoshimura, T. Nakagawa, K. Nakamura, K. Tokunaga, U. I. Chung and H. Kawaguchi (2010). "Transcriptional regulation of endochondral ossification by HIF-2 α during skeletal growth and osteoarthritis development." *Nat Med* 16(6): 678-686.
- Sakkas, L. I., C. Scanzello, N. Johanson, J. Burkholder, A. Mitra, P. Salgame, C. D. Katsetos and C. D. Platsoucas (1998). "T cells and T-cell cytokine transcripts in the synovial membrane in patients with osteoarthritis." *Clin Diagn Lab Immunol* 5(4): 430-437.
- Saklatvala, J. (1987). "Interleukin 1: purification and biochemical aspects of its action on cartilage." *J Rheumatol* 14 Spec No: 52-54.
- Saklatvala, J. (2007). "Inflammatory signaling in cartilage: MAPK and NF-kappaB pathways in chondrocytes and the use of inhibitors for research into pathogenesis and therapy of osteoarthritis." *Curr Drug Targets* 8(2): 305-313.
- Saklatvala, J., L. M. Rawlinson, C. J. Marshall and M. Kracht (1993). "Interleukin 1 and tumour necrosis factor activate the mitogen-activated protein (MAP) kinase kinase in cultured cells." *FEBS Lett* 334(2): 189-192.
- Sakurai, H., H. Kohsaka, M. F. Liu, H. Higashiyama, Y. Hirata, K. Kanno, I. Saito and N. Miyasaka (1995). "Nitric oxide production and inducible nitric oxide synthase expression in inflammatory arthritides." *J Clin Invest* 96(5): 2357-2363.
- Salvemini, D., T. P. Misko, J. L. Masferrer, K. Seibert, M. G. Currie and P. Needleman (1993). "Nitric oxide activates cyclooxygenase enzymes." *Proc Natl Acad Sci U S A* 90(15): 7240-7244.
- Sampieri, C. L., R. K. Nuttall, D. A. Young, D. Goldspink, I. M. Clark and D. R. Edwards (2008). "Activation of p38 and JNK MAPK pathways abrogates requirement for new protein synthesis for phorbol ester mediated induction of select MMP and TIMP genes." *Matrix Biol* 27(2): 128-138.

Sandy, J. D., R. E. Boynton and C. R. Flannery (1991). "Analysis of the catabolism of aggrecan in cartilage explants by quantitation of peptides from the three globular domains." *J Biol Chem* 266(13): 8198-8205.

Sauerland, K., R. X. Raiss and J. Steinmeyer (2003). "Proteoglycan metabolism and viability of articular cartilage explants as modulated by the frequency of intermittent loading." *Osteoarthritis Cartilage* 11(5): 343-350.

Scherle, P. A., M. A. Pratta, W. S. Feeser, E. J. Tancula and E. C. Arner (1997). "The effects of IL-1 on mitogen-activated protein kinases in rabbit articular chondrocytes." *Biochem Biophys Res Commun* 230(3): 573-577.

Scherle, P. A., M. A. Pratta, W. S. Feeser, E. J. Tancula and E. C. Arner (1997). "The effects of IL-1 on mitogen-activated protein kinases in rabbit articular chondrocytes." *Biochem Biophys Res Commun* 230(3): 573-577.

Schmid, T., J. Zhou and B. Brune (2004). "HIF-1 and p53: communication of transcription factors under hypoxia." *J Cell Mol Med* 8(4): 423-431.

Schuerwegh, A. J., E. J. Dombrecht, W. J. Stevens, J. F. Van Offel, C. H. Bridts and L. S. De Clerck (2003). "Influence of pro-inflammatory (IL-1 alpha, IL-6, TNF-alpha, IFN-gamma) and anti-inflammatory (IL-4) cytokines on chondrocyte function." *Osteoarthritis Cartilage* 11(9): 681-687.

Schulz, R. M. and A. Bader (2007). "Cartilage tissue engineering and bioreactor systems for the cultivation and stimulation of chondrocytes." *Eur Biophys J* 36(4-5): 539-568.

Scott, D. L., A. C. Wainwright, K. W. Walton and N. Williamson (1981). "Significance of fibronectin in rheumatoid arthritis and osteoarthritis." *Ann Rheum Dis* 40(2): 142-153.

Seguin, C. A. and S. M. Bernier (2003). "TNFalpha suppresses link protein and type II collagen expression in chondrocytes: Role of MEK1/2 and NF-kappaB signaling pathways." *J Cell Physiol* 197(3): 356-369.

Shlopov, B. V., M. L. Gumanovskaya and K. A. Hasty (2000). "Autocrine regulation of collagenase 3 (matrix metalloproteinase 13) during osteoarthritis." *Arthritis Rheum* 43(1): 195-205.

Shlopov, B. V., W. R. Lie, C. L. Mainardi, A. A. Cole, S. Chubinskaya and K. A. Hasty (1997). "Osteoarthritic lesions: involvement of three different collagenases." *Arthritis Rheum* 40(11): 2065-2074.

Siebelt, M., H. C. Groen, S. J. Koelewijn, E. de Blois, M. Sandker, J. H. Waarsing, C. Muller, G. J. van Osch, M. de Jong and H. Weinans (2014). "Increased physical activity severely

induces osteoarthritic changes in knee joints with papain induced sulfate-glycosaminoglycan depleted cartilage." *Arthritis Res Ther* 16(1): R32.

Simon, S. R., E. L. Radin, I. L. Paul and R. M. Rose (1972). "The response of joints to impact loading. II. In vivo behavior of subchondral bone." *J Biomech* 5(3): 267-272.

Singh, G., J. D. Miller, F. H. Lee, D. Pettitt and M. W. Russell (2002). "Prevalence of cardiovascular disease risk factors among US adults with self-reported osteoarthritis: data from the Third National Health and Nutrition Examination Survey." *Am J Manag Care* 8(15 Suppl): S383-391.

Smith, R. L. (1999). "Degradative enzymes in osteoarthritis." *Front Biosci* 4: D704-712.

Sondergaard, B. C., N. Schultz, S. H. Madsen, A. C. Bay-Jensen, M. Kassem and M. A. Karsdal (2010). "MAPKs are essential upstream signaling pathways in proteolytic cartilage degradation--divergence in pathways leading to aggrecanase and MMP-mediated articular cartilage degradation." *Osteoarthritis Cartilage* 18(3): 279-288.

Song, R. H., M. D. Tortorella, A. M. Malfait, J. T. Alston, Z. Yang, E. C. Arner and D. W. Griggs (2007). "Aggrecan degradation in human articular cartilage explants is mediated by both ADAMTS-4 and ADAMTS-5." *Arthritis Rheum* 56(2): 575-585.

Souza-Tarla, C. D., J. A. Uzuelli, A. A. Machado, R. F. Gerlach and J. E. Tanus-Santos (2005). "Methodological issues affecting the determination of plasma matrix metalloproteinase (MMP)-2 and MMP-9 activities." *Clin Biochem* 38(5): 410-414.

Spirito, S. and R. L. Goldberg (1997). "The ability of nitric oxide (NO) inhibitors to reverse an interleukin-1 (IL-1) induced depression of proteoglycan synthesis is age dependent." *Inflamm Res* 46 Suppl 2: S131-132.

Squires, G. R., S. Okouneff, M. Ionescu and A. R. Poole (2003). "The pathobiology of focal lesion development in aging human articular cartilage and molecular matrix changes characteristic of osteoarthritis." *Arthritis Rheum* 48(5): 1261-1270.

Stadler, J., M. Stefanovic-Racic, T. R. Billiar, R. D. Curran, L. A. McIntyre, H. I. Georgescu, R. L. Simmons and C. H. Evans (1991). "Articular chondrocytes synthesize nitric oxide in response to cytokines and lipopolysaccharide." *J Immunol* 147(11): 3915-3920.

Stanton, H., F. M. Rogerson, C. J. East, S. B. Golub, K. E. Lawlor, C. T. Meeker, C. B. Little, K. Last, P. J. Farmer, I. K. Campbell, A. M. Fourie and A. J. Fosang (2005). "ADAMTS5 is the major aggrecanase in mouse cartilage in vivo and in vitro." *Nature* 434(7033): 648-652.

Stefanovic-Racic, M., M. O. Mollers, L. A. Miller and C. H. Evans (1997). "Nitric oxide and proteoglycan turnover in rabbit articular cartilage." *J Orthop Res* 15(3): 442-449.

- Stefanovic-Racic, M., T. I. Morales, D. Taskiran, L. A. McIntyre and C. H. Evans (1996). "The role of nitric oxide in proteoglycan turnover by bovine articular cartilage organ cultures." *J Immunol* 156(3): 1213-1220.
- Steinmeyer, J. and S. Knue (1997). "The proteoglycan metabolism of mature bovine articular cartilage explants superimposed to continuously applied cyclic mechanical loading." *Biochem Biophys Res Commun* 240(1): 216-221.
- Stevens, C. R., R. B. Williams, A. J. Farrell and D. R. Blake (1991). "Hypoxia and inflammatory synovitis: observations and speculation." *Ann Rheum Dis* 50(2): 124-132.
- Studer, R. K., E. Levicoff, H. Georgescu, L. Miller, D. Jaffurs and C. H. Evans (2000). "Nitric oxide inhibits chondrocyte response to IGF-I: inhibition of IGF-IRbeta tyrosine phosphorylation." *Am J Physiol Cell Physiol* 279(4): C961-969.
- Studer, R. K., H. I. Georgescu, L. A. Miller and C. H. Evans (1999). "Inhibition of transforming growth factor beta production by nitric oxide-treated chondrocytes: implications for matrix synthesis." *Arthritis Rheum* 42(2): 248-257.
- Taskiran, D., M. Stefanovic-Racic, H. Georgescu and C. Evans (1994). "Nitric oxide mediates suppression of cartilage proteoglycan synthesis by interleukin-1." *Biochem Biophys Res Commun* 200(1): 142-148.
- Tchetina, E. V., J. A. Di Battista, D. J. Zukor, J. Antoniou and A. R. Poole (2007). "Prostaglandin PGE2 at very low concentrations suppresses collagen cleavage in cultured human osteoarthritic articular cartilage: this involves a decrease in expression of proinflammatory genes, collagenases and COL10A1, a gene linked to chondrocyte hypertrophy." *Arthritis Res Ther* 9(4): R75.
- Teeple, E., K. A. Elsaid, B. C. Fleming, G. D. Jay, K. Aslani, J. J. Crisco and A. P. Mechrefe (2008). "Coefficients of friction, lubricin, and cartilage damage in the anterior cruciate ligament-deficient guinea pig knee." *J Orthop Res* 26(2): 231-237.
- Tetlow, L. C., D. J. Adlam and D. E. Woolley (2001). "Matrix metalloproteinase and proinflammatory cytokine production by chondrocytes of human osteoarthritic cartilage: associations with degenerative changes." *Arthritis Rheum* 44(3): 585-594.
- Tew, S. R., Y. Li, P. Pothacharoen, L. M. Tweats, R. E. Hawkins and T. E. Hardingham (2005). "Retroviral transduction with SOX9 enhances re-expression of the chondrocyte phenotype in passaged osteoarthritic human articular chondrocytes." *Osteoarthritis Cartilage* 13(1): 80-89.
- Tokmina-Roszyk, M., D. Tokmina-Roszyk and G. B. Fields (2013). "The synthesis and application of Fmoc-Lys(5-Fam) building blocks." *Biopolymers* 100(4): 347-355.

- Tower, G. B., C. I. Coon, K. Belguise, D. Chalbos and C. E. Brinckerhoff (2003). "Fra-1 targets the AP-1 site/2G single nucleotide polymorphism (ETS site) in the MMP-1 promoter." *Eur J Biochem* 270(20): 4216-4225.
- Towle, C. A., H. H. Hung, L. J. Bonassar, B. V. Treadwell and D. C. Mangham (1997). "Detection of interleukin-1 in the cartilage of patients with osteoarthritis: a possible autocrine/paracrine role in pathogenesis." *Osteoarthritis Cartilage* 5(5): 293-300.
- Troyer, H. (1982). "Experimental models of osteoarthritis: a review." *Semin Arthritis Rheum* 11(3): 362-374.
- Ulivi, V., P. Giannoni, C. Gentili, R. Cancedda and F. Descalzi (2008). "p38/NF-kB-dependent expression of COX-2 during differentiation and inflammatory response of chondrocytes." *J Cell Biochem* 104(4): 1393-1406.
- van Baar, M. E., W. J. Assendelft, J. Dekker, R. A. Oostendorp and J. W. Bijlsma (1999). "Effectiveness of exercise therapy in patients with osteoarthritis of the hip or knee: a systematic review of randomized clinical trials." *Arthritis Rheum* 42(7): 1361-1369.
- van den Berg, W., P.M. van der Kraan, H.M van Beuningen (1999). "Role of growth factors in cartilage repair." In: Reginster J-Y, Pelletier JP, Martel-Pelletier J, et al., editors. *Osteoarthritis: clinical and experimental aspects*. Heidelberg: Springer-Verlag 188-209.
- van Weeren, P. R., E. C. Firth, H. Brommer, M. M. Hyttinen, A. E. Helminen, C. W. Rogers, J. Degroot and P. A. Brama (2008). "Early exercise advances the maturation of glycosaminoglycans and collagen in the extracellular matrix of articular cartilage in the horse." *Equine Vet J* 40(2): 128-135.
- Vane, J. R. and R. M. Botting (1998). "Anti-inflammatory drugs and their mechanism of action." *Inflamm Res* 47 Suppl 2: S78-87.
- Varfolomeev, E., T. Goncharov, A. V. Fedorova, J. N. Dynek, K. Zobel, K. Deshayes, W. J. Fairbrother and D. Vucic (2008). "c-IAP1 and c-IAP2 are critical mediators of tumor necrosis factor alpha (TNFalpha)-induced NF-kappaB activation." *J Biol Chem* 283(36): 24295-24299.
- Veihelmann, A., J. Landes, A. Hofbauer, M. Dorger, H. J. Refior, K. Messmer and F. Krombach (2001). "Exacerbation of antigen-induced arthritis in inducible nitric oxide synthase-deficient mice." *Arthritis Rheum* 44(6): 1420-1427.
- Venn, G., J. J. Nietfeld, A. J. Duits, F. M. Brennan, E. Arner, M. Covington, M. E. Billingham and T. E. Hardingham (1993). "Elevated synovial fluid levels of interleukin-6 and tumor necrosis factor associated with early experimental canine osteoarthritis." *Arthritis Rheum* 36(6): 819-826.

- Vignon, E., J. P. Valat, M. Rossignol, B. Avouac, S. Rozenberg, P. Thoumie, J. Avouac, M. Nordin and P. Hilliquin (2006). "Osteoarthritis of the knee and hip and activity: a systematic international review and synthesis (OASIS)." *Joint Bone Spine* 73(4): 442-455.
- Villiger, P. M., A. B. Kusari, P. ten Dijke and M. Lotz (1993). "IL-1 beta and IL-6 selectively induce transforming growth factor-beta isoforms in human articular chondrocytes." *J Immunol* 151(6): 3337-3344.
- Vodovotz, Y., N. S. Kwon, M. Pospischil, J. Manning, J. Paik and C. Nathan (1994). "Inactivation of nitric oxide synthase after prolonged incubation of mouse macrophages with IFN-gamma and bacterial lipopolysaccharide." *J Immunol* 152(8): 4110-4118.
- von der Mark, K., T. Kirsch, A. Nerlich, A. Kuss, G. Weseloh, K. Gluckert and H. Stoss (1992). "Type X collagen synthesis in human osteoarthritic cartilage. Indication of chondrocyte hypertrophy." *Arthritis Rheum* 35(7): 806-811.
- Vuolteenaho, K., T. Moilanen, M. Hamalainen and E. Moilanen (2003). "Regulation of nitric oxide production in osteoarthritic and rheumatoid cartilage. Role of endogenous IL-1 inhibitors." *Scand J Rheumatol* 32(1): 19-24.
- Wachi, H., H. Sugitani, H. Murata, J. Nakazawa, R. P. Mecham and Y. Seyama (2004). "Tropoelastin inhibits vascular calcification via 67-kDa elastin binding protein in cultured bovine aortic smooth muscle cells." *J Atheroscler Thromb* 11(3): 159-166.
- Walev, I., J. Klein, M. Husmann, A. Valeva, S. Strauch, H. Wirtz, O. Weichel and S. Bhakdi (2000). "Potassium regulates IL-1 beta processing via calcium-independent phospholipase A2." *J Immunol* 164(10): 5120-5124.
- Walker, P. S., J. Sikorski, D. Dowson, D. Longfield and V. Wright (1969). "Behaviour of synovial fluid on articular cartilage." *Ann Rheum Dis* 28(3): 326.
- Wann, A. K., J. Mistry, E. J. Blain, A. T. Michael-Titus and M. M. Knight (2010). "Eicosapentaenoic acid and docosahexaenoic acid reduce interleukin-1beta-mediated cartilage degradation." *Arthritis Res Ther* 12(6): R207.
- Webb, G. R., C. I. Westacott and C. J. Elson (1997). "Chondrocyte tumor necrosis factor receptors and focal loss of cartilage in osteoarthritis." *Osteoarthritis Cartilage* 5(6): 427-437.
- Weinblatt, M. E., E. C. Keystone, D. E. Furst, L. W. Moreland, M. H. Weisman, C. A. Birbara, L. A. Teoh, S. A. Fischkoff and E. K. Chartash (2003). "Adalimumab, a fully human anti-tumor necrosis factor alpha monoclonal antibody, for the treatment of rheumatoid arthritis in patients taking concomitant methotrexate: the ARMADA trial." *Arthritis Rheum* 48(1): 35-45.

- Wernike, E., Z. Li, M. Alini and S. Grad (2008). "Effect of reduced oxygen tension and long-term mechanical stimulation on chondrocyte-polymer constructs." *Cell Tissue Res* 331(2): 473-483.
- Westacott, C. I. and M. Sharif (1996). "Cytokines in osteoarthritis: mediators or markers of joint destruction?" *Semin Arthritis Rheum* 25(4): 254-272.
- Westacott, C. I., A. F. Barakat, L. Wood, M. J. Perry, P. Neison, I. Bisbinas, L. Armstrong, A. B. Millar and C. J. Elson (2000). "Tumor necrosis factor alpha can contribute to focal loss of cartilage in osteoarthritis." *Osteoarthritis Cartilage* 8(3): 213-221.
- Westacott, C. I., R. M. Atkins, P. A. Dieppe and C. J. Elson (1994). "Tumor necrosis factor-alpha receptor expression on chondrocytes isolated from human articular cartilage." *J Rheumatol* 21(9): 1710-1715.
- Wickstrom, S. A., K. Alitalo and J. Keski-Oja (2002). "Endostatin associates with integrin alpha5beta1 and caveolin-1, and activates Src via a tyrosyl phosphatase-dependent pathway in human endothelial cells." *Cancer Res* 62(19): 5580-5589.
- Williams, J.M., J. Zhang, Y. Kang, G.A. Homandberg (2003). "Effect of intra-articular injection of high molecular weight hyaluronic acid in joints of skeletally mature rabbits on protection against cartilage chondrolysis induced by fibronectin fragments." *Osteoarthritis Cartilage* 11: 44-49.
- Williams, J.M., V.L Plaza, J. Wen, D.G. Karwo, G.A. Homandberg (1996). "Short and Long Term Effects of Multiple Intra-articular Injections of Fibronectin Fragments on the Articular Cartilage of Adolescent Rabbits." *Orthop Trans* 21: 313.
- Williams, R.J. (2007). "Cartilage Repair Strategies: Analysis and Strategies." Humana Press, 4-11. ISBN: 1588296296, 9781588296290.
- Willoughby, D. A., A. R. Moore, P. R. Colville-Nash and D. Gilroy (2000). "Resolution of inflammation." *Int J Immunopharmacol* 22(12): 1131-1135.
- Woessner, J.F.J., D.S. Howell (1993). "Joint Cartilage Degradation." Marcel Dekker, New York, NY.
- Wright, M. O., K. Nishida, C. Bavington, J. L. Godolphin, E. Dunne, S. Walmsley, P. Jobanputra, G. Nuki and D. M. Salter (1997). "Hyperpolarisation of cultured human chondrocytes following cyclical pressure-induced strain: evidence of a role for alpha 5 beta 1 integrin as a chondrocyte mechanoreceptor." *J Orthop Res* 15(5): 742-747.
- Wurster, N. B. and G. Lust (1984). "Synthesis of fibronectin in normal and osteoarthritic articular cartilage." *Biochim Biophys Acta* 800(1): 52-58.

- Xie, D. and G. A. Homandberg (1993). "Fibronectin fragments bind to and penetrate cartilage tissue resulting in proteinase expression and cartilage damage." *Biochim Biophys Acta* 1182(2): 189-196.
- Xie, D. L., F. Hui, R. Meyers and G. A. Homandberg (1994). "Cartilage chondrolysis by fibronectin fragments is associated with release of several proteinases: stromelysin plays a major role in chondrolysis." *Arch Biochem Biophys* 311(2): 205-212.
- Xie, D. L., R. Meyers and G. A. Homandberg (1992). "Fibronectin fragments in osteoarthritic synovial fluid." *J Rheumatol* 19(9): 1448-1452.
- Xie, D., F. Hui and G. A. Homandberg (1993). "Fibronectin fragments alter matrix protein synthesis in cartilage tissue cultured in vitro." *Arch Biochem Biophys* 307(1): 110-118.
- Xu, Z., M. J. Buckley, C. H. Evans and S. Agarwal (2000). "Cyclic tensile strain acts as an antagonist of IL-1 beta actions in chondrocytes." *J Immunol* 165(1): 453-460.
- Yang, S., J. Kim, J. H. Ryu, H. Oh, C. H. Chun, B. J. Kim, B. H. Min and J. S. Chun (2010). "Hypoxia-inducible factor-2alpha is a catabolic regulator of osteoarthritic cartilage destruction." *Nat Med* 16(6): 687-693.
- Yasuda, T. (2011). "Activation of Akt leading to NF-kappaB up-regulation in chondrocytes stimulated with fibronectin fragment." *Biomed Res* 32(3): 209-215.
- Yasuda, T.T., F. Mwale, J. Burgess, A.R. Poole (1999). "Cartilage destruction by matrix degradation products." *Trans Orthop Res Soc* 45 336.
- Yellowley, C. E., C. R. Jacobs, Z. Li, Z. Zhou and H. J. Donahue (1997). "Effects of fluid flow on intracellular calcium in bovine articular chondrocytes." *Am J Physiol* 273(1 Pt 1): C30-36.
- Young, A. A., S. McLennan, M. M. Smith, S. M. Smith, M. A. Cake, R. A. Read, J. Melrose, D. H. Sonnabend, C. R. Flannery and C. B. Little (2006). "Proteoglycan 4 downregulation in a sheep meniscectomy model of early osteoarthritis." *Arthritis Res Ther* 8(2): R41.
- Zack, M. D., E. C. Arner, C. P. Anglin, J. T. Alston, A. M. Malfait and M. D. Tortorella (2006). "Identification of fibronectin neoepitopes present in human osteoarthritic cartilage." *Arthritis Rheum* 54(9): 2912-2922.
- Zadow, J.G. (1992). "Whey and Lactose Processing". Elsevier Applied Science Publ.
- Zahn, G. and A. Greischel (1989). "Pharmacokinetics of tumor necrosis factor alpha after intravenous administration in rats. Dose dependence and influence of tumor necrosis factor beta." *Arzneimittelforschung* 39(9): 1180-1182.

Zhang, D., N. Burton-Wurster, G. Lust (1995). "Antibody specific for extra domain B of fibronectin demonstrates elevated levels of both extra domain B[+] and B[-] fibronectin in osteoarthritic canine cartilage." *Matrix Biol* 14: 623-633.

Zhou, M., A. Zhang, B. Lin, J. Liu and L. X. Xu (2007). "Study of heat shock response of human umbilical vein endothelial cells (HUVECs) using cDNA microarray." *Int J Hyperthermia* 23(3): 225-258.

Zwerina, J., S. Hayer, K. Redlich, K. Bobacz, G. Kollias, J. S. Smolen and G. Schett (2006). "Activation of p38 MAPK is a key step in tumor necrosis factor-mediated inflammatory bone destruction." *Arthritis Rheum* 54(2): 463-472.

Publications and Conference Proceedings

Publications

Tilwani, R. K., S. Vessillier, B. Pinguan-Murphy, D. A. Lee, D. L. Bader and T. T. Chowdhury (2017). "Oxygen tension modulates the effects of TNF α in compressed chondrocytes." *Inflamm Res* 66(1): 49-58.

Conference Proceedings

R.K Tilwani, D.A Lee, B Pinguan-Murphy, WAB Wan Abas and T.T Chowdhury (2013). Hypoxia Amplified Catabolic Effects Induced by TNF α in Chondrocytes – response reduced with biomechanical signals. British Society for Matrix Biology Autumn Conference – “Under pressure: the cell response”, Cardiff, Sept. 2013.